

**ENDOCANNABINOID MODULATION OF NOCICEPTIVE
PROCESSING**

Leonie Norris, (BSc)

**Thesis submitted to the University of Nottingham for the
degree of Doctor of Philosophy**

September 2009

**MEDICAL LIBRARY
QUEENS MEDICAL CENTRE**

Abstract

The analgesic effects of cannabis-based medicines are widely described and elevation of the endocannabinoids (ECLs), by inhibition of endocannabinoid metabolism, also produces analgesia. Measurement of endocannabinoids (ECLs) and metabolites, in low weight biological tissue, provides an important tool for investigating the potential therapeutic effects of this receptor system.

The main aims of this thesis were to develop an analytical method to measure ECLs, and cyclooxygenase-2 (COX-2) metabolites of anandamide (AEA) and 2-arachidonoylglycerol (2-AG), and to apply the method to determine their role in nociceptive processing in models of acute and chronic inflammatory pain.

A liquid chromatography-tandem mass spectrometry (LC-MS/MS) method, which allowed for the simultaneous measurement of AEA, oleoylethanolamide (OEA), palmitoylethanolamine (PEA) and 2-AG, as well as COX-2 metabolites of AEA and 2-AG was developed and validated. This method was demonstrated to be able to quantify ECLs and related compounds in rat hindpaw, brain, spinal cord and cell samples.

The effects of TRPV1 activation on levels of intracellular calcium $[Ca^{2+}]_i$ and ECLs in sensory nerves were investigated. The TRPV1 agonist, capsaicin, dose dependently increased $[Ca^{2+}]_i$, which was blocked by the TRPV1 antagonist *iodoresiniferatoxin* (IRTX). Although synthesis of ECLs is activity and calcium dependent, there

was no relationship between the TRPV1-mediated increases in $[Ca^{2+}]_i$, and levels of intracellular or extracellular ECLs. The mechanism of sensitization of primary afferent nociceptors by the proinflammatory cytokine tumor necrosis factor- α (TNF α), which is heavily implicated in inflammatory responses, was also studied. TNF α facilitated capsaicin-evoked calcium responses, an effect which was mediated by p38MAPK-induced phosphorylation.

The ability of inhibition of fatty acid amide hydrolase (FAAH) to modulate inflammatory pain responses, and the sites at which ECLs were elevated, was studied in the carrageenan model of inflammatory pain. This model was considered ideal for the investigation of the role of alternative metabolism of ECLs by COX-2 as inflammatory pain is associated with an up-regulation of COX-2. The effects of acute and repeated administration of URB597 (0.3 mgkg⁻¹), a selective inhibitor of FAAH metabolism of ECLs, on carrageenan-evoked changes in weight bearing and hindpaw oedema were determined. Behavioural effects were considered in parallel with the changes in levels of ECLs and COX-2 metabolites of AEA and 2-AG in the hindpaw and spinal cord. Acute administration of URB597 delayed the onset and attenuated carrageenan-induced hyperalgesia, an effect which was associated with increased levels of AEA, OEA and PEA in the spinal cord. By contrast, carrageenan-induced hyperalgesia was not altered by repeated administration of URB597 and levels of AEA in the spinal cord were not significantly increased by this treatment. There was no evidence for the

metabolism of ECLs via COX-2 in the hindpaw, or spinal cord, of carrageenan-treated rats, under basal conditions or following inhibition of FAAH.

The role of the endocannabinoid system in a model of osteoarthritis (OA) pain was also investigated. Intra-articular injection of the chondrocyte inhibitor monosodium iodoacetate (MIA, 1mg/50 μ l) produced histological changes reminiscent of joint damage in OA patients, and a time dependant decrease in paw withdrawal thresholds and weight bearing on the injured (ipsilateral) side. These behavioural pain responses were accompanied with an increase in ECLs in the spinal cord, suggestive of a role of ECLs in modulation of OA-induced pain.

Declaration

All of the experiments and analysis detailed within this thesis were carried out by myself, unless otherwise stated. Collaborators are acknowledged in appropriate chapters.

Acknowledgements

I would firstly like to thank my supervisors, Professor Victoria Chapman, Professor David Kendall, and Dr David Barrett for all their help and guidance throughout my PhD, and for taking a chance on me with a pharmacology and neuroscience PhD in the first place!

I would also like to thank Paul Millns and Liaque Latiff for their invaluable training, and introducing me to the 'dark place' of calcium imaging and the 'dull world' of western blotting, respectively. I would also like to mention Steve Alexander for the (unwanted) attempts to improve my articulateness, when a bit of cannabinoid advice was all that was asked for!

I would also like to thank all the members of the E31 Chapman group (too numerous to name individually!) for all the support and good times, but in particular Dr Devi Rani Sagar-Cooper for being there from Day One with advice and Badger Balm.

Outside the lab, I would like to thank all my friends in Biomedical Sciences particularly Amy Warnerberry, Caitlin 'Welshit' Jones,

Boobie Woods, Ian Robinson-Bennett, and (F)Annie Patel, for the many cups of tea, and for making the whole PhD process an enjoyable one.

Finally I would like to acknowledge the support given to me by my family throughout the course of this PhD, but also in the preceding years. Without that I would not have made it to this stage. So, thanks to mam, dad, Imelda, Fintan, and Tony (and thanks for the 'financial hardship grant's too!). And thank you to Judith and Alex, for the umpteen lifts, and 'meals on wheels'! A special shout out goes to Ben, for without him, I'd be lost!

Abbreviations

2-AG : 2-arachidonoyl glycerol

2-AG-d8 : deuterated 2-arachidonoyl glycerol

2-EGs : 2-epoxyeicosatrienoyl-glycerols

AA-5HT: N-arachidonoyl serotonin

Aβh4 : N-acylphosphatidylethanolamine lipase

AEA : N-arachidonoyl ethanolamine; Anandamide

AEA-d8 : deuterated anandamide

AM251: 1-(2,4-dichlorophenyl)-5-(4-iodophenyl)-4-methyl-N-(1-piperidyl)pyrazole-3-carboxamide

AMPA : ionotropic glutamate receptor

ATP : Adenosine Tri-Phosphate

cAMP : cyclic adenosine monophosphate

B1 : Bradykinin 1 receptor

B2 : Bradykinin 2 receptor

CB₁ : Cannabinoid 1 receptor

CB₂ : Cannabinoid 2 receptor

CBD : Cannabidiol

CCI : Chronic constriction injury

CFA : Complete Freund's adjuvant

CHO : Chinese hamster cells

COX-2: Cyclooxygenase type 2

CRGP : calcitonin gene-related peptide

CYP450 : Cytochrome P450

Cyclic AMP : Cyclic adenosine monophosphate

DAG(L) : Diacylglycerol (Lipase)

dH₂O : distilled water

DH : Dorsal horn

DHETE-GE : Dihydroxyeicosatrienoic acid glycerol ester

DRG : Dorsal root ganglion

DSE : Depolarisation induced suppression of excitation

DSI : Depolarisation induced suppression of inhibition

ECL : Endocannabinoid and like compounds

EP : Prostaglandin receptor

EET-EA : Epoxyeicosatrienoic acid ethanolamide

EGTA ; ethylene glycol tetraacetic acid
EMT : Endocannabinoid membrane transporter
ESI : Electrospray ionisation
FAAH : Fatty acid amide hydrolase
FDA : Food and drug administration
Fura-2AM : L-[2-(carboxyoxazol-2-yl)-6-amino-benzofuran-5-oxy]-2-(2'-amino-5'methylphenoxy) ethane-N,N,N,N-tetraacetic acid pentaacetoxymethylester)
GABA : gamma-aminobutyric acid
GAPDH : Glyceraldehyde 3-phosphate dehydrogenase
GC-MS : Gas chromatography Mass spectrometry
GDE1 : glycerophosphoinositol phosphodiesterase
GDNF : Glial derived neurotrophic factor
GpAEA - glycerophospho-N-arachidonoyl ethanolamine
GpNAE - glycerophospho-N-acyl ethanolamine
HCl : Hydrochloric acid
HETE : Hydroxyeicosatetraenoic acid
HEK : Human embryonic kidney
HBSS : Hanks balanced saline solution
HPETE-GE : Hydroxyperoxyeicosa-5,8,10,14-tetraenoic acid glycerol ester
HPLC : High performance liquid chromatography
HU210 : 1,1-dimethylheptyl-11-hydroxytetrahydrocannabinol
IL-1 : Interleukin 1
i.p. : Intraperitoneal administration
i.pl. : Intraplantar administration
IRTX : Iodoresiniferatoxin, 7-Deepoxy-6,7-didehydro-5-deoxy-21-dephenyl-21-(phenylmethyl)-daphnetoxin,20-(4-hydroxy-5-iodo-3-methoxybenzeneacetate)
JWH133 : (6aR,10aR)-3-(1,1-Dimethylbutyl)-6a,7,10,10a-tetrahydro -6,6,9-trimethyl-6H-dibenzo[b,d]pyran
KCl : Potassium chloride
LC-MS/MS : Liquid chromatography- mass spectrometry mass spectrometry
LOX : Lipoxygenase
LPS : Lipopolysaccharide
MAGL : Monoacylglycerol lipase
MAPK : Mitogen activated protein kinase

MEM : Minimum Essential Medium
MIA : Monosodium iodoacetate
mGluR : metabotropic glutamate receptor
MRM : Multiple reaction monitoring
mRNA : Messenger ribonucleic acid
NAAA : N-acylethanolamine hydrolysing acid amidase
NADA : N-arachidonoyl dopamine
NAE : N-acylethanolamines
NaF : Sodium Fluoride
NAPE : N-phosphatidyl ethanolamine
NAPE-PLD : N-acyl phosphatidylethanolamine phospholipase D
NArPE : arachidonoyl containing NAPE
NGF : neurotrophin nerve growth factor
NMDA : N-methyl-D-aspartic acid
NMR : Nuclear magnetic resonance
NO : Nitric Oxide
NSAIDs : Non-steroidal anti-inflammatory drugs
OEA : N-oleoyl ethanolamine
P2X₃ : Purinergic receptor ligand-gated ion channel 3
PA : Phosphatidic acid
pAEA : phospho anandamide
PAG : Periaqueductal grey
PB : parabrachial nucleus
PBS : Phosphate buffered saline
PE : phosphatidylethanolamine
PEA : N-palmitoyl ethanolamine
PI : Phosphoinositides
PKA : Protein kinase A
PKC : Protein kinase C
PLA1 : Phospholipase A1
PLC : Phospholipase C
PLD : Phospholipase D
p.o. : Oral administration
PPAR : Peroxisome proliferator-activated receptor
PG-EA : Prostaglandin ethanolamide
PGD2-EA : Prostaglandin D2 ethanolamide
PGE2-EA : Prostaglandin E2 ethanolamide

PGF2 α -EA : Prostaglandin F2 α ethanolamide
PGF2 α -EA-d4 : deuterated prostaglandin F2 α ethanolamide
PGE2-GE : Prostaglandin E2 glycerol ester
PGF2 α -GE : Prostaglandin F2 α glycerol ester
PGE₂-G : Prostaglandin E₂-glycerol
PTPN22 : Protein tyrosine phosphatase, non-receptor type 22
Q-TOF : quadrupole time-of-flight
QTRAP : Quadruple linear ion trap
RA : Rheumatoid arthritis
RFU : Relative fluorescent intensity
RVM : rostral ventromedial medulla
SDS : Sodium dodecyl sulphate
SHIP1 : SH2-containing phosphatase
STT : spinothalamic tract
SNL : Spinal nerve ligation
SR141716a : 5-(4-Chlorophenyl)-1-(2,4-dichloro-phenyl)-4-methyl-N-(piperidin-1-yl)-1*H*-pyrazole-3-carboxamide
SR144528 : 5-(4-chloro-3-methylphenyl)-1-[(4-methylphenyl)methyl]-N-[(1*S*,4*R*,6*S*)-1,5,5-trimethyl-6-bicyclo[2.2.1]heptanyl]pyrazole-3-carboxamide
SRM : Selected reaction monitoring
TBST : Tris-Buffered Saline Tween-20
TEA : Triethylamine
TFA : Trifluoroacetic Acid
 Δ^9 -THC : Δ^9 -Tetrahydrocannabinol
TLC : Thin layer chromatography
TNF α : Tumour necrosis factor α
TNFR1 : Tumour necrosis factor receptor 1
TNFR2 : Tumour necrosis factor receptor 2
TRIS : Tris(hydroxymethyl)aminomethane
TrKA : Neurotrophic tyrosine kinase, receptor for NGF
TRPV1 – Transient receptor potential vanilloid type 1

1	General Introduction	16
1.1	Pain	16
1.2	Primary afferent nociceptors	17
1.2.1	TRPV1	19
1.3	The dorsal horn of the spinal cord	21
1.3.1	Ascending pathways	23
1.3.2	Descending pathways	27
1.4	Peripheral sensitisation	28
1.5	Central sensitisation	34
1.6	Animal models of pain	36
1.7	Inflammatory Pain	37
1.7.1	The carrageenan model of inflammation	39
1.8	Current analgesic treatments	40
1.9	Cannabinoids	41
1.10	Cannabinoid Receptors	42
1.10.1	Cannabinoid receptor-mediated analgesia	45
1.11	Endocannabinoids	47
1.12	Measurement of Endocannabinoids	48
1.12.1	Endocannabinoid synthesis	49
1.12.2	Endocannabinoid modulation of nociception	53
1.12.3	Endocannabinoid metabolism	54
1.12.4	Attenuation of endocannabinoid catabolism	59
1.13	Aims:	62
2	Development and validation of a quantitative analytical method to measure levels of endocannabinoids and COX-2 metabolites in rat tissue	64
2.1	Introduction	64
2.1.1	Endocannabinoid metabolism	65
2.1.2	Measured levels of endocannabinoids metabolites using LC- MS/MS	65
2.2	Aims and objectives	69
2.3	Method	70
2.3.1	Chemicals	70
2.3.2	LC-MS/MS conditions	71
2.3.3	Sample extraction	73
2.3.4	Validation	75
2.3.5	Quantification of endocannabinoids, prostaglandin ethanolamides and prostaglandin glycerol esters	79
2.3.6	Direct comparison of two MS systems to ensure consistency in data	80
2.3.7	Data Analysis	81
2.4	Results and Discussion	82
2.4.1	Analytical Development	82
2.4.1.1	MS parameters	82
2.4.2	HPLC Development	83
2.4.2.1	Effects of column stationary phase on separation	85
2.4.2.2	Effects of mobile phase composition on separation	86
2.4.3	Extraction of ECLs and related compounds	88
2.4.4	Effect of extraction solvent on recovery	88
2.4.4.1	Effect of silanisation of glassware	91
2.4.4.2	Evaluation of solid phase extraction	92

2.4.5	Validation	93
2.4.6	Analysis of rat brain extract	96
2.4.7	Comparison of two analytical methods	98
2.4.8	Quantification of EC in biological matrices	100
3	The role of TRPV1 in modulating endocannabinoid levels and neuronal responses to TNFα.	106
3.1	Introduction	106
3.1.1	Capsaicin and TRPV1	106
3.1.2	CB ₁ and TRPV1	107
3.1.3	Calcium driven EC synthesis	110
3.1.4	Endocannabinoid uptake, release and degradation	111
3.1.5	TRPV1 sensitisation by inflammatory mediators	113
3.1.6	Inflammatory mediators and TRPV1	114
3.1.7	TNF α	116
3.1.8	The objectives of this chapter are:	119
3.2	Materials and Methods	120
3.2.1	DRG Preparation	120
3.2.1.1	Glass coverslip preparation	120
3.2.1.2	Dorsal root ganglion (DRG) neurone preparation	121
3.2.1.3	Fura-2AM cell loading	123
3.2.1.4	Calcium imaging studies of DRG neurones	123
3.2.2	Measurement of changes in [Ca ²⁺] _i in hTRPV1- SHSY5Y cells	126
3.2.2.1	Cell Culture	126
3.2.2.2	Fluorimetric measurement of intracellular free calcium	127
3.2.3	Western Blotting	128
3.2.3.1	hTRPV1-SHSY5Y sample preparation for western blot analysis	129
3.2.3.2	Lowry protein assay	130
3.2.3.3	Antibodies Used	131
3.2.3.4	Running the gels	132
3.2.3.5	Visualising the protein bands- ECL	133
3.2.3.6	Densitometry	134
3.2.3.7	Running Gels- Odyssey	134
3.2.4	Endocannabinoid Measurements	135
3.3	Results	137
3.3.1	Effects of varying concentrations of capsaicin on intracellular calcium responses in adult rat dorsal root ganglion neurones <i>in vitro</i>	138
3.3.2	The role of CB ₁ receptors in modulation of intracellular calcium responses	141
3.3.3	Effects of capsaicin on endocannabinoid levels in rat DRG neurones	142
3.3.4	hTRPV1 SHSY5Y	144
3.3.5	Capsaicin concentration/response in hTRPV1 transfected SHSY5Y cells	144
3.3.6	Cannabinoid response in hTRPV1-SHSY5Y cells	146
3.4	Endocannabinoid levels in <i>htrpv1</i> -SHSY5Ys cells and supernatant	150

3.4.1.1	Effects of varying concentrations of capsaicin on ECL levels	150
3.4.1.2	Effects of IRTX (100nM) and capsaicin (10nM) on ECL levels.....	153
3.4.1.3	Effects of URB597 (1 μ M) and capsaicin (10 nM) on ECL levels.....	155
3.5	Modulation of TRPV1 function by TNF α	158
3.5.1	Effects of varying concentrations of TNF α on intracellular calcium responses in adult rat dorsal root ganglion neurones <i>in vitro</i>	158
3.6	Effects of TNF α on capsaicin-evoked changes in intracellular calcium concentrations in DRG neurons	161
3.7	Effects of SB706504 on TNF α and capsaicin-evoked changes in intracellular calcium concentrations in DRG neurones	165
3.7.1	Effect of TNF α on P38 MAPK phosphorylation and TRPV1 receptor expression	166
3.8	Discussion	172
4	Effects of inhibition of fatty acid amide hydrolase in the carrageenan model of inflammation	187
4.1	Introduction	187
4.1.1	FAAH inhibitors in inflammatory pain.....	187
4.1.2	Effects of inhibiting FAAH on pain responses	189
4.1.3	Inhibition of FAAH in animals models of pain.....	191
4.1.4	COX-2 metabolism of ECs and its role in inflammatory pain	195
4.2	Aims.....	199
4.3	Methods	200
4.3.1	Overview of Studies	200
4.3.2	Animals	203
4.3.3	Measurement of carrageenan-induced inflammation and drug treatment.	203
4.3.3.1	Weight bearing Behaviour	203
4.3.3.2	Measurement of Paw Circumference and Volume	205
4.3.4	Measurement of ECLs and prostamides in rat hindpaw and spinal cord	206
4.3.5	FAAH enzyme activity	207
4.3.6	Data Analysis	207
4.4	Results.....	209
4.4.1	Carrageenan-induced hyperalgesia.....	209
4.4.2	Levels of ECLs in the hindpaw and spinal cord of carrageenan treated rats.....	213
4.4.2.1	Levels of ECs at 2 hours post-carrageenan injection ...	213
4.4.2.2	Levels of ECLs at 3 hours post-carrageenan injection .	215
4.4.3	Effects of a single systemic administration of URB597 on carrageenan induced hyperalgesia	218
4.4.4	Effects of a single systemic administration of URB597 on FAAH enzyme activity in the Midbrain and Liver	220
4.4.5	Effects of a single systemic administration of URB597 on levels of ECLs and related compounds.....	221

4.4.5.1	Levels of ECLs 2 hours post-carrageenan injection	222
4.4.5.2	Levels of ECLs 3 hours post-carrageenan injection	230
4.4.6	Effects of a repeated systemic administration of URB597 on carrageenan induced hyperalgesia	240
4.4.7	Effects of repeated systemic injection of URB597 on FAAH enzyme activity in the Midbrain and Liver.....	241
4.4.8	Effects of repeated systemic injection of URB597 on levels of ECLs in the hindpaw and spinal cord of carrageenan treated rats	242
4.5	Discussion	255
4.5.1	The effects of carrageenan at 2 hours and 3 hours on carrageenan-induced hyperalgesia and levels of ECLs.....	256
4.5.2	Effects of URB597 on carrageenan-induced changes in weight bearing and paw oedema.	259
4.5.3	Central versus peripheral effects of FAAH inhibition in inflammatory pain.	260
4.5.4	Effects of repeated administration of URB597 on carrageenan-induced hindpaw inflammation and endocannabinoid levels.....	262
4.5.5	Is the lack of effect of repeated administration of URB597 due to changes in endocannabinoid biosynthesis and catabolism?	263
5	The role of the endocannabinoid system in MIA model of Osteoarthritis.	268
5.1	Introduction	268
5.2	Synovial Joint Histology	269
5.3	Pathophysiological changes in the joint in OA.....	271
5.3.1	Animal models of OA.....	274
5.3.2	MIA model of OA pain	275
5.3.3	The cannabinoid receptor system: implications for OA	277
5.3.4	Aims	279
5.4	Methods	280
5.4.1	Intra-articular injections	280
5.4.2	Behavioural testing.....	280
5.4.3	Histology	282
5.4.4	Measurement of endocannabinoids.....	283
5.5	Results.....	285
5.5.1	MIA-induced changes in pain behaviour.....	285
5.5.2	Levels of ECLs in the hindpaw and spinal cord of MIA and saline treated rats	289
5.5.2.1	ECL levels in rat hindpaw PO14 and PO28	289
5.5.3	ECL levels in rat spinal cord PO14 and PO28	293
5.6	Discussion	302
6	General Discussion.....	310
7	Reference:.....	317
8	Appendix.....	356

Chapter 1.

General Introduction

1 General Introduction

1.1 Pain

Pain is defined as “an unpleasant sensory and emotional experience associated with actual or potential tissue damage, or described in terms of such damage” (Merskey, 1994). The term pain encompasses the emotional, behavioural and cognitive responses to the physiological sensation of a noxious stimulus. Pain is part of the body's defense system, triggering a reflex reaction to retract from a painful stimulus. It is a major symptom in many diseases and pathological conditions, significantly interfering with a person's quality of life and general functioning. This problem can be difficult to treat, particularly when it is present in addition to other pathological conditions such as cancer and inflammation. Although there are many different types of pain, the mechanisms involved in producing the pain can be loosely separated into inflammatory or neuropathic pain. However, in order to develop effective medicines to treat this wide ranging problem, the basic mechanisms by which pain is perceived and transduced into a behavioural response must be understood.

In 1906 Sherrington defined a nociceptor as a receptor that responds to stimuli which damage tissue, or have the potential to do so (Sherrington, 1906). Importantly nociceptors do not respond to innocuous stimuli (Sherrington, 1906, Meyer, 2006). Some time later, the gate control theory of pain was proposed, which is a

complex mechanism of nociceptive transmission, where activation of nerves that do not transmit pain signals can interfere with signals from pain fibers and inhibit an individual's perception of pain. (Melzack and Wall, 1965). When pain is sensed, there is usually an increase in neuronal activity, resulting in the perception of pain, however when the gating mechanism is activated, the pain signal can be curtailed due to pre-synaptic inhibition (Melzack and Wall, 1965). This mechanism involves a sequence of complex interactions at peripheral, spinal and supraspinal sites, and provides various potential pharmacological targets (Melzack and Wall, 1965).

1.2 Primary afferent nociceptors

Pain is associated with increased electrical firing in small diameter sensory nerve afferent fibres. Nociceptors transduce mechanical, thermal and chemical stimuli and the generated electrical signals are propagated along sensory neurones to the spinal cord and brain. Cell bodies of these fibres are located in the dorsal root ganglia (DRG), and are categorised into 3 different classes, according to their diameter, structure, and conduction velocity (Meyer, 2006). Cells with the largest cell bodies give rise to large diameter ($>10\mu\text{m}$) fastest conducting, myelinated $A\beta$ fibres, these fibres are cutaneous mechanoreceptors which respond to innocuous stimulation such as light touch; however, they are also thought to play a minor role in nociceptive transmission (Koltzenburg et al., 1994). The two major sensory fibres associated with nociceptive processing are thin, myelinated, relatively fast $A\delta$ fibres and un-myelinated, slow

conducting C-fibres. A δ fibres respond to mechanical and thermal noxious stimulation, with varying receptor thresholds, with the lowest threshold in the innocuous range. A δ fibres discharge increasingly upon stimulation in a stimulus intensity-dependent manner. C-fibres are sensitive to thermal, chemical and mechanical stimuli, and are often termed 'polymodal receptors'. However, sub-populations of C-fibre nociceptors have been identified. These nociceptors are not activated equally by thermal, chemical and mechanical stimuli. Some mechanically sensitive C-fibres are unresponsive to heat (Schmidt et al., 1997), while another group are only responsive to heat (Schmidt et al., 1995), however can be sensitised to mechanical stimuli following repeated noxious mechanical stimulation (Schmidt et al., 2000). Other differences in C fibre sub-populations include their neurochemical content. One class of fibre, classed as the peptidergic population, contains substance P and CRGP (Averill et al., 1995, Molliver et al., 1997). They require the neurotrophin nerve growth factor (NGF) for development during embryonic life and express the receptor for NGF, TrKA (Molliver et al., 1997). However not all neurones express TrKA, and these form the non-peptidergic population. These fibres are sensitive to glial cell derived neurotrophic factor (GDNF), and express GDNF receptors, the ATP-gated ion channel P2X₃ receptors, and IB4-lectin binding site. In addition a sub group of nociceptors, named sleeping nociceptors, are insensitive to mechanical and thermal stimuli under normal conditions, but can become sensitised under pathological conditions

such as inflammation (Schaible and Schmidt, 1988, Schmidt et al., 1995). It has been suggested that these nociceptors are recruited and thought to contribute to hyperalgesia (an increased response to a noxious stimulus) (Schmidt et al., 1995, Besson, 1999).

Responses of primary afferent fibres are part of the normal protective response to pain. However, increased intensity of firing or prolonged firing of these fibres can lead to hyperalgesia or allodynia. Hyperalgesia as defined above is an increased response to a noxious stimulus and occurs when nociceptive responses are increased and prolonged (Merskey, 1994). Allodynia is a noxious response to a previously innocuous stimulus, due to normally innocuous A β -fibre input into a sensitized area perceived as noxious (Merskey, 1994), which can occur from biochemical changes peripherally and centrally.

1.2.1 TRPV1

TRPV1 channels are non-selective cation channels belonging to the transient receptors potential family (TRP). TRPV1 is a ~ 95kDa protein that has six transmembrane domains (Caterina, 1997). TRPV1 is expressed primarily by small to medium diameter primary afferent fibres and is activated by noxious heat (>43 °C), low pH and capsaicin, an ingredient of chilli peppers. Activation increases the permeability of the plasma membrane to cations, such as sodium and calcium (Szallasi, 1994, Caterina, 1997). Several phosphorylation sites for PKC and PKA, as well as several

glycosylation sites play a pivotal role in the regulation of the activity of the TRPV1 receptor (see review (Nagy et al., 2004)). Evidence suggests that post-translation modification of TRPV1, such as phosphorylation increase the activity of TRPV1 receptor, PKA-mediated phosphorylation increased the response of TRPV1 receptor to external activators such as prostaglandin E2 and AEA (Lopshire and Nicol, 1998, De Petrocellis et al., 2001c), and reduces the heat threshold of the receptor (Rathee et al., 2002). PKC-mediated phosphorylation of TRPV1 has been shown to be involved in the sensitising effects of some inflammatory mediators such as bradykinin, prostaglandins, and NGF released from injured tissue (Cesare and McNaughton, 1996, Caterina, 1997, Tominaga et al., 1998, Premkumar and Ahern, 2000), lowering the threshold of activation, thus implementing a role of TRPV1 in inflammation. Furthermore, TRPV1 expression is essential for the development of inflammatory heat hyperalgesia, which is absent in TRPV1 knock out mice (Caterina et al., 2000, Davis et al., 2000), and is upregulated following inflammation (Ji et al., 2002b, Amaya et al., 2003) (see chapter 3 for more detail).

In contrast to this pro-nociceptive role of TRPV1 activation, prolonged activation the primary afferent neuron by an increase in intracellular calcium results in desensitisation, reduced activity of the sensory nerves (Cholewinski et al., 1993, Koplas et al., 1997) leading to reduced pain, and thus represents an intriguing target for the treatment of pain (Sasamura and Kuraishi, 1999). However the

mechanisms underlying desensitisation is unclear. The acute loss of neuronal activity may be due to a voltage-dependant inhibition of sodium or calcium channels that occurs at positive membrane potentials (Docherty et al., 1991), whereas the long term inhibition through repeated exposure or high concentrations, capsaicin exerts neurotoxic effects in primary sensory neurones (Bevan and Szolcsanyi, 1990). The increase in intracellular calcium following capsaicin application causes the activation of Ca^{2+} -dependant enzymes and a decrease in mitochondrial function. Excessive influx of Na^+ induces passive transport of Cl^- into the cells, with a rise in osmotic pressure and finally cell death (Bevan and Szolcsanyi, 1990). Desensitisation has been shown to depend on a variety of factors including capsaicin concentration, the duration and time between applications and the presence of extracellular calcium (Craft and Porreca, 1992; Liu and Simon, 1998)

1.3 The dorsal horn of the spinal cord

The dorsal horn of the spinal cord is comprised of 6 laminae (figure 1.1), first described by Rexed in 1952, with laminae I, V, VI and X, and the outer part of laminae II associated with nociceptive processing (Todd, 2006). Dorsal horn neurones are made up of projection cells and interneurones. Projection neurones relay information from the white mater to various supra-spinal sites, while interneurones process information within the spinal cord. Interneurones make up the majority of the neuronal population in the

dorsal horn, and can be divided into two main functional classes: inhibitory interneurons, which use gamma amino butyric acid (GABA) as a transmitter, and excitatory interneurons, which are glutamatergic. The release of GABA, and, in many cases, co-releasing glycine (Todd and Sullivan, 1990) is particularly relevant spinally and supraspinally in the modulation of nociceptive transmission (Malcangio and Bowery, 1996). This is illustrated by the finding that local blockade of GABA_A receptors (GABA_ARs) and glycine receptors (GlyRs) replicates symptoms of neuropathic and inflammatory pain (Yaksh, 1989, Sivilotti and Woolf, 1994). Furthermore blocking this form of inhibition also allows low threshold input to be relayed to nociceptive specific neurons (Baba et al., 2003, Torsney and MacDermott, 2006).

With regards to their processing of nociceptive input, neurones in the dorsal horn can be divided into 3 populations. The first type consists of non-nociceptive low threshold neurones located in laminae II, III, and VI, and receive input from A β fibres. The second type consists of nociceptive-specific neurones, these are high threshold neurones, which are typically silent, and activated by noxious stimuli via A δ and C fibres. The third are wide dynamic range neurones, which are typically found in laminae IV, V, X, however also located in laminae I and II. These neurones encode information from a wide range of stimuli including noxious and innocuous inputs relayed by A β , A δ and C fibres (Millan, 1999b, Willis, 2004). Interneurones relay information from primary afferent fibres between and within each of

the laminae, while projection neurones transmit nociceptive information from laminae I, V, and VI to higher brain centres (Millan, 1999a).

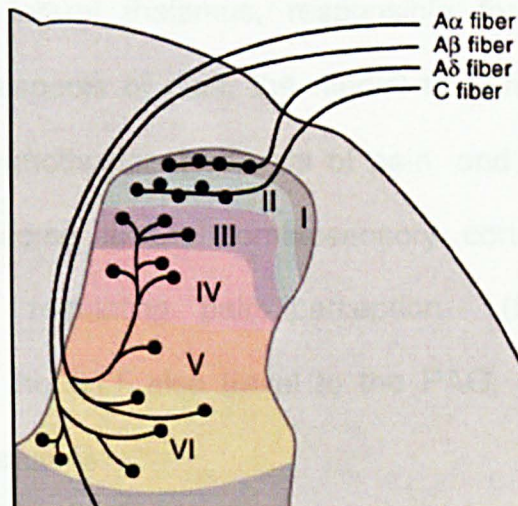


Figure 1.1

Anatomy of the dorsal horn, divided into laminae I –VI and primary afferent fibre innervation. Taken from (Squire, 2003)©.

1.3.1 Ascending pathways

From the dorsal horn neurones, noxious messages are relayed to the brain via various ascending pathways. The major pathways involved in pain processing are the spinothalamic tract (STT), and the spinobulbar tracts (consisting of the the spinomesencephalic tract, the spinoparabrachial tracts, the spinohypothalamic tract and the spinoreticular tract) (Millan, 1999b, Dostrovsky, 2006) see Figure 1.2.

The STT originates from 3 distinct regions, laminae I accounting for approximately 50% of the STT cells, laminae IV–V, accounting for 25% of the STT cells and the remaining 25% are found in laminae VII-VIII. These neurones project to various parts of the thalamus, which plays a key role in the integration and transmission of nociceptive information (Millan, 1999b). The thalamus can be divided into lateral thalamus, responsible for the sensory and discriminative aspects of pain, the medial thalamus, involved in the affective and motivational aspects of pain, and the ventroposterior thalamus, leading to the somatosensory cortex, thought to be important in regulating pain perception (Dostrovsky, 2006). Branches of the STT also travel to the PAG, and drive inhibitory control mechanisms.

The spinobulbar tract projections terminate in 4 main regions; the regions of catecholamine cell groups (A1-A7); the parabrachial nucleus (PB); the periaqueductal grey (PAG); the brain stem reticular formation (Dostrovsky, 2006). Catecholamine cell groups form part of the autonomic nervous system and activate somato-autonomic reflexes as well as descending pro and anti nociceptive mechanisms (Dostrovsky, 2006). A major target of the spinomesencephalic tract is the parabrachial nucleus (PB) of the pons. The PB projects to the hypothalamus, amygdala, midline and intralaminar thalamus, and to part of the ventrobasal thalamus (VMb, or VPMpc). Two pathways also run to the PB; the spinoparabrachiohypothalamic and spinoparabrachioamygdaloid pathways, thus the PB can be

accessed by several ascending pathways making it the main pathway by which nociceptive information reaches areas involved in the emotional aspects of pain. The hypothalamus and medial thalamus also have projections to the periaqueductal gray (PAG) and are again involved in emotional aspects of pain (Dostrovsky, 2006).

The PAG is a major site of homeostatic and limbic motor output, as well as having ascending and descending projections to the spinal cord. Activation of this region produces descending inhibitory control of nociceptive processes, making it a region involved in antinociception.

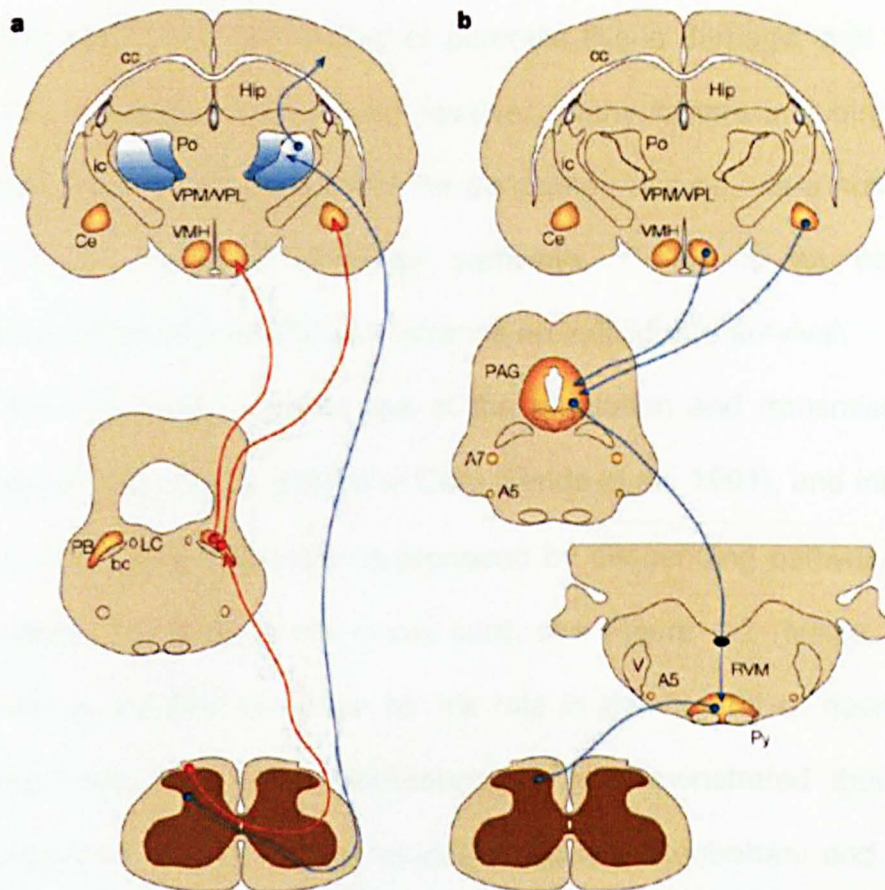


Figure 1.2

The major ascending and descending spinal pathways involved in nociceptive processing. The prominent ascending pathways shown in (a) are the spinoparabrachial pathway (red), and the spinothalamic pathway (blue) originating in superficial layers of the dorsal horn, projecting to the thalamus and hypothalamus. The descending pathway shown in (b) originates from the amygdala and hypothalamus and terminates in the periaqueductal grey (PAG). Subsequently neurones project from to the rostral ventral medulla (RVM) and control many of the antinociceptive and autonomic responses that follow noxious stimulation.

(A, adrenergic nucleus; bc, brachium conjunctivum; cc, corpus callosum; Ce, central nucleus of the amygdala; Hip, hippocampus; ic, internal capsule; LC, locus coeruleus; PB, parabrachial area; Po, posterior group of thalamic nuclei; Py, pyramidal tract; RVM, rostroventral medulla; V, ventricle; VMH, ventral medial nucleus of the hypothalamus; VPL, ventral posteriolateral nucleus of the thalamus; VPM; ventral posteromedial nucleus of the thalamus.) (take from (Hunt and Mantyh, 2001).

1.3.2 Descending pathways

Pain can arise from actual or potential tissue damage, and serves as a protective mechanism; however, many factors including other stimuli and stress can affect the perception of pain, via a number of centrally mediated inhibitory pathways. This is an essential mechanism of protection to enhance an individual's survival.

The PAG plays a major role in the mediation and transmission of nociceptive signals within the CNS (Fields et al., 1991), and inhibition of nociceptive responses is produced by descending pathways from supraspinal sites to the spinal cord, see Figure 1.2 (Millan, 2002). Indeed, the first evidence for its role in the control of nociceptive responses was when Behbehani et al demonstrated that direct stimulation of the PAG produces analgesia (Behbehani and Fields, 1979). The PAG projects to the rostral ventromedial medulla (RVM) and nociceptive information and modulation of the pain response in the dorsal horn is under bi-directional control from the PAG and the RVM (Fields and Heinricher, 1985). The RVM contains two types of neurones that mediate the inhibitory effects from the RVM to DH, 'ON' and 'OFF' cells, which either produce a burst of activity prior to a behavioural response or stop firing prior to the behavioural response, respectively. Descending inhibition is thought to be modulated by 'OFF' cells, whereas, 'ON' cells are involved in descending facilitation of nociception, with neurones terminating in the dorsal horn. The RVM is an important site of action for opioid mediated analgesia (Mitchell et al., 1998), as well as analgesic actions of cannabis-based

compounds (Meng et al., 1998). Microinjection of WIN55,212-2, the CB₁/CB₂ agonist into the RVM produced an increase in tail-flick latency (Meng et al., 1998), however this effect was not inhibited by the opioid receptor antagonist, naloxone, suggesting that the inhibitory effects of cannabinoids is not mediated by opioids (Meng et al., 1998), demonstrating a role of endogenous cannabinoid receptor system in nociceptive processing.

1.4 Peripheral sensitisation

Peripheral sensitisation contributes to the pain hypersensitivity found at the site of tissue damage and inflammation. Peripheral sensitisation is a reduction in threshold and an increase in responsiveness of the peripheral ends of nociceptors that transfer nociceptive information from peripheral targets (skin, muscle, joints and the viscera) through peripheral nerves to the central nervous system. Sensitisation arises due to the action of inflammatory mediators released around the site of tissue damage or inflammation. Tissue damage can either directly, or indirectly, cause the release of glutamate, bradykinin, cytokines, substance P, opioids, calcitonin gene related protein (CGRP), histamine, protons, nitric oxide, adenosine phosphates (including adenosine triphosphate, ATP) and arachidonic acid metabolites, such as prostaglandins from neighboring cells including neutrophils and mast cell. These mediators can exert direct effects by activating nociceptors, or indirectly by activating immune cells, thus increasing the

responsiveness of peripheral nociceptors to produce hyperalgesia (Meyer, 2006). In addition to these mediators, cytokines and neurotrophins are also generated during tissue damage which can contribute to changes in receptor expression and ion channels permeability, decreasing the threshold required for their activation, such as the TRPV1 (figure 1.3).

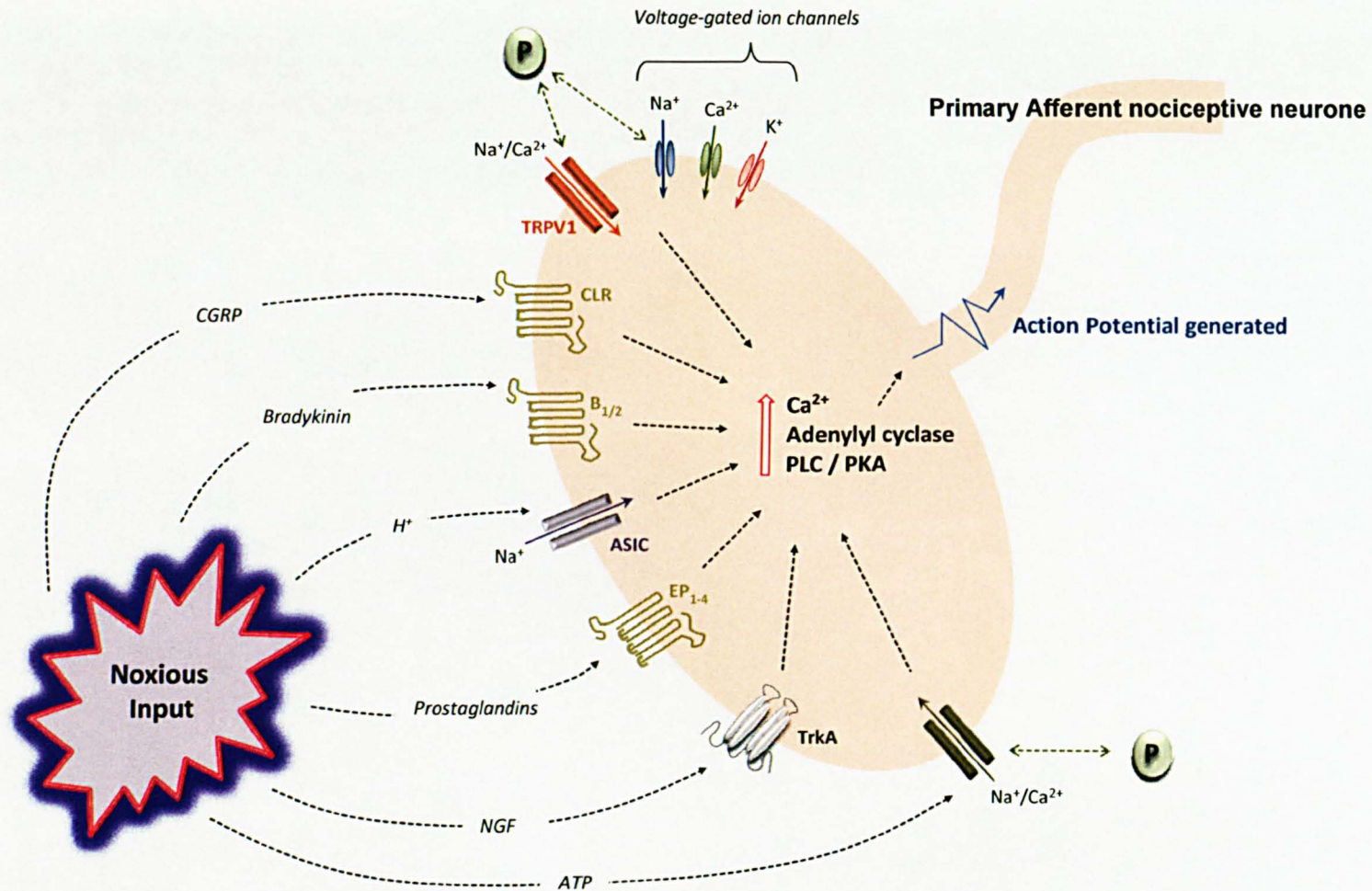


Figure 1.3 Overview of peripheral sensitisation of nociceptive neurons following tissue injury. Tissue injury leads to the synthesis and release of pro-inflammatory mediators from tissue around the site of injury, this leads to the activation of respective receptors and voltage gated ion channels. Collectively this leads to an increase in intracellular calcium, activation of adenylyl cyclase and subsequent activation of PLC/PKA pathways, leading to the sensitisation and phosphorylation TRPV1 receptors, Na⁺ channels of the peripheral terminals of nociceptive neurons,

ASIC, acid-sensing ion channel; TRPV1, transient receptor potential vanilloid receptor 1; CLR, Calcitonin-like receptor; B1/2, Bradykinin receptor; EP1-4, prostaglandin receptors; TrKA, neurotrophic tyrosine kinase receptor; CGRP, calcitonin gene related protein; ATP, adenosine triphosphate; NGF, nerve growth factor; PGE2, prostaglandin E2; PKA, protein kinase A; PKC, protein kinase C; PLC, phospholipase C; Many changes are effected by phosphorylation of receptors or channels (P), (adapted from Meyer., 2006).

The mechanisms by which inflammatory mediators exert their effects differ greatly depending on the compound in question.

Bradykinin is formed from kininogen precursor's proteins following tissue damage and plays an important role in inflammatory pain and hyperalgesia. It acts at G protein coupled B1 and B2 receptors. B2 receptors are constitutively expressed on a wide range of cells, including nociceptive neurones. B1 receptors are not expressed under normal conditions, but are induced following tissue injury, thought to be as a result of cytokine release (Perkins and Kelly, 1994). Bradykinin mediated activation of sensory neurons is via a marked rise in $[Ca^{2+}]_i$ and activation of the diacylglycerol (DAG) and protein kinase C (PKC) pathway (Burgess et al., 1989, Bleakman et al., 1990b). However another route by which bradykinin is thought to exert its effects is via sensitisation of TRPV1 receptor in a PKC-dependent manner (Premkumar and Ahern, 2000, Sugiura et al., 2002). B2 receptor agonists have also been shown to drive the generation of prostaglandins (Lembeck et al., 1976, Sauer et al., 1998), which in turn can sensitise neurones (Dray et al., 1992, Maubach and Grundy, 1999). Prostaglandins are synthesized from arachidonic acid, derived from membrane phospholipids which are metabolised by cyclooxygenase enzymes (COX-1 and COX-2). COX-2 is induced following inflammation, and is responsible for the production of PGE₂ and PGI₂, which play a role in acute and chronic inflammation (Minami et al., 2001; Stock et al., 2001). Prostaglandins act upon distinct prostanoid

receptors including EP₁, EP₂, EP₃, EP₄ and IP that activate several different G protein-coupled signalling pathways including the stimulation of adenylyl cyclase and subsequent increase in cAMP (Narumiya et al., 1999, Breyer et al., 2001, Narumiya and FitzGerald, 2001). PGE₂ and PGI₂ sensitise afferent neurones via a PKC and PKA dependant pathway (Pitchford and Levine, 1991, Lopshire and Nicol, 1998, Smith et al., 2000) as well as increasing intracellular calcium (Gu et al., 2003) ATP also plays an important role in nociceptive processing; it is released following damage to cells or activation of nociceptors. ATP binds to P2X receptors, which are cation selective ATP-gated ion channels on neurones and activation results in rapid depolarisation and increase in intracellular calcium (Millan, 1999b). An increase in extracellular protons, results in a reduction in pH, which has also been demonstrated to produce sustained discharges in DRG neurons (Steen et al., 1995, Vyklicky et al., 1998). The role of neurotrophins such as NGF and brain-derived neurotrophic factor (BDNF) in mediating neuronal responses under pathological conditions is becoming more evident. NGF stimulates mast cells to release histamine and serotonin and can induce heat hyperalgesia by acting directly on the peripheral terminals of primary afferent fibres (Chuang et al., 2001). Furthermore NGF increases the percentage A δ fibres that respond to mechanical stimuli (Stucky et al., 1999) and is implicated in inflammation-induced changes in nociceptor response properties, such as an increase in incidence of ongoing activity of dorsal root ganglion neurons (Djouhri et al., 2001). Cultured DRG neurons innervating inflamed tissue exhibit

spontaneous activity, and cultured DRG neurons from non-inflamed tissue exhibit spontaneous activity when cultivated for 1 day with NGF (Kasai and Mizumura, 2001), suggesting a role of NGF in spontaneous activation of DRG neurones. Moreover, NGF also potentiates the responses of the TRPV1 receptor (and NGF-induced hyperalgesia is absent in TRPV1-knockout mice (Chuang et al., 2001) indicating that this channel protein plays a critical role in inflammation-induced heat hyperalgesia (Caterina et al., 2000, Davis et al., 2000).

1.5 Central sensitisation

Central sensitisation is an increase in the excitability of neurons within the central nervous system, so that normal inputs begin to produce abnormal responses, resulting in hypersensitivity to pain signals. The increased excitability is triggered by a burst of activity in nociceptors (such as that evoked by an injury), which alter the strength of synaptic connections between the nociceptor and the neurons of the spinal cord (namely activity-dependent synaptic plasticity), which ultimately causes an increase in membrane excitability, or reduced inhibition. Low-threshold sensory fibers activated by innocuous stimuli activate normally high-threshold nociceptive neurons, producing allodynia. The pain, although evoked by a stimulus in the periphery, essentially arises as a result of changes in sensory processing within the CNS, and represents an abnormal state of responsiveness or an increased gain of the nociceptive system. Repetitive discharge of primary afferent nociceptors results in a release of modulators such as glutamate,

neuropeptides (substance P and (CGRP)) and BDNF from the central terminals of the nociceptors (Kidd and Urban, 2001) which on binding to their corresponding receptors contribute to central sensitisation. For example, substance P, which is co-released with glutamate (Afrah et al., 2002), binds to neurokinin-1 receptor (NK1), and causes long-lasting membrane depolarization, which is abolished following NK1 ablation using SPR-expressing neurons using the selective cytotoxin conjugate substance P-saporin (SP-SAP) (Khasabov et al., 2002). Furthermore, CGRP, also synthesised in small diameter neurones (Woolf and Wiesenfeld-Hallin, 1986), potentiates the effects of substance P and participate in central sensitisation through activation of postsynaptic CGRP1 receptors, which also activate PKA and PKC pathways (Sun et al., 2004).

The excitatory neurotransmitter glutamate acts at ionotropic glutamate receptors (AMPA, kainate and NMDA) or metabotropic glutamate receptors (mGluRs). Activation of the ionotropic glutamate receptors have been shown to play a role in central sensitisation. Phosphorylation of ionotropic glutamate receptors leads to an increase in synaptic efficacy by changing channel open time, increasing bursting, and removing the Mg^{2+} channel blockade at these receptors (Dickenson et al., 1997; Woolf and Salter, 2000). Inhibition of phosphorylation via the deletion of genes for isoforms of adenylate cyclase, protein kinase A and protein kinase C, impairs the development of pain hypersensitivity in transgenic mice (Malmberg et al., 1997; Wei et al., 2002). The role of activated glial cells in sensitisation of neurones in pathological

conditions has become more evident (Bruce-Keller, 1999, Hains and Waxman, 2006, Moalem and Tracey, 2006), with dorsal horn astrocytes and microglia activated following peripheral inflammation (Fu et al., 1999) and spinal nerve injury (Hashizume et al., 2000), activating p38 mitogen activated protein kinases (p38MAPK), and releasing pro-inflammatory cytokines such as IL-1 β and TNF α , which increase COX-2 activity and produces prostaglandins (Seybold et al., 2003), such as PGE₂, which binds to EP2 receptors to potentiate AMPA and NMDA receptors (Kohno et al., 2008), thus reducing inhibitory glycine transmission (Ahmadi et al., 2002).

1.6 Animal models of pain

Experiments on pain using human subjects are practically challenging, subjective, and ethically self-limiting, and thus laboratory animal models of pain are widely used. Animal models of pain are critical in understanding the mechanistic aspects of nociception, as well as understanding the analgesic activity of novel, or existing compounds. There are a number of different models commonly used, often in rodents, which mimic different clinical manifestations of pain. Models of acute nociception include the tail-flick, hot-plate and writhing tests (Walker et al., 1999, Le Bars et al., 2001), are useful for analysing the analgesic properties of drugs, but, bear few similarities to chronic pathological pain conditions observed in humans. Models of the mechanisms underlying chronic pain include injection of formalin, capsaicin, carrageenan or complete Freund's adjuvant (CFA) for inflammatory pain (Chapman et al., 1985), and a nerve ligation to

induce neuropathic pain (Bennett and Xie, 1988). These models produce complex pathologies, similar to the clinical situation, with time-dependent changes in nociceptive processing.

1.7 Inflammatory Pain

Inflammation is an essential protective reaction to irritation, injury or infection of tissue. It can be characterised by four signs; heat (calor), pain (dolor), redness (rubor), and swelling (tumor) as defined by Celsus in 1489. Pain arising from inflamed or injured tissues may arise spontaneously in the absence of an external trigger. Alternatively, responses to noxious stimuli may be enhanced (hyperalgesia) or normally innocuous stimuli may produce pain (allodynia). Tissue damage can be divided into 2 regions of pain, primary hyperalgesia, and secondary hyperalgesia. Primary hyperalgesia is an area of actual tissue damage, which displays an increase in sensitivity to mechanical, thermal and chemical stimuli. This is due to a decrease in activation threshold, and therefore sensitisation of primary afferent fibre. Thresholds to mechanical stimuli are unaltered following heat or mechanical injury; however there is evidence that mechanical insensitive afferents become sensitised following inflammation (Thalhammer and LaMotte, 1982, Campbell et al., 1988). Responsiveness to suprathreshold stimuli maybe augmented, where inflammation of the rat hindpaw resulted in an enhanced response to mechanical stimuli, spontaneous activity, and an expansion of receptor

fields for both A- and C-fibre nociceptors results in the activation of a greater number of fibres (Levine, 1999). Under normal circumstances, the production of pain from activation of nociceptors with mechanical stimuli is modulated in the CNS by the simultaneous activation of low-threshold mechanoreceptors. Injury decreases the responsiveness of low-threshold mechanoreceptors (Beck et al., 1974), thus hyperalgesia to mechanical stimuli may be due to injury to low-threshold mechanoreceptors, which would lead to a central disinhibition of nociceptor input. Injury also results in the local release of pro-inflammatory mediators, such as TNF α , bradykinin, prostaglandins, and histamine, and can lead to recruitment of immune cells local to the site of injury, such as T-cells, B-cells, mast cells and leukocytes (Levine and Reichling, 1999). Proinflammatory mediators can lead to a sensitisation of the nociceptor response, as well as having synergistic effects in potentiating nociceptor responses. Secondary hyperalgesia involves the area surrounding the region of tissue damage and displays an increase to mechanical stimuli only. When nociceptive input from the CNS is spared at the time of injury, hyperalgesia does not develop (LaMotte et al., 1991), suggesting that central sensitisation, not peripheral sensitisation, plays a major role in secondary hyperalgesia (Levine, 1999). As mentioned previously, in order to investigate the mechanisms underlying inflammatory pain, several animal models of inflammatory pain have been developed, one of which is the carrageenan model of inflammation.

1.7.1 The carrageenan model of inflammation

Carrageenan is a polysaccharide extract of the red seaweed, *chondrus crispus* used to induce inflammation in animals. Injection of the noxious stimulant, first described by Winter et al, 1962, is a model of rapid onset inflammatory pain (Winter et al., 1962). Inflammation induced by carrageenan, is an acute, and non-immune response. In rats, carrageenan, when injected subcutaneously into the plantar surface of a paw, produces characteristic inflammation, oedema, redness and associated hyperalgesia, which can be assessed through changes in weight bearing and paw pressure sensitivity (Hargreaves et al, 1988). Tissue damage following carrageenan results in the release of inflammatory mediators such as prostaglandins (Blackman et al, 1979), Nitric Oxide (NO) (Salvemini et al, 1996) Histamine (Al-Haboubi et al, 1983), bradykinin (Buritova et al, 1997), pro-inflammatory cytokines (Loram et al, 2006) and NGF (McMahon et al, 1996), from the site of injury or by infiltrating cells which migrate to the site of inflammation, such as neutrophils and mast cells. Carrageenan-induced pain behaviour is dependant on the release of histamine (Di Rosa et al., 1971, Stochla and Maslinski, 1982, Al-Haboubi and Zeitlin, 1983), as well as NGF from mast cells (Friedman et al., 1990, Leon et al., 1994), which can activate and/or sensitise receptors and primary afferent fibres leading to an increase in hindpaw receptive field size (Elmes et al., 2005). These pain-related behaviours peak at approximately 3 hours following carrageenan injection (Hargreaves et al, 1988). This model

can therefore be used to quantify the anti-inflammatory or anti-hyperalgesic actions of drugs.

1.8 Current analgesic treatments

Opioids are the major analgesics in the treatment of moderate to severe pain, however due to their adverse side effects such as constipation, nausea, respiratory depression, and tolerance towards the compounds (Ikeda et al., 2002), further pharmacological agents are necessary.

Non-selective NSAIDs such as aspirin, ibuprofen and diclofenac are commonly used for the treatment of mild to moderate acute and inflammatory pain. They act both centrally and peripherally (during inflammation), by inhibiting COX metabolism of arachidonic acid to pro-inflammatory and pro-nociceptive prostaglandins (see review (Rao and Knaus, 2008)). Two isoforms of the COX enzyme have been identified namely COX1 (Vane, 1971, 1976) and COX2 (Masferrer et al., 1990, Xie et al., 1991). The COX-1 isoform is constitutively expressed in high levels in cells and tissues such as endothelium, monocytes, and platelets (Smith and Dewitt, 1996), and is thought to be responsible for unwanted effects of NSAIDs on the gastrointestinal tract (Chan et al., 1995). The COX-2 enzyme is induced by mediators of inflammation such as, IL-1, and TNF- α in a wide variety of cells and tissues such as vascular endothelium, and macrophages, hence play a prominent role in inflammation. Therefore it was thought that targeting the COX-2 isoform would improve current anti-inflammatory and analgesic agents, with reduced adverse side effects compared to current NSAIDs. In

1999, Pfizer launched the first selective COX-2 inhibitor celecoxib, which was followed by the launch of Merck's selective COX-2 inhibitor rofecoxib prescribed for long term pain relief with reduced side effects associated with NSAIDs. However both drugs were removed from the markets due to adverse cardiovascular effects (Melnikova, 2005, Sanghi et al., 2006). Thus inhibition of COX2 may not be an ideal target for the development of analgesic medicines. There is still a lack of effective treatments for chronic inflammatory conditions such as rheumatoid arthritis (RA), without adverse effects. Furthermore, some conditions require specific treatment targeting key inflammatory mediators specific to the condition. TNF α levels are increased in the synovial fluid of patients suffering from RA (McNearney et al., 2004), hence TNF α antagonists are used to treat RA patients unresponsive to NSAIDs (Rankin et al., 1995, Maini et al., 1999a, Maini et al., 1999b, Curtis et al., 2007, Wendling et al., 2008, Li et al., 2009).

1.9 Cannabinoids

Cannabinoid drugs have emerged as novel analgesics for the treatment of pain. The evidence for this is based on both clinical and preclinical research many individuals self-medicate with cannabis to relieve a range of conditions including MS and depression (Consroe et al., 1997, Goodin, 2004, Prentiss et al., 2004, Bottorff et al., 2009). Additionally cannabis relieved chronic neuropathic pain from HIV-associated peripheral neuropathy (Abrams et al., 2007), while MS patients self-medicate with cannabis to relieve spasticity and chronic pain associated

with the disease (Consroe et al., 1997, Goodin, 2004). In addition to smoking cannabis, Δ^9 -tetrahydrocannabinol (Δ^9 -THC) was found to alleviate chronic pain condition (Naef et al., 2003, Svendsen et al., 2004, Nurmikko et al., 2007, Narang et al., 2008) suggesting a clinical potential of cannabis based medicines. This led to the development and licensing of Δ^9 -THC based medicines such as Marinol (dronabinol) Sativex. Marinol is a pure synthetic version of Δ^9 -THC and is used to treat loss of appetite in people with AIDS, and to treat severe nausea and vomiting associated with cancer chemotherapy (Seamon, 2006). Sativex is a whole plant extract containing Δ^9 -THC and cannabidiol (CBD) (another active constituent of cannabis) in a known quantity/ratio of each compound and is used for the treatment of chronic pain, such as neuropathic pain in patients with MS and cancer-related pain (Nurmikko et al., 2007, Rog et al., 2007). It has also been reported that Sativex produces a significant analgesic effect and suppresses disease activity in patients with RA (Blake et al., 2006). Collectively, these applications suggest a clinical potential of cannabis-based medicines.

1.10 Cannabinoid Receptors

The analgesic properties of the *cannabis sativa* plant have been known for thousands of years. Cannabis contains 60 or more bioactive phytocannabinoid compounds including Δ^9 -THC which is the major psychoactive component (Mechoulam and Gaoni, 1967). These compounds interact with cannabinoid receptors, two of which (CB₁ and CB₂) have been cloned.

The CB₁ receptor is expressed in neuronal tissue, both centrally and peripherally, as well as in other peripheral organs. CB₁ receptors are also present at lower densities in the heart, lung, testis, ovary, bone marrow, thymus, uterus and immune cells (Galiegue *et al.*, 1995). The CB₁ receptor is the most abundant G protein-coupled receptor in the brain (Herkenham *et al.*, 1990), with particularly high levels of expression in the striatum, cerebellum, basal ganglia, cerebral cortex and hippocampus (Herkenham *et al.*, 1990, Herkenham *et al.*, 1991). The widespread distribution of the CB₁ receptor is consistent with the range of effects of cannabinoid agonists, including hypomotility, increased food intake, disruption of short term memory, antinociception, and anxiolysis effects. The distribution of CB₁ receptors in the PNS and CNS corresponds with several major sites involved pain transmission and modulation, such as dorsal root ganglion (DRG), spinal cord, thalamus, periaqueductal grey (PAG), amygdala and rostroventromedial medulla (Tsou *et al.*, 1998, Hohmann and Herkenham, 1999, Ahluwalia *et al.*, 2000).

CB₂ receptors are mainly expressed, at high densities, in immune tissues, including macrophages, mast cells, and the spleen. However, recent work has reported the presence of CB₂ mRNA in the spinal cord of control rats (Beltramo *et al.*, 2006) and CB₂ receptor protein in brain tissue (Van Sickle *et al.*, 2005, Gong *et al.*, 2006). However a functional imaging study demonstrated that CB₂ receptor antagonism did not alter brain activation evoked by systemic administration of a non-selective cannabinoid agonist, whereas CB₁ receptor antagonism

did (Chin *et al.*, 2008), suggesting that there is little CB₂-mediated cannabinoid-induced changes in brain activity under control conditions.

Both CB₁ and CB₂ receptors are inhibitory G_i protein-coupled receptors reducing the formation of the key second messenger, cyclic AMP (Matsuda *et al.*, 1990). CB₁ receptor activation also inhibits N-, L-, and P/Q-type Ca²⁺ channels and activates K⁺ channels and MAP kinases (for review see Howlett *et al.*, 2002). Thus, CB₁ activation inhibits neurotransmitter release and neuronal excitability. CB₁ receptors are present pre-synaptically on axons and terminals of neurones (Egertova and Elphick, 2000) and are ideally located for the modulation of synaptic activity.

CB₂ receptors are also coupled to similar signal transduction mechanism to CB₁ in terms of their actions on adenylyl cyclase and MAP kinases, but do not share the same interactions with ion channels as CB₁ receptors (for review see Howlett *et al.*, 2002).

A third G protein-coupled receptor, GPR55, binds a number of cannabinoid ligands and, therefore, has been proposed to be a member of the cannabinoid receptor family (Brown, 2007, Johns *et al.*, 2007, Ryberg *et al.*, 2007, Lauckner *et al.*, 2008, for review see Ross, 2009).

There is increasing evidence for cannabinoid receptor-independent effects of cannabinoids, some of which are mediated through the peroxisome proliferator activator receptor (PPAR) family of nuclear receptors (Rockwell *et al.*, 2006, O'Sullivan, 2007, Russo *et al.*, 2007b, Sun *et al.*, 2007, Costa *et al.*, 2008). Three major isoforms (α , β and γ -)

of this ligand-dependent transcription factor have been identified, with their roles in the regulation of lipid metabolism are well characterised and studied. Recent studies have demonstrated the involvement of PPAR- α and γ in pain and inflammation (Genovese et al., 2005, Cuzzocrea et al., 2006, Sun et al., 2007, Costa et al., 2008, Jhaveri et al., 2008b, Sagar et al., 2008a, Staumont-Salle et al., 2008).

1.10.1 Cannabinoid receptor-mediated analgesia

The analgesic effects produced by activation of CB₁ receptors are well described and extensively reviewed (for reviews see Pertwee, 2001, Iversen and Chapman, 2002, Walker and Huang, 2002a). Activation of CB₁ receptors in the spinal cord (Hohmann et al., 1998, Kelly and Chapman, 2001) and in the periphery (Kelly et al., 2003) attenuates nociceptive responses of dorsal horn neurones in naïve rats. Spinal CB₁ receptors contribute to the antinociceptive effects of cannabinoids in models of acute pain (Welch and Stevens, 1992, Lichtman et al., 1996, Welch et al., 1998, Martin et al., 1999). In addition to the analgesic effects seen following systemic and spinal administration of cannabinoids, peripheral mechanisms of cannabinoid analgesia have also been demonstrated. Anti-nociceptive effects of a CB₁ receptor agonist were substantially reduced in mice with CB₁ receptor gene deletion in the peripheral nociceptors (Agarwal et al., 2007) and hindpaw injection of CB₁ receptor agonists produces antinociceptive effects in models of inflammatory and chronic pain (Richardson et al., 1998b, Clayton et al., 2002, Kelly and Chapman,

2002, 2003, Kelly *et al.*, 2003, Scott *et al.*, 2004, Elmes *et al.*, 2005). However, the broad distribution of CB₁ receptors in the brain promotes both therapeutic effects, such as analgesia, as well as their unwanted psychotropic side-effects.

A number of studies have demonstrated analgesic effects of CB₂ receptor agonists in models of acute and chronic pain, and have been reported to be devoid of CNS-mediated side effects (reviewed elsewhere by Jhaveri *et al.*, 2007a, Guindon and Hohmann, 2008). Administration of CB₂ receptor agonists systemically (Malan *et al.*, 2001, Valenzano *et al.*, 2005, Ibrahim *et al.*, 2006) or locally into the hindpaw (Malan *et al.*, 2001, Elmes *et al.*, 2004) attenuates nociceptive responses in naïve rats. Furthermore, there is evidence for a functional role of CB₂ receptors in the spinal cord (Sagar *et al.*, 2005, Romero-Sandoval *et al.*, 2008, Yamamoto *et al.*, 2008) and thalamus (Jhaveri *et al.*, 2008a) of neuropathic rats. CB₂ receptors are functionally up-regulated in the ipsilateral spinal cord (Beltramo *et al.*, 2006) and ipsilateral dorsal horn (Wotherspoon *et al.*, 2005) in neuropathic rats. CB₂ knockout mice exhibit exacerbated neuropathic pain behaviour, thought to be caused by enhanced microglia and astrocyte activation, where CB₂ receptors are highly expressed, and may play important role in regulating neuropathic pain behaviour (Maresz *et al.*, 2005, Racz *et al.*, 2008). Collectively there is broad base of evidence supporting an important role of spinal CB₂ receptors in the modulation of neuropathic pain responses.

1.11 Endocannabinoids

Anandamide (*N*-arachidonyl ethanolamine, AEA) was the first endogenous ligand of the cannabinoid receptor to be isolated and characterised (Devane et al., 1992a). It was identified by screening solvent extracts of porcine brain in a cannabinoid receptor radioligand binding assay, where AEA displaced radiolabelled cannabinoid receptors ligands. Determination of structure was performed using collision-induced dissociation GC-MS and NMR (Devane et al., 1992b). Following advances in sensitivity and specificity of mass spectrometry, further ECs have been identified, namely, 2-arachidonoyl glycerol (2-AG; Mechoulam *et al.*, 1995), noladin ether (Hanus *et al.*, 2001), virodhamine (Porter *et al.*, 2002) and *N*-arachidonoyl dopamine (NADA; Huang *et al.*, 2002). The structurally-related, *N*-acylethanolamines (NAEs) *N*-oleoyl ethanolamine (OEA) and *N*-palmitoyl ethanolamine (PEA) are also widely distributed in the CNS and periphery but are not considered endocannabinoids due to their lack of binding affinity for CB₁ and CB₂ receptors. They are, however, PPAR ligands (Guzman et al., 2004, LoVerme et al., 2006b). AEA, 2-AG, noladin ether, virodhamine and NADA display sub μ M affinity for cannabinoid receptors (Sugiura et al., 1995, Huang et al., 2001, Porter et al., 2002), however 2-AG has been suggested to be the most biologically important EC, as it occurs in greater concentrations in tissues, and shows greater binding efficacy at CB₁ and CB₂ receptors, than AEA (Sugiura et al., 1997, Sugiura et al., 1999, Sugiura et al., 2000).

Endocannabinoids are widely believed to be synthesised on demand (i.e. not stored in any cellular compartment awaiting release) and their actions are rapidly terminated by being taken up into cells where they are subject to enzymatic hydrolysis. The anti-nociceptive effects of exogenously administered endocannabinoids have been well described. AEA has antinociceptive effects in behavioural models of acute and chronic pain (for review see Pertwee, 2001). Similarly, 2-AG reduces pain behaviour in tail-flick (Mechoulam *et al.*, 1995) and formalin tests (Guindon *et al.*, 2007).

1.12 Measurement of Endocannabinoids

Much research has been devoted to studying the formation and deactivation of ECLs in mammalian tissues. These analyses have initially relied on techniques such as thin-layer chromatography (TLC) and gas chromatography–mass spectrometry (GC/MS) (Giuffrida and Piomelli, 1998, Okamoto *et al.*, 2005). However, these techniques often require multiple analytical steps which are very time-consuming. Recent progress in liquid chromatography/mass spectrometry (LC/MS) has greatly facilitated these efforts, making it possible for the simultaneous measurements of varying components of the endocannabinoid system (precursors and metabolites), rather than its individual components, invaluable to the elucidation of the physiopathological roles of this signalling system. LC/MS allows the identification and quantification of individual endocannabinoid molecules in a single step. Furthermore, tandem mass spectrometry (MS/MS) provides detailed structural information necessary for the characterization of lipids in complex

biological matrices (Hansen *et al.*, 1999). Ionization techniques such as electrospray ionization (ESI) and atmospheric pressure chemical ionization (APCI), which permit the direct coupling of LC to MS, has allowed researchers to identify and quantify the endocannabinoids with greater sensitivity than was possible with other techniques (Weber *et al.*, 2004, Richardson *et al.*, 2007, Schreiber *et al.*, 2007, Williams *et al.*, 2007). Thus LC/MS is the ideal method for endocannabinoid analyses. These techniques have primarily used solvent based extractions methods to extract ECLs from biological matrix (Schmid *et al.*, 1995, Giuffrida *et al.*, 2000a, Di Marzo *et al.*, 2000 (a), Richardson *et al.*, 2007). Levels of ECLs, particularly 2-AG are rapidly increased post-mortem (Sugiura *et al.*, 2001), hence tissue must be snap-frozen to prevent artificial changes that may occur and interfere with the analysis.

1.12.1 Endocannabinoid synthesis

Several different pathways are suggested to contribute to the synthesis of the ECLs (Figure 1.4). NAEs (AEA, OEA and PEA) are synthesised via their corresponding *N*-acylphosphatidyl ethanolamine (NAPE) precursor and are synthesized through the action of acyltransferase, which hydrolyses fatty acids from *sn*-1 position of phosphatidylcholine, and transfers it to the amine of phosphatidylethanolamine (PE). This was initially identified as a calcium dependant pathway (Hansen *et al.*, 1995, Cadas *et al.*, 1996), however a calcium-independent PE *N*-acyltransferase has recently been described (Jin *et al.*, 2007). The

NAPE-phospholipase D (PLD) pathway of NAE synthesis has been most widely studied (for review see Ahn *et al.*, 2009), producing NAEs and phosphatidic acid (Schmid *et al.*, 1983). The regional expression of NAPE-PLD in the mouse brain has been reported (Egertova *et al.*, 2008). Disruption of NAPE-PLD gene in mice increased levels of the precursor NAPE, and decreased brain levels of saturated *N*-acyl chains (OEA and PEA) (Leung *et al.*, 2006). By contrast, levels of longer chain polyunsaturated NAEs, including AEA (C20:4) were unaltered in knock-out mice, compared to NAPE-PLD^{+/+} mice (Leung *et al.*, 2006). Furthermore, in HeLa cells over expressing NAPE-PLD, cellular levels of OEA and PEA were increased, while levels of AEA were unaltered (Fu *et al.*, 2008). This suggests that other pathways may contribute to the synthesis of AEA in the brain under control conditions.

Two alternative pathways involving phospholipase-C (PLC)-PTPN22 (Liu *et al.*, 2008) and $\alpha\beta$ hydrolase ($\alpha\beta$ H4)-GDE1 (Simon and Cravatt, 2008) are able to generate NAEs, including AEA (Figure 1.4). The functional relevance of these multiple pathways is yet to be determined, but they may subserve differential synthesis of NAEs that might be dependent on the tissue in question. Production of NAEs occurs following the PLC hydrolysis of NAPE producing acylethanolamine-O-phosphates, which can be further hydrolysed by phosphatases PTPN22 or SHIP1 (Liu *et al.*, 2008). The role of PTPN22 and SHIP1 in EC synthesis, to date, requires further investigation. *In vitro* studies have suggested cross-talk between the PLC-PTPN22 pathway and the NAPE-PLD pathway (Liu *et al.*, 2008). Lipopolysaccharide (LPS)

treatment of RAW264.7 cells increased levels of AEA despite reducing NAPE-PLD mRNA. siRNA knockdown of NAPE-PLD in RAW264.7 cells did not alter basal levels of AEA, but increased LPS-stimulated AEA generation, compared to mock-transfected cells (Liu *et al.*, 2008), providing further support for cross-talk between these synthetic pathways. These *in vitro* data suggest that when NAPE-PLD generation of AEA is compromised, the PLC-PTPN22 pathway may have a compensatory role in maintaining levels of AEA.

Recent work has shown that biosynthesis of NAEs, such as AEA, occurs via a $\alpha\beta\text{H4}$ -GDE1 pathway in mouse brain and testes (Simon and Cravatt, 2008). $\alpha\beta\text{H4}$ is a lysophospholipase/phospholipase B that hydrolyses NAPEs through removal of both *O*-acyl chains from NAPE to yield glycerophosphoNAE (GpNAE) (Simon and Cravatt, 2006). $\alpha\beta\text{H4}$ shows little selectivity between acyl groups, generating PEA at an equal rate to AEA (Simon and Cravatt, 2006). GDE1, an acyl chain specific phosphodiesterase, then converts GpNAE to NAE (Simon and Cravatt, 2008). Blockade of this phosphodiesterase activity with EDTA increased levels of long chain polyunsaturated GpNAEs (C20:4, GpAEA) as well as shorter chain saturated and monounsaturated GpNAEs, (C16:0, GpPEA; C18:1, GpOEA) with no effects on long chain saturated (C20:0) species detected (Simon and Cravatt, 2008). The identification of these additional synthetic pathways is essential for the further investigation of the relative contribution of these pathways to functional levels of endocannabinoids under control conditions, as well

as under different pathological conditions, such as chronic pain states which are associated with elevated levels of endocannabinoids.

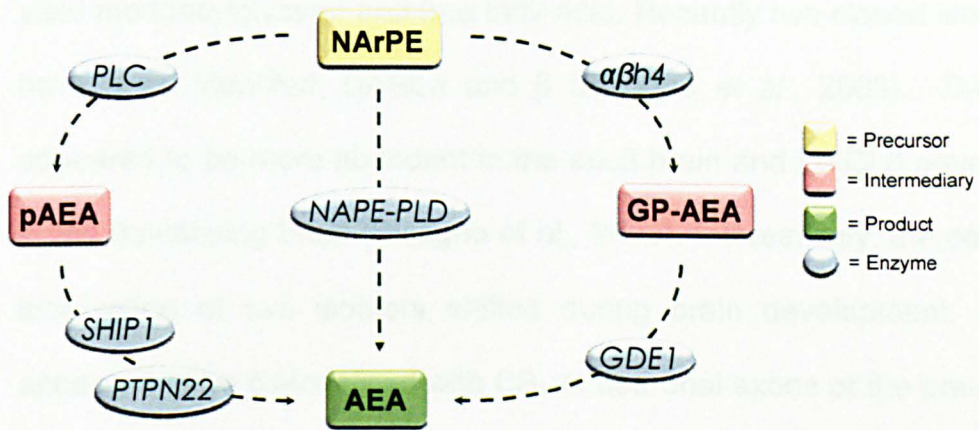


Figure 1.4 Proposed biosynthetic pathways for the generation of AEA from its arachidonoyl containing NAPE (NArPE) precursor. Abrev: PLC, phospholipase c; pAEA, phospho anandamide; SHIP1, SH2-containing inositol phosphatase; PTPN22, Protein tyrosine phosphatase, non-receptor type 22; AEA, anandamide; NArPE, N-arachido- noylphosphatidylethanolamine; NAPE-PLD, N-acyl phosphatidyl ethanolamine; $\alpha\beta h4$ N-acylphosphatidylethanolamine lipase; GP-AEA, glycerophospho anandamide; GDE1, glycerophosphoinositol phosphodiesterase. (Adapted from (Liu et al., 2008, Simon and Cravatt, 2008))

The major pathway for the biosynthesis of 2-AG comprises sequential hydrolysis of arachidonic acid-containing inositol phospholipids by PLC and DAGL. 2-AG, is produced from hydrolysis of arachidonate-containing membrane phosphoinositides (PI) or phosphatidic acid (PA) depending on the cell type (for review see; Bisogno *et al.*, 2005). 2-AG is synthesized in response to many extracellular stimuli, such as, neurotransmitters, antigens, and growth factors (see review (Di Marzo, 2008, Wang and Ueda, 2008)), PLCs catalyze the hydrolysis of phosphatidylinositol-4,5-bisphosphate, thereby generating two second messengers, inositol 1,4,5-trisphosphate and diacylglycerol (Sugiura *et*

al., 1995). DAGL exhibits strong selectivity for diacylglycerols over phospholipids, monoacylglycerols, triacylglycerols and fatty acid amides, and prefers the acyl group at *sn*-1 position to that at *sn*-2, to yield monoacylglycerol and free fatty acid. Recently two cloned isomers have been identified, DAGL α and β (Bisogno *et al.*, 2003). DAGL α appeared to be more abundant in the adult brain and DAGL β abundant in the developing brain (Bisogno *et al.*, 2003). Interestingly, the cellular localization of two isomers shifted during brain development. They appeared to be co-localized with CB $_1$ in neuronal axons of the pre-natal nervous system, while they moved to a location corresponding to CB $_1$, i.e. to post-synaptic neurons, in the adult brain (Bisogno *et al.*, 2003). Recent morphological studies confirmed that DAGL α is localized on postsynaptic sites that face CB $_1$ -expressing terminals in the cerebellum and hippocampus, (Yoshida *et al.*, 2006, Suarez *et al.*, 2008) supporting the role of 2-AG as a retrograde messenger (Hashimoto *et al.*, 2008). Although DAGL has long been identified and well characterised, its role in modulation of nociceptive processing is only just starting to emerge. DAGL α mRNA is present in the superficial dorsal horn neurones of the spinal cord (Nyilas *et al.*, 2009), a region that plays a key role in the receipt and processing of nociceptive inputs.

1.12.2 Endocannabinoid modulation of nociception

It is well established that cannabinoid receptor ligands produce analgesia, however investigating whether endogenously produced

ECLs have anti-nociceptive effects is more complex. Electrical stimulation of the PAG produced anti-nociceptive effects, which was associated with an increase in AEA in microdialysate (Walker *et al.*, 1999a). Levels of endocannabinoids are altered under pathological conditions such as inflammation and neuropathic pain (see review (Jhaveri *et al.*, 2007a)). We have demonstrated a significant reduction in levels of AEA and PEA in the hindpaw of rats with carrageenan-induced hindpaw inflammation (Jhaveri *et al.*, 2008a). Similarly, levels of AEA, 2-AG and PEA were decreased in the hindpaw following intraplantar injection of formalin (Maione *et al.*, 2007). By contrast, Beaulieu *et al.*, reported no significant alteration in levels of AEA, 2-AG and PEA in the hindpaw of formalin-treated rats (Beaulieu *et al.*, 2000b). In addition to altering levels of endocannabinoids at the site of injury, inflammation can cause an increase in levels of ECLs at other sites involved in nociceptive processing. Intraplantar injection of formalin increased levels of AEA in the PAG indicating a role for endocannabinoids in descending control of pain processing (Walker *et al.*, 1999b). Furthermore, levels of ECLs are altered in different pain states, which may reflect altered synthesis or catabolism. Levels of ECLs are increased in the spinal cord (Jhaveri *et al.*, 2006, Petrosino *et al.*, 2007, Jhaveri *et al.*, 2008b) and DRG (Mitrirattanakul *et al.*, 2006) following peripheral nerve injury.

1.12.3 Endocannabinoid metabolism

To date, hydrolase and oxygenase pathways have been shown to be the major pathways responsible for the metabolism of the

endocannabinoids, in particular AEA and 2-AG (Figure 1.5). Hydrolysing enzymes include fatty acid amide hydrolase (FAAH), monoacylglycerol lipase (MAGL) and *N*-acylethanolamine-hydrolysing acid amidase (NAAA). AEA and other NAEs are mainly hydrolysed by FAAH through the hydrolytic cleavage of the amide bond to form arachidonic acid and ethanolamine (Deutsch and Chin, 1993, Cravatt et al., 1996, Vandevorde and Lambert, 2007). FAAH is a membrane bound enzyme found predominately in microsomal and mitochondrial fractions (Schmid et al., 1985, Desarnaud et al., 1995, Hillard et al., 1995, Ueda et al., 1995a). FAAH has an intracellular substrate binding site for fatty acid ethanolamides (Cravatt et al., 1996) and has a high level of expression in rat brain and liver (Desarnaud et al., 1995, Egertova et al., 1998, Watanabe et al., 1998), as well widespread distribution in neuronal cells throughout the CNS (Thomas et al., 1997). The distribution of FAAH is correlated with that of the CB₁ receptor, FAAH enzyme activity is high in the hippocampus, neocortex, cerebellum and olfactory bulb regions of the rat brain, areas which are also enriched with cannabinoid receptors (Herkenham, 1991). FAAH is expressed in neurons that are postsynaptic to CB₁-expressing axons (Egertova et al., 1998). An additional isoform of FAAH, FAAH2, has been identified in humans and other primates, but not in rodents (Wei et al., 2006).

2-AG is mainly metabolised by MAGL to arachidonic acid and glycerol (Dinh et al., 2002, Vandevorde and Lambert, 2007). NAAA is a lysosomal enzyme with optimum activity at an acid pH. It can

metabolise AEA and PEA to their corresponding fatty acids and ethanolamine, but 2-AG is a poor substrate (Tsuboi *et al.*, 2007). It is poorly expressed in the brain and is unlikely to be an important route of endocannabinoid metabolism under normal conditions.

AEA and 2-AG are also substrates for the oxidative enzymes, such as COX-2, lipoxygenase (LOX) and cytochrome p450s (CYP450s) (see review (Kozak and Marnett, 2002). COX, LOX and CYP450 are not specific to endocannabinoid catabolism, however their effects on endocannabinoids is of great interest, due to the potential production of pharmacologically active metabolites.

COX-2 is constitutively expressed in the kidney, spinal cord, hippocampus, cortex and hypothalamus (Vandevorde and Lambert, 2007) and it is up-regulated in pathological states, such as inflammation (Samad *et al.*, 2001). AEA and 2-AG can be converted by COX-2 to prostaglandin-ethanolamides (Prostamides; PG-EA) and prostaglandin glyceryl esters (PG-GE), respectively (Burstein *et al.*, 2000, Kozak *et al.*, 2001a, for reviews see; Kozak and Marnett, 2002), of which seem to be biologically active. The PG-EAs are weakly active at cannabinoid CB₁ and CB₂ receptors and PGF₂ α -EA has weak agonist effects at TRPV1 (Matias *et al.*, 2004, Fowler, 2007). Numerous *in vitro* studies have shown the ability of COX-2 to metabolise ECLs (Kozak *et al.*, 2001a, Kozak *et al.*, 2002a, Kim and Alger, 2004, Ho and Randall, 2007, Rockwell *et al.*, 2008), however, evidence for a physiological role *in vivo* is more elusive. PGD₂-EA and PGE₂-EA are present, following systemic administration of AEA, in mouse lung and kidney, with higher

levels seen in AEA-treated FAAH knockout mice, compared to control mice. PGF₂ α -EA was only detected in the liver, kidney, lung and small intestine of AEA-treated FAAH knockout mice (Weber *et al.*, 2004).

Biological effects of the COX2 metabolite of 2-AG, PG-GEs have been demonstrated in the hippocampus where they modulate GABAergic mediated inhibitory synaptic transmission (Sang *et al.*, 2006) and enhance hippocampal glutamatergic transmission and neurotoxicity (Sang *et al.*, 2007). The potential role of COX2 metabolites of 2-AG in pain processing have not been widely studied. Intraplantar injection of PGE₂-GE produced mechanical analgesia and thermal hyperalgesia, suggesting that pro-nociceptive ligands could be generated by the COX2 metabolism of 2-AG *in vivo* (Hu *et al.*, 2008). They also detected the presence of PGE₂-GE in the naïve and inflamed rat hindpaw, with levels unaltered following inflammation when COX-2 would be upregulated. Levels of PGE₂-GE were below detection limits in the spinal cord and brain in naïve rats and inflamed rats (Hu *et al.*, 2008). Further studies are required to determine whether PG-EA and PG-GE are produced, and involved in nociceptive processing in models of inflammatory or neuropathic pain.

The ECs are also metabolised by lipoxygenases (LOX) and cytochrome p450s (CYP450s). The main isoforms of lipoxygenase that metabolise AEA and 2-AG are 5-LOX, 12-LOX and 15-LOX generating hydroperosyeicosatetraenoic acids (HPETEs) (see review (Kozak and Marnett, 2002). LOX metabolites are also pharmacologically active at CB₁ and CB₂ receptors (Edgemond *et al.*,

1998), TRPV1 receptors (Craib *et al.*, 2001) and PPAR receptors (Kozak *et al.*, 2002b). CYP450 enzymes 2D6, 3A4 and 4F2 produce several metabolites of NAEs including 5,6-epoxyeicosatrienoic acid ethanolamide (5,6-EET-EA), which is more stable than AEA in brain homogenate and is a potent and selective CB₂ agonist *in vitro*. Activated BV-2 microglial cells had an increased capacity to convert AEA to 5,6-EET-EA, which may have relevance to neuropathic pain states. However, the role of CYP450s metabolites such as 5,6-EET-EA in the modulation of central sensitisation in models of chronic pain is unknown, and warrants investigation. A group of CYP450 metabolites of AA were identified in the spleen, kidney and brain and were termed 2-epoxyeicosatrienoyl-glycerols (2-EGs). Some of these products, 2-(11,2-epoxyeicosatrienoyl)glycerol (2-11,12-EG) and 2-(14,15-epoxyeicosatrienoyl)glycerol (2-14,15-EG) have high affinity for CB₁ and CB₂ receptors in transfected CHO cells (Chen *et al.*, 2008). 2-EG is present in the brain, however, whether 2-EG produces CB₁ receptor-mediated analgesia remains to be determined. Overall these studies have shown that the metabolism of endocannabinoids via the hydrolase and oxidative pathways has the potential to generate various modulators of physiological / pathophysiological processing.

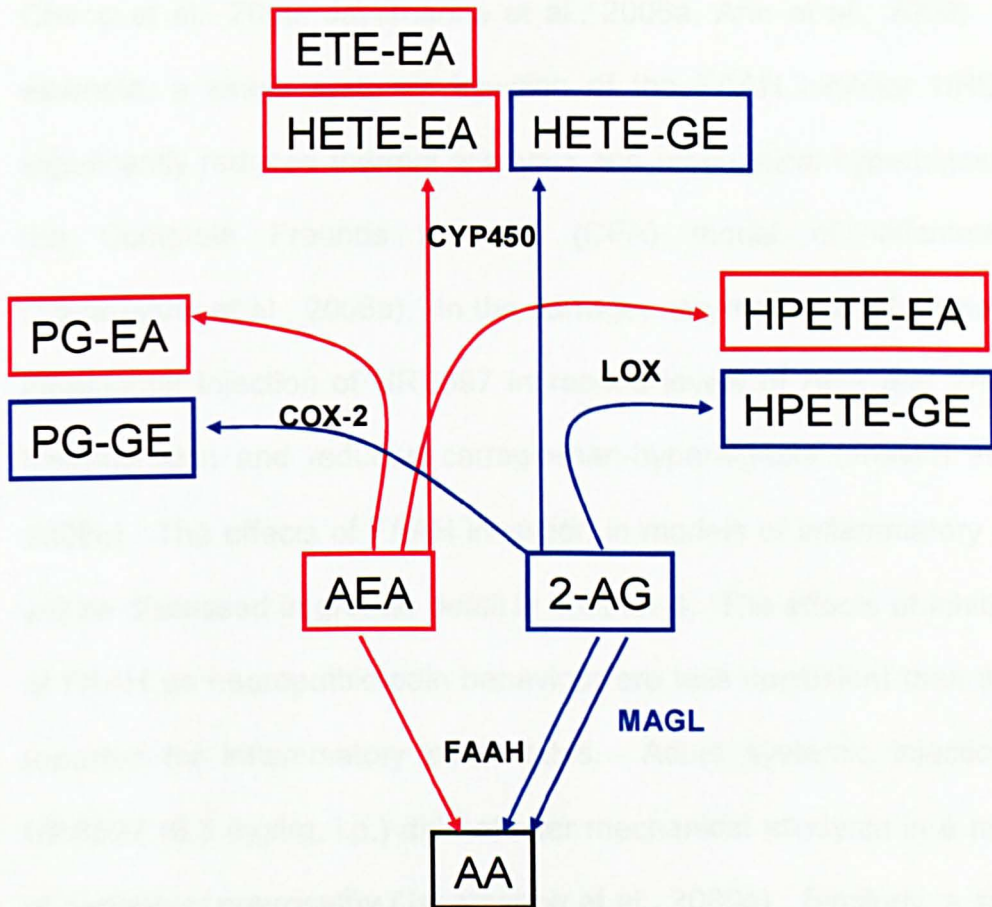


Figure 1.5 Proposed metabolic pathways for the breakdown of AEA (red) and 2-AG (blue) via hydrolase and oxygenase pathways. Red=metabolites of AEA, Blue=metabolites of 2-AG.

1.12.4 Attenuation of endocannabinoid catabolism

The role of FAAH in the metabolism of endocannabinoids has been demonstrated in mice lacking FAAH, which exhibit 15 fold elevated levels of AEA, compared to wild-type mice. FAAH^{-/-} mice display phenotypic hypoalgesia in models of acute and inflammatory pain (Cravatt et al., 2001, Lichtman et al., 2004b), but not neuropathic pain (Lichtman *et al.*, 2004b). Furthermore, pharmacological inhibition of FAAH is antinociceptive in models of acute and inflammatory pain (Kathuria et al., 2003a, Lichtman et al., 2004a, Fegley et al., 2005,

Chang et al., 2006, Jayamanne et al., 2006a, Ahn et al., 2009). For example, a single systemic injection of the FAAH inhibitor URB597 significantly reduced thermal allodynia and mechanical hyperalgesia in the Complete Freund's adjuvant (CFA) model of inflammation (Jayamanne et al., 2006a). In the carrageenan model of inflammation, intraplantar injection of URB597 increased levels of AEA and 2AG in hindpaw skin and reduced carrageenan-hyperalgesia (Jhaveri *et al.*, 2008b). The effects of FAAH inhibition in models of inflammatory pain will be discussed in greater detail in chapter 4. The effects of inhibition of FAAH on neuropathic pain behaviour are less consistent than those reported for inflammatory pain states. Acute systemic injection of URB597 (0.3 mg/kg, i.p.) did not alter mechanical allodynia in a model of peripheral neuropathy (Jayamanne et al., 2006a). Similarly, a single oral dose of URB597 (10 mg/kg, p.o.) had limited effects on mechanical hyperalgesia in the chronic constriction injury (CCI) model of peripheral neuropathy (Russo *et al.*, 2007a). By contrast, repeated administration of URB597 (10 mg/kg, for 4 days p.o.) significantly reduced thermal and mechanical hyperalgesia (Russo *et al.*, 2007a), suggesting that repeated administration of a FAAH inhibitor may produce analgesia, and have more therapeutic relevance.

The focus of research in this area has centred on prevention of AEA catabolism by FAAH, largely due to the lack of selective inhibitors for the major 2-AG catabolic enzyme; MAGL (Comelli et al., 2007, Guindon et al., 2007, Vandevorde et al., 2007). Recently a novel compound, JZL184, which has over 300 fold selectivity for MAGL over FAAH *in*

vitro, significantly increases levels of 2-AG *in vivo* and produces analgesia in mouse models of acute and inflammatory pain has been described (Long *et al.*, 2009).

Indeed, the quantification of ECLs and their metabolites in tissues involved in pain processing is required in order to understand the mechanisms involved, and may lead to a more targeted approach to the development of cannabinoid-based analgesics.

Considerable progress has been made in understanding the physiological and pathological roles of endocannabinoids. Advances liquid chromatography (LC) and mass spectrometry (MS) have aided these developments, and can be combined with genetic and pharmacological studies to address many unexplained questions on the roles and regulation of endocannabinoid signalling

1.13 Aim and objectives:

The aim of this thesis is to develop a sensitive LC-MS/MS method capable of measuring levels of endocannabinoids and COX-2 metabolites of AEA and 2-AG, in one analytical step, and determine their role in nociceptive processing in acute and chronic models of inflammation.

Objectives

1. The development of sensitive LC-MS/MS method capable of measuring levels of ECLs and COX-2 metabolites of AEA and 2-AG in biological tissue.
2. To determine the role of FAAH and other catabolic pathways in the regulation of ECs in models of inflammatory pain.
3. To investigate the contribution of peripheral versus spinal sites of action of elevated ECLs in mediating the analgesic effects of FAAH inhibition.

Chapter 2.

Development and validation of a quantitative analytical method to measure levels of endocannabinoids and COX-2 metabolites in rat tissue

2 Development and validation of a quantitative analytical method to measure levels of endocannabinoids and COX-2 metabolites in rat tissue

2.1 Introduction

Measurement of levels of ECLs and related compounds in biological tissue can provide vital information regarding the role of the EC system in various disease states, and the therapeutic relevance of the ECL system.

Quantification of ECLs by LC/MS has been carried out in a wide variety of biological matrices, including brain (Gonzalez et al., 2002, Valenti et al., 2004, Richardson et al., 2007), cell (Ahluwalia et al., 2003a, van der Stelt et al., 2005, Vellani et al., 2008), and blood plasma (Giuffrida et al., 2000a, Balvers et al., 2009, Di Marzo et al., 2009, Koppel et al., 2009), but current methods do not allow for the simultaneous profiling of ECLs and related compounds, such as COX-2 metabolites, now known to be potentially involved in physiological and pathophysiological conditions. For example, bimatoprost a structural analogue of prostaglandin-F₂ α ethanolamide (PGF₂ α -EA), has therapeutic potential as an anti-glaucoma agent due to its effects on ocular hypotension (Woodward et al., 2004), and prostaglandin-E₂ glycerol ester (PGE₂-GE) has been shown to modulate inhibitory synaptic transmission in primary

hippocampal neurons (Hu et al., 2008). Thus, the development of new analytical methodology would help to gain an insight into ECL regulation, such as monitoring their synthesis and metabolism, thus providing a better insight into the role of the ECL system in many disease states.

2.1.1 Endocannabinoid metabolism

Although many aspects of endocannabinoid metabolism are under investigation (see reviews (Di Marzo, 1999, Alexander and Kendall, 2007, Basavarajappa, 2007, Jhaveri et al., 2007a), the specific contributions of each of the biosynthetic and degradative enzymes that have been identified in ECL generation and metabolism are still not fully understood. There is great interest in delineating the detail of ECL metabolic pathways, but progress is difficult with the available analytical methodology. AEA is predominately metabolised by fatty acid amide hydrolase (FAAH), and 2-AG by monoacyl glycerol lipase (MAGL), however, AEA and 2-AG can be also be metabolized, via oxidation, by cyclooxygenase-2 (COX-2), 12- and 15-lipoxygenase (LOX), and cytochrome P450 (CYP450) to generate ethanolamide and glycerol derivatives respectively (see Figure 1.5, chapter 1).

2.1.2 Measured levels of endocannabinoids metabolites using LC-MS/MS

To date, there are limited studies which demonstrate the presence of metabolites of AEA and 2-AG *in vivo*. LC/MS/MS analysis of rat hindpaw detected the ammonium adduct of PGE₂-GE, which was

Development and validation of a quantitative analytical method to measure levels of endocannabinoids and COX-2 metabolites in rat tissue further confirmed using quadrupole time of flight mass spectrometer (Hu et al., 2008). The hindpaw extract was partially purified on solid-phase extraction columns and further purified on a HPLC column prior to structural identification using nano-LC Q-TOF. However, the extraction and LC/MS method was not validated and quantification was via direct injection of standards of only one metabolite of 2-AG (Hu et al., 2008). COX-2 metabolites of AEA were present in mice liver, kidney lung and small intestine following the exogenous administration of AEA in FAAH knock-out mice (Weber et al., 2004). However, they were unable to separate PGD₂-EA and PGE₂-EA, therefore, the concentrations of these two PG-EAs were reported as the sum, PG-E₂-EA and PGD₂-EA. Furthermore, quantification was performed using two sets of MRM transitions: one MRM set involved monitoring parent ions $[M+H]^+$ \rightarrow water loss $[M+H]^+ - H_2O$ daughter ions; and the second set of MRM monitored parent ions $[M+H]^+$ \rightarrow ethanolamide selective m/z 62 daughter ions, where $[M+H]^+$ \rightarrow water loss $[M+H]^+ - H_2O$ was used for the quantification of prostamides, however the MRM ion pair of $[M+H]^+ >$ ion of m/z 62 and retention times, confirmed that these were PG-EAs containing the ethanolamide moiety, and that the peaks quantitated were PG-EAs (Weber et al., 2004). Mouse brain homogenates contain CYP450 metabolites of AEA (5,6-epoxyeicosatrienoic acid ethanolamide (5,6-EET-EA)) which were detected using the less sensitive and specific selected reaction monitoring (SRM) (Snider et al., 2009). Many of the analytical methods used for ECL metabolites lack full validation of the extraction and quantification procedures. The lack

Development and validation of a quantitative analytical method to measure levels of endocannabinoids and COX-2 metabolites in rat tissue

of consistent data on ECL metabolites may be due to the low sensitivity of available methods, or the lack of specific extraction procedures to provide adequate recovery of the less lipophilic ECL metabolites. The extraction solvent usually contains appropriate internal standards, which also act to compensate for analyte loss during sample preparation. Careful consideration of extraction procedures, may extract other relevant lipids, such as the more polar metabolites of AEA and 2-AG, known to be biologically relevant, such as COX-2 metabolites of AEA and 2-AG.

Prior to analysis, ECLs and metabolites must first be efficiently extracted from the biological matrix. The extraction procedures, unless managed carefully can lead to several problems leading to false results such as the rapid biosynthesis or metabolism of ECLs *in vivo*, and variable recovery of the polar/non-polar lipids. Also, levels of ECLs can rapidly increase post mortem (Sugiura et al., 2001), therefore the amount of time between death and tissue collection and snap freezing must be as quick as possible to prevent artificial changes in levels and consistency between tissues for comparison.

Due to the relatively hydrophobic nature of the ECLs, a variety of mixtures of organic solvents have been utilized to extract lipid classes from biological samples, including 1:1 methanol:acetonitrile (Koppel et al., 2009), 9:1 ethyl acetate:hexane (Kingsley and Marnett, 2003, Richardson et al., 2007), 2:1 chloroform/methanol (Di et al., 2005, Williams et al., 2007, Vellani et al., 2008). However, metabolites of

Development and validation of a quantitative analytical method to measure levels of endocannabinoids and COX-2 metabolites in rat tissue

ECLs, such as COX-2 metabolites of AEA and 2-AG, are more polar, thus requiring more polar extraction solvents, such as acetonitrile (Weber et al., 2004), acetonitrile:water (Kozak et al., 2000) and methanol (Hu et al., 2008). The extraction procedure for both class of compounds are not necessarily compatible, thus leading to potential difficulties in their simultaneous quantitative measurement in biological samples.

There is also significant interest in the quantification of ECLs and related compounds in biological matrixes with very low sample weight such as synovial fluid, and microdysate samples. Furthermore, metabolites of ECs are expected to be in low concentration, so also would require a sensitive method for the detection of these compounds. Recently published data has shown the amount of PGE₂-GE in the hindpaw to be in the femtomole range, whereas 2-AG is found in the nanomole range (Hu et al., 2008). Thus, there is the requirement for a more sensitive method capable of measuring ECLs in low weight tissue, as well as their metabolites. This type of sample requires methods to have even more increased sensitivity but with sufficient robustness to allow routine analysis. Use of nanospray ionisation in mass spectrometry has, for example, increased sensitivity but has not proved very useful, with blocked columns, leaks and pressure drops to name but a few problems (for review see(Noga et al., 2007). Thus there is the need for a single analytical method, capable of quantifying ECLs, PG-EA's and PG-GE's, in one analytical step, which could provide important

Development and validation of a quantitative analytical method to measure levels of endocannabinoids and COX-2 metabolites in rat tissue mechanistic detail in models of pain, and perhaps other models involving the EC signalling system.

2.2 Aims and objectives

The main specific objectives are:

1. To optimise LC separation and MS conditions for the simultaneous and high sensitivity analysis of ECLs and their COX-2 metabolites
2. To assess tissue extraction methods to give optimal recovery of ECLs and metabolites.
3. To validate the LC-MS/MS method for application to rat bio fluids and tissue.
4. To evaluate the method and compare with existing methodologies.

Upon successful completion of these aims, the developed method will then be used in subsequent chapters of this thesis, to quantify ECLs and related compounds in spinal cord, paw, and cell samples, as well as other tissue of interest in *in vivo* models of peripheral inflammation and *in vitro* model of sensory sensitisation, to investigate the role of the EC system in nociceptive processing.

2.3 Method

2.3.1 Chemicals

Acetonitrile, anhydrous chloroform, ethanol, toluene, ethyl acetate, hexane, ammonium acetate, triethylamine (TEA), trifluoroacetic acid (TFA) and formic acid were all from Fisher Scientific (Loughborough, UK). AEA, 2-AG, virodhamine, OEA, PEA, PGD2-EA, PGE2-EA, PGF2 α -EA, PGE2-GE, PGF2 α -GE, deuterated anandamide (AEA-d8), deuterated 2-AG (2-AG-d8), and deuterated prostaglandin F2 α ethanolamide (PGF2 α -EA-d4) were from Cayman Chemicals (Cayman Europe, Estonia). HPLC grade water, (Elga Ltd., High Wycombe, UK) was used for all experiments. Trichlorotrimethyl silane was from Sigma-Aldrich (Steinheim, Germany). All solvents and chemicals were of HPLC grade or higher.

Mobile phases were filtered using 0.47 μ m nylon filters before use (Whatman, Maidstone, UK). 100 mg silica, solid phase extraction cartridges were used (Phenomenex, Macclesfield, UK).

AEA, AEA-d8, virodhamine, OEA, PEA, PGD2-EA, PGE2-EA, PGF2 α -EA, and PGF2 α -EA-d4 stock solutions were prepared in ethanol. 2-AG is known to be more stable in acetonitrile and, therefore, this solvent was used in all dilutions of 2-AG and the structurally related glycerol compounds such as 2-AG-d8, PGE2-GE, and PG F2 α -GE. All stock solutions were stored at -80°C. Further dilutions were carried out as

Development and validation of a quantitative analytical method to measure levels of endocannabinoids and COX-2 metabolites in rat tissue appropriate in LC mobile phase, acetonitrile or ethanol, and were used within two weeks, following storage at -80°C. There was no evidence of degradation of the standards under these conditions of storage.

2.3.2 LC-MS/MS conditions

A triple quadrupole Quattro Ultima mass spectrometer (Waters Micromass, Manchester, UK) was used in conjunction with an Agilent 1100 LC system (Agilent Technologies, Waldbron, Germany), with cooled 4°C autosampler. The final optimised method LC column was a Waters Symmetry C18 column (100 x 2.1 mm id, 3.5µm particle size, Hertfordshire, UK), maintained at 40°C with a mobile phase flow rate of 0.3 ml/min. When more sensitivity was required, a triple quadrupole/linear ion trap (4000QTRAP) mass spectrometer (AB Sciex Instruments, UK) was used in conjunction with Shimadzu LC system (Shimadzu, Milton Keynes, UK) using a Thermo Hypersil-Keystone BDS C18 (150 x 1mm i.d 5µm particle size, Thermo Fisher Scientific, Runcorn, UK). Gradient elution mobile phases consisted of A (water, 1g/L ammonium acetate, 0.1% formic acid at pH 3.6) and B (acetonitrile, 1g/L ammonium acetate, 0.1% formic acid). The gradient and flow rates for both LC/MS systems were slightly different and are summarised in table 2.1.

Sample temperature was maintained at 4°C in the auto sampler prior to analysis. During method development stages other LC columns and

Development and validation of a quantitative analytical method to measure levels of endocannabinoids and COX-2 metabolites in rat tissue conditions were tested and used to optimise results, and are discussed later in the chapter.

Quattro				Qtrap			
Time	%A	%B	Flow(ml/min)	Time	%A	%B	Flow(ml/min)
0	15	85	0.3	0	15	85	0.15
2	25	75	0.3	2	25	75	0.15
6	25	75	0.3	4	25	75	0.15
8	35	65	0.3	10	45	55	0.15
9	0	100	0.3	12	100	0	0.15
15	0	100	0.3	14	100	0	0.15
16	85	15	0.3	14.2	15	85	0.15
20	85	15	0.3	20	15	85	0.15

Table 2.1 HPLC conditions

Quantification of analytes was undertaken using tandem electrospray mass spectrometry, in positive ion mode (ES⁺). MS parameters, such as cone voltage and positioning (for Quattro MS), and declustering potential (for QTRAP MS) were optimised to maximise production of the precursor ion by direct infusion of the standard into the MS, using single MS monitoring. Cone and desolvation gas flows of 174 and 844 L/hr with source and desolvation temperatures of 125°C and 350°C respectively were used. Subsequently, MS-MS product ion spectra were acquired, monitoring for each precursor [M+H]⁺ ion with varying entry, collision and exit energies. The dominant product ion for each compound was selected for monitoring in MRM mode, with optimisation of collision energy (argon gas induced dissociation). Identification of

Development and validation of a quantitative analytical method to measure levels of endocannabinoids and COX-2 metabolites in rat tissue compounds in biological tissue was confirmed by comparison of precursor and product ion m/z values and LC retention times, with standards. Peaks were then integrated and the software package MassLynx version 4 (Waters, Micromass, Manchester, UK) for Quattro, or using Analyst (for QTRAP) used to quantify levels of the ECLs. Optimised m/z values for Quattro MS showing the chosen precursor and product ions, cone voltages and retention times for each compound are shown in Table 2.2, whereas table 2.3 shows the optimised m/z values for QTRAP MS, including precursor and product ions, declustering potential, retention times, and entrance and exit energies.

2.3.3 Sample extraction

The extraction solvents acetonitrile, methanol, hexane and ethyl acetate/hexane were investigated in various combinations, to determine optimal conditions for maximum recovery of analytes from rat brain tissue (male Sprague-Dawley rats, Charles River UK).

Because some of the analytes are endogenously produced in brain tissue there is a lack of an appropriate 'blank' matrix. Analytes were, therefore, spiked into rat brain tissue to determine accuracy, precision and recovery of method, correcting for the presence of endogenous analytes. To ensure homogeneity, brain tissue was placed into liquid nitrogen, and ground in a porcelain pestle and mortar, before being split into approximately equal 100 mg aliquots for recovery and validation experiments. This ensured that there were constant and equivalent

background concentrations of all the endogenous cannabinoids in the samples used for recovery and validation.

Recoveries were calculated by spiking 20 μ l of 1 nM, 10 nM and 100 nM of AEA, OEA, PEA and virodhamine, 10 nM, 100 nM and 1 μ M of 2-AG, PGD₂-EA, PGE₂-EA, PGF₂ α -EA, PGE₂-GE, and PG F₂ α -GE into 100mg rat brain tissue. The peak area obtained was then subtracted from background concentrations and expressed as a percentage of non-extracted standards at the same concentration. Recovery experiments were replicated a minimum of 3 times. Homogenisations were carried out on ice to prevent any degradation of analytes or internal standards. Adaptations of the extraction procedure were also investigated in order to allow extraction from other types of biological tissue including rat paw, rat spinal cord tissue, and cell tissue. ECLs were extracted from rat brain tissue in the final method using an acetonitrile extraction, adapted from a previously published method (Weber et al., 2004). Tissue was minced using scalpel blades, and transferred into a glass tube with acetonitrile and internal standards. This mixture was then briefly homogenised to break up the tissue and shaken at 4°C for 60 min. Samples were centrifuged (7,000xg, 5 min, 4°C) and the supernatants transferred to clean glass tubes. The homogenisation, mixing and centrifugation steps were repeated twice, with the supernatants pooled, to optimise recovery. The pooled supernatants were then evaporated to dryness under vacuum and stored at -80 °C until analysis.

2.3.4 Validation

For each of the analytes of interest triplicate six-point calibration curves were prepared at concentrations of 0.001 nmol/g, 0.01 nmol/g, 0.1 nmol/g, 0.5 nmol/g, 2.5 nmol/g, and 10 nmol/g using rat brain tissue. The peak area of each analyte, expressed as a ratio to internal standard peak area was then calculated and used to ensure linearity of the method. The appropriate internal standard for each analyte was selected based on structural similarities, as shown in Figure 2.1. The slope, intercept and regression coefficient of each calibration line was determined.

Analyte	Retention time (min)	Precursor ion (<i>m/z</i> value)	Product ion (<i>m/z</i> value)	Cone voltage (eV)	Collision energy (eV)
PEA	14.22	300.30	62.00	35	15
OEA	14.30	326.40	62.00	51	16
AEA	13.42	348.30	62.00	35	12
Virodhamine	12.55	348.30	62.00	35	12
AEA-d8	13.42	356.33	62.00	48	21
PGD2-EA	9.81	378.24	62.00	35	24
PGE2-EA	8.58	378.24	62.00	35	24
PGF2 α -EA	8.24	380.50	62.00	35	37
PGF2 α -d4-EA	8.17	384.5	62.00	35	37
2-AG	13.78	379.20	287.50	55	15
2-AG-d8	13.78	387.35	96.17	43	34
PGE2-GE	11.31	409.20	91.30	43	70
PGF2 α -GE	10.31	411.20	91.30	43	70

Table 2.2

Selected precursor and product *m/z* values with appropriate retention times, cone and collision voltages used to identify and quantify analytes, using MRM mode on the Quattro tandem-mass spectrometry machine.

Analyte	Retention Time	Q1 Mass (amu)	Q3 Mass (amu)	Declustering Potential	Entrance Potential	Collision Energy	Exit Potential
AEA	15.6	348.5	62.2	51	10	41	15
PEA	15.47	300.5	62.2	50	10	35	15
OEA	15.53	326.4	62.2	70	5	35	5
2-AG	15.35	379.2	287.02	60	10	17	15
AEA-d8	15.14	356.5	63.2	50	10	41	15
2-AG-d8	15.32	387.2	96	60	10	80	15
PGD2-EA	9.56	378.5	62.2	80	10	36	10
PGE2-EA	9.10	378.4	62.2	80	10	38	10
PGF2 α -EA	9.10	380.4	62.2	65	10	40	10
PGE2-GE	10.51	409.3	91.3	80	10	75	15
PGF2 α -GE	10.40	411.3	91.3	80	10	90	15
PGF2 α -EA-d4	9.10	384.3	62	70	10	35	15

Table 2.3 Selected precursor and product m/z values with appropriate retention times, cone and collision voltages used to identify and quantify analytes, using MRM mode on the QTRAP4000 mass spectrometry machine.

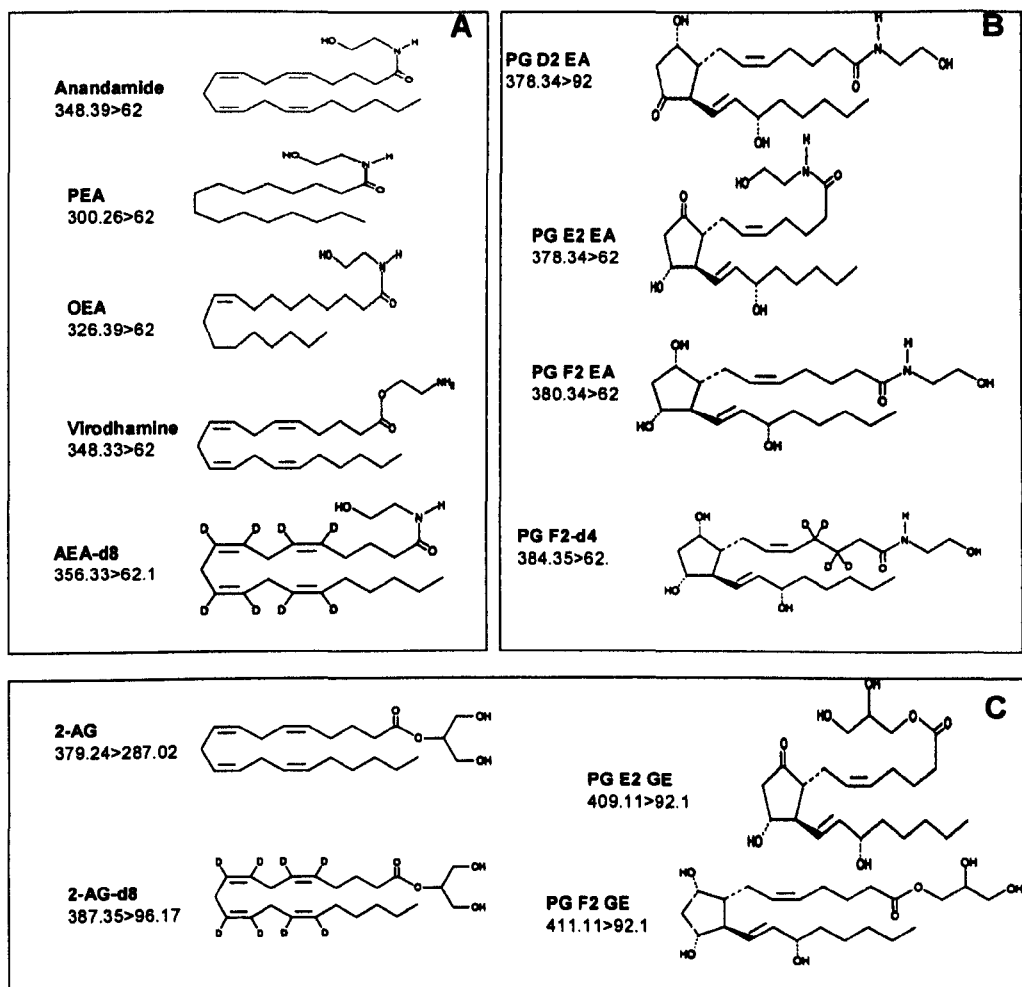


Figure 2.1 Chemical structures of the endocannabinoids and related compounds, (A) - shows AEA and structurally related compounds using AEA-d₈ as an internal standard; (B) shows prostamides using prostaglandin ethanolamide as an internal standard (C) - shows 2-AG and structurally related compounds using 2-AG-d₈ as an internal standard.

To determine intra-day (n=6) and inter-day (n=6 over a period of 5 separate days) precision and accuracy, analyte concentrations of 0.001 nmol/g, 0.1 nmol/g and 1 nmol/g of AEA, PEA, OEA and virodhamine, 0.1 nmol/g, 1 nmol/g, 10 nmol/g 2-AG, 0.005 nmol/g, 0.1 nmol/g, 1 nmol/g PG-EAs, and 0.5 nmol/g, 2.5 nmol/g, and 10 nmol/g PG-GEs were spiked into rat brain tissue and homogenised with extraction

Development and validation of a quantitative analytical method to measure levels of endocannabinoids and COX-2 metabolites in rat tissue solvent then analysed for all compounds. Due to the reduced MS ionisation efficiency of 2-AG and PG-GEs higher concentrations were used for these analytes. Precision was calculated from the RSD% of the replicates, and accuracy by comparison of measured levels of spiked analytes with expected concentrations (RSD%). A RSD% of 20% was considered acceptable for accuracy and precision at the lower limit of quantitation (LLOQ). The limit of detection (LOD) of each compound was defined as the concentration at which a signal to noise ratio of greater than 3:1 was achieved following direct analysis from a stock solution. Recovery was calculated by comparison of the integrated area under the curve for each of the eight analytes at the low, medium and high analyte concentrations with 100% standards. To allow accurate calculation of recovery, endogenous levels of ECs and related compounds were determined and corrections made to calculations. The recovery of all three internal standards (AEA-d8, 2-AG-d8 and PGF2 α -EA-d4) was also determined, but as they are not present in biological tissue, without any correction for endogenous concentration.

Validation procedures were based on the recommendation of Bioanalytical method validation published by the US Food & Drug administration (FDA).

2.3.5 Quantification of endocannabinoids, prostaglandin ethanolamides and prostaglandin glycerol esters

Quantification was accomplished through at least a five point calibration curve. The peak area was expressed as a ratio of the peak area of the

Development and validation of a quantitative analytical method to measure levels of endocannabinoids and COX-2 metabolites in rat tissue corresponding internal standard, based on structure similarity, as shown in figure 2.1. AEA-d8 was used for the quantification of AEA, OEA and PEA, PGF2 α -d4 was used for the quantification of PG-EA's, and 2-AG-d8 was used for 2-AG and PG-GEs as there is no commercially available internal standard for PG-GE. A standard regression curve was plotted to ensure linearity. The slope, intercept, and regression coefficient was calculated, and the slope was used in calculation for amounts of each compound of interest, with correction for dilution and weight. Data are expressed as pmol/g for AEA, PGD2-EA, PGE2-EA, PGF2 α -EA, PGD2-GE, and PG F2 α -GE and nmol/g for OEA, PEA and 2-AG

2.3.6 Direct comparison of two MS systems to ensure consistency in data

To ensure direct comparison of methods used in this research, samples were also ran on a triple quadrupole Quattro Ultima mass spectrometer and compared to the data obtained using a triple quadrupole/linear ion trap (4000QTRAP) mass spectrometer.

Animals were killed by stunning and then decapitation (see chapter 4 for further details). Hindpaw were dissected rapidly on ice and placed immediately onto dry ice. Tissue collection was standardised as far as possible to minimise differences between researchers, and samples were stored immediately at $-80\text{ }^{\circ}\text{C}$ to minimize postmortem increases in ECL levels. Then this tissue was extracted and analysed, as previously described on both systems, to provide a direct quantitative comparison

Development and validation of a quantitative analytical method to measure levels of endocannabinoids and COX-2 metabolites in rat tissue of levels of ECLs and related compounds in rat hindpaw on both instruments. Samples were stored at $-80\text{ }^{\circ}\text{C}$ to prevent degradation of compounds prior to analyses.

2.3.7 Data Analysis

Comparison of concentrations of ECs between treatment groups was carried out using Mann-Whitney non-parametric test, as these data were shown not to be normally distributed. Significance level was set at the $P < 0.05$. Data are expressed as mean \pm SEM.

2.4 Results and Discussion

2.4.1 Analytical Development

2.4.1.1 MS parameters

The LC-MS/MS method was optimised from Richardson et al., (2007) to allow for the quantification of COX-2 metabolites of AEA and 2-AG.

The strong ethanolamine fragment (m/z 62) was selected as the product ion for ethanolamine containing ECs (AEA, OEA, PEA), PGD₂-EA, PGE₂-EA and PGF₂ α -EA which are consistent with other work done in both our group (Richardson et al., 2007) and others (Weber et al., 2004, Yang et al., 2005), respectively. PGD₂-EA and PGE₂-EA had identical fragmentation patterns, with both compounds having identical precursors at m/z 378 and product ion at m/z 62, but were distinguishable by a difference in chromatographic retention time. The parent ions of PGD₂-EA, PGE₂-EA and PGF₂ α -EA (m/z 395.5 and 397.5 respectively) were not detected due to in source fragmentation; hence 378 and 380 (loss of water) was used as the precursor for these compounds. AEA and virodhamine also have identical precursors and product ions, having $[M+H]^+$ at m/z 348 \rightarrow 62, however they have a different LC retention time. The precursor/product ion values for PGF₂ α -EA were selected at m/z 380, which corresponds to the parent compound, with a loss of water, and the ethanolamine product ion at m/z 62. It was also noticed that the MS responses of 2-AG, COX-2 metabolites of 2-AG, and other glycerol-containing compounds had reduced MS responses compared to other compounds. This is due to

Development and validation of a quantitative analytical method to measure levels of endocannabinoids and COX-2 metabolites in rat tissue

reduced ion field from these compounds when using ESI method of fragmentation. The glycerol containing compounds did not produce such an obvious product ion, although continuing with previous studies m/z 92 was selected which corresponded to the loss of glycerol fragment (Bradshaw et al., 2006, Richardson et al., 2007, Hu et al., 2008). It was also noticed in the product ion spectra of compounds such as AEA, 2-AG, PG-EA, and PG-GE, the MS spectra looked more noisy, this was due to an increase in product ions that were spaced at approximately 14amu and 18 amu intervals, which may represent the systematic loss of methyl groups from the alkyl chain, and the loss of water from the prostaglandin-containing compounds (Figure 2.2).

2.4.2 HPLC Development

The main requirements of the HPLC method development were to

- 1) Provide optimised retention/separation of ECLs and the various metabolites.
- 2) Separate PGE₂-EA and PGD₂-EA, as well as between AEA and virodhamine as they share the same molecular weight and give identical fragmentation patterns by ES⁺ MS (m/z values of precursor and product ions on MS).

Development and validation of a quantitative analytical method to measure levels of endocannabinoids and COX-2 metabolites in rat tissue

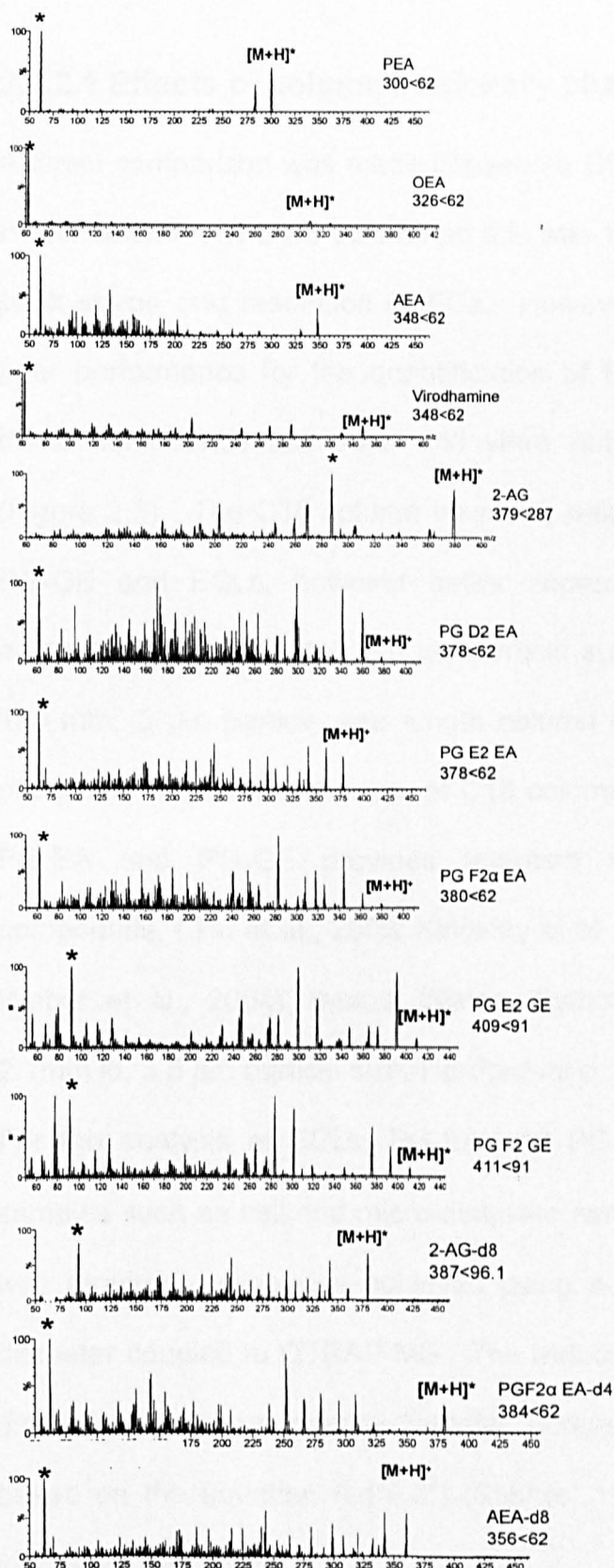


Figure 2.2 Product ion mass spectrums for each of the EC and PG-EA and PG-GE compounds, with the chosen precursor ion indicated with $[M+H]^+$ and product ion indicated by *. The common product fragment of all ethanolamide-containing compounds (m/z of 62) represents the ethanolamide portion of the compound.

2.4.2.1 Effects of column stationary phase on separation

A direct comparison was made between a C8 and C18 reversed phase HPLC column. The C8 column as this was found to give good analyte peak shape and resolution of ECs. However the C8 column gave a poor performance for the quantification of PG-EA and PG-GE, since these compounds are polar and were not retained on the column (Figure 2.3). The C18 column however, retained both the PG-EA and PG-GE and ECLs, however better separation and resolution was achieved with a 100 mm, 3.5 μm particle size column, compared to a 150 mm, 5 μm particle size length column (Figure 2.3). It has been previously shown that the use of C18 columns for the quantification of PG-EA and PG-GE provides retention and resolution of these compounds, (Hu et al., 2008; Kingsley et al., 2005; Kozak et al., 2002; Weber et al., 2004), thus a Waters Symmetry C18 column (100 x 2.1mm id, 3.5 μm particle size, Hertfordshire, UK) was used.

For the analysis of ECLs, PG-EA and PG-GE in low weight tissue samples such as cell and micro-dialysate samples maximum sensitivity was required, which was achieved using a C18 micro column, 1mm diameter coupled to QTRAP MS. The reduction from a 2.1mm internal diameter to a 1 mm internal diameter increases the sensitivity 5 times, based on the equation $(i.d^2/i.d^2)$ (Steiner, 1991), thus $(2.1^2/1^2)=4.41x$ increase in sensitivity.

2.4.2.2 Effects of mobile phase composition on separation

Mobile phase composition was varied to determine the optimum separation composition and condition. This was based on the previous analytical method used within our group (Richardson et al., 2007) and on currently used analytical methods for the measurement of COX-2 metabolites (Kozak et al., 2002a, Weber et al., 2004, Kingsley et al., 2005). This included varying the amount of acetonitrile as the organic component, varying the acid and buffer concentrations and trying isocratic and gradient based methods. It was also noted that for PGF2 α -EA, a peak was detected in biological tissue at approximately 15 min, however due to the retention time of the synthetic standard being approximately 8 min; this was deemed to be an unknown compound and not PGF2 α -EA (Figure 2.5). Obtaining the correct organic starting composition proved vital in this method, as this controlled whether separation of PGD2-EA and PGE2-EA was achieved, and it was found that 15% organic achieved this, the final gradient conditions are summarised in table 2.1 There was a subtle effect of mobile phase pH on the retention of analytes, and varying the pH of the mobile phase did not significantly improve separation of PGD2-EA and PGE2-EA, therefore as in previous studies, a pH of 3.6 was used (Richardson et al, 2007). A typical extracted ion chromatogram of the optimised method is shown in Figure 2.4. Therefore for modified LC method a C18 column, with internal diameter of either 2.1mm or 1 mm was used depending on the tissue, with a starting acetonitrile organic concentration of 15% was used to

successfully retain and separate PGD₂-EA from PGE₂-EA, and AEA from virodhamine. The final method is described in section 2.3.2- 2.3.3.

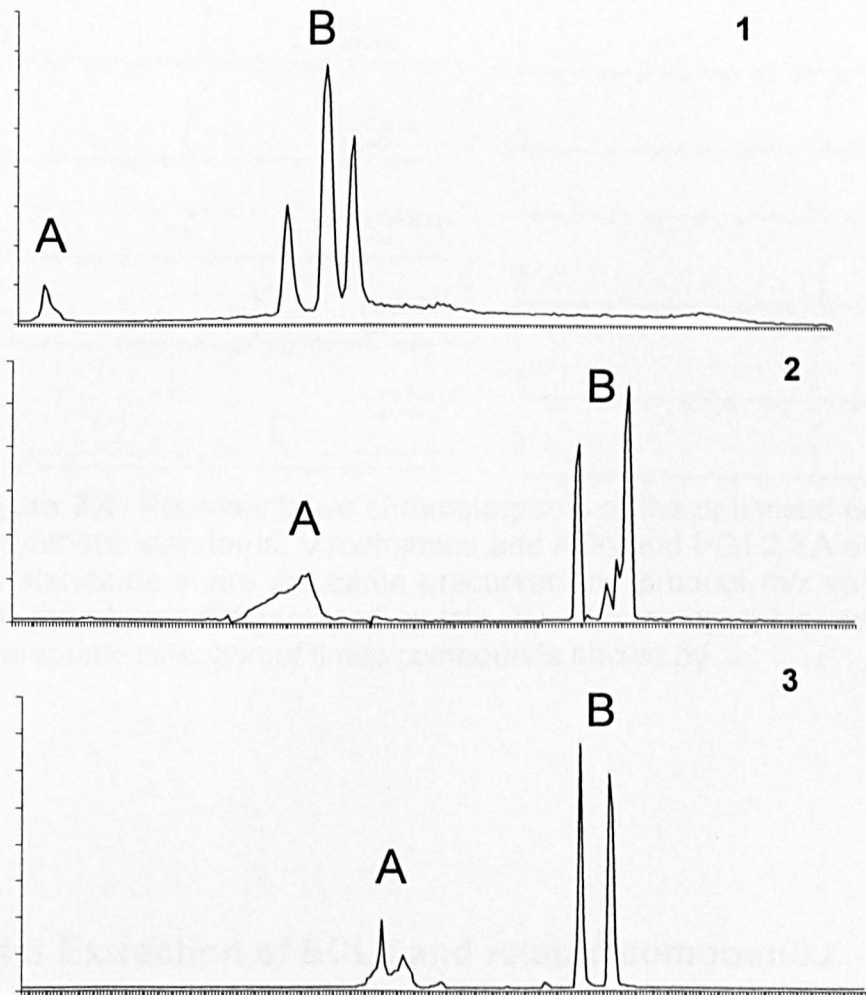


Figure 2.3 Comparison of chromatographic separation of A, PG-EA and PG-GE; B, AEA, OEA, PEA, 2-AG and virodhamine; using 2 different stationary phases, C8 and C18 . **(1)** Initially a Thermo Hypersil-Keystone HyPurity Advance column was used (150 x 2.1mm internal diameter, 5 μ particle size)(Richardson et al., 2007). **(2)** Improvements in PG-EA and PG-GE retention were seen with a Waters Symmetry C18 column, (150 x 3.5mm internal diameter, 5 μ particle size) **(3)** However, the most significant improvement observed was with a shorter Waters Symmetry C18 column (100 x 2.1mm id, 3.5 μ m particle size, Hertfordshire, UK), with further retention of prostamides. Chromatograms were obtained using a Hewlett Packard 1100 LC system.

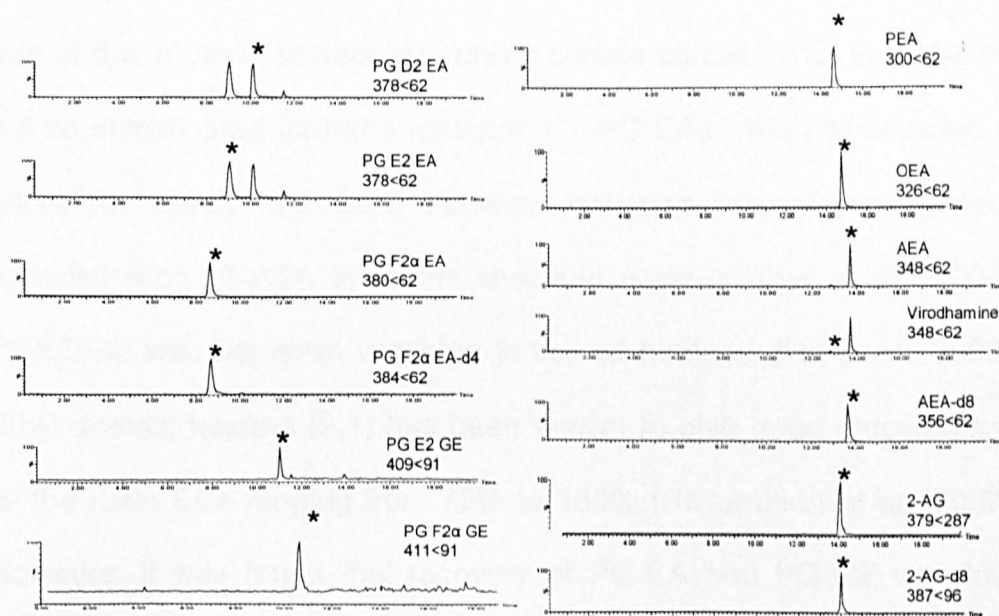


Figure 2.4 Representative chromatograms of the optimised separation of synthetic standards. Virodhamine and AEA and PGE2 EA and PGD2 EA standards share the same precursor and product m/z values, and are therefore, differentiated solely by chromatographic separation. Appropriate retention of times compounds shown by *.

2.4.3 Extraction of ECLs and related compounds

After optimisation of the MS settings and LC separation the next stage was to evaluate a range of extraction solvents to enable the efficient extraction of ECs, PG-EAs and PG-GE from rat brain tissue.

2.4.4 Effect of extraction solvent on recovery

Previous studies have confirmed the presence of ECs in a variety of biological tissues, but there are conflicting reports regarding the presence of PG-EA and PG-GE in naïve animal tissue. The majority of

evidence for the presence of PG-EA and PG-GE is derived from *in vitro* studies (Yu et al., 1997, Kozak et al., 2002a), yet there is evidence for a role of this route of metabolism under certain conditions *in vivo*, (which will be investigated further in chapter 4). PG-EAs were not detected in naïve rat tissue, but were however detected following exogenous administration of AEA in FAAH knockout mice (Weber et al., 2004). PGE2-GE was however, detected in the rat hindpaw (Hu et al., 2008). Ethyl acetate:hexane (9:1) has been shown to give good recoveries of all the main ECs ranging from 78% to 138% (Richardson et al., 2007). However, it was found that recovery of PG-EA and PG-GE was low, ranging from 38% to 57%. Therefore a new extraction solvent was needed. Literature searches have shown that methanol or acetonitrile can be used in the extraction of ECs, PG-EA and PG-GE (Kozak et al., 2000, Kozak et al., 2001a, Weber et al., 2004, Hu et al., 2008). We therefore investigated the extraction of these compounds with various solvents at varying compositions (Table 2.4).

Extraction Solvent	% Recovery						
	AEA	2-AG	PGD2-EA	PGE2-EA	PGF2-EA	PGD2-GE	PGE2-GE
Acetonitrile	91.2±3.5	87.3±8.1	87.1±13.5	92.1±3.4	94.2±13.7	71.6±14.9	76.3±12.2
Methanol	89.1±5.1	74.2±9.1	42.2±16.5	23.7±5.7	43.7±12.5	65.2±15.8	75.3±10.2
50:50	92.3±2.9	71.3±5.8	48.3±11.5	63.1±8.2	72.1±18.4	58.2±11.7	68.9±6.1
Acetonitrile:Methanol							
50:50 Acetonitrile:Ethyl Acetate	89.39±7.2	69.2±6.7	79.2±11.5	92.8±3.5	87.2±13.7	39.7±14.2	47.3±12.0
9:1 Ethyl Acetate	98.8±8.2	85.3±2.4	36.5±19.5	56.2±9.2	42.0±10.2	27.8 ±3.7	38.2±7.2
Hexane							
9:1 Acetonitrile	86.2±9.5	71.2±8.5	59.3±19.4	63.4±14.2	43.8±19.3	49.3±17.4	87.3±7.7
Methanol							
9:1 Ethyl Acetate	91.2±6.3	88.3±7.5	56.2±17.5	78.2±12.3	77.2±13.5	59.1±13.2	68.1±10.3
Acetonitrile							
8:1:1 Ethyl Acetate	83.2±7.2	66.3±8.2	31.2±15.8	21.8±5.2	28.7±9.8	33.4±9.8	42.0±8.4
Acetonitrile:Hexane							
8:1:1Ethyl Acetate	84.2±10.2	68.3±6.1	58.7±16.3	28.7±7.9	18.7±4.2	51.2±11.0	49.2±7.9
Methanol Hexane							

Table 2.4 The recovery of a representative structurally similar compound, AEA for ethanolamine containing EC, 2-AG, for glycerol containing compounds, prostaglandin E2 ethanoloamide and prostaglandin E2 glycerol ester for COX-2 metabolites of AEA and 2-AG respectively. (n=4).

To control for variability in recovery, and to ensure accurate quantification of ECs and related compounds, we used three internal standards (AEA-d8, 2-AG-d8, and PGF2 α EA-d4).

2.4.4.1 Effect of silanisation of glassware

Silanisation of glassware was previously used to improve reproducibility, however further work showed that recovery and reproducibility was not affected by silanisation (Table 2.5). A comprehensive washing schedule was therefore used to prevent contamination. For some low weight sample such as whole cell and cell supernatant, these were extracted in an Eppendorf tube, which did not require silanisation.

Analyte		% recovery	
		Silanised Glassware	Non-silanised Glassware
AEA	0.001	86.8 \pm 3.8	89.0 \pm 4.8
	0.01	85.1 \pm 2.3	93.2 \pm 7.2
	0.5	91.8 \pm 4.7	94.3 \pm 3.1
2-AG	0.001	79.3 \pm 6.3	75.1 \pm 3.6
	0.01	75.3 \pm 2.1	78.7 \pm 5.9
	0.5	81.3 \pm 5.2	85.5 \pm 8.3
PGE2-EA	0.001	91.3 \pm 4.3	89.7 \pm 7.3
	0.01	87.3 \pm 2.3	85.8 \pm 4.5
	0.5	93.6 \pm 7.5	91.2 \pm 5.3

Table 2.5 Recovery of Anandamide, 2-AG and PGE2 ethanolamide from spiked synthetic standards at 0.001, 0.01, and 0.5 μ M into silanised and non-silanised glass ware (n=3).

2.4.4.2 Evaluation of solid phase extraction

The inclusion of solid phase extraction step in previous methods (Schmid et al., 2000, Richardson et al., 2007) was found to increase MS specificity and sensitivity as well as prolonging the HPLC column life. However SPE (based on (Richardson et al., 2007)) for the extraction of PG-EAs and PG-GEs was not viable as very poor recovery was achieved (Table 2.6). Furthermore, SPE is useful when in preventing HPLC overload with large amounts of tissue (>200 mg), however due to the small tissue weight (<70 mg) used in future experiments, it was therefore decided to exclude this step from the extraction procedure.

Analyte	% Recovery	
	SPE	Non-SPE
AEA	87.2±7.3	91.2±9.2
prostaglandin ethanolamide	E2 21.9±10.5	92.2±12.3
prostaglandin glycerol ester	E2 15.2±6.9	86.3±8.2

Table 2.6 Comparison of percentage recovery of AEA, prostaglandin E2 ethanolamide, and prostaglandin E2 glycerol ester, with, or without the use of solid phase extraction for sample preparation.

After extraction, samples were reconstituted in 100%, and a reconstitution volume of 200 µl was used for tissues with high sample weight (>50 mg), whereas 100 µl was used for low sample weight tissue (<50 mg).

2.4.5 Validation

The validation data for the method are shown in Table 2.7. The results confirm that the method provides high recoveries of all analytes and is sufficiently linear, sensitive, precise and accurate for application to the measurement of these analytes in small amounts (100 mg) of brain tissue using Quattro MS.

The intra-run precision was within an RSD% of 5.67 % to 19.8 % and the inter-run precision was between 8.02% to 20.1%. The values for recovery of the ECs and related compounds were greater than 71% at all concentrations (Table 2.3). AEA, OEA and PEA demonstrated a lower limit of quantification (LLOQ) of 2.5 pmol/g, PG-EAs had a LLOQ of 10 pmol/g, 2-AG demonstrated a LLOQ of 50 pmol/g, and the PG-GEs had a LLOQ of 100 pmol/g. The LLOQ of ECs reported here of 2.5-50 pmol/g consistent with previous studies in our group (Richardson et al., 2007). The LLOQ for ECs, PG-EAs, and PG-GEs were determined from spiked rat brain tissue, and hence are more realistic compared to values determined using standard solutions. However, using direct injection of standards the LLOD for our method were 5 fmol for AEA, virodhamine, OEA, and PEA, 20 fmol for PG-EAs, 100 fmol for 2-AG, and 200 fmol for PG-GEs. Other studies quote on column limits of quantification using direct injection of standards of between 8 fmol- 2 pmol for AEA (Beaulieu et al., 2000a, Giuffrida et al., 2000b, Clarke and Guttman, 2002, Kingsley and Marnett, 2003), 1.25 pmol PEA and 0.6 pmol OEA using LC-single quadrupole MS (Giuffrida et al., 2000a) and 1 pmol-13 fmol 2-AG (Beaulieu et al., 2000a, Kingsley and Marnett,

2003). LLOD and LOQ for PG-EAs and PG-GEs are less documented, with only one study to date providing LOD values for PGE₂-GE (Hu et al., 2008), even though other groups have quantified PG-EAs (Kozak et al., 2000, Kozak et al., 2001a, Kozak et al., 2002a, Weber et al., 2004). The limits of detection for ECLs are better than the majority of methods published and allow the quantification of these compounds in mg amounts of tissue, whilst maintaining a high level of analyte specificity. Previously, there have been very few details reported regarding percentage recovery of ECLs and associated compounds from a biological matrix. Calculations of recovery are hindered by the endogenous nature of some of these compounds, and post mortem changes. However, subtracting 'spiked' areas from endogenous levels area, or from synthetic standard areas (for non-endogenous compounds) supported the efficient extraction of all the analytes from brain tissue (Table 2.7). These data show the high and reproducible recovery of ECLs, PG-EAs and PG-GEs for a range of concentrations, providing high confidence in this method for the extraction and detection of ECLs, PG-EAs and PG-GEs in biological tissue.

Development and validation of a quantitative analytical method to measure levels of endocannabinoids and COX-2 metabolites in rat tissue

Analyte	R ²	Slope (ratio to Concentration (nmol/g))	Concentration (nmol/g)	Recovery % (±SD)	Intraday (n = 5)		Interday (n = 4)	
					Precision (RSD%)	Accuracy (RSD%)	Precision (RSD%)	Accuracy (RSD%)
PEA	0.975	2.075±0.404	0.001	98.2±6.21	7.34	104	16.1	116
			0.1	111±19.3	15.1	98	19.3	112
			1	96.3±15.7	8.99	94.7	13.2	94.3
OEA	0.993	1.564±0.387	0.001	101±4.76	10.1	83.0	8.02	81.2
			0.1	102±11.5	12.4	123	11.2	125
			1	98.8±13.5	7.53	98.4	11.4	112
Virodhamine	0.987	0.473±0.093	0.001	71.1±22.1	14.5	123	18.4	135
			0.1	91.0±19.3	15.9	102	16.8	142
			1	74.1±13.3	14.6	134	18.9	98.7
AEA	0.992	1.053±0.263	0.001	111.3±19.2	12.6	81.3	15.7	78.2
			0.1	105.9±21.6	11.4	99.4	20.1	114
			1	98±15.7	5.67	113	17.1	109
2-AG	0.984	1.563±0.395	0.1	125±19.9	17.1	109	11.5	111
			1	111±13.1	19.8	123	21.3	127
			10	112±19.7	17.4	106	11.2	121
PGD2 EA	0.95	0.401±0.103	0.005	112±12.9	8.72	100	14.05	102
			0.01	101±8.51	12.8	109	16.7	101
			0.1	118±22.9	9.04	121	14.8	96.2
PGE2 EA	0.993	0.473±0.132	0.005	109±5.45	12.4	103	12.4	107
			0.01	97.4±15.6	11.7	192	21.0	98.3
			0.1	103±12.4	15.3	88.8	7.32	112
PGF2α EA	0.984	0.621±0.0.171	0.005	102±11.9	11.2	100	9.75	103
			0.01	95.2±14.5	19.4	119	15.8	111
			0.1	121±22.7	11.0	105	10.8	107
PE2 GE	0.971	0.441±0.0.099	0.5	111±4.06	14.1	93.7	7.42	91.2
			2.5	102±7.5	9.24	103	14.6	108
			10	98.9±12.8	10.3	104	11.9	102
PGF2α GE	0.964	0.397±0.0.078	0.5	99.4±11.7	9.67	107	14.0	101
			2.5	103±12.9	13.1	94.8	14.9	109
			10	111±13.7	17.1	103	9.03	121

Table 2.7 Recovery and intraday, interday assay precision and assay of the LC-MS/MS method for the measurement of ECs and COX-2 metabolite compounds in rat brain tissue, based on 100mg tissue.

2.4.6 Analysis of rat brain extract

The validated method was used to extract, identify and quantify concentrations of AEA (43.4 ± 11.2 nmol/g), OEA (0.16 ± 0.03 nmol/g), PEA (0.21 ± 0.08 nmol/g) and 2-AG (11.24 ± 3.48 nmol/g) in rat brain, which is consistent with previous studies analysing whole brain tissue (Kathuria et al., 2003b, de Lago et al., 2005, Fegley et al., 2005, Bradshaw et al., 2009). This provides confidence in the modified extraction and quantification method. Figure 2.5 shows a representative chromatogram of the analytes detected in rat brain. The method validated here was unable to detect the presence of virodhamine, PG-EA and PG-GEs rat brain analysed, consistent with previous studies. Richardson et al., (2007) was unable to detect virodhamine in various rat brain regions, while virodhamine was reported to be present in rat brain microdialysate and tissue (Clarke and Guttman, 2002). Due to the close structural similarities of AEA/virodhamine, and similar retention times, it may be possible that, under particular conditions AEA may be mislabelled/detected as virodhamine. The lack of COX-2 metabolites of AEA and 2-AG *in vivo* is conflicting, with the detection of PG-EAs in FAAH^{-/-} mice following exogenous administration of AEA (50mg/kg), however not in naïve tissue (Weber et al., 2004). This suggests that *in vivo* these compounds are formed only when levels of AEA are high, or when EC metabolism has been compromised (see chapter 4 for more details). PG-GEs have however, been detected and quantified in naïve rat paw tissue (Hu et al., 2008).

The LC-MS/MS method used for PGE₂-GE had a limit of detection from injection of synthetic standards of 15 fmol. This is lower than our reported limit of detection, however Hu et al., (2008) method was not validated, the lack of detailed information on limits of quantification cast doubt as to whether this limit is correct for biological tissue. PG-EAs, have however been quantified *in vitro* using either sodium-containing mobile phases to generate $[M^+Na]^+$ ions of PG-EA and PG-GE (Kozak et al., 2000, Kozak et al., 2001a). The use of ammonium cation (NH_4^+) utilised this technique for the analysis of PG-GEs and prostaglandins from cell media (Kingsley et al., 2005) as PGE₂-GE from an *in vivo* sample (Hu et al., 2008). The precursor ion is the $[M^+NH_4]^+$ complex and the fragment ion is one of several masses m/z 409 and m/z 391 are dehydration products which result from the loss of NH_3 and one or two molecules of H_2O . Hu et al., (2008) also used these fragments as precursor ions and used m/z 91 and m/z 79 as fragment ions to verify the presence of PGE₂-GE in rat tissue, similar to our method, which looked at m/z 409 < 91 for PGE₂ GE. It may also be feasible that the enzymes required for the conversion of the intermediate products of metabolism, may not be present in our sample tissue. Indeed incubation of 2-AG with COX-2 and specific prostaglandin H₂ (PGH₂) isomerases in cell cultures and isolated enzyme preparations results in PG-GE formation (Kozak et al., 2002a), suggesting these compounds may only be produced in certain types of tissue.

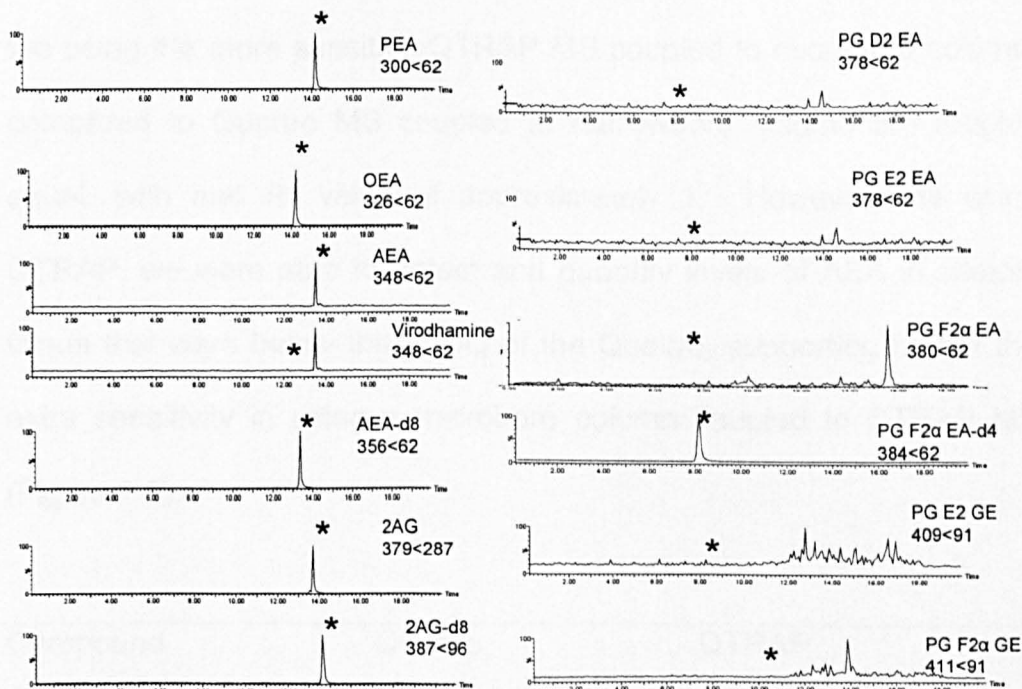


Figure 2.5 Representative chromatograms of the optimised separation of endogenous compounds in rat brain. PGD2-EA, PGE2-EA, PGF2 α -EA, PGE2-GE and PGF2 α -GE were below the limit of detection. Appropriate retention of times compounds shown by *.

2.4.7 Comparison of two analytical methods

When higher sensitivity was required, depending on tissue/biological matrix under investigation (for example neuroblastoma cells), HP 1100 LC system was coupled to QTRAP for extra sensitivity, and in some cases the LLOQ was 5 times lower, allowing quantification of ECs and related compounds in lower weight tissue. For example AEA, OEA and PEA demonstrated a lower limit of quantification (LLOQ) of 0.5 pmol/g, the PG-EAs had a LLOQ of 5 pmol/g, 2-AG demonstrated a LLOQ of 10 pmol/g, and the PG-GEs had a LLOQ of 100 pmol/g (see Table 2.8). The relative amounts of analytes present in sample was tissue was comparable when using both the QTRAP, and Quattro to analyse the same samples (Figure 2.5), for example: the endogenous levels of AEA,

OEA, PEA and 2-AG quantified in hindpaw tissue data acquired from the using the more sensitive QTRAP MS coupled to microbore column, compared to Quattro MS coupled to narrowbore column are roughly equal, with and R^2 value of approximately 1. However, the using QTRAP, we were able to detect and quantify levels of AEA in sample tissue that were below the LLOQ of the Quattro, supporting further the extra sensitivity in using a microbore column coupled to QTRAP MS (Figure 2.6).

Compound	Quattro	QTRAP
AEA pmol/g	2.5	0.5
OEA pmol/g	2.5	0.5
PEA pmol/g	2.5	0.5
2-AG pmol/g	50	10
PGD2-EA pmol/g	10	5
PGE2-EA pmol/g	10	5
PGF2 α -EA pmol/g	10	5
PGE2-GE pmol/g	100	100
PGF2 α -GE pmol/g	100	100

Table 2.8 A comparison of the LOQ for two different MS instruments for the quantification of ECs and COX-2 metabolites in rat brain tissue.

2.4.8 Quantification of EC in biological matrices

The method was developed and validated in rat brain tissue, however it has also allowed the quantification of ECs and related compounds in a wide range of biological matrixes, such as rat paw, brain, liver, bone and spinal tissue. Table 2.9 shows the basal values of ECs and related compounds quantified in spinal cord, paw, liver, cell and bone samples. The development of these methods allow for the identification and quantification of ECs and COX-2 metabolites of AEA and 2-AG, giving the equivalent quantitative values of endogenous levels of ECs in biological matrices, no matter what MS instrument has been used. This allows for comparisons between samples that have been analysed on both MS instruments, allowing the use of QTRAP detector when sensitivity is compromised. The exclusion of SPE from sample preparation has proved not to affect chromatography or sensitivity, and has allowed for faster extraction of biological samples.

The specific and sensitive method described in this chapter allows quantitative profiling of AEA, OEA, PEA, and 2-AG in biological tissue, and the detection of COX-2 metabolites of AEA and 2-AG, although their production *in vivo* and *in vitro* remains to be investigated further. The measurement of ECs and their metabolites is vital in understanding the role of the endocannabinoid system in pathological conditions.

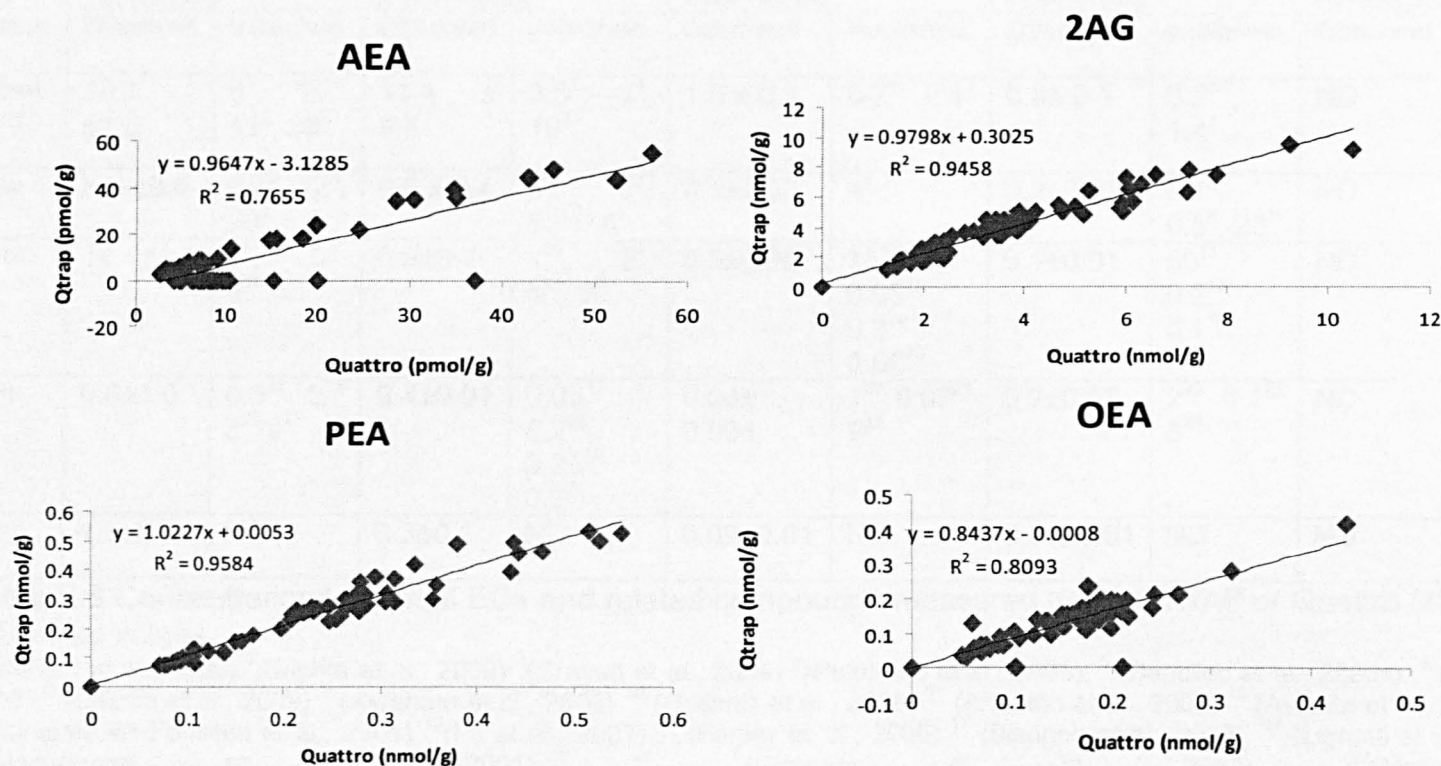


Figure 2.6 Levels of AEA, OEA, PEA and 2-AG obtained using both analytical methods coupled to either QTRAP or Quattro MS. Levels of AEA, PEA, OEA and 2-AG are comparable using both methods, however the red arrow shows levels of AEA, that were where previously below the LLOQ using Quattro are now quantifiable using QTRAP.

Rat Tissue	AEA pmol/g		2-AG nmol/g		OEA nmol/g		PEA nmol/g		PG-EA pmol/g		PG-GE pmol/g	
	Observed	published	Observed	published	Observed	Published	Observed	published	Observed	published	Observed	published
spinal cord	18.7 ±1.6	5 ¹ , 10 ² , 11 ³ , 30 ⁴	51.4 ± 9.6	0.5 ¹ , 1 ⁴ , 10 ²	1.0 ± 0.1	0.2 ^{4,3} 0.4 ¹	0.8± 0.1	0.2 ^{3,4} , 1.4 ¹	ND	ND	ND	ND
Paw	6.5 ±0.5	0.7 ⁵ , 12 ⁶ , 20 ¹	9.6 ± 0.4	3 ⁶ , 5 ¹ , 51 ⁵ 0.8 ⁷	0.1±0.03	1 ¹	0.2±0.02	0.1 ⁶ , 0.5 ⁵ , 20 ¹	ND	ND	ND	0.002 ⁷
Liver	14.4±1.1	1 ⁸ , 5 ¹⁰ , 6 ¹⁶	6.9±0.7	1 ¹⁰ , 2 ⁹ , 5 ¹¹ , 6 ⁸	0.3±0.05	15 ¹² , 0.05 ¹³ , 0.3 ¹⁴ , 0.08 ¹⁵	0.1±0.01	50 ¹¹ , 0.2 ¹³ , 0.1 ¹⁶	ND	ND	ND	ND
Cell	6.0±1.0	0.5 ¹⁸ , 2 ¹⁹ , 3 ²⁰ 9 ²¹	0.4±0.01	0.05 ¹⁷ , 0.2 ¹⁸ , 0.25 ²⁰ , 0.1 ²¹	0.03± 0.004	1 ²⁰ 0.07 ²¹ , 9 ²²	0.2±0.03	2 ²⁰ 0.1 ²¹ , 3 ²²	ND	ND	ND	ND
Bone	4.1±0.5	ND	0.3±0.1	ND	0.09±0.01	ND	0.08±0.01	ND	ND	ND	ND	ND

Table 2.9 Concentrations of basal ECs and related compounds measured using QTRAP or Quattro MS in a variety of rat tissue and published values.

¹ (Jhaveri et al., 2006) ²(Suplita et al., 2006) ³(Cravatt et al., 2004) ⁴(Petrosino et al., 2006), ⁵ (Beaulieu et al., 2000a), ⁶ (Guindon et al., 2007), ⁷ (Hu et al., 2008) ⁸ (Batetta et al., 2009) ⁹ (Avraham et al., 2008) ¹⁰ (Guijarro et al., 2008) ¹¹ (Artmann et al., 2008) ¹² (Astarita et al., 2006) ¹³ (LoVerme et al., 2006a) ¹⁴ (Rodriguez de Fonseca et al., 2001) ¹⁵(Fu et al., 2007) ¹⁶ (Fegley et al., 2005) ¹⁷ (Bisogno et al., 2009), ¹⁸ (Ligresti et al., 2003) ¹⁹ (Burstein et al., 2002), ²⁰(Maccarrone et al., 2001), ²¹ (Gonthier et al., 2007), ²²(Matias et al., 2007).

This newly developed analytical method has been shown to be suitable for quantitative profiling of ECLs and is readily adaptable to different types of biological samples. Concentrations of ECLs have been successfully measured in rat paw, rat spinal cord, and human cell lines, and rat neurones (see future chapters), with levels similar to that published from other groups (Table 2.9). The similarity in these levels provides confidence with the validated extraction and quantification method developed, and casts doubt as to whether PG-EA and PG-GE are present in naïve tissue under normal pathological conditions, at least to the limit of quantification of the method. Chapter 4 investigates the production of these compounds under inflammatory conditions.

Profiling not only ECLs, but also their precursors and metabolites in diseased tissue or following noxious stimulation is crucial in understanding the role and fate of the endocannabinoid in various disease states. Many questions still remain on the regulation of the biosynthesis and catabolism of the ECLs, however this system represents a novel therapeutic target for the treatment of pain, with modulators of the system shown to produce analgesic effects both clinically and in animal models of pain, reviewed by (Gauldie et al., 2001, Huang et al., 2002, Iversen and Chapman, 2002, Hohmann and Suplita, 2006). With insufficient methods allowing the simultaneous quantification of ECs and their metabolites, as well as sensitivity issues for AEA detection, actual concentrations of ECLs

Development and validation of a quantitative analytical method to measure levels of endocannabinoids and COX-2 metabolites in rat tissue and the production of COX-2 metabolites *in vitro* and also in *in vivo* models of pain are often unclear, thus this new analytical method will help provide some further insight into the regulation of ECLs in various *in vivo* and *in vitro* models of pain.

Chapter 3.

The role of TRPV1 in modulating endocannabinoid levels and neuronal responses to TNF α .

3 The role of TRPV1 in modulating endocannabinoid levels and neuronal responses to TNF α .

3.1 Introduction

Following the successful development and validation of a LC/MS method capable of quantifying ECs and related compounds, we wanted to investigate the generation of ECs in sensory neurones. In particular, our intention was to address the hypothesis that they act in an autocrine fashion such that TRPV1 activation, and subsequent increases in cytosolic calcium, could drive ECL synthesis and release. The second part was to investigate the role of the pro-inflammatory mediator TNF α , which has been shown to sensitise receptors and ion channels, including TRPV1 leading to hyperalgesia. Hence, we investigated the effects of TNF α on capsaicin-evoked calcium responses as a measure of neuronal excitability.

3.1.1 Capsaicin and TRPV1

The activation of TRPV1 channels on sensory fibres and non-neuronal cells initiates Ca²⁺ and Na⁺ influx (Wood et al., 1988, Bleakman et al., 1990a, Docherty et al., 1991) and the corresponding

release of tachykinin neuropeptides such as substance P (Go and Yaksh, 1987, Holzer, 1988, Bevan and Szolcsanyi, 1990), and calcitonin-gene-related-peptide (CGRP) (Meng et al., 2009). Various resident immune cells (e.g., macrophages), peripheral target cells (endothelia, epithelia), respond to these neuropeptides and mediate the tissue response characteristic of inflammation, namely redness, swelling, and pain (Richardson and Vasko, 2002).

Capsaicin also causes the release of endogenous antinociceptive ligands, such as β -endorphin (Bach and Yaksh, 1995) and somatostatin (Szolcsanyi et al., 1998a, Szolcsanyi et al., 1998b); therefore, it is conceivable that capsaicin via the activation of TRPV1 leads to elevation of cytoplasmic calcium levels and a consequent increase in endocannabinoid synthesis, which could attenuate neuronal activation via inhibition of Ca²⁺ channels, opening of K⁺ channels, and inhibiting adenylyl cyclase activity, thereby providing a negative feedback system.

3.1.2 CB₁ and TRPV1

Cannabinoid CB₁ receptors and TRPV1 receptors are co-expressed in the dorsal horn of the spinal cord, and on primary sensory neurons (Szallasi et al., 1995, Szallasi and Blumberg, 1999, Ahluwalia et al., 2000, Binzen et al., 2006). The receptors can engage in cross-talk when expressed on the same or neighboring cells, such as in the striatum, where exogenous AEA application leads to inhibition of 2-

AG formation, via down regulation of diacylglycerol lipase- α (DAGL α). This inhibition of DAGL α activity was prevented by inhibition of TRPV1 receptors with I-resiniferatoxin (Maccarrone et al., 2008), and is thought that AEA, via TRPV1 interferes with glutathione-dependant 2-AG synthesis; however the validity of this mechanism throughout the brain is still unknown. However, these data suggest that AEA might be critically involved in the control of the excitability of striatal neurons through a direct depressant action at excitatory synapses and an indirect interference with inhibitory inputs regulated by 2-AG. Furthermore, the endocannabinoids AEA and NADA can also act as endovanilloids (Smart et al., 2000, Zygmunt et al., 2000, Huang et al., 2002, Chu et al., 2003, Van Der Stelt and Di Marzo, 2004), with AEA activating the TRPV1 channel via an intracellular binding site (De Petrocellis et al., 2001a). Several pieces of evidence suggest that AEA and capsaicin bind to the same site on TRPV1. AEA displaces [3 H]-RTX from TRPV1 with a K_i of $\sim 2 \mu\text{M}$ in transfected (Chinese hamster ovary) CHO cells, which is similar to that of capsaicin (De Petrocellis et al., 2001b, Ross et al., 2001). Although AEA has similar affinity for TRPV1 as capsaicin in binding assays, it often shows lower potency in functional assays. In heterologous expression systems, such as human embryonic kidney (HEK) cells or *Xenopus* oocytes, the concentrations of AEA required to fully activate TRPV1 as assessed by measuring intracellular Ca^{2+} are 1- to 10-fold higher than those required to evoke CB $_1$ -mediated functional responses (Zygmunt et al., 1999, De Petrocellis et al.,

2000, Smart et al., 2000, Ross et al., 2001). In native systems *in vitro*, the potency of AEA ranges between 0.3 and 0.8 μ M in blood vessels (relaxation) compared with 6–10 μ M in DRG neurones (elevation of intracellular calcium, $[Ca^{2+}]_i$ and stimulation of inward currents) (Zygmunt et al., 1999, Smart et al., 2000, Olah et al., 2001, Ralevic et al., 2001, Jerman et al., 2002). The functional activity of AEA at TRPV1 can be masked or enhanced by its activity on CB₁ receptors, especially in those cells when the 2 receptors are co-expressed (Ahluwalia et al., 2003a), where AEA produces a greater increase in CB₁/TRPV1 over-expressing cells, compared to TRPV1 over-expressed cells (Hermann et al., 2003). Thus, it appears that cell and experimental factors such as receptor levels and possibly metabolic enzymes can affect the affinity and efficacy of AEA. Given that the binding site of AEA is on the intracellular side of TRPV1, and that AEA is produced from the hydrolysis of membrane phospholipids, via an increase in cytosolic calcium, this makes the generation of AEA and other ECs by TRPV1 activation highly likely. Furthermore, Di Marzo's group proposed that AEA acts as an intracellular amplifier for Ca²⁺ and AEA synthesis, where TRPV1 activation leads to an increase in Ca²⁺, AEA synthesis, which in turn can further activate TRPV1 receptors allowing more AEA synthesis (van der Stelt et al., 2005). This cycle, however, can be interrupted by AEA activating extracellular CB₁ receptors, and thus inhibiting TRPV1 function and calcium release (Millns et al., 2001).

3.1.3 Calcium driven EC synthesis

The role of calcium in endocannabinoid synthesis is well documented (Di Marzo et al., 1994, Ohno-Shosaku et al., 2005, Wang and Ueda, 2008) (see Chapter 1 for more detail). Indeed, in various brain regions, it has been demonstrated that postsynaptic depolarization-induced Ca^{2+} elevation causes endocannabinoid release, and suppresses neurotransmitter release through activation of presynaptic CB_1 receptors (Kreitzer and Regehr, 2001, Ohno-Shosaku et al., 2001, Wilson and Nicoll, 2001, Diana et al., 2002, Yoshida et al., 2002). However, these studies did not measure ECLs. To date there is a lack of studies linking capsaicin-induced increase in calcium-driven ECL synthesis with direct measurements in sensory nerves. Previous studies have reported that DRG neurones make AEA by direct measurement using LC/MS (Ahluwalia et al., 2003a, van der Stelt and Di Marzo, 2005, Vellani et al., 2008), either cooperatively with, or independently from, Ca^{2+} -influx, where intracellular Ca^{2+} mobilisation by thapsigargin, or by receptors coupled to the PLC/ IP_3 pathway leads to the formation of intracellular anandamide in HEK293 cells and primary sensory neurons, and anandamide-induced TRPV1-dependent influx of extracellular Ca^{2+} in these cells (van der Stelt and Di Marzo, 2005). However, the studies did not simultaneously measure levels of the other ECL compounds, such as OEA, PEA and 2-AG, which are also reported to be produced in a calcium-dependant manner (Hansen et al., 1995, Cadas et al., 1996, Bisogno et al., 2005). However, levels of OEA,

PEA and 2-AG may not be regulated in the same way as levels of AEA. In fact, AEA and 2-AG have entirely different biosynthetic routes originating from precursors, whose levels in turn depend on the amount of arachidonic acid in the *sn*-1 and 2-position of phosphoglycerides, respectively (see review (Di Marzo and Petrosino, 2007)). AEA, PEA, and OEA although belonging to the same class of lipids, the *N*-acylethanolamines, are likely to be biosynthesised via different enzymes from the corresponding *N*-acylphosphatidylethanolamine (NAPE) precursors (Liu et al., 2006, Simon and Cravatt, 2006). Therefore, it is possible that neuronal AEA, OEA, PEA and 2-AG levels may be regulated via differing mechanisms, and it's not definite that the same stimulus would have the same effects on all ECL synthesis.

3.1.4 Endocannabinoid uptake, release and degradation

AEA is inactivated through cellular reuptake and enzymatic degradation mechanisms (see Chapter 1 for more detail). It is widely accepted that degradation of AEA occurs intracellular; however, the mechanisms by which AEA is taken into cells, are yet to be fully elucidated. Once inside the cell, actions of AEA are terminated by hydrolysis primarily by the enzyme fatty acid amide hydrolase (FAAH), which hydrolyzes AEA to arachidonic acid (AA) and ethanolamine.

It still remains unclear as to how ECLs are released into the postsynaptic plasma membrane and taken into the cell, or even if

these are the same mechanisms. ECLs are highly lipophilic and so are capable of crossing the plasma membrane of cells via passive diffusion down concentration gradients (Di Marzo et al., 1994, Beltramo et al., 1997, Hillard et al., 1997), but carrier proteins are probably required to extrude ECLs from the lipid environment of the membrane into the aqueous intracellular and extracellular media (Di Marzo et al., 1994, Piomelli et al., 1998). AEA uptake has been demonstrated in many cell lines (Deutsch and Chin, 1993, Bisogno et al., 1997, Rakhshan et al., 2000) and in culture from primary neurons (Di Marzo et al., 1994, Hillard et al., 1997). Uptake is independent of sodium (Beltramo et al., 1997) and ATP (Hillard et al., 1997), and is moderately temperature dependant. However, the suggestion that ECLs can cross the cell membrane via an endocannabinoid membrane transporter remains controversial. Ligand binding studies have indicated that the putative carrier protein is stereoselective and requires well defined structural requirements (Khanolkar and Makriyannis, 1999, Jarrahian et al., 2000). Furthermore, AEA uptake was blocked by the arachidonic acid derivative AM404, which is proposed to act as a competitive inhibitor of AEA uptake (Rakhshan et al., 2000, Fegley et al., 2004). AM404 has been shown to inhibit efflux of accumulated AEA in striatal and endothelial cells (Gerdeman et al., 2002, Maccarrone et al., 2002), further supporting the existence of a transporter. However it should also be noted that AM404 is also a ligand of the TRPV1 receptors, and may be able to modulate ECL synthesis through mobilisation of intracellular calcium (Di Marzo et

al., 1994, Ralevic et al., 2001, van der Stelt and Di Marzo, 2005). Thus, it is probable that an increase in cytosolic calcium via TRPV1 activation can drive ECL release and uptake via a membrane transporter.

3.1.5 TRPV1 sensitisation by inflammatory mediators

The ability of TRPV1 to become sensitised by pro-analgesic and inflammatory mediators has raised interest in it being a novel drug target for the treatment of chronic pain and hyperalgesia (see(Gunthorpe and Szallasi, 2008, Gunthorpe and Chizh, 2009). There is evidence that the combination of direct and indirect mechanisms finely tunes TRPV1 activity (Nagy et al., 2004), and each of the known activators of TRPV1 (heat, protons and vanilloids) can sensitise the channel to other stimuli. For example, capsaicin is more potent in the presence of sub-threshold concentrations of protons as well as slight increases in temperature (Ryu et al., 2003, Ahern et al., 2005, Lee et al., 2005). Protons induce a leftward shift of the capsaicin and temperature response curves of TRPV1 leading to a lower EC₅₀ and activation threshold, respectively (Tominaga et al., 1998). Thus, proton activation of TRPV1 and sensitisation of heat-induced currents is consistent with the dual role of protons as nociceptor activator and inflammatory mediator. Thus, a combination of otherwise innocuous heat and tissue acidosis may become painful (Steen et al., 1995). In addition to protons, other inflammatory

agents, such as bradykinin and prostaglandin E2 together in acidic solution, can activate TRPV1 in a similar conductance to capsaicin. The response is smaller or absent if any one of the constituents is lacking, and is prevented in the presence of capsazepine (Vyklícky et al., 1998). Inflammatory mediators can act as second messengers (Dray, 1995, Hingtgen et al., 1995), by sensitizing TRPV1 to other, direct activators, confirming the general hypothesis that, under inflammatory circumstances, a 'sensitised' TRPV1 can be activated by agonist concentrations much lower than those required under conventional experimental conditions.

3.1.6 Inflammatory mediators and TRPV1

During inflammation, various cell types, including mast cells and immune cells, release pro-inflammatory cytokines (e.g., IL1 β , IL6, and TNF α) (Cunha et al., 1992, Jonakait, 1993, Davis and Perkins, 1994), which cause an increase in TRPV1 expression (see Chapter 1, figure 1.1). For example, in complete Freund's adjuvant-induced inflammation in the rat hind paw, TRPV1 protein levels are known to increase in the plantar skin (Ji et al., 2002), DRG and spinal cord (Luo et al., 2004)). Additionally, TRPV1 can be indirectly sensitised by several inflammatory mediators from the surrounding inflamed area, e.g. nerve growth factor (Chuang et al., 2001) (Ji et al., 2002), bradykinin (Chuang et al., 2001), and ATP (Tominaga et al., 2001). Inflammatory mediator signaling cascades could, via allosteric modulation, post-translationally modify TRPV1 or increase TRPV1

protein expression to produce sensitisation. Increased TRPV1 expression which has been shown to occur 12–24 h following inflammation, appears to be crucial to the development of thermal sensitization (Ji et al., 2002).

TRPV1 is known to have several phosphorylation sites, and sensitisation can occur via modification of several serine and threonine residues on the receptor through phosphorylation to sensitize receptor activity (Bhave et al., 2002, Numazaki et al., 2003, Jordt et al., 2004). In particular, protein kinase A (PKA) (Bhave et al., 2002) and protein kinase C (PKC) (Cesare et al., 1999a, Cesare et al., 1999b) appear to have a significant role in TRPV1 phosphorylation. Mitogen-activated protein kinases (MAPK) have also been implicated in nociceptors sensitisation associated with inflammation and peripheral neuropathy. P38 MAPK is activated in response to inflammation (Ji et al., 2002), and activation of TRPV1 by intraplantar injection of capsaicin leads to p38-MAPK dependant hyperalgesia (Mizushima et al., 2005). Inflammation, axotomy and spinal nerve ligation also activate p38 MAPK in spinal cord and DRG neurones, possibly contributing to neuropathic pain (Kim et al., 2002b, Jin and Gereau, 2006). Furthermore, TNF α was reported to be central to p38 phosphorylation and mechanical hyperalgesia in the spinal nerve ligation model of peripheral neuropathy (Pollock et al., 2002, Schafers et al., 2003b, Jin and Gereau, 2006). Endogenous NGF-dependent p38 activation, leading to an increase in TRPV1 expression, has been shown to occur following

inflammation (Ji et al., 2002). Therefore, inflammatory mediators such as TNF α , can activate p38MAPK signaling pathway, leading to sensitisation and up-regulation or modification of TRPV1 receptors in regions of tissue injury, which could play important roles in inflammatory nociception.

3.1.7 TNF α

TNF α is a pro-inflammatory cytokine produced in response to injury and inflammation and is reported to play a critical role in the development and maintenance of neuropathic and inflammatory pain states (Woolf et al., 1997, Junger and Sorkin, 2000, Sommer and Kress, 2004). TNF α has also been implicated in many autoimmune diseases including rheumatoid arthritis and multiple sclerosis (Feldmann et al., 1996, Spuler et al., 1996, Ledeen and Chakraborty, 1998) and it is involved in nociceptive processes causing hyperalgesia (Cunha et al., 1992, Watkins et al., 1995, Ignatowski et al., 1999, Junger and Sorkin, 2000). Thus, after nerve injury, TNF α expression is increased in both DRG (Schafers et al., 2002, Schafers et al., 2003a) and spinal cord (Hashizume et al., 2000).

Two distinct TNF receptor subtypes have been identified, TNFR1 (type I, p55TNFR) and TNFR2 (type II, p75TNFR), with molecular weights of 55 and 75 kDa, respectively (Lewis et al., 1991), and both have previously been identified in nociceptive neurones (Shubayev and Myers, 2001, Marchand et al., 2005). Occupation of these receptors can activate a number of intracellular signaling pathways

The role of TRPV1 in modulating endocannabinoid levels and neuronal responses to TNF α

including nuclear factor kappa-light-chain-enhancer of activated B cells (NF- κ B), p38 MAPK and c-jun N-terminal kinase (JNK) resulting in a number of responses including inflammation, apoptosis and necrosis (Eissner et al., 2000, Harashima et al., 2001, Eissner et al., 2004, Ware, 2005). TNFR1 appears to be particularly important in the pain-sensitizing actions of TNF α . Mechanical hypersensitivity induced by exogenous TNF α is reduced in TNFR1-null animals (Cunha et al., 2005) and antisense knockdown of TNFR1 reduces hyperalgesic priming after inflammation in the rat (Parada et al., 2003). However, there are conflicting reports as to whether activation of these receptors can lead to an increase in intracellular calcium. Some reports have shown modulation of Ca $^{2+}$ responses, but not direct Ca $^{2+}$ mobilisation by TNF α . Moreover, the effects that have been observed only occur after long-term exposure to TNF α and usually involve TNF α -induced cell death mechanisms (Amrani et al., 1997, Kong et al., 1997, Parris et al., 1999, Yorek et al., 1999). TNF α , acting via TNFR1, has also been shown to increase the frequency of spontaneous miniature synaptic currents in cultured rat hippocampal neurones, albeit without increased cytosolic Ca $^{2+}$ concentration (Grassi et al., 1994) and it has also been shown to increase the calcium current density in sympathetic neurones (Soliven and Albert, 1992). Application of TNF α results in the release of Ca $^{2+}$ via TNFR1 from intracellular stores in rat DRG neurons (Pollock et al., 2002) and human microglia cells (McLarnon et al., 2001) which appears to be independent of calcium influx and

intracellular IP₃ stores. TNF α increases the proportion of DRG neurons expressing the TRPV1 receptor 24 hours following application (Hensellek et al., 2007), and studies have revealed that p38 MAPK are involved in this increased TRPV1 expression (Ji et al., 2002, Bron et al., 2003). Activation of p38 MAPK has been implicated in nociceptor sensitisation associated with inflammation (Joseph and Levine, 2004, Wu, 2004). Furthermore, activation of TRPV1 leads to p38-dependent hyperalgesia, following injection of capsaicin in rats hindpaw (Mizushima et al., 2005), and an up-regulation of TRPV1 protein expression in cell bodies of DRG neurons following intraplantar administration of Complete Freund's adjuvant (CFA), which is mediated by NGF and p38MAP kinase (Ji et al., 2002). Inflammation and spinal nerve ligation similarly activate p38 in spinal cord and DRG neurons, contributing to neuropathic pain (Kim et al., 2002b, Jin and Gereau, 2006). In the spinal nerve ligation model of peripheral neuropathy, TNF α was central to p38 phosphorylation and mechanical hyperalgesia (Pollock et al., 2002, Schafers et al., 2003a, Jin and Gereau, 2006). Thus, it is clear that, during inflammation, mediators released into the external milieu can indirectly sensitize neuronal TRPV1 receptors.

Collectively these data suggest that it may be possible for TNF α to activate the p38MAPK pathway to increase the phosphorylation of TRPV1 receptors and allow pronociceptive inflammatory mediators to sensitize TRPV1 responses, thus promoting hyperalgesia.

3.1.8 The objectives of this chapter are:

- To determine the effect of capsaicin on intracellular and extracellular ECL levels in rat DRG neurons and *hTRPV1*-SHSY5Y cells.
- To determine the effect of FAAH inhibition on the synthesis and release of ECLs.
- To examine the effects of TNF α on calcium release from sensory neurones.
- The potential sensitisation of TRPV1 by TNF α in sensory neurones and the mechanisms by which it does so.

3.2 Materials and Methods

All chemicals and biochemical were purchased from Sigma, unless otherwise stated.

3.2.1 DRG Preparation

3.2.1.1 Glass coverslip preparation

Glass coverslips (19mm diameter) were washed in 10% Decon (Decon Sciences) overnight, before being rinsed twice in distilled water (dH2O) and then in tap water for 2hours. The coverslips were rinsed again in dH2O, and then soaked in concentrated hydrochloric acid (HCl) for 30 minutes. Cover-slips were rinsed again in dH2O, and then again in tap water for 2 hours, before being rinsed three times in dH2O. Cover-slips were autoclaved before being stored at room temperature in sterile water.

Cover-slips were coated with 100 μ l sterile 0.1 mg/ml poly-L-lysine and left for 90minutes at room temperature. Cover-slips were washed once in sterile water and left to dry. Laminin (1 mg/ml) was added to the centre of the cover-slip, and left to air dry for a minimum of 60 minutes. Cover-slips were washed once with sterile water and dried via vacuum before use.

3.2.1.2 Dorsal root ganglion (DRG) neurone preparation

Dorsal root ganglion (DRG) neurones were dissected from adult rats using a similar method to that described by Lindsay (1988), with minor modifications.

Adult male Sprague –Dawley rats (180-200g) were killed by exposure to CO₂. The dorsal surface of the rat was swabbed with 70% alcohol, and the fur and skin was lifted and cut, to expose the underlying vertebral column. Incisions were made close to either side of the vertebral column using scissors, and then the spinal column lifted out and place into a culture dish containing Dulbecco's Ca²⁺ and Mg²⁺-free phosphate-buffered saline (PBS) (Sigma) at 37°C. Excess back muscle was removed to expose the spinal column and cord. The column was held using a pair of rat toothed forceps and the bone was removed. Following the midline of the ventral plate, the column was halved. The DRGs were exposed in their recesses by carefully removing the spinal cord. The DRGs are visible as swellings of each spinal nerve that are slightly more translucent than the rest of the nerve. The DRGs were carefully dissected out by cutting the peripheral and central trunks (Approximately 30-40 DRGs can be removed from a single rat). The isolated DRGs are placed in a tube containing PBS and washed once under gravity, and then incubated (37 °C, 5%CO₂) for 90mins in 5ml Neurobasal media (Gibco) containing collagenase (2.5 mg/ml) supplemented with horse serum (10%).

DRGs were then washed three times under gravity in PBS. The PBS was removed and 2.5 ml trypsin (1x) was added. Ganglia were incubated (37 °C, 5%CO₂) for 5 minutes, then 1ml Neurobasal medium containing 10% horse serum added. This was triturated up and down, approximately 15 times to form a cell suspension using a pastette. The suspension was then carefully layered on top of 6ml of bovine serum albumin solution (16% in Hanks balanced saline solution (HBSS) at pH 7.4) at room temperature. This was then centrifuged (1000 x g, 20 °C) for 5 minutes and the supernatant layer removed to leave the cell pellet, which was re-suspended in 180 μ l neurobasal media containing 50 mg/ml glial cell line-derived neurotrophic factor (GDNF), 2 mM L-glutamine, 1 mg/ml nerve growth factor (NGF), 200 units/ml penicillin and 200 ng/ml streptomycin. 20 μ l of the cell suspension was pipetted onto sterilised glass cover slips, and incubated (37 °C, 5%CO₂) for 30minutes, (this was to produce a densely populated cell area in the centre of the cover-slip for ease of imaging) and then the remaining media was added to each sterilized cover-slip coated with poly-L-lysine and laminin and incubated (37 °C, 5%CO₂) overnight before intracellular calcium measurements.

3.2.1.3 Fura-2AM cell loading

Intracellular calcium concentrations were visualized by incubating cells with the calcium sensitive dye Fura-2AM (L-[2-(carboxyoxazol-2-yl)-6-amino-benzofuran-5-oxy]-2-(2'-amino-5'-methylphenoxy) ethane-N,N,N,N-tetraacetic acid pentaacetoxymethylester).

Cells were washed in Ca²⁺ buffer (see appendix for recipe), before a solution of 5 μ L Fura-2AM (see appendix for recipe) was added to the cells, which were incubated in the dark for 30minutes (37°C). Cells were washed in Ca²⁺ to remove extracellular Fura-2AM and kept in Ca²⁺ buffer for use in imaging.

3.2.1.4 Calcium imaging studies of DRG neurones

Intracellular Ca²⁺ concentration ([Ca²⁺]_i) in individual neurones was estimated as the ratios of the peak fluorescence emission intensities (measured at 500 nm) at excitation wavelengths of 340 and 380 nm respectively using an Improvion imaging system. Ratiometric imaging is a quantitative fluorescence application that provides a way to measure the concentration of intracellular calcium. Fura-2AM reversibly binds to cytosolic calcium, shifts its absorption maximum towards lower wavelengths upon binding to calcium. In its free form, Fura-2 has high excitation efficiency at 380 nm and low excitation efficiency at 340 nm. With calcium bound, the reverse is true: at 380 nm Fura-2 fluoresces with low excitant efficiency and at 340 nm with high excitant efficiency. Subsequently, the ratio between the two

fluorescence intensities measured at the two excitation wavelengths can be calculated.

The major advantage of ratiometric imaging is the ability to normalise for changes in fluorescence intensities that are unrelated to changes in dye loading. The temporal and spatial distribution of the measured fluorescence intensity can fluctuate, typically due to an unequal distribution of the fluorophore within the specimen, uneven cell thickness, or noise introduced by the imaging system itself, such as variations in the illumination intensity. Changes in calcium concentration are expressed as changes in ratio units. The Grynkiewicz equation (Grynkiewicz *et al.*, 1985) can be used to convert the ratio values into absolute calcium concentrations; however, the constants required by the equation such as the dissociation constant for Fura-2, R_{\max} and R_{\min} , are difficult to determine accurately and, as this study was concerned with changes in internal calcium levels, we have chosen to quote the fluorescence ratios which are directly proportional to the absolute calcium concentrations.

The mean diameter of the neurones studied was 25.7 ± 1.9 μm ($n=537$ neurones). This was estimated using Scion Image software (Scion Corporation).

Coverslips were fixed to a Perspex chamber using vacuum grease and DRG neurones were superfused (2 ml/min) with Ca^{2+} buffer.

The role of TRPV1 in modulating endocannabinoid levels and neuronal responses to TNF α

Drugs were initially dissolved in 100% ethanol to form a stock solution of 1mM, except tumor necrosis factor α (TNF α (10 μ g/ml) which was purchased as a solution in phosphate buffered saline.

DRG neurones were superfused (2 ml/min) with either the TRPV1 receptor agonist capsaicin (1 nM-1 μ M), or the cytokine TNF α (10, 30, 50, 100, or 200 ng/ml), or pretreated with TNF α (50 ng/ml) for 4 min before application of capsaicin (50 nM) for 1 min. Experiments were repeated in the presence of the P38 MAPK inhibitor SB706504 (10 μ M). Neurones were finally superfused (2 ml/min) with KCl (60 mM in Ca²⁺ buffer; 60s) to cause depolarisation-induced Ca²⁺ influx.

All drugs were made up in calcium buffer, and 45 minute washout periods with calcium buffer were carried out between applications of drugs to ensure drug application did not cause desensitisation.

Superfusion of neurones with KCl (60 mM) resulted in a depolarization-induced calcium influx, which was acted as a control response. The stimulated ratio was obtained by subtracting the basal conditions, from the ratio obtained during drug addition. Neurones with an increase in ratio less than 0.1units following KCl superfusion were considered to be non-responsive and excluded from analysis.

Changes in ([Ca²⁺]_i) were expressed as a percentage of the response to KCl. Data are expressed as mean \pm standard error of the mean (SEM). Statistical analysis was carried out using an unpaired Student's t-test. P values < 0.05 were deemed significantly different.

The Fura-2 pseudo-colour image of DRG neurons shows individual neurones under basal and stimulated conditions at excitation 340nm and 380nm, emission 510. Neurones fluoresce green at excitation wavelengths, and fluorescence appears more intense following capsaicin application, due to the increase in cytosolic calcium. The ratio pseudo-image shows neurones appearing red/yellow having an increase in $[Ca^{2+}]_i$ (figure 3.1).

3.2.2 Measurement of changes in $[Ca^{2+}]_i$ in hTRPV1-SHSY5Y cells

A human neuroblastoma cell line SHSY5Y transfected with TRPV1 receptors was used in this study. The cells were a generous gift from Prof Dave Lambert (University of Leicester). They were originally produced by GlaxoSmithKline (Stevenage, UK) as described in (Lam *et al*, 2007). Whilst it is possible to study neuronal activation *in vitro*, in primary cell cultures, such as DRGs, large cell numbers are required to measure endocannabinoid levels. These cultures only provide low yields, thus the neuronal cell line was used.

3.2.2.1 Cell Culture

Transfected SHSY5Y cells were grown to 80% confluence in T75 culture flasks and maintained in minimum essential media (MEM), supplemented with 10% foetal calf serum, 0.2 mmol/L L-glutamine, 2.5 μ g/ml fungizone, 100 IU/ml penicillin, 100 μ g/ml streptomycin and

The role of TRPV1 in modulating endocannabinoid levels and neuronal responses to TNF α

300 μ g/ml hygromycin B at 37°C in 5% CO₂. The initial transfection was sub-cloned in this medium.

3.2.2.2 Fluorimetric measurement of intracellular free calcium

Assay buffer for intracellular calcium measurements were freshly made on the day of experiments.

Confluent SHSY5Y cells were seeded into black walled clear base 96-well plates at a density of 30,000 cells/well over night in supplemented MEM excluding hygromycin B (Marshall et al, 2006).

Fluo-4AM aliquots (50 μ g) were initially prepared as a 1 mM solution in DMSO containing 10% pluronic acid. Cells were loaded in 2.3 μ M Fluo-4AM in MEM supplemented with 10% FCS and 2.5 mM probenecid (see appendix for recipe) for 30 minutes at 37°C in a humidified atmosphere of 5% CO₂.

Agonists and antagonists at varying concentrations were incubated with Fluo-4AM for 30 minutes (light sensitive). After an incubation period, the plate was loaded on the Flexstation (Molecular Devices) before the addition of varying concentrations of capsaicin or TNF α prepared in loading buffer (for recipe see appendix).

The Flexstation is a benchtop scanning fluorometer and integrated fluid transfer workstation used to measure fluorescence which can measure concentrations of free cytoplasmic calcium, ([Ca²⁺]_i) in cultured cells, using a 96-well plate format. The Ca²⁺-insensitive fluorescent dye, Fluo-4AM, permeates cell membranes as an ester and is hydrolyzed in the cell to its Ca²⁺-sensitive acidic form.

Fluorescence in the adherent cells is measured over time by using a bottom read of a 96-well plate. The machine monitors all the wells in a column over a time course, during which up to three compounds can be added robotically. Multiple columns are read sequentially for additional run times. Data are expressed as relative fluorescent units (RFU). Intracellular calcium levels were measured at excitation 485 nm and emission 520 nm. Capsaicin or TNF α was added after 20seconds. In separate experiments TNF α was added after 20 seconds, followed by capsaicin addition at 260 seconds. This was expressed as relative fluorescence intensity. Note: Fluo-4-AM and agonists/antagonists were not washed away before application of capsaicin or TNF α .

3.2.3 Western Blotting

DRGs were prepared as described earlier; with the exception that 33 μ l of cell suspension was added to a 6 well plate and incubated overnight in supplemented media. The following day, cells were washed with PBS, and treated with either TNF α , or buffer for 4 minutes. In separate experiments, cells were incubated with either the p38 MAPK inhibitor SB706504 (10 μ M) and TNF α or SB706504 alone for 4minutes. The supernatant was aspirated and DRGs were harvested in ice cold PBS by scraping. The cell suspension was centrifuged, supernatant removed and the cell pellet was lysed in 100 μ l lysis buffer (for composition see appendix a) containing Complete Mini protease inhibitor cocktail (from Roche). 1 tablet was added to 10 ml lysis buffer before use. The cell lysate was shaken for 30

The role of TRPV1 in modulating endocannabinoid levels and neuronal responses to TNF α

minutes at 4°C to ensure complete lysis. 10 μ l cell solution was transferred to another Eppendorf tube for protein quantification. The remaining solution was stored at -80°C Note: due to the low protein yield of DRG cultures, n=3 rats per drug treatment, and DRGs were re-suspended in a minimal volume of lysis buffer.

However, in cell membrane preparations, cells were lysed in 100 μ l TRIS/HCl buffer (see appendix for recipe). The cell solution was shaken for 30 minutes at 4°C to ensure lysis of cells, and then centrifuged at 40,000 x g for 30 minutes to pellet cell membranes. The cell supernatant was transferred to another Eppendorf tube, with 10 μ l of solution used for protein quantification.

3.2.3.1 hTRPV1-SHSY5Y sample preparation for western blot analysis

Cells were grown in T75 culture flask in supplemented MEM until 80% confluent. Medium was removed by aspiration, cells were washed with PBS, and harvested via scraping using ice cold PBS. The cell suspension was centrifuged, the supernatant removed and the cell pellet lysed in 200 μ l lysis buffer containing Complete Mini protease inhibitor cocktail. Whole cell samples were then prepared as described earlier.

15 μ l of 6x Laemmli solubilisation buffer (for recipe see appendix) were added to samples. Note: 6 x solubilisation buffers was used instead of 2 x due to low protein content.

The cell fraction was often very viscous after addition of solubilisation buffer, so samples were boiled at 95°C using a hotplate for 5 minutes, followed by centrifugation at 15,000 x g at 4°C for 5 minutes. Samples were used immediately or stored at -20°C for immunoblotting analysis.

3.2.3.2 Lowry protein assay

In order to compensate for the variation in cell numbers between different cell treatments, lysed cell pellets were assayed for total protein content using the Lowry method (Lowry *et al.*, 1951). Serial dilutions of standards were prepared as outlined in Table 3.1 using

Conc. (mg/ml)	0	0.05	0.10	0.15	0.20	0.25	0.30	0.35	0.40
H ₂ O (μ l)	500	475	450	425	400	375	350	325	300
BSA (μ l)	0	25	50	75	100	125	150	175	200

Table 3.1 Protein concentration serial dilutions from BSA.

200 μ l of each standard concentration and 200 μ l of diluted samples were transferred into a new microfuge tube. 1 ml of Lowry reagent (for composition, see appendix) was added to the samples and the standards. After 10 minutes, 100 μ l of Folin phenol reagent (1:1 diluted in Milli-Q-water) were added to the samples and the standards. After 45 minutes, 200 μ l of samples, blank and standards were loaded into a 96-well plate (in triplicate) and absorbance was

The role of TRPV1 in modulating endocannabinoid levels and neuronal responses to TNF α

measured at 750 nm, on a Dynatech Laboratories MRX spectrophotometric plate reader, using Dynex Revelation software. The correct protein concentration was calculated by multiplying the final value by the dilution factor of the samples, and protein concentrations were expressed in mg/ml.

3.2.3.3 Antibodies Used

Phospho-p38 (p-p38MAPK) primary antibody and p38 MAPK primary antibody were supplied by Cell Signalling Technology Inc. (NEW ENGLAND BIOLABS, UK). CB1 primary antibody was supplied by Calbiochem, TRPV1 primary antibody were supplied by Tocris, TNFR1 primary antibody was supplied by Abcam. P-p38 MAPK antibody detects p38 MAPK that is dually phosphorylated Thr180 (threonine 180) and Tyr182 (Tyrosine182). p38 MAPK detects endogenous levels of total p38 α , - β or - γ MAPK protein. CB₁ antibody detects amino acid sequence 1-77 of rat CB₁ receptor, TRPV1 detects C-terminal amino acids 822 to 838 of rat TRPV1 with a cysteine added at the N-terminus of the peptide for conjugation to keyhole limpet haemocyanin (KLH). TNFR1 antibody detects Synthetic peptide sequence: GLVPHLGDREKRDSV, corresponding to amino acids 29-43 of Human TNF Receptor I. A polyclonal infrared goat anti-rabbit secondary antibody supplied by LiCor Biosciences (Cambridge, UK) was used to label antibodies at 700-800nm infrared emission wavelengths for all antibodies except p-p38 MAPK, where Goat anti-mouse antibody was used. These secondary antibodies were used for samples analysed using

Odyssey system. For samples quantified using ECL, A polyclonal goat anti-rabbit secondary antibody (used for all antibodies, excluding p-p38MAPK, where goat anti-mouse secondary antibody was used) supplied by Sigma (UK) was used to bind to the primary antibodies. GAPDH and β -actin was used to confirm equal protein loading of samples.

3.2.3.4 Running the gels

10% Sodium dodecyl sulphate (SDS) polyacrylamide gel electrophoresis (SDS-PAGE) gels (resolving gel) were prepared according to the manufacture's instruction for use with a Bio-Rad Mini Protean III apparatus for Western blotting. A 4% SDS-PAGE gel (stacking gel) layered on top of the resolving gel was used for loading samples. Precision Plus Protein all blue standards (5 μ l) were used as markers supplied by Bio-Rad Laboratories Ltd (UK). This marker contains ten proteins of the following molecular weights: 10, 15, 20, 25, 37, 50, 75, 100, 150, and 250 kD. Samples containing about 1 μ g protein per lane were loaded (in 10 lane gels). The gels were run in loading buffer (for composition, see appendix-A) at 200 V (constant) for 45 minutes, or until the dye front ran off the gel.

The proteins were then transferred onto nitrocellulose membranes in transfer buffer (for composition, see appendix-A) using a Bio-Rad Kit at 100 V for 60 minutes in a cold room (at 4°C). Nitrocellulose membranes (blots) were tested for satisfactory protein transfer with Ponceau red stain (supplied by Bio-Rad). The stain was then washed away with Milli-Q-water. The blots were then blocked in blocking

buffer [5% fat-free dried milk powder in TBST buffer (for composition, see Appendix) for 60 minutes at room temperature with gentle shaking. The blots were washed twice with TBST buffer and incubated with the primary antibody at a 1:1000 dilution, made up in blocking buffer, overnight at 4°C. Next day, the blots were washed three times with TBST buffer, and washed three times with TBST for 15 minutes.

The blots were then incubated with secondary antibody at a 1:2000 dilution, made up in blocking buffer, for 60 minutes at room temperature. The blots were then washed with TBST buffer as previously, and finally washed with Milli-Q-water.

3.2.3.5 Visualising the protein bands- ECL

The blots were exposed to ECL detection solution (equal volumes of solution 1 (luminal/enhancer solution) & 2 (peroxide buffer solution) prepared just prior to the use) for one minute. The blots were dried (by placing between two filter papers) and wrapped in SaranWrap® cling film. The blots were placed in an X-ray cassette and exposed to Hyperfilm ECL autoradiography film (from Amersham Biosciences, U.K.), in dark room for up to 5 minutes. The films were then developed and fixed using Kodak GBX developer (from Sigma-Aldrich, U.K.) and Ilford Hypam rapid fixer (From Ilford Imaging Ltd, U.K.). Proteins bands were detected based on the principle of enhanced chemiluminescence.

3.2.3.6 Densitometry

The developed Western blot films were scanned using a GS-710 Imaging Densitometer (Bio-Rad) on transmission mode using the Quantity One software package for image analysis.

3.2.3.7 Running Gels- Odyssey

Carried out by Liaque Latif

Unlike conventional Western blotting, where diffusion is the primary means of reagent transport, the SNAP i.d. system applies a vacuum to actively drive reagents through the membrane, which is less time consuming. The Snap ID cassettes were soaked in dH₂O for approximately 1 minute and laid out for immunoblotting. The nitrocellulose was placed in the cassette (molecular marker face down), and rolled to remove bubbles. The cassette was placed in Snap ID and the nitrocellulose is blocked with 1.5% concentration of fish skin gelatine. (Stock is 45%, so need to dilute 1:30 in TBST). The blocking agent was poured over the nitrocellulose blot and pulled through via vacuum. A 1/1000 dilution of primary antibody was used in 1.5% fish skin gelatine, antibodies are left on for 10 minutes, ran through Snap ID and then washed three times with TBST. 1/2000 dilution of the 2^o antibody was also used in 1.5% fish skin gelatine, and was pipetted over nitrocellulose for a further 10 minutes (Note: secondary antibodies are light sensitive, thus Snap ID box was

covered). This was then run through Snap ID, washed three times with TBST and the nitrocellulose removed and placed in dH₂O.

The nitrocellulose blot was placed moist, upside down and analysed using Odyssey infrared imaging system.

3.2.4 Endocannabinoid Measurements

DRG neurones were prepared in a similar manner to that of the Western blot sample analysis. Neurones were treated with capsaicin (1 nM, 10 nM, 100 nM, or 1 μ M) for 1 minute (as in calcium imaging experiments). The supernatant was removed and stored at -80°C and neurones were removed via scraping. However, due to low cell number and sample weight, we were unable to measure endocannabinoids in DRG neurones, therefore the effects of various agonists and antagonists on endocannabinoid levels were investigated in hTRPV1 SHSY5Y. Experiments were designed to mimic previous calcium imaging experiments. hTRPV1 SHSY5Y cells were grown to approximately 80% confluence in supplemented MEM. Cells were washed with PBS before the addition of capsaicin (1 nM-1 μ M) for 1 minute. The supernatant was removed and stored on dry while, while cells were harvested via scraping in ice cold PBS. The effects of IRTX (100 nM) and URB597 (1 μ M) on capsaicin-evoked endocannabinoid release were also investigated.

Cells were washed in PBS followed by addition of either IRTX (100 nM) for 1 minute or URB597 (1 μ M) for 4 minutes (Millins *et al*, 2006),

followed by addition of 10 nM capsaicin (EC_{50} value) for 1 minute. The supernatant was removed and stored on dry while, while cells were harvested via scraping in ice cold PBS. Following collection, samples were stored at -80°C until analysis.

The processing of samples with extraction and analysis of analytes is described in detail in Chapter 2. Cells were homogenised in ice-cold acetonitrile, samples were shaken twice at 4°C for 1 hour and the supernatant collected. Samples were dried under vacuum and reconstituted in 100 μL Acetonitrile. 5 ml Acetonitrile was added was added to the supernatant collected from cell treatment. Samples were shaken twice at 4°C for 1 hour and the supernatant collected. Samples were dried under vacuum and reconstituted in 100 μL acetonitrile.

The LC-MS/MS method allowed for the quantification of AEA, 2-AG, virodhamine, OEA, PEA, 2-LG, and COX-2 metabolites of AEA, and 2-AG (i.e. PG-EA and PG-GE). AEA-d8, 2-AG-d8 and PGF2 α -EA-d4 were used as internal standards.

3.3 Results

The response of DRG neurones to 100nM capsaicin, Figure 3.1 shows examples of images captured during calcium imaging experiments. The DRGs examined had a mean diameter of 25.7 ± 1.9 μm and are, thus, classified as small diameter neurones.

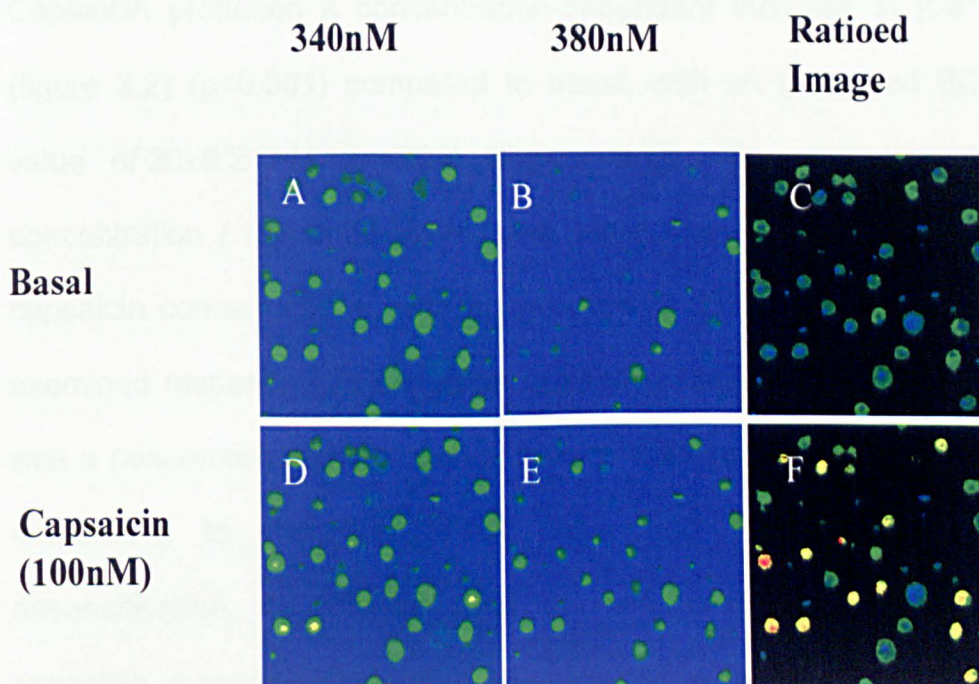


Figure 3.1 Ratiometric calcium pseudocolour images of DRG neurones in the presence and absence of capsaicin. Fluorescence emission measured at wavelengths: 340nm and 380nm under basal conditions (A+B) and after capsaicin administration (D+E). Fluorescing cells appear green. The ratio image shows the ratio between light emitted at 340/500 nm and 380/500 nm, under basal conditions (C), and after capsaicin (100nM) administration (F). Cells that appear yellow/orange after capsaicin administration, compared to green under basal conditions, have an increase in intracellular calcium.

3.3.1 Effects of varying concentrations of capsaicin on intracellular calcium responses in adult rat dorsal root ganglion neurones *in vitro*

In untreated DRG neurones, the 340/380 nm ratio (reflecting basal intracellular calcium concentration $[Ca^{2+}]_i$) was 3.4 ± 1.5 % KCl response ($n = 364$).

Capsaicin produced a concentration-dependent increase in $[Ca^{2+}]_i$ (figure 3.2) ($p < 0.001$) compared to basal, with an estimated EC_{50} value of 20 ± 0.2 nM, ($n = 204$) (Figure 3.2). In generating the concentration / response curve, cells were exposed to a range of capsaicin concentrations, with an average of 38% of the neurones examined responding to capsaicin at varying concentrations. There was a concentration-dependant increase in the number of neurones responding to capsaicin (Table 3.2), and little evidence of desensitisation. 45 Minutes after an initial exposure to 100nM capsaicin, a second exposure of the cells to the same concentration, produced a signal that was $81 \pm 7\%$ ($n = 26$) of the first response (Figure 3.3).

Capsaicin concentration (μ M)	% cell responding
0.001	9.2 \pm 3.4
0.01	24.8 \pm 9.6
0.05	29.7 \pm 11.3
0.1	36.3 \pm 14.2
0.3	49.2 \pm 19.1
1	67.1 \pm 23.1

Table 3.2 percentage of small diameter DRG neurones responding to varying concentrations of capsaicin.

To confirm that this response was TRPV1-mediated, DRG neurones were pre-treated with the competitive TRPV1 antagonist IRTX (100 nM), and then superfused with varying concentrations of capsaicin. Pretreatment with IRTX (100 nM) significantly inhibited capsaicin-evoked increases in $[Ca^{2+}]_i$ causing a rightwards shift in the capsaicin concentration/ response curve. This allowed an inhibition constant (K_i) of 7 nM to be calculated.

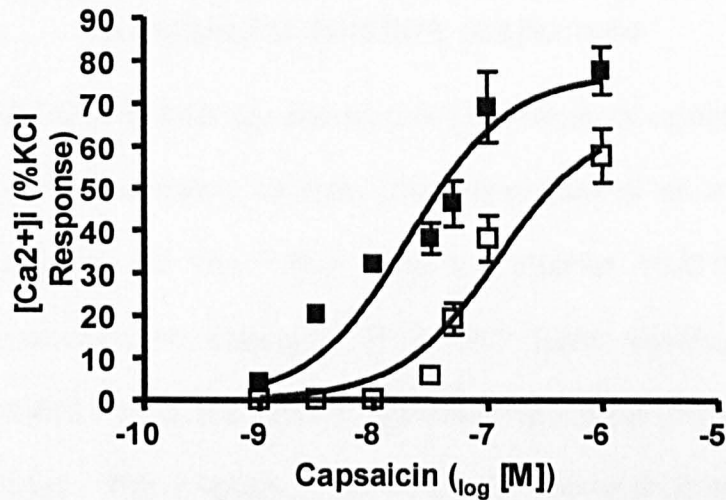


Fig 3.2 Effects of capsaicin (closed bars) and capsaicin + IRTX (100 nM) (open symbols) on $[Ca^{2+}]_i$ in DRG neurones, expressed as a percentage of KCl response. $n=37-61$ neurones per concentration from 3 rats.

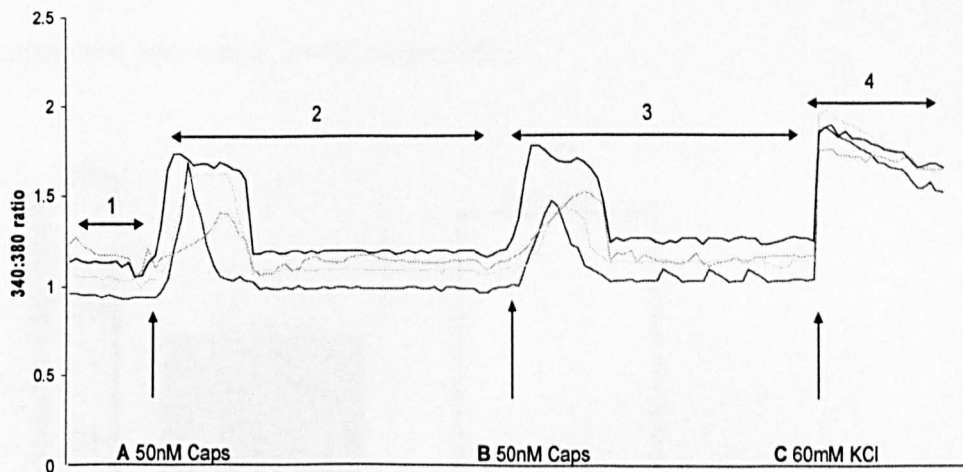


Figure 3.3 A representative trace showing changes in 340: 380 nm ratios in four individual DRG neurones, in response to capsaicin. Recordings of 340:308 ratio were made at various time points, where 1= 2minute recording, 2 and 3 = 46 minute recording, 4= 3 minute recording. At point A, the cell was exposed to capsaicin (50 nM) for 60 s. Forty-five minutes later, at point B, capsaicin (50 nM) was reapplied with no evidence of desensitisation. After another 45 min (C) KCl (60 mM) was applied to depolarize neurones.

3.3.2 The role of CB₁ receptors in modulation of intracellular calcium responses

We have previously shown that CB₁ receptor agonists can modulate capsaicin-evoked calcium responses (Millns et al., 2001). In the presence of the CB_{1/2} receptor agonist HU210 (1 μ M), peak responses to capsaicin (100 nM) were significantly reduced to $44.4\pm 2.7\%$ of the control capsaicin response (Figure 3.4; $P < 0.001$, $n = 58$). Pre-incubation with the CB₁ receptor antagonist AM251 (1 μ M) partly reversed the inhibitory effect of HU210 (1 μ M) on the capsaicin (100 nM)-evoked response ($67.9\pm 2.8\%$ of control response, $n = 48$ neurones, Figure 3.4). AM251 alone had no significant effect on capsaicin-evoked responses ($92\pm 2\%$ of control capsaicin response, $n = 37$ neurones).

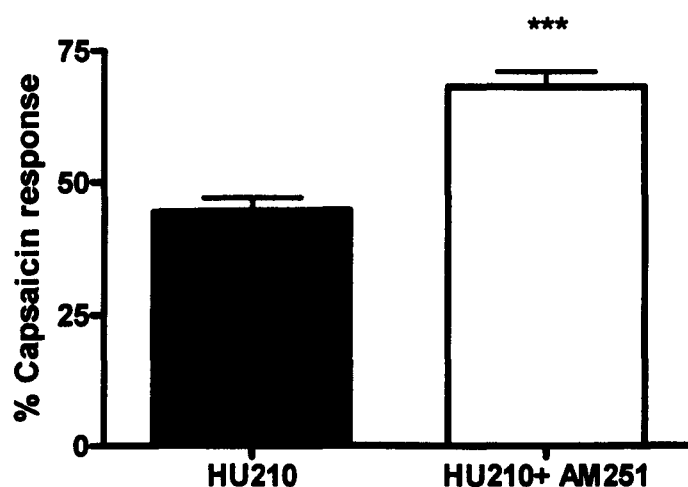


Figure 3.4 Inhibition of capsaicin-evoked calcium responses in the presence of HU210 and reversal by AM251 in DRG neurones. Results are expressed as percentages of the responses to 100 nM capsaicin alone. In the presence of HU210 (1 μ M) the capsaicin response was reduced to $44.4\pm 2.7\%$ of control ($P < 0.001$, $n = 58$). Co-administration of AM251 (1 μ M) partially reversed this to $67.9\pm 2.8\%$ of control ($***P < 0.001$, Mann Whitney, compared with HU210).

3.3.3 Effects of capsaicin on endocannabinoid levels in rat DRG neurones

The effects of varying concentrations of capsaicin on levels of endocannabinoids (ECs) in rat DRG neurons were investigated. Levels of OEA were significantly reduced following capsaicin application, while levels of PEA and 2-AG were unaltered following capsaicin application; however, levels of AEA were below the limit of quantification (Table 3.3), due to the small cell yield from DRG cultures. Therefore, as an appropriate alternative, a neuronal cell line was used to investigate the role of TRPV1 activation in EC synthesis.

Treatment	AEA pmol/g		OEA nmol/g		PEA nmol/g		2-AG nmol/g	
	Cell	Super	Cell	Super	Cell	Super	Cell	Super
Capsaicin	ND	ND	6.45 \pm 0.89**	5.28 \pm 0.16**	15.49 \pm 3.57	38.77 \pm 8.45	ND	ND
Vehicle	ND	ND	13.39 \pm 1.75	14.02 \pm 1.46	14.50 \pm 0.73	89.20 \pm 65.38	ND	ND

Table 3.3 Levels of ECs in rat DRG neurone cultures expressed as g wet weight, following treatment for 1 minute with 100nM capsaicin or vehicle. Data were analysed using Mann-Whitney non-parametric testing, **P<0.01 vs vehicle treated cells. Abbreviations; ND=not detected (below level of quantification; AEA=2.5pmol/g, 2-AG=10nmol/g), super=supernatant.

3.3.4 hTRPV1 SHSY5Y

Primary neuronal cell culture produces low cell yields, which proved to be insufficient for the routine measurement of ECs. Currently, there is a lack of neuronal models available that natively express TRPV1 receptors, TRPV1 have been studied in heterologous expression systems such as HEK cells and CHO cells (Caterina et al., 1997, Hayes et al., 2000, Lam et al., 2005); however, these do not provide a neuronal environment that models the situation in sensory nerves. It has proved to be difficult to obtain stable TRPV1 transfects in neuronal host cells but we have been fortunate to obtain SHSY5Y human neuroblastoma cells that stably express TRPV1 receptors from Prof David Lambert (University of Leicester). The cells exhibit a pharmacological profile consistent with endogenous TRPV1 receptor expression in neurones (Lam et al., 2007) .

3.3.5 Capsaicin concentration/response in hTRPV1 transfected SHSY5Y cells

Capsaicin produced a statistically significant, concentration-related increase in $[Ca^{2+}]_i$ ($p < 0.001$), compared to basal, with an estimated EC_{50} value of 9 nM, ($n=4$) (Figure 3.5). This was similar to the EC_{50} of 20nM in primary DRGs (Figure 3.2). To confirm that this response was TRPV1-mediated, SHSY5Ys were pre-treated with the TRPV1 selective antagonist IRTX (100 nM), and then superfused with

increasing concentrations of capsaicin. IRTX treatment significantly inhibited capsaicin-evoked increases in $[Ca^{2+}]_i$ causing a rightwards shift in the capsaicin concentration/ response curve, allowing calculation of a K_i value of 30 nM for IRTX (compared with 7 nM in DRGs; Figure 3.2).

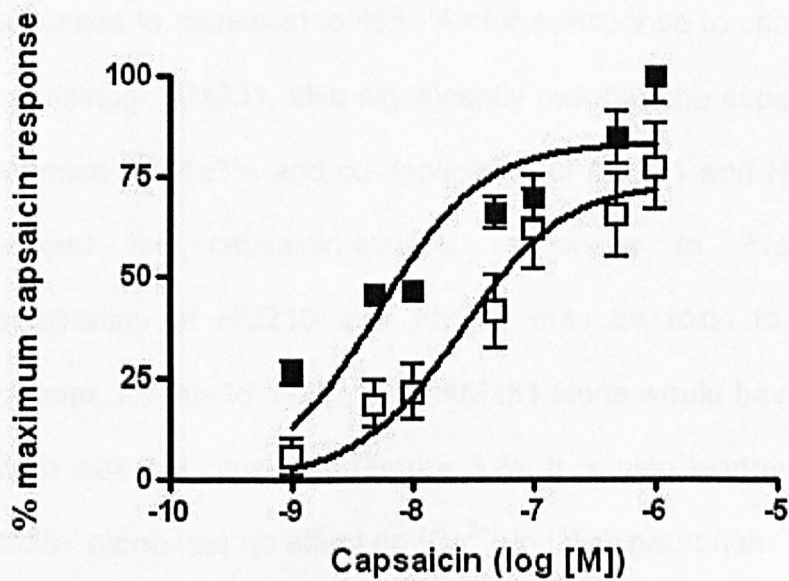


Figure 3.5 Effects of capsaicin (closed symbols) and capsaicin + IRTX (10nM) (open symbols) on $[Ca^{2+}]_i$ in hTRPV1 SHSY5Y cells, expressed as a percentage of the maximum capsaicin response. n=3 separate experiments carried out on Flexstation.

We and others have shown that CB_1 receptors present on rat DRGs are functional and that they can modulate nociceptive responses (Hohmann and Herkenham, 1999, Ahluwalia et al., 2000, Millns et al., 2001, Sagar et al., 2005, Millns et al., 2006). Therefore, the effects of CB_1 agonists and antagonists in SHSY5Ys were investigated.

3.3.6 Cannbinoid response in hTRPV1-SHSY5Y cells

Cells were incubated with either the CB_{1/2} receptor agonist HU210 (1 μ M), the CB₁ receptor antagonist AM251 (1 μ M) or a combination of both for 30 minutes prior to exposure to 10 nM capsaicin (approximate EC₅₀ value). Neither HU210 (1 μ M) nor AM251 (1 μ M) had any effect alone on [Ca²⁺]_i. HU210 significantly reduced calcium responses to capsaicin to 49 \pm 4% of the response to capsaicin alone. Surprisingly, AM251, also significantly reduced the capsaicin-evoked response to 71 \pm 3% and co-application of AM251 and HU210 further reduced the capsaicin-evoked responses to 21 \pm 3%. The combination of HU210 and AM251 may be toxic to these cells; however, for this to be the case AM251 alone would have to be toxic, which was not observed (Figure 3.6). It is also worthy of note that AM251 alone had no effect on [Ca²⁺]_i in DRG neurones.

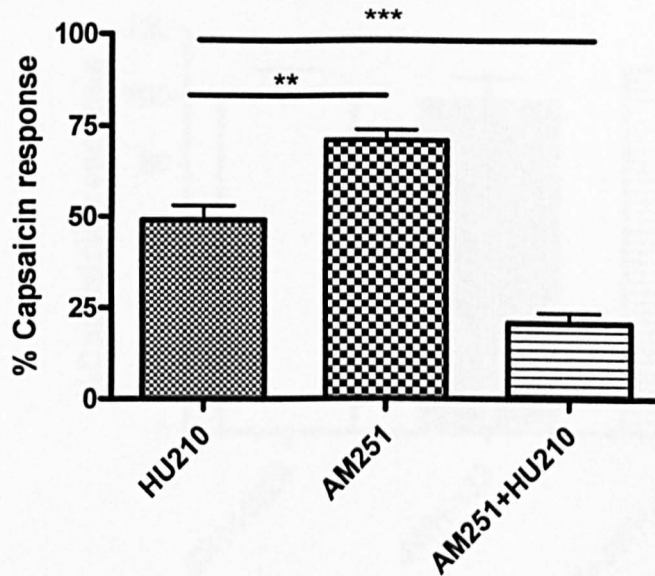


Figure 3.6 Inhibition of capsaicin responses in the presence of HU210 or AM251 separately and in combination. Results are expressed as percentages of the responses to 10 nM capsaicin alone. In the presence of HU210 (1 μ M) the capsaicin response was reduced to 49 \pm 4% of control (P <0.001, n =3). AM251 also reduced the capsaicin response to 71 \pm 3% (P <0.05, n =3). Co-administration of AM251 (1 μ M) further reduced this response to 21 \pm 3% of control (** P <0.005), compared with HU210 plus capsaicin.

The potential function of CB₂ receptors in SHSY5Y was also investigated to see if activation could modulate calcium responses. The CB₂ receptor agonist JWH-133 (1 μ M) and CB₂ antagonist SR144528 (1 μ M) were, however, without effect on capsaicin responses (Figure 3.7).

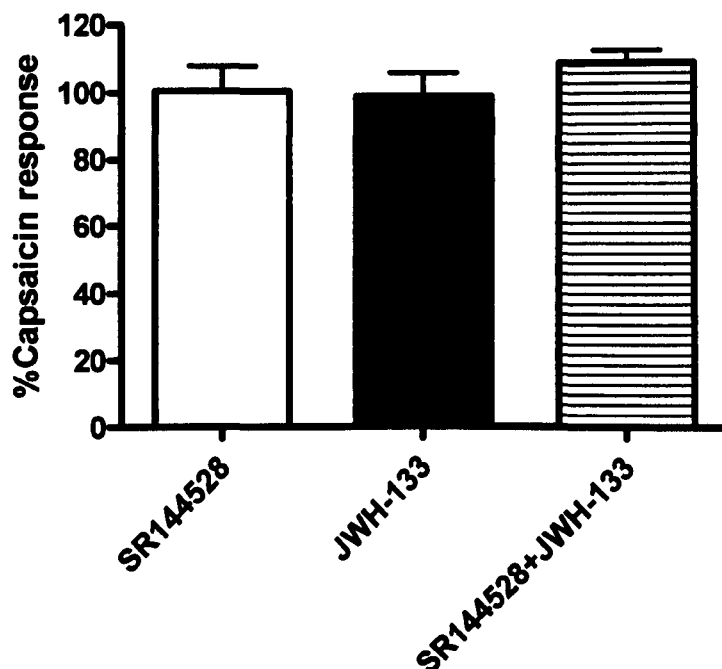


Figure 3.7 Capsaicin responses in the presence of SR144528, JWH-133 separately and in combination. Results are expressed as percentages of the responses to 10 nM capsaicin alone.

CB₁ receptor expression in TRPV1-transfected SHSY5Y cells was compared to CB₁ receptor expression in rat DRG neurones and untransfected SHSY5Y cells. Due to the lack of effect of CB₂ receptor ligands in modulating capsaicin-evoked calcium responses, it was decided only to investigate CB₁ receptor expression.

CB₁ receptor protein appeared to be expressed by rat DRG neurones; in immunoblots; a faint band was detected at approx 60 kDa, (Figure 3.8), consistent with previous reports (Song and Howlett, 1995, Matias et al., 2002, Porcella et al., 2002, Wager-Miller et al., 2002).

Both hTRPV1 and native SHSY5Y stained positive for the CB₁ receptor protein, although the bands were detected at a slightly lower

The role of TRPV1 in modulating endocannabinoid levels and neuronal responses to TNF α

mass than the rat CB₁ band, which may be due to species differences in post-translational modification (Figure 3.8).

On the basis of desitometric analysis, CB₁ bands from the native and transfected SHSY5Y cells and rat DRG neurones appeared to show equal levels of expression when normalised to GAPDH.

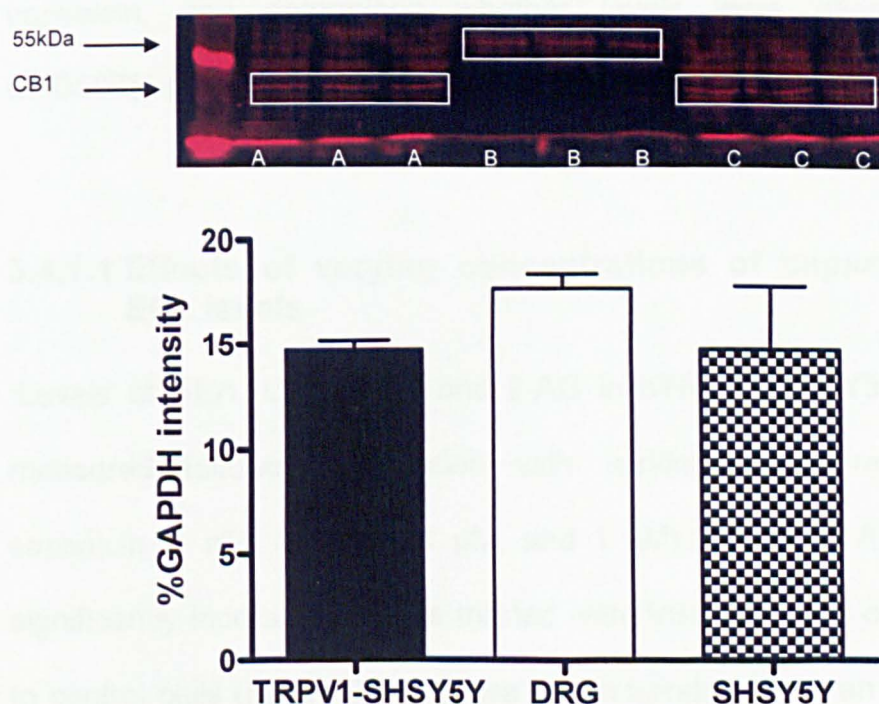


Figure 3.8 Quantification of CB₁ receptor protein expression in rat DRG neurones (B), hTRPV1 SHSY5Y (A), and SHSY5Y (C) cells detected by Western blotting and quantified using Odyssey. Rat DRG primary neuronal cultures were prepared from 3 rats. SHSY5Y cells were from 1 flask 70% confluent at passage numbers 14-23. Data are expressed as percentages of GapDH intensity mean \pm SEM (n=3 separate experiments).

3.4 Endocannabinoid levels in htrpv1-SHSY5Ys cells and supernatant

It is well documented that ECL synthesis is stimulated by increases in intracellular calcium and previous authors have suggested that TRPV1 might be a key player in controlling synthesis via intracellular AEA activation of the receptor channel. To investigate this further, we measured ECL levels in hTRPV1-SHSY5Y cells, and in the cell supernatant following stimulation with a range of concentrations of capsaicin, and determined whether levels were altered with URB597 (1 μ M) or IRTX (100 nM) treatment.

3.4.1.1 Effects of varying concentrations of capsaicin on ECL levels

Levels of AEA, OEA, PEA and 2-AG in hTRPV1-SHSY5Ys were measured following incubation with varying concentrations of capsaicin (1 nM, 10 nM, 0.1 μ M, and 1 μ M). Levels of AEA were significantly increased in cells treated with 1nM capsaicin compared to control cells (Figure 3.9). There was a trend towards an increase in 10 nM, 0.1 μ M, and 1 μ M capsaicin-treated cells; although significance was not reached. Levels of 2-AG were significantly higher only in cells treated with 0.1 μ M capsaicin compared to control cells. Interestingly, there was a decrease in levels of PEA following capsaicin treatment (1 nM, 10 nM, 0.1 μ M, and 1 μ M), whereas levels of OEA were not significantly altered by capsaicin (Figure 3.9). Given the concentration-dependent effects of capsaicin on $[Ca^{2+}]_i$,

shown earlier, it is, therefore, clear that there was no correlation between whole cell endocannabinoid levels and $[Ca^{2+}]_i$.

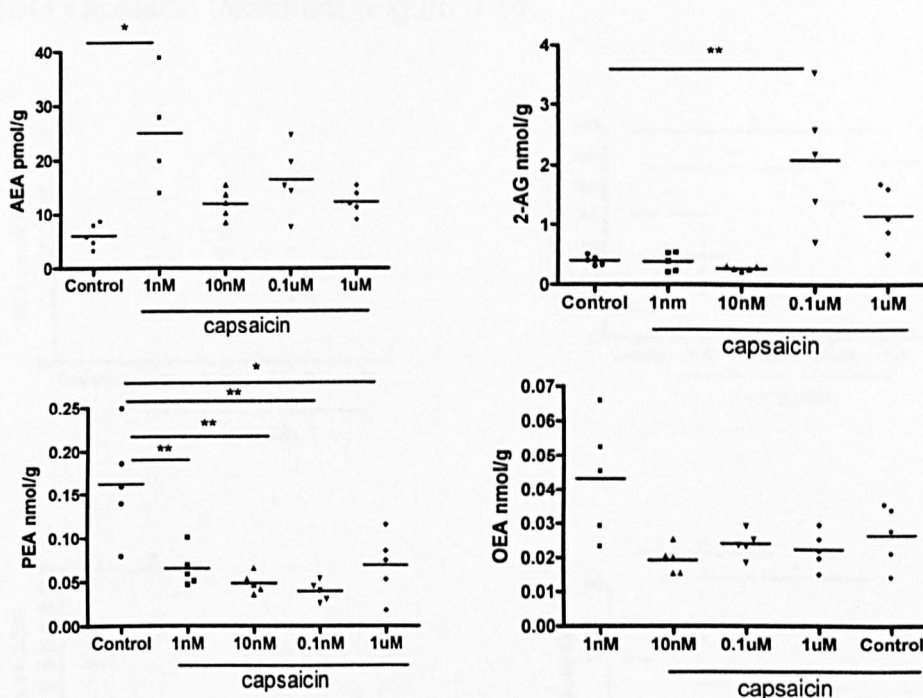


Figure 3.9 Effects of varying concentrations of capsaicin or PBS (control) on the levels of endocannabinoids in hTRPV1 SHSY5Y cells. Data were analysed using the Mann-Whitney non-parametric test and expressed as the median and range, (n=4-5 separate experiments). *P<0.05, **P<0.01 vs. control treated cells.

Levels of ECs in the supernatant followed a similar trend to that observed in the whole cells after capsaicin treatment. Levels of AEA in the supernatant appeared, if anything, to decrease with increasing capsaicin concentration and were undetectable/below the limit of detection in control and 1uM capsaicin-treated cells. Capsaicin treatment had no clear effect on levels of PEA and OEA, with levels significantly lower following 10 nM and 1 μ M capsaicin treatment, compared to control supernatants (Figure 3.10).

Interestingly, levels of 2-AG were elevated following treatment with capsaicin, with levels of 2-AG at their highest following 0.1 μ M and 1 μ M capsaicin treatment (Figure 3.10).

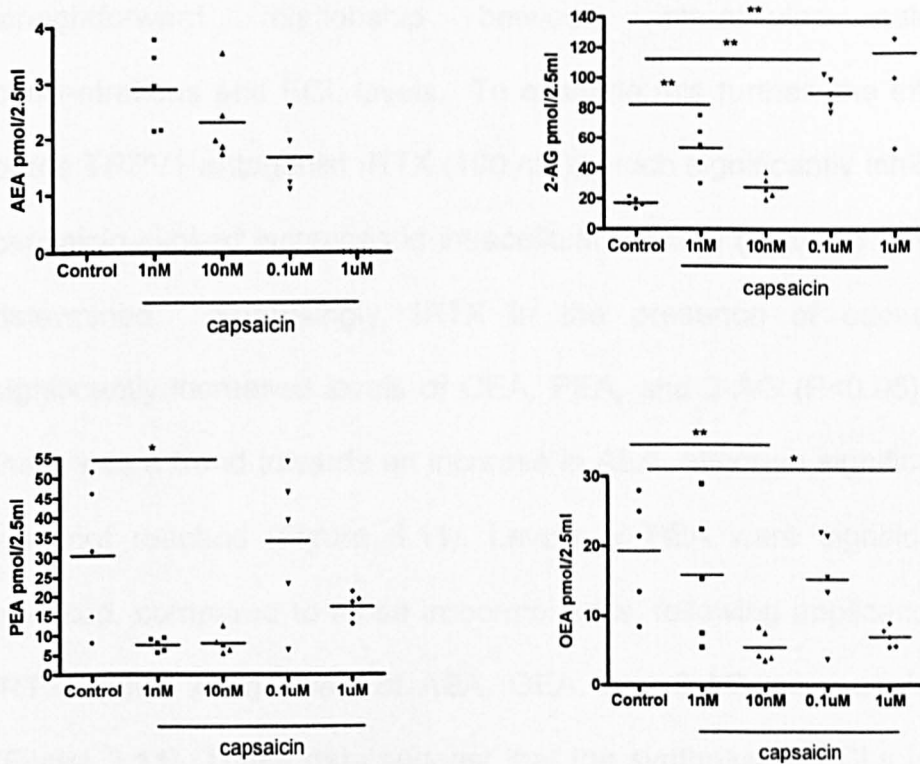


Figure 3.10 Effects varying concentrations of capsaicin or PBS (control) on the levels of endocannabinoids in hTRPV1 SHSY5Y cell supernatant. Data were analysed using the Mann-Whitney non-parametric test and are expressed as the median and range, (n=4-5 separate experiments). *P<0.05, **P<0.01 vs. control cell supernatant.

A correlation analysis of the levels of ECLs in the whole cells and cell supernatants was undertaken to investigate the relationship between cell and released ECLs. Spearman rank correlation coefficients (R^2) were calculated and demonstrated that there was no correlation between intracellular and extracellular levels of ECLs, regardless of the concentration of capsaicin (data not shown).

3.4.1.2 Effects of IRTX (100nM) and capsaicin (10nM) on ECL levels

It is apparent from the data shown above that there is no straightforward relationship between intracellular calcium concentrations and ECL levels. To examine this further, the effects of the TRPV1 antagonist IRTX (100 nM), which significantly inhibited capsaicin-evoked increases in intracellular calcium (Figure 3.5) were determined. Surprisingly, IRTX in the presence of capsaicin, significantly increased levels of OEA, PEA, and 2-AG ($P < 0.05$) and there was a trend towards an increase in AEA, although significance was not reached (Figure 3.11). Levels of PEA were significantly elevated, compared to those in control cells, following application of IRTX alone, while levels of AEA, OEA, and 2-AG were unaltered (Figure 3.11). These data suggest that the synthesis of ECLs is not simply enhanced by increasing $[Ca^{2+}]$, at least via TRPV1 activation.

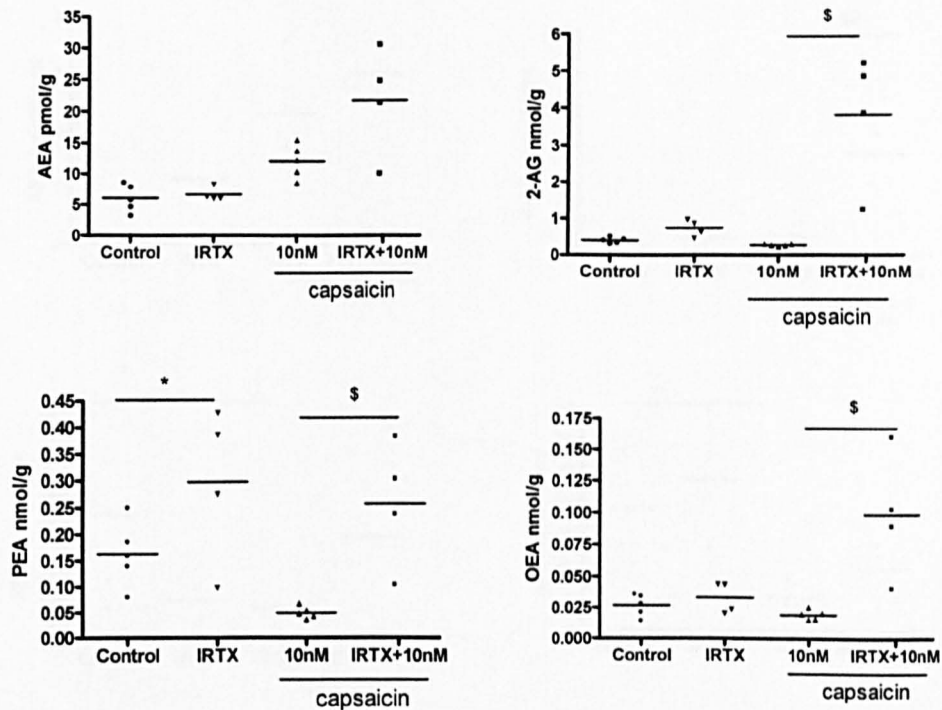


Figure 3.11 Effects capsaicin (10 nM) and IRTX(100 nM) on the levels of endocannabinoids in hTRPV1 SHSY5Y cells. Data were analysed using Mann-Whitney non-parametric testing and are expressed as the median and range, (n=4-5 separate experiments). *P<0.05 vs. c ontrol treated cells, \$P<0.05 vs. IRTX (100 nM) + capsaicin (10 nM). The control and 10nm EC levels were taken from the previous set of experiments.

However, in the extracellular medium, levels of PEA, OEA and 2-AG were decreased following pre-treatment with IRTX (10 nM) compared to control (Figure 3.12). Treatment with capsaicin and IRTX did not further alter levels of PEA, OEA or 2-AG; levels of AEA were unaltered following IRTX treatment, in the presence and absence of capsaicin (Figure 3.12).

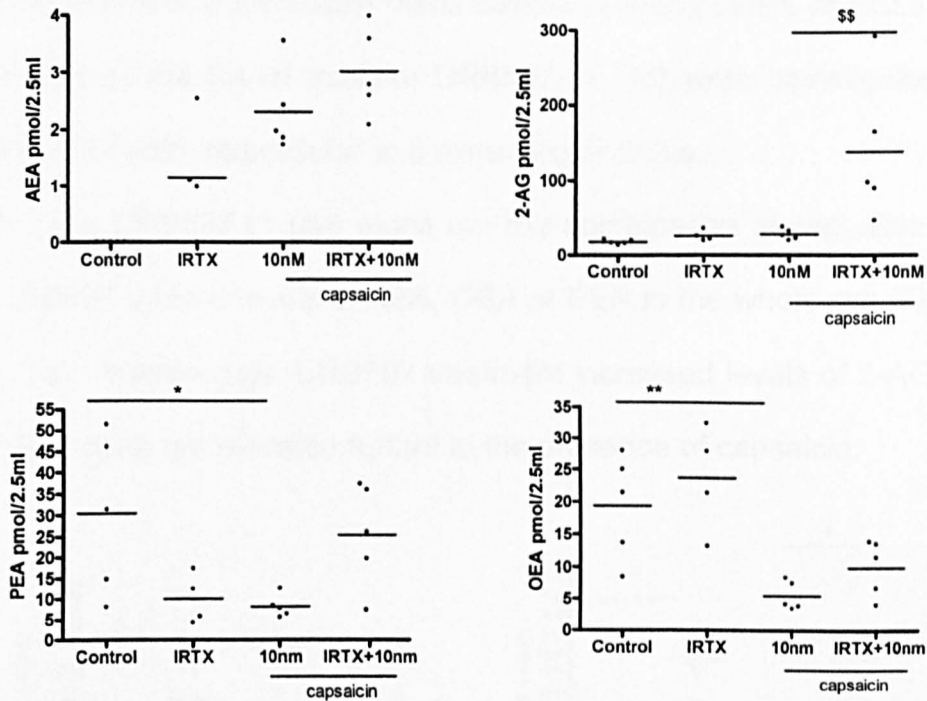


Figure 3.12 Effects of capsaicin (10 nM) and IRTX (100 nM) on the levels of endocannabinoids in hTRPV1 SHSY5Y cell supernatants. Data were analysed using Mann-Whitney non-parametric testing and are expressed as the median and range, (n=4-5 separate experiments). *P<0.05, **P<0.01 vs. control treated cell supernatant, \$\$P<0.01 vs. IRTX (100nM) + capsaicin (10nM). The control and 10nm EC levels were taken from the previous set of experiments.

3.4.1.3 Effects of URB597 (1 μ M) and capsaicin (10 nM) on ECL levels

It was expected that capsaicin-induced increases in $[Ca^{2+}]_i$ would enhance ECL synthesis. However, this was not reflected in increased levels of ECLs in the cells or supernatants. Given that extracellular levels were unaltered, it is unlikely that the effects of any increased synthesis were masked by transport out of the cells. Another possibility is that capsaicin also increased ECL metabolism, thereby blunting any increases in parent ECL levels. To investigate the

The role of TRPV1 in modulating endocannabinoid levels and neuronal responses to TNF α

potential role of increased metabolism in altering levels of ECLs, the effects of the FAAH inhibitor URB597 (1 μ M) were investigated on levels of both intracellular and extracellular ECLs.

Neither URB597 (1 μ M) alone nor the combination of capsaicin and URB597 altered levels of AEA, OEA or PEA in the whole cell (Figure 3.13). Interestingly, URB597 treatment increased levels of 2-AG but these were not elevated further in the presence of capsaicin.

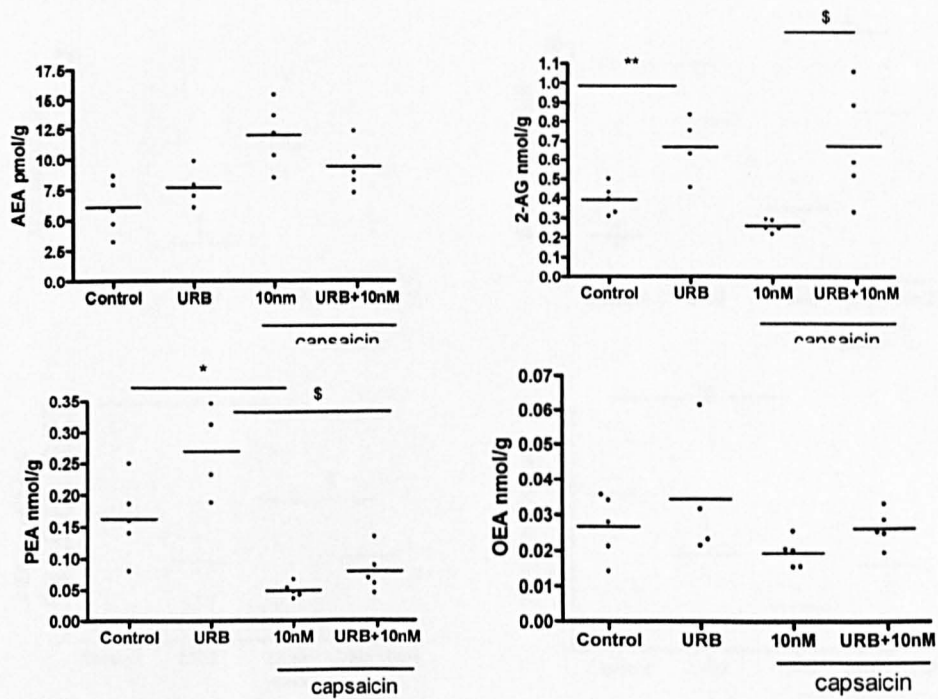


Figure 3.13 Effects of capsaicin (10 nM) and URB597 (1 μ M) on the levels of endocannabinoids in hTRPV1 SHSY5Y cells. Data were analysed using the Mann-Whitney non-parametric test and are expressed as the median and range, (n=4-5 separate experiments). **P<0.01 vs. control treated cells, \$P<0.05 vs. URB597 + capsaicin (10 nM). The control and 10 nM ECL levels were taken from the previous set of experiments.

In relation to the cell supernatants, neither URB597 (1 μ M) alone nor the combination of capsaicin and URB597 altered the levels of AEA, PEA and OEA compared to control (Figure 3.14). The effects on 2-AG supernatant levels mirrored those in the whole cells; URB597 alone increased 2-AG but this was not enhanced further in the presence of capsaicin.

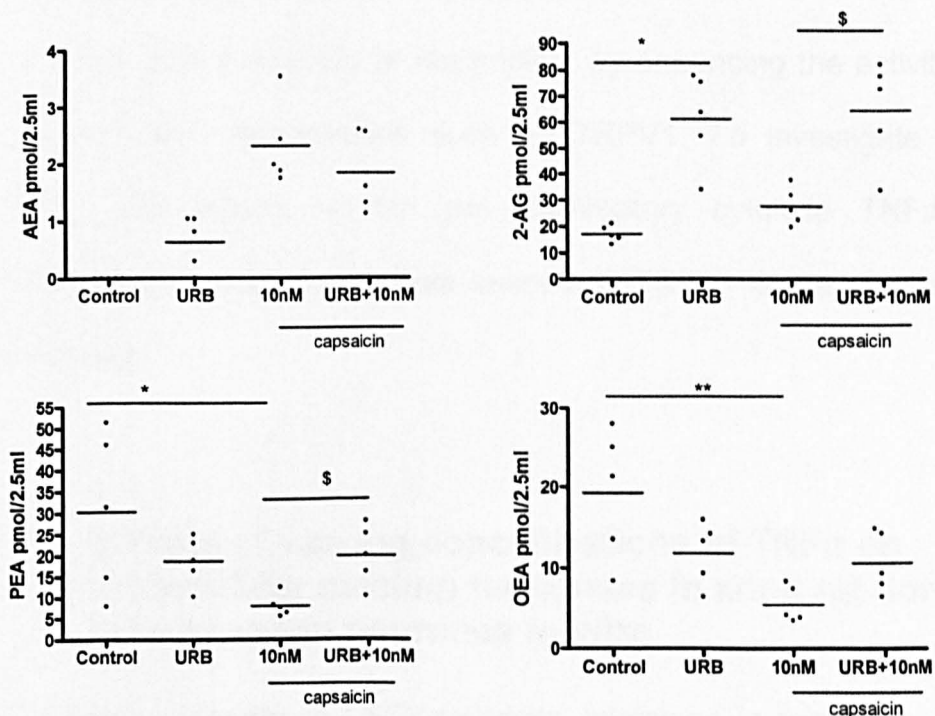


Figure 3.14 Effects of capsaicin (10 nM) and URB597 (1 μ M) on the levels of endocannabinoids in hTRPV1 SHSY5Y cell supernatant. Data were analysed using Mann-Whitney non-parametric testing and are expressed as the median and range, (n=4-5 separate experiments). *P<0.05, **P<0.01 vs. control treated cell supernatant, $^{\$}$ P<0.05 vs. URB597 (1 μ M) + capsaicin (10 nM). The control and 10 nm ECL levels were taken from the previous set of experiments.

A correlation analysis of the levels of ECLs in the cell and cell supernatant was also undertaken following URB597 application in

The role of TRPV1 in modulating endocannabinoid levels and neuronal responses to TNF α

the presence and absence of capsaicin (10 nM). Spearman rank correlation coefficient (R^2) analysis demonstrated that there was no correlation between levels of intracellular and extracellular, ECLs following URB597 treatment (data not shown).

3.5 Modulation of TRPV1 function by TNF α

Pro-inflammatory mediators such as TNF α are known to increase the sensitivity and excitability of nociceptors by enhancing the activity of receptors and ion-channels such as TRPV1. To investigate this further, the effects of the pro-inflammatory cytokine TNF α in modulating intracellular calcium levels and TRPV1 expression were examined.

3.5.1 Effects of varying concentrations of TNF α on intracellular calcium responses in adult rat dorsal root ganglion neurones *in vitro*

The mean diameter of DRG neurones examined in this study was 28.3 ± 2.1 μm . In untreated DRG neurones, the 340/380 nm ratio (reflecting basal $[\text{Ca}^{2+}]_i$) was $2.5 \pm 0.7\%$ KCl response ($n = 81$).

Neurones were exposed to increasing concentrations of TNF α (3 ng/ml-200 ng/ml); this produced an increase in $[\text{Ca}^{2+}]_i$ ($p < 0.005$) compared to basal, with a maximal effect seen at 100 ng/ml (Figure 3.15). In this case, TNF α was applied via Pasteur pipette, rather than superfusion (to save on material costs) and left in contact with neurones for 4 minutes before removal via aspiration. A

representative trace of TNF α -induced increases in $[Ca^{2+}]_i$ is shown in Figure 3.16. An estimated EC₅₀ value of 72 ng/ml was calculated for TNF α . An average of only 6% of the neurones examined responded directly to TNF α at varying concentrations, with a maximum of 9% responding at 100 ng/ml. The increase in $[Ca^{2+}]_i$ that was observed following 50ng/ml TNF α was abolished in experiments that were performed without extra-cellular calcium (Figure 3.15b) showing that the increases were due to mobilisation of intra-cellular calcium. We were unable to record from neurones treated with concentrations of TNF α above 200 ng/ml at which concentration neurones were washed off the cover slip, suggesting cell toxicity.

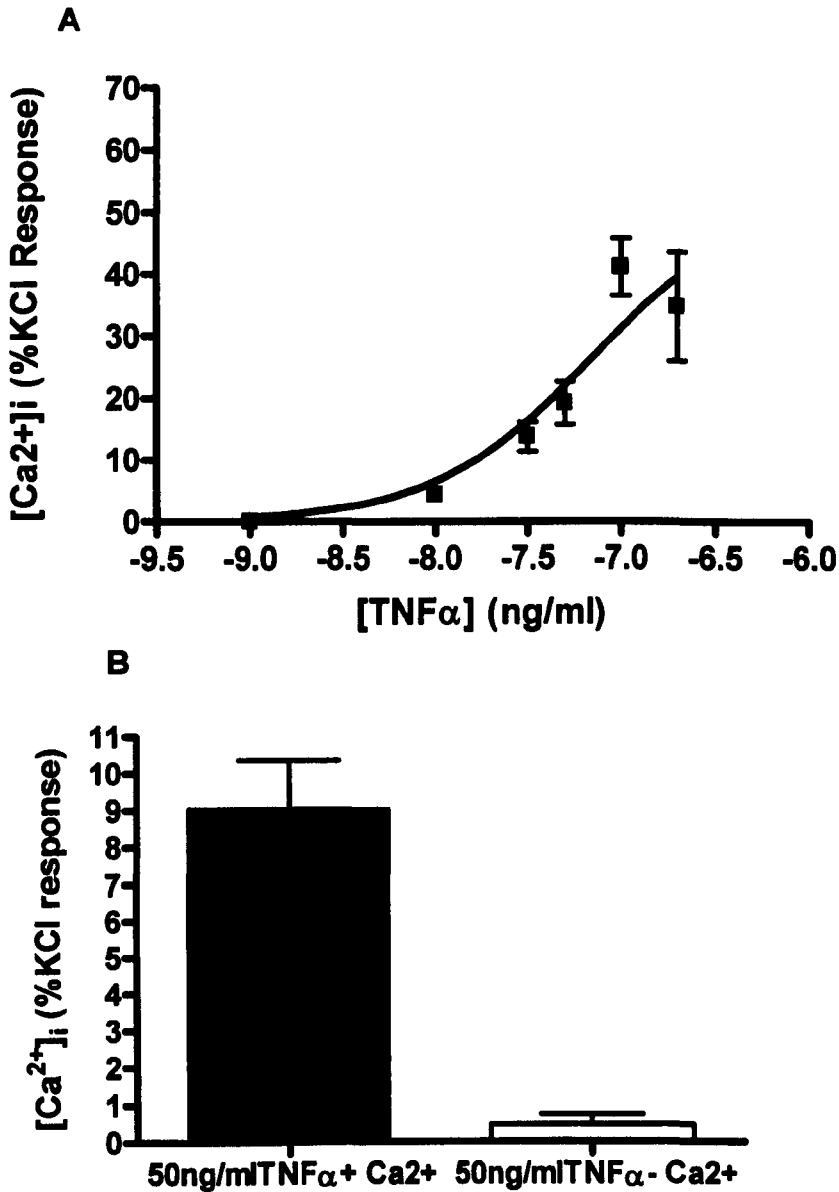


Figure 3.15 (A+B) Effects of TNF α on [Ca²⁺]_i in DRG neurones. (A) This concentration/ response curve shows the change in [Ca²⁺]_i, expressed as a percentage of a control KCl, response, evoked by increasing concentrations of TNF α . n=7-21 neurones per concentration from 4 rats (B). The effects of calcium and calcium free buffer on changes in [Ca²⁺]_i, expressed as a percentage of a control KCl, response, evoked by 50ng/ml TNF α . n=9-47 neurones from 3 rats.

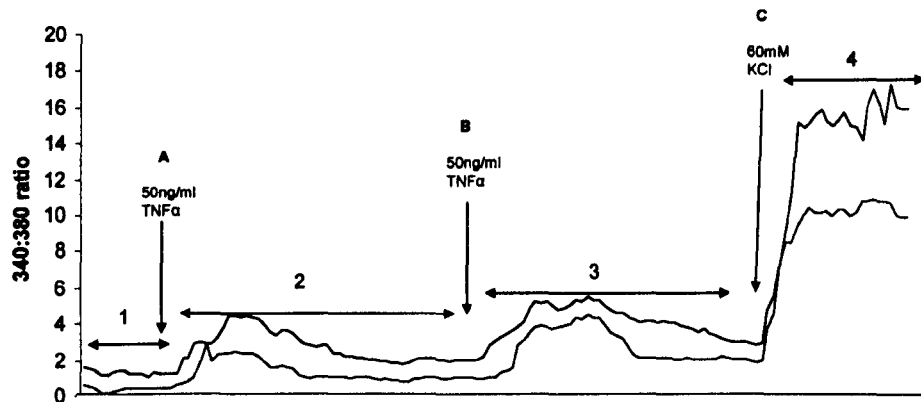


Figure 3.16 A representative trace showing changes in 340: 380 nm ratios in two individual DRG neurones, in response to TNF α 50 ng/ml. Recordings of 340:308 ratio were made at various time points, where 1= 2minute recording, 2 and 3 = 46 minute recording, 4= 3 minute recording. At point A, the cell was exposed to TNF α (50 ng/ml) for 4minutes. Forty-five minutes later, at point B, TNF α (50 ng/ml) was reapplied with no evidence of desensitisation. After another 45 min (C) KCl (60 mM) was applied to depolarize neurones.

3.6 Effects of TNF α on capsaicin-evoked changes in intracellular calcium concentrations in DRG neurones

To determine whether exposure to TNF α affected the capsaicin response in DRG cells, neurones were treated with TNF α (50ng/ml) for 4 minutes; 50ng/ml was used as it produced approximately 50% of the maximal effect and 4 minutes was the optimum time to induce an increase in $[Ca^{2+}]_i$ without washing neurones off the cover slip. 50nM capsaicin was used as this was the approximate EC₅₀ value for the calcium response (figure 3.17). 50nM capsaicin alone produced a peak $[Ca^{2+}]_i$ response of $34.3 \pm 5.9\%$ KCl which was increased to $42.1 \pm 6.9\%$ in the presence of TNF α ($P < 0.05$; Student's *t* –test).

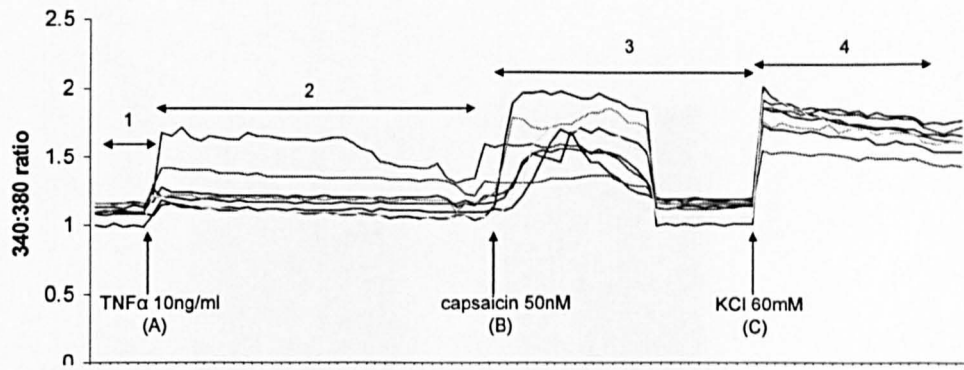


Figure 3.17 A representative trace showing changes in $[Ca^{2+}]_i$ (340:380nm ratios) in response to TNF α 50 ng/ml (A), exposure to 50 nM capsaicin(B), and following KCl (60 mM) (C) to depolarize neurones. Recordings of 340:308 ratio were made at various time points, where 1= 2minute recording, 2 and 3 = 46 minute recording, 4= 3 minute recording. Following each application of drug there was a 45 minute washout period.

To see if this effect was simply additive, in further experiments, TNF α was applied to neurones for 4 minutes, before removal by aspiration, followed by capsaicin supra-fusion for 60 seconds.

Pre-treatment with TNF α for 4 minutes, significantly increased capsaicin-evoked $[Ca^{2+}]_i$ from $46.6 \pm 5.4\%$ with capsaicin to $58.67 \pm 1.9\%$ ($P < 0.05$) (Figure 3.18). TNF α pre-treatment also increased the percentage of neurones responding to 50nM capsaicin from $27.5 \pm 1.9\%$ to $35.1 \pm 1.1\%$ for TNF α and capsaicin-treated neurones (Figure 3.19) ($P < 0.01$; t- test)

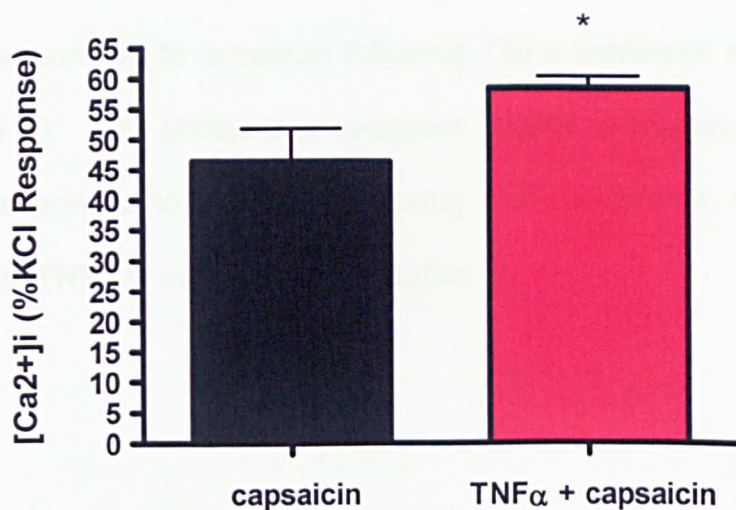


Figure 3.18 Effects of pre-treatment with TNF α (50 ng/ml) on capsaicin-evoked calcium responses in DRG neurones. Pre-treatment with TNF α significantly increased capsaicin-evoked [Ca²⁺]_i responses (n=59-88 neurones, p<0.05).

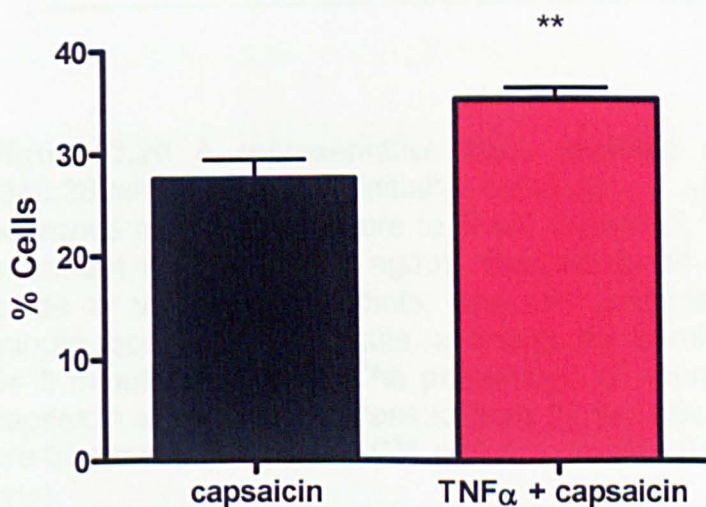


Figure 3.19. Effects of pre-treatment with TNF α on the number of neurones responding to capsaicin. TNF α significantly increased the percentage of neurones that responded to capsaicin, compared to neurones treated with capsaicin alone, (n=59-88 neurones; p<0.01).

The role of TRPV1 in modulating endocannabinoid levels and neuronal responses to TNF α

A representative trace of the increase in percentage of cells responding to capsaicin following TNF α treatment is shown in figure 3.20. This shows that neurones initially unresponsive to capsaicin, responded to capsaicin following TNF α treatment, suggesting a role for TNF α in neuronal sensitisation.

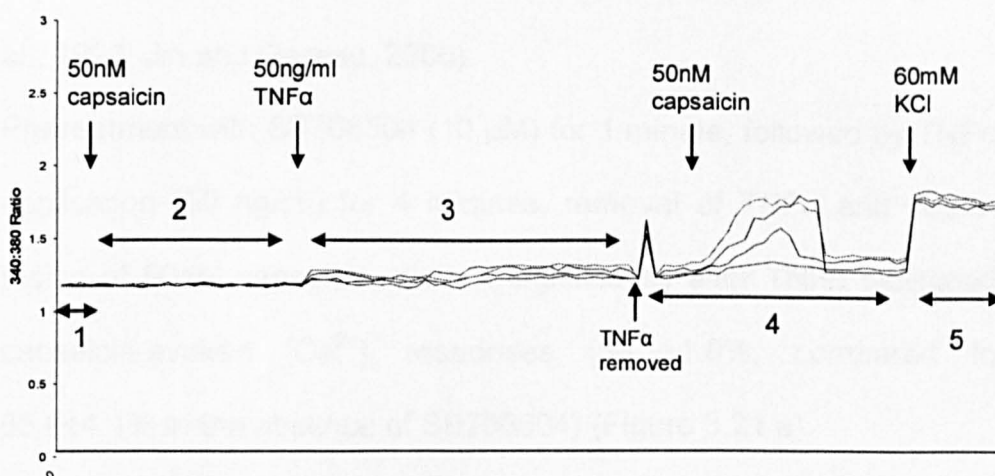


Figure 3.20 A representative trace showing changes in $[Ca^{2+}]_i$ (340:380nm ratios) in initially capsaicin – unresponsive DRG neurones following exposure to 50nM capsaicin, with or without pre-treatment with TNF α (50 ng/ml). Recordings of 340:308 ratio were made at various time points, where 1= 2minute recording, 2= 46 minute recording, 3=4 minute recording, 4= 46 minute recording, and 5= 3 minute recording. The percentage of neurones responding to capsaicin significantly increased from $27.5 \pm 1.9\%$ to $35.1 \pm 1.1\%$ after pre-treatment with TNF α (***) $p < 0.001$; $n = 84-103$ neurones, from 4 rats).

3.7 Effects of SB706504 on TNF α and capsaicin-evoked changes in intracellular calcium concentrations in DRG neurones

To investigate the mechanism underlying the TNF α sensitisation of DRG neurones to capsaicin, experiments were performed in the presence of a phospho-38 mitogen-activated protein kinase (p38MAPK) inhibitor SB706504 (10 μ M); this concentration has been reported to inhibit TNF α regulation of p38MAPK (Vanden Berghe et al., 1998, Jin and Gereau, 2006).

Pretreatment with SB706504 (10 μ M) for 1 minute, followed by TNF α application (50 ng/ml) for 4 minutes, removal of TNF α and superfusion of 50nM capsaicin, did not significantly alter TNF α facilitated capsaicin-evoked $[Ca^{2+}]_i$ responses ($58.1 \pm 1.8\%$, compared to $65.0 \pm 4.1\%$ in the absence of SB706504) (Figure 3.21 a)

However, pre-exposure to SB706504 did significantly reduce the percentage of neurones responding to the combination of TNF α and capsaicin ($14.6 \pm 2.3\%$ compared with $35.3 \pm 1.1\%$ in the absence of SB706504, ($p < 0.05$ Figure 3.21b).

Pretreatment with SB 706504 alone, or in combination with either TNF α or capsaicin did not alter the capsaicin or TNF α -evoked $[Ca^{2+}]_i$ responses or the percentage of neurones responding to either TNF α or capsaicin alone (data not shown).

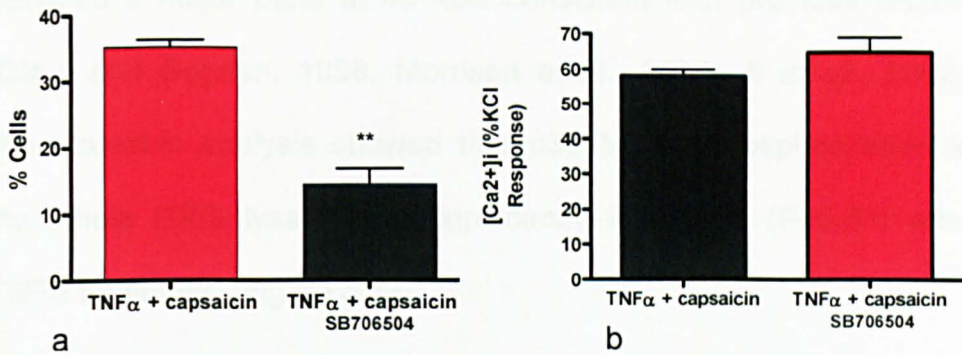


Figure 3.21 a+b Effects of pre-exposure to SB706504 and pre-treatment with TNF α on the responsiveness of DRG neurones to capsaicin.

a) Pre-exposure of DRG neurones to SB706504 significantly reduced the percentage of neurones responding to capsaicin following pre-incubation with TNF α ($14.6 \pm 2.3\%$ compared to $35.3 \pm 1.1\%$) ($n=72-101$ neurones from 4 rats)

b) Pre-exposure to SB706504 did not alter TNF α facilitated capsaicin-evoked $[Ca^{2+}]_i$ responses ($58.1 \pm 1.8\%$, compared to $65.0 \pm 4.1\%$ in the absence of SB706504) ($n=49-91$ neurones from 4 rats).

3.7.1 Effect of TNF α on P38 MAPK phosphorylation and TRPV1 receptor expression

To investigate whether TNF α stimulates p38 MAPK phosphorylation, Western blot analysis using phosphospecific antibodies was carried out to assess MAP kinase activation in whole cell lysates of DRG neurones exposed (or not) to TNF for 4 minutes.

DRGs were prepared following the same protocol used in calcium imaging experiments. The cells were harvested via scraping from 6 well plates, instead of mounting on cover-slips, and levels of phospho p38MAPK were normalized to the amount of β -actin present in the DRG neurone lysates.

Immunoblotting for phospho p38 MAPK expression in DRG neurons detected a major band at 40 kDa consistent with previous reports (Clerk and Sugden, 1998, Morrison et al., 2000, Ji et al., 2002). Densitometric analysis showed that p38 MAPK phosphorylation in the whole DRG lysate was significantly increased ($P < 0.01$) after TNF α treatment, (Figure 3.22).

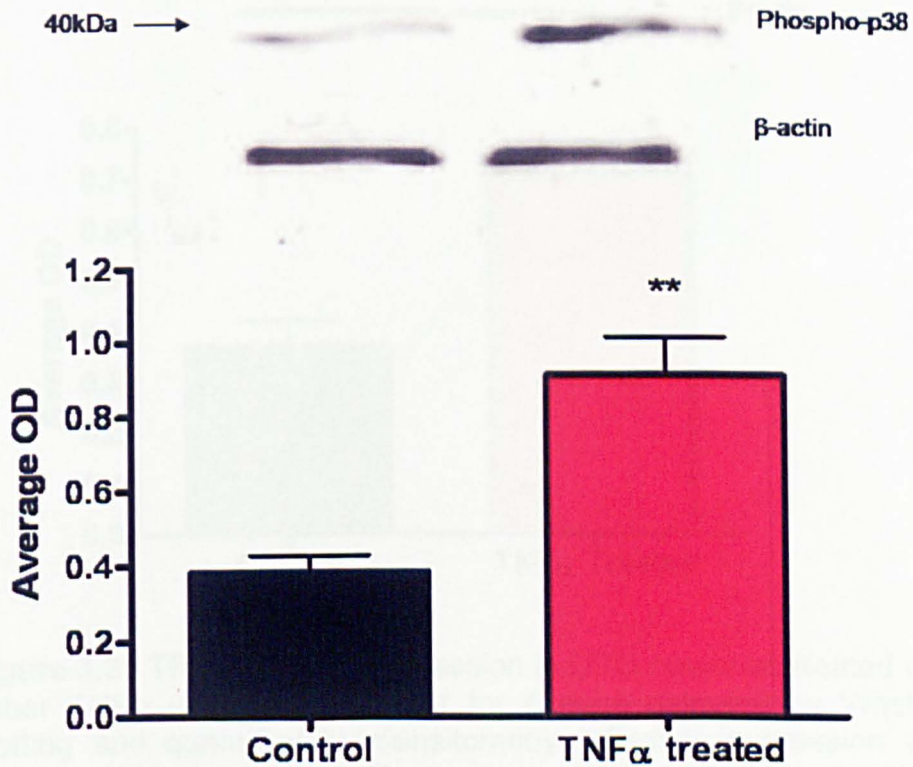


Figure 3.22 Expression of phosphoP38 MAPK protein expression in DRG neurones treated with either TNF α (50 ng/ml) or buffer for 4 mins detected by Western blotting and quantified by densitometry. Protein expression was calculated as percentage of expression of the internal control, β -actin. Data are shown as means \pm SEM of the expression of phosphoP38MAPK assessed in 3 separate experiments. (n=4 rats per treatment).

The role of TRPV1 in modulating endocannabinoid levels and neuronal responses to TNF α

The levels of TRPV1 expression following TNF α treatment were measured in DRG neurones treated with either 50 ng/ml TNF α or PBS (control) by Western blot analysis. A band at approximately 103 kDa was detected consistent with the antibody manufacturer's specification. TNF α significantly increased TRPV1 expression in whole cell lysates compared to control cells (Figure 3.23).

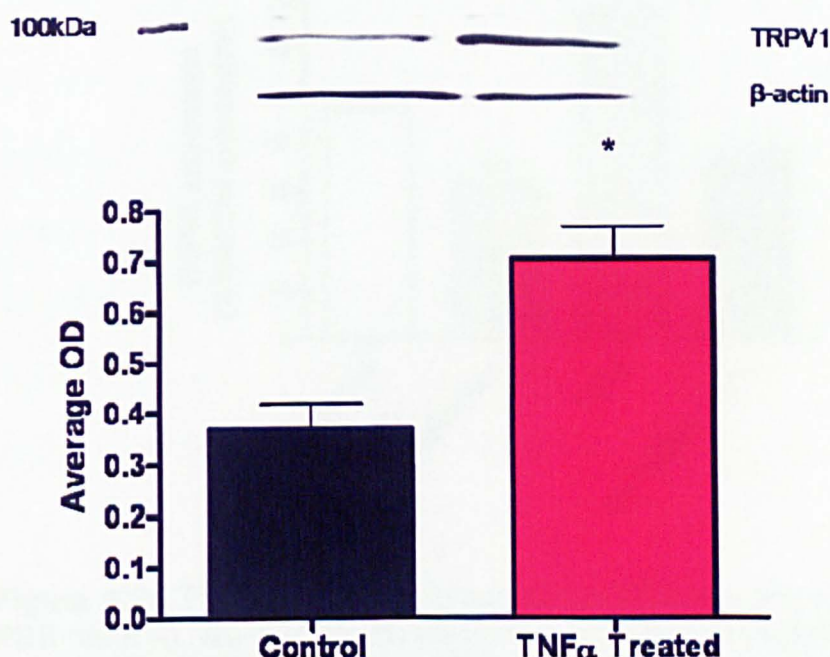


Figure 3.23 TRPV1 protein expression in DRG neurones treated with either TNF α (50ng/ml) or buffer for 4 mins detected by Western blotting and quantified by densitometry. Protein expression was calculated as percentage of expression of the internal control, β -actin. Data are means \pm SEM of the expression of TRPV1 assessed in 3 separate experiments.

The effect of the p38 MAPK inhibitor SB706504 on TNF α induced TRPV1 expression was also investigated, and SB706504 (10M μ M) significantly ($P<0.01$) inhibited TNF α -induced increase in TRPV1 expression (Figure 3.24). Note: The expression of TRPV1 receptors

The role of TRPV1 in modulating endocannabinoid levels and neuronal responses to TNF α

in DRG neurones in the presence or absence of TNF α and SB706504 was analyzed using Odyssey software, unlike previous experiments which were analysed using ECL.

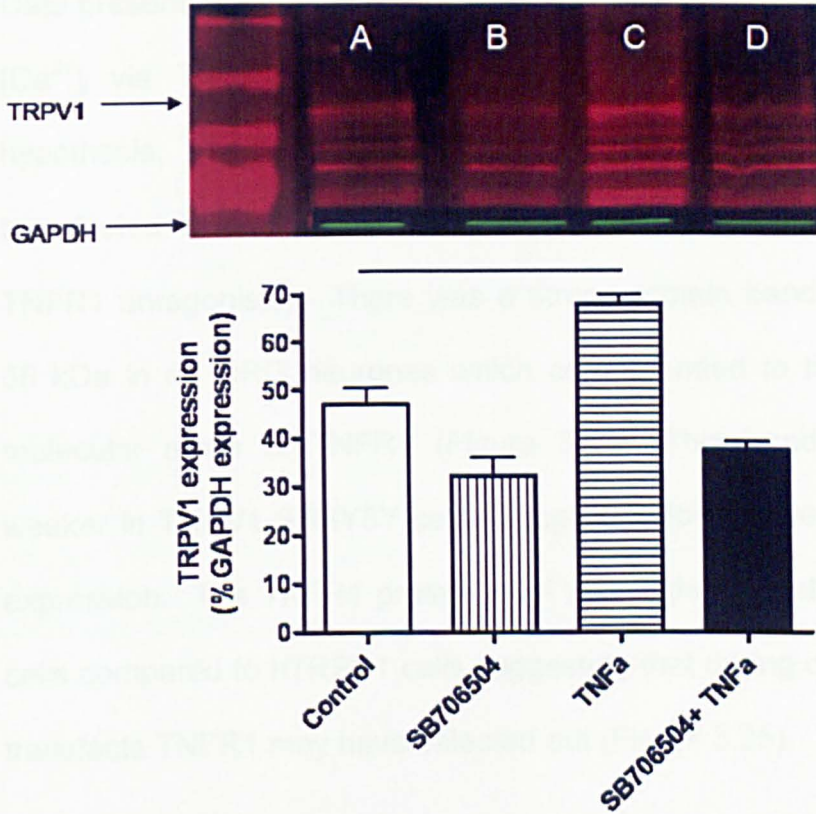


Figure 3.24 TRPV1 protein expression in DRG neurons treated with PBS (lane A), SB706504 (10 μ M) (Lane B), TNF α (50ng/ml) (lane C), or SB706504 (10 μ M) +TNF α (50 ng/ml) (lane D) for 4 mins detected by western blotting and quantified by densitometry. Protein expression was calculated as percentage of expression of the internal control, GAPDH. Data are means \pm SEM of the expression of TRPV1 assessed in 3 separate experiments.

The effects of TNF α (50ng/ml) in the SHSY5Y cells were investigated to see if responses were modulated as was the case for DRG neurones.

Exposure of SHSY5Ys to varying concentrations of TNF α did not cause an increase in $[Ca^{2+}]_i$. Cells were then exposed to capsaicin following a 4 minute pre-incubation with 50 ng/ml TNF α (as

previously used in DRG neurones). However, TNF α did not alter capsaicin-evoked calcium responses (capsaicin + TNF α =104.2 \pm 0.4% capsaicin response).

Data presented earlier in this chapter suggested that TNF α increases [Ca²⁺]_i via TNFR1 in rat DRG neurones. To investigate this hypothesis, TNFR1 expression in DRG neurones and TRPV1-transfected SHSY5Y cells was investigated (there are no specific TNFR1 antagonists). There was a strong protein band detected at 55 kDa in rat DRG neurones which corresponded to the predicted molecular mass of TNFR1 (Figure 3.25). This band was much weaker in TRPV1-SHSY5Y cells, suggesting lower levels of TNFR1 expression. The TNFR1 protein level was higher in native SHSY5Y cells compared to hTRPV1 cells suggesting that during cloning of the transfects TNFR1 may have selected out (Figure 3.25).

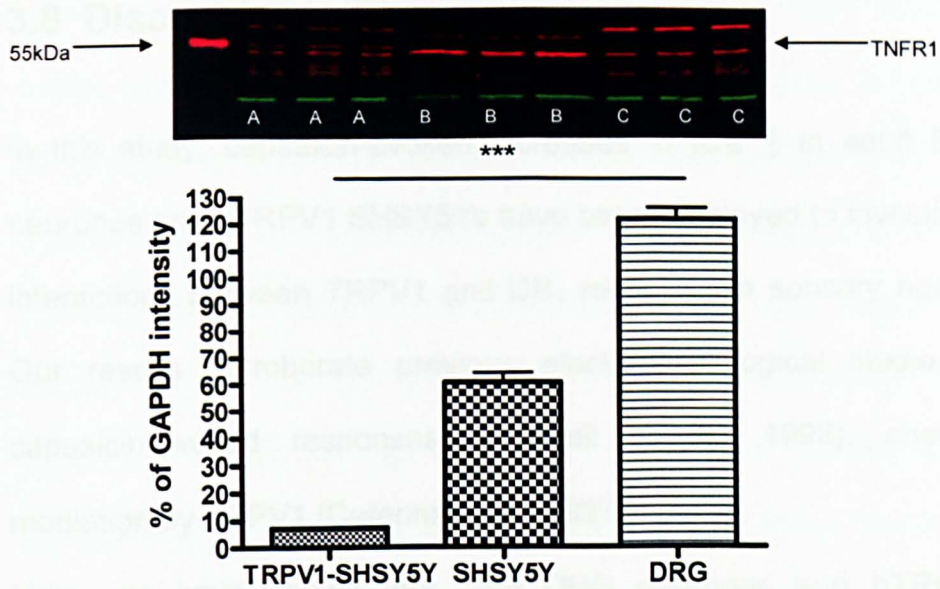


Figure 3.25 Quantification and expression of TNFR1 protein in rat primary DRG neurones (n=3 rats) (C), hTRPV1 SHSY5Y cells (A), and untransfected SHSY5Y cells (B) detected by Western blotting and quantified using Odyssey. Data are expressed as percentages of GAPDH intensity (means \pm SEM) in triplicate determinations. There was equal loading of protein as confirmed by GAPDH expression.

3.8 Discussion

In this study, capsaicin-evoked increases in $[Ca^{2+}]_i$ in adult DRG neurones and hTRPV1 SHSY5Ys have been employed to investigate interactions between TRPV1 and CB₁ receptors in sensory nerves. Our results corroborate previous electrophysiological studies of capsaicin-evoked responses (Helliwell et al., 1998), showing mediation by TRPV1 (Caterina et al., 1997).

Here, we have shown that both DRG neurones and hTRPV1-SHSY5Y cells express active and functional TRPV1 receptors. The excitatory effects of capsaicin and the presence of TRPV1 receptors on DRG neurones reported here are in agreement with previous studies (Helliwell et al, 1988, Caterina et al, 1997), and calcium imaging of these small diameter neurones with the TRPV1 agonist capsaicin provided a robust and concentration-dependant increase in intracellular calcium, which was attenuated with the TRPV1 specific antagonist IRTX. Capsaicin application in DRG neurones can desensitize TRPV1 channels via a rapid influx of Ca^{2+} and activation of voltage-sensitive ion channels (Bevan and Szolcsanyi, 1990, Koplas et al., 1997). Thus, the experimental protocols were designed so that multiple additions of capsaicin could be applied without desensitisation. Effects of capsaicin were readily reversible on washout, further suggesting that desensitisation does not markedly affect responses; however desensitisation can be dependant on the dose and time intervals of capsaicin exposure

(Winter et al., 1988, Maggi et al., 1990, Craft and Porreca, 1992). It is also well known that CB₁ receptor and TRPV1 are co-expressed on primary sensory neurons see reviews (Szallasi et al., 1995, Szallasi and Blumberg, 1999, Hohmann, 2002, Rice et al., 2002) and in small diameter DRGs (Ahluwalia et al., 2002, Bridges et al., 2003, Price et al., 2003, Binzen et al., 2006). As reported by Millns et al., (2001) we found that the synthetic cannabinoid agonist HU210 inhibited capsaicin-evoked Ca²⁺ responses in DRG neurones. This effect of HU210 was reversed by the cannabinoid CB₁ receptor antagonist AM251 (Millns et al., 2001). Thus, HU210 appears to modify TRPV1 responses through CB₁ receptor activation and it is unlikely that HU210 inhibition of capsaicin-evoked responses is via interaction with the TRVR1, as HU210 alone had no effect on capsaicin-evoked responses.

To investigate the relationship between calcium-driven endocannabinoid synthesis and TRPV1 activation, levels of ECLs in rat DRG neurons were investigated following stimulation with capsaicin. However, due to the low yield of DRG neurones in primary culture preparations, we were unable to quantify ECLs in the rat DRG. Some groups have quantified ECLs in both control and stimulated DRGs (Ahluwalia et al., 2003b, van der Stelt et al., 2005, Vellani et al., 2008); however, the limits of quantification (LOQ) of the analytical instruments used in these studies were not given, although very low levels of AEA have been reported (0.05 pmol in some cases, e.g. (van der Stelt et al., 2005), whereas the LOQ used in the present

experiments is 0.5pmol/g for AEA. The DRG cell number observed following our culture is approximately 10,000 to 20,000 cells per rat (observation), however for the quantification of AEA, cell number was approximately 10 times this (Vellani et al., 2008). Therefore, excessive numbers of animals would be needed to produce such cell numbers. Some of the other experiments were also performed in the presence of MAFP, to prevent AEA and 2-AG hydrolysis by FAAH (Ahluwalia et al., 2003b), which complicates interpretation, or using atmospheric pressure chemical ionization (Vellani et al., 2008), instead of electrospray ionisation, as used in the present studies which may increase sensitivity. In all cases, samples were analysed using LC/MS, and monitored using selected ion monitoring (SIM), which is less specific compared to multiple reaction monitoring (MRM); however, an advantage of SIM is that the detection limit is lower since the MS instrument is only looking at a small number of fragments (see Chapter 2).

In order to investigate the roles of calcium and TRPV1 in neuronal endocannabinoid synthesis and release, we needed an appropriate cell model expressing the receptor channel that would generate large enough cell yields to enable quantification of ECLs. Previous studies have used TRPV1-transfected HEK cells (van der Stelt et al., 2005, Vellani et al., 2008), mouse neuroblastoma cells (Bisogno et al., 1997), rat cortical neurones (Stella and Piomelli, 2001) to investigate ECL levels *in vitro*. However, to date, there is only one stable neuronal cell line available that expresses the hTRPV1 receptor

(Lam et al., 2007), with previous studies using recombinant TRPV1 receptors in non-neuronal cell lines, such as HEK and CHO. Thus, the SHSY5Y neuroblastoma cell line transfected with TRPV1 (Lam et al., 2007) was used to investigate the relationship between TRPV1-mediated modulations of cell calcium and endocannabinoid synthesis.

SHSY5Y cells transfected with TRPV1 receptors responded to the TRPV1 agonist capsaicin, with increases in intracellular calcium, which were attenuated by the antagonist IRTX (figure 3.5), and there was good agreement in terms of agonist and antagonist potencies compared to primary neuronal DRG cultures. HU210 in the presence of capsaicin, significantly decreased the capsaicin response, consistent with previous studies (Millns et al., 2001). Unexpectedly however, AM251 alone reduced the capsaicin response, and the combination of AM251 and HU210 appeared to have an additive effect. The mechanisms behind this inhibition remain unclear. However it is surprising that AM251 did not have the same effect as SR141716A as seen in DRG neurones (Millns et al., 2001), suggesting that there is a difference in the selectivity or specificity of these CB₁ antagonists. Indeed, a recent report indicated that SR141716A may also antagonize TRPV1 (De Petrocellis et al., 2001a) therefore, one might conclude that in TRPV1-expressing SHSY5Y cells AM251 may act as a TRPV1 antagonist although there is no existing evidence to support this hypothesis and the antagonist had no such effect in DRG neurones. Further pharmacological

studies are required to address this unexpected finding, starting with an examination of the effects of SR141716A on capsaicin-evoked calcium responses in TRPV1-SHSY5Y cells. The existing literature reports that treatment of cells co-expressing CB₁ and TRPV1 receptors with CB₁ receptor agonists leads to either an inhibition or enhancement of TRPV1 activity, depending on the state of activation of the cAMP-signalling pathway (Hermann et al., 2003). Thus, there is the possibility that in TRPV1 transfected SHSY5Y cells, AM251 could inhibit cAMP formation, thereby attenuating capsaicin-evoked increases in calcium. Another possibility is that the combination of AM251 and HU210 is toxic to these cells, although for this to be a viable explanation; AM251 alone would have to be toxic, which was not observed.

Western blot analysis of TRPV1-transfected SHSY5Y cells was consistent with the presence of CB₁ receptors in both rat DRG neurones (Hohmann and Herkenham, 1999, Ahluwalia et al., 2000) and native SHSY5Y cells (Klegeris et al., 2003) (Marini et al., 2009). The protein band appearing to correspond with CB₁ for human SHSY5Y cells exhibited a slightly lower molecular weight than the CB₁ band in rat DRG, which could be due to a difference in post-translational modification of the protein between the species. Thus, the effects of HU210 in attenuating the response to capsaicin are largely consistent with CB₁ mediation in DRG neurones (albeit with the uncertainty over AM251's effects in SHSY5Y cells).

Having confirmed the role of TRPV1 receptors in mediating capsaicin-evoked increases in intracellular calcium and the presence of CB₁ receptors in SHSY5Y cells, we investigated the roles of calcium and TRPV1 receptors in controlling endogenous endocannabinoid levels. The measurement of ECLs provides a snapshot in time, and estimates an uncertain balance between synthesis, catabolism and export of ECLs, and mechanisms governing these relationships are unclear. Endocannabinoid generation is reported to be triggered by two well known pathways, depolarization-induced elevation of Ca²⁺ (Kreitzer and Regehr, 2001, Ohno-Shosaku et al., 2001, Wilson and Nicoll, 2001) and activation of G_q-coupled receptors, including group I metabotropic glutamate receptors (mGluRs) (Maejima et al., 2001a, Varma et al., 2001). Levels of ECLs varied following capsaicin application in both whole cell, and cell supernatant, and there appeared to be no clear relationship between an increase in intracellular calcium, and endocannabinoid synthesis and release. Levels of AEA were significantly higher following treatment with 1 nM capsaicin, while levels were unaltered following higher concentrations of capsaicin. Further experiments are required to generate more statistical confidence in these observations. It has previously been suggested that receptor activation with weak depolarization enhances endocannabinoid release (Varma et al., 2001, Kim et al., 2002a, Ohno-Shosaku et al., 2002) (Ohno-Shosaku et al., 2003). This can be related to the capsaicin concentration response curve, where 1 nM capsaicin,

produced the lowest response to intracellular calcium elevation, but significantly elevated AEA levels. Levels of OEA were unaltered at all capsaicin concentrations, while capsaicin caused a significant decrease in PEA levels. A higher concentration (0.1 μ M) of capsaicin was required to elevate levels of 2-AG. Levels of individual ECLs may vary depending on intracellular calcium levels, with some compounds, such as AEA requiring lower calcium levels for their synthesis, and others such as 2-AG, requiring higher calcium levels. However, it is not surprising that AEA and 2-AG levels are not comparable, with AEA and 2-AG belonging to two different classes of lipids, although AEA, OEA and PEA belong to the same class, the *N*-acylethanolamines, and are synthesised via their corresponding *N*-acyl phosphatidyl ethanolamine (NAPE) precursors; thus, it is possible that other pathways may contribute to the synthesis of each compound, due to their difference in structure (namely the number of carbon atoms). Indeed, disruption of NAPE-PLD gene in mice increased levels of the precursor NAPE, and decreased brain levels of longer chain NAEs, specifically saturated *N*-acyl chains with 20 or more carbon atoms (OEA and PEA) (Leung *et al.*, 2006). By contrast, levels of longer chain polyunsaturated NAEs, including AEA (C20:4) were unaltered in knock-out mice, compared to NAPE-PLD^{+/+} mice (Leung *et al.*, 2006, Liu *et al.*, 2006, Simon and Cravatt, 2006, Liu *et al.*, 2008). These data further highlight the differences in ECLs, and differing unknown pathways potentially involved in ECL synthesis and metabolism for AEA, OEA PEA and 2-AG which warrants further

investigation. In the present study we have found little evidence for capsaicin-induced Ca²⁺ mobilisation elevating levels of ECLs, which does not support a recent study by Van der Stelt (2005). In the latter study it was proposed that AEA acts as an intracellular agonist of TRPV1, providing an amplification system for increasing cell calcium, whereby activation of TRPV1 leads to an elevation of cytosolic calcium, which increases AEA levels, thus providing a positive feedback mechanism. Release of AEA is then suggested to act on extracellular facing CB₁ receptors, to inhibit TRPV1 function (Millns et al., 2001). Other 'entourage compounds' such as OEA and PEA could, potentially, potentiate these effects. Furthermore, TRPV1 receptors are activated/sensitised by activation of PKC, leading to an increase in AEA levels, but not 2-AG and PEA (Vellani et al., 2008). This suggests that the generation of second messengers, following TRPV1 activation has the potential to modulate ECL levels, and to potentiate AEA activity at either CB₁ or TRPV1 receptors.

There was no clear relationship between intra- and extracellular levels of ECLs and capsaicin concentration. However, it does suggest that ECLs are released into the extracellular medium, possibly via the proposed endocannabinoid membrane transporter (EMT), (see reviews (Glaser et al., 2005, Ho and Hillard, 2005, Hermann et al., 2006). Surprisingly, the TRPV1 antagonist, IRTX appeared to elevate intracellular levels of AEA, 2-AG, PEA and OEA in the presence of capsaicin. This puzzling observation, may suggest other unknown properties of IRTX, such as inhibition of

The role of TRPV1 in modulating endocannabinoid levels and neuronal responses to TNF α

endocannabinoid membrane transporter (EMT); however, further studies, such as the use of the EMT inhibitor, AM404 are required to test this hypothesis. The effects of FAAH inhibition and increases in levels of ECLs are well documented (Cravatt et al., 2001, Maione et al., 2006, Piomelli et al., 2006, Jhaveri et al., 2007a, Jhaveri et al., 2008b); however, following incubation with URB597 (1 μ M) for 30 minutes, followed by capsaicin (10 nM) for 1 minute, there were no changes in the levels of AEA, PEA and OEA, although 2-AG levels were significantly increased both in the presence and absence of URB597, suggesting that this increase is via a mechanism independent of FAAH inhibition, as 2-AG is not a good substrate for FAAH. However, some evidence suggests that 2-AG can also be metabolized by FAAH (Goparaju et al., 1998) and microinjection of an FAAH inhibitor into the peri-aqueductal grey increases 2-AG levels in that region (Maione et al., 2006) A cautious interpretation is that both FAAH and MAGL participate in 2-AG inactivation to an extent depending on the tissue or cell type, although 2-AG levels, unlike those of AEA, are not increased in FAAH "knockout" mice (Lichtman et al., 2002).

Collectively, these puzzling data suggest that increasing cell calcium via TRPV1 does not elevate ECL levels, and there is no correlation with intracellular and extracellular levels. However, the possibility of calcium-independent ECL synthesis must not rule out. Indeed, most of the enzymes identified to date that catalyse endocannabinoid formation are Ca²⁺-sensitive, however Ca²⁺-independent

endocannabinoid biosynthesis has been suggested to occur during certain types of synaptic plasticity (Brenowitz and Regehr, 2003), furthermore Di Marzo's group have shown that AEA levels can be elevated in intact neurons independent from elevation of intracellular Ca²⁺ (Vellani et al., 2008).

In the second part of this study, we showed that TNF α facilitates capsaicin-evoked calcium responses via the activation of p38 MAPK, and that inhibition of this pathway may prevent sensitisation of sensory neurones to inflammatory mediators.

The pro-inflammatory cytokine TNF α , increased intracellular calcium levels in adult rat DRG neurones; however, the mechanism underlying this increase remains unclear. TNF α , acts either on TNF receptor 1 (TNFR1), or TNF receptor 2 (TNFR2). Most TNF α effects including cell growth and death, development, oncogenesis, and immune, inflammatory, and stress responses (for review see (Chen and Goeddel, 2002) are mediated through TNFR1, although both TNFR1 and TNFR2 have been localised in rat DRG neurones (Pollock et al., 2002, Schafers et al., 2002, Schicho et al., 2004). TNF receptor activation can lead to the mobilisation of intracellular stores of calcium (Amrani et al., 1996, Bick et al., 1997, Parris et al., 1999) but, due to the lack of selective TNFR1 antagonists, we were unable to investigate if the mobilisation of intracellular calcium was TNFR1-mediated. Other reports have shown an increase in intracellular calcium levels in human microglia following TNF α

The role of TRPV1 in modulating endocannabinoid levels and neuronal responses to TNF α application (McLarnon *et al.*, 2001), which appeared to be independent of Ca²⁺ influx and intracellular IP₃ stores. However, in astrocytes (Koller *et al.*, 1996), and hen granulosa cells (Sobloff *et al.*, 1995), TNF α induced an increase in intracellular calcium which was dependant on extracellular calcium, which concurs with our findings. The inhibition of increased [Ca²⁺]_i via TNF α , in the absence of extracellular calcium suggests that the increase in [Ca²⁺]_i is via influx through ion channels, however, further work with calcium ion channel antagonists is required to investigate this. It appears that depending on the cell type, multiple mechanisms contribute to TNF α -induced increases in intracellular calcium.

Pre-treatment of DRG neurones with TNF α , prior to capsaicin administration, increased both the percentage of neurones responding to capsaicin, and the evoked changes in intracellular calcium. These data are supported by previous studies showing the ability of TNF α to sensitise neurones to capsaicin (Nicol *et al.*, 1997, Hensellek *et al.*, 2007) via TRPV1. Analysis of TNF α (50ng/ml) pre-treated DRG neurones prior to capsaicin application, revealed an increase in TRPV1 protein levels, indicating an increase in TRPV1 receptor expression. Increases in TRPV1 receptor expression *in vivo* (Carlton and Coggeshall, 2001, Ji *et al.*, 2002, Amaya *et al.*, 2003, Bron *et al.*, 2003) and *in vitro* (Ji *et al.*, 2002, Hensellek *et al.*, 2007, Constantin *et al.*, 2008) under inflammatory conditions are well documented and consistent with our findings that TNF α application caused an increase in TRPV1 protein levels in whole cells, while

levels were undetectable in membrane lysates, due to insufficient samples being available for reliable measurements.

There are reports of increases in TRPV1 protein levels but not TRPV1 mRNA levels in the DRG after complete Freund's adjuvant-induced inflammation (Ji et al., 2002b) suggesting a translational regulation, however, the short time frame (4 minutes) of TNF α application and associated increase in TRPV1 suggests that this is not a translational effect; but possibly liberation of a protein recognised by the TRPV1 antibody resulting from p38MAPK activation. The increase in TRPV1 protein levels occurred in conjunction with an increase in the activity of phospho-p38 MAPK in DRG lysates, and inhibition with the p38 MAPK inhibitor, SB706504 caused a significant reduction in the percentage of cells that responded to capsaicin, while having no effect on intracellular calcium levels. Previous studies conducted by Pollock et al. 2002 demonstrated a significantly increased level of phospho p38 MAPK activity after five minutes (Pollock et al., 2002); however, to date there are no other studies that have investigated TRPV1 protein levels after short exposure to TNF α . The involvement of p38 MAPK in mediating heat hyperalgesia after peripheral inflammation is well documented (Ji et al., 2002, Boyle et al., 2006, Jin and Gereau, 2006). Furthermore, p38 MAPK is activated in spinal cord by injection of carrageenan or formalin into the paw, and inhibition of p38MAPK reduces pain behaviour associated with peripheral inflammation (Kim et al., 2002b, Svensson et al., 2003). TNF α

activates p38 MAPK *in vitro* (Schafers *et al.*, 2002) while neurones treated with anti-TNF α antibodies exhibited an attenuation of mechanical hypersensitivity, an effect mimicked by treatment with SB706504, (the inhibitor of p38 MAPK; (Schafers *et al.*, 2003b). This presents the possibility that the effects observed in these studies were due to TNF α , via p38 MAPK activation, inducing phosphorylation of TRPV1 receptors, and subsequently sensitising nociceptive neurones to capsaicin.

Another possible explanation is TNF α , via p38 MAPK, causes a release or an activation of an inactive form of TRPV1 receptor protein translocated to the DRG membrane, which is detectable by our antibody, however to further investigate this, protein levels in DRG membrane lysates need to be higher, demanding the use of large numbers of experimental animals. The increase in the number of neurones responding to capsaicin following TNF α application corresponds to an increase in TRPV1 expression, however for this to be viable, TRPV1 would have to be functional TRPV1 in the cell membrane, and due to low protein levels is immeasurable. These data imply that TNF α increases the percentage of neurones, and increases levels of $[Ca^{2+}]_i$, via a phosphorylation of p38MAPK and subsequent sensitisation of TRPV1. It is unknown as to whether TNF α phosphorylates TRPV1, as unlike other protein kinases, there is a lack of specific phosphorylated TRPV1 antibodies.

To determine a link between TNF α and ECL release we were interested in measuring EC release following TNF α treatment, however the TRPV1-SHSY5Y cells used for the quantification of ECLs did not express TNFR1, and thus unsurprisingly the potentiating effects of TNF α on capsaicin-evoked increases in calcium observed in DRG were not seen in SHSY5Y cells.

In conclusion we have shown the inflammatory cytokine TNF α has the potential directly, and indirectly, perhaps by way of a p38 MAPK-mediated phosphorylation and sensitisation of TRPV1 receptors, to augment inflammatory nociceptive states.

Developing inhibitors of TNF α -mediated sensitisation of nociceptive neurones represents a potential therapeutic avenue for treating inflammatory pain states.

Chapter 4

Effects of inhibition of fatty acid amide hydrolase in the carrageenan model of inflammation.

4 Effects of inhibition of fatty acid amide hydrolase in the carrageenan model of inflammation

4.1 Introduction

Following the development of a LC-MS-MS method capable of quantifying the ECs and the COX-2 metabolites of AEA and 2-AG in the rat brain and neuronal cell line, the effects of acute noxious stimulation on levels of ECs were investigated, alongside measurement of pain related behaviour in the rat. The effects of carrageenan-induced inflammation on nociceptive behaviour and on levels of ECs in the hindpaw and spinal cord were investigated along with the effects of a FAAH inhibitor in this model of inflammation.

4.1.1 FAAH inhibitors in inflammatory pain

The analgesic effects of cannabinoid agonists acting at CB₁ and CB₂ have been widely documented and reviewed (Pertwee, 2001, Walker and Huang, 2002b, Hohmann and Suplita, 2006). One of the major drawbacks of this approach to analgesia is the wide spread distribution of CB₁ receptor in the brain and the associated side

effects of CB₁ receptor activation, including sedation, dependence and psychosis (Thomas, 1996, Kalant, 2004, Pacher et al., 2006).

The endocannabinoids AEA (Devane et al., 1992c) and 2-AG (Sugiura et al., 1995) act at CB₁ and CB₂ receptors to modulate many physiological responses, including nociception (see review (Fowler et al., 2005, Pacher et al., 2006). Recent studies have investigated targeting the ECLs, rather than the receptors as an alternative mechanism to achieve analgesia without the unwanted associated side effects. The rapid termination of the biological actions of the ECLs, via metabolism and transport, does limit their analgesic effects. Nevertheless, systemic administration of anandamide produces analgesia in a number of animal models of inflammatory pain (Devane et al, 1992, Jaggar et al, 1998, Richardson et al, 1998), thus supporting the targeting of the endocannabinoid system as an alternative approach to achieving analgesia.

As discussed in Chapter 1, a number of studies have shown that FAAH is the predominant enzyme responsible for the hydrolysis of fatty acid amides (FAAs) including AEA (Cravatt et al., 2001, Lichtman et al., 2002, Cravatt et al., 2004). 2-AG is predominantly metabolised by MAGL (Dinh et al., 2002). There is, however, evidence that 2-AG is also metabolised by FAAH (Di Marzo et al., 1998) and both 2-AG and AEA can be metabolised by COX-2 (Yu et al., 1997, Kozak et al., 2002a, Kozak et al., 2004).

4.1.2 Effects of inhibiting FAAH on pain responses

Deletion of the gene encoding FAAH results in the endogenous levels of anandamide and other fatty acid amides being elevated over 10- fold throughout the nervous system (Cravatt et al., 2001). These data strongly support the notion that FAAH is the primary enzyme responsible for the hydrolytic degradation of these lipids *in vivo* (Cravatt et al., 2001). Deletion of FAAH attenuates inflammation in the carrageenan-induced paw edema model (Cravatt et al., 2004, Lichtman et al., 2004 (b)), allergic contact dermatitis model (Karsak et al., 2007) and dinitrobenzene sulfonic (DBNS) model of colitis (Massa et al., 2004). FAAH^(-/-) mice do not, however, display a reduction of thermal hyperalgesia in the CCI model (Lichtman et al., 2004b). Consistent with the crucial role of FAAH in the catabolism of anandamide, exogenous administration of anandamide in FAAH^(-/-) mice produced exaggerated behavioural effects including hypomotility, analgesia, hypothermia, and catalepsy. The effects of AEA in FAAH^(-/-) mice were blocked by a CB₁ antagonist (Cravatt et al, 2001, Cravatt et al, 2004, Litchman et al 2004b).

The analgesic phenotype of FAAH inhibition is thought to be mediated through an increase in ECs in both central and peripheral tissues. Comparison of CNS-spared FAAH knockout mice (FAAH present in CNS, however not in peripheral tissue) with complete FAAH knockout mice, showed that analgesic effects in tests of acute pain (tail immersion & hot plate tests) were only noted in the complete FAAH knockout mice, whereas both CNS-spared and

complete FAAH knockout mice displayed reduced oedema in the carrageenan-inflammation model. Levels of ECs in the brain and spinal cord of CNS-spared FAAH knockout mice were similar to wild-type levels of ECLs in the brain and spinal cord, but levels were significantly elevated in peripheral tissues (Cravatt et al., 2004). These data indicate a role of peripheral FAAH in modulating oedema, whereas acute pain responses are modulated by FAAH through the central elevation of ECLs. The outcomes of these knockout studies has resulted in considerable interest in the potential analgesic effects of the pharmacological manipulation of FAAH, which has clear therapeutic potential for the treatment of pain. Inhibition of FAAH with compounds such as URB597 elevates levels of AEA both *in vivo* and *in vitro* (Cravatt et al., 2001, Kathuria et al., 2003b, Fegley et al., 2005), and produces similar effects to that seen with FAAH gene deletion (Table 4.1)

Potential Therapeutic Effects	CB1 Agonist*	FAAH(-) Mice*	Chemical FAAH inhibition*
Analgesia	Yes	Yes	Yes
Anxiolysis	Yes/No	Unknown	Yes
Anti-inflammatory	Yes	Yes	Unknown
Anti-spasticity	Yes	Unknown	Unknown
Anti-emesis	Yes	Unknown	Unknown
Side effects			
Hypermotility	Yes	No	No
Hypothermia	Yes	No	No
Catalepsy	Yes	No	No

Table 4.1 Comparison of the behavioral effects of CB1 agonists versus genetic deletion of FAAH gene, and chemical inhibition of FAAH using FAAH inhibitor.

*For a comprehensive review see (Kumar et al., 2001, Lichtman et al., 2002)

4.1.3 Inhibition of FAAH in animals models of pain

A number of studies have investigated the effects of FAAH inhibition on pain behavior, as is often the case, there are inconsistencies in the reported effects. Inhibition of FAAH has been consistently reported to produce analgesia and reduce inflammation in models of acute inflammatory pain (Lichtman et al., 2004 (a), Holt et al., 2005b, Chang et al., 2006, Jayamanne et al., 2006b, Maione et al., 2006, de Novellis et al., 2008, Jhaveri et al., 2008b, Sagar et al., 2008a, Ahn et al., 2009) (Table 4.2). By contrast, inconsistent effects of inhibition of FAAH have been reported in models of neuropathic pain (Jayamanne et al., 2006b) or anti-nociceptive effects (Chang et al., 2006, Maione et al., 2006, Russo et al., 2007b, Karbarz et al., 2009)

in models of neuropathic pain. In mice, repeated oral administration of URB597 attenuated CCI-induced thermal hyperalgesia and mechanical allodynia (Russo et al., 2007a). These effects were blocked by CB₁ and CB₂ receptor antagonists. Local injection of URB597 and URB602, which inhibits both FAAH and MAGL, into rat paws ipsilateral to the ligated nerve, also attenuated thermal hyperalgesia and mechanical allodynia (Desroches et al., 2008). Similarly, the reversible FAAH inhibitor, OL-135, reversed mechanical allodynia in a rat spinal nerve ligation model (Chang et al., 2006). This anti-allodynic effect was blocked by the CB₂ receptor antagonist, SR144528. In contrast to mice treated with FAAH inhibitors, FAAH^(-/-) mice do not display a phenotypic reduction of thermal hyperalgesia in the CCI model (Lichtman et al., 2004b). Collectively, these studies indicate FAAH inhibitors are efficacious in animal models of inflammatory and neuropathic pain.

Pain Model	FAAH inhibitor	Route of Administration	Analgesic	Suggested Mechanism			Endogenous Cannabinoid levels	Reference
				CB1	CB2	Other		
Carra (Mouse)	URB597 Pre-carra	0.3, 1 and 3mgkg ⁻¹ i.p. SYSTEMIC	Dose dependent reduction in oedema	Not inhibited by pretreatment SR141716A, 1mgkg ⁻¹ i.p.,	Prevented with pretreatment SR144528, 1mgkg ⁻¹ i.p.,	Not inhibited by co-ad BADGE 30mgkg ⁻¹ /capsazepine 10mgkg ⁻¹	Not measured	(Holt et al., 2005a)
Carra (Rat)	URB597 Pre-carra	25 & 100µg i.pl, LOCAL	Yes – MH (WB) No effect on inflammation	-	-	Not inhibited by co-ad PPAR γ agonist GW9662 (30µg, i.pl.), prevented by PPAR α agonist GW6471 (30µg, i.pl.)	↑AEA and 2-AG in URB inflamed HP with 25µg. ↑spinal AEA and OEA following 100µg URB597	(Jhaveri et al., 2008b)
Carra (Rat)	URB597 Pre-carra	25µg i.pl, LOCAL	No effect on evoked responses or inflammation	Not inhibited by co-ad with AM251, 30µg,	-	Prevented by PPAR α agonist GW6471, 30µg, i.pl,	Not measured	(Sagar et al., 2008b)
CFA (Rat)	PF-3845	1-30mg/kg p.o ORAL	Yes- MA (PWT)	Prevented with co-ad SR141716A 10mg/kg	Reduced with co-ad SR144528 30mg/kg	-	↑brain and liver levels of AEA, PEA and OEA	(Ahn et al., 2009)
CFA (Rat)	URB597 Post-CFA	0.3mgkg ⁻¹ , i.p., SYSTEMIC	Yes - MA, TH	Reduced by SR141716A, 1mgkg ⁻¹ , i.p. Co-ad	Reduced by co-ad SR144528, 1mgkg ⁻¹ , i.p	Prevented by co-ad of both antagonists	Not Measured	(Jayamanne et al., 2006)
Formalin (Mouse)	OL-135 Pre-Formalin	3, 10, & 30mgkg ⁻¹ , i.p., SYSTEMIC	Yes – both phases	Prevented with pre-treatment i.p SR141716A, 3mgkg ⁻¹	Not inhibited by pretreatment i.p SR144528, 3mgkg ⁻¹	-	Not Measured	(Lichtman et al., 2004a)
Formalin (Rat)	AA-5-HT Pre-Formalin	1mg, i.pl., LOCAL	Yes – 2 nd phase	Prevented with co-administration of AM251, 0.35mg, s.c.,	-	Prevented by co-administration with TRPV1 antagonist capsazepine, 50µg, s.c	↑AEA and 2AG in formalin treated hindpaw receiving AA-5-HT compared to vehicle	(Maione et al., 2007)
		5mgkg ⁻¹ , i.p., SYSTEMIC	Yes – 2 nd phase	Prevented with co-administration AM251, 3mgkg ⁻¹ , i.p	-	Prevented by co-ad i.p of TRPV1 antagonist capsazepine, 2.5mgkg ⁻¹ , and by I-RTX, 0.1 & 0.2mgkg ⁻¹	No change in AEA, PEA or 2AG in spinal tissue or PAG.	
Formalin (Mouse)	5mgkg ⁻¹ , i.p., SYSTEMIC	Yes – both phases	Prevented by co-ad AM251, 3mgkg ⁻¹ , i.p.	Not inhibited by co-administration AM630, 3mgkg ⁻¹ , i.p.,	Not inhibited by TRPV1 antagonist capsazepine 2.5 or 10mgkg ⁻¹ , or by I-RTX, 0.1 & 0.2mgkg ⁻¹ , i.p., C	↑AEA, PEA and 2AG in formalin treated hindpaw receiving AA-5-HT		
Formalin (Rat)	AA-5-HT Pre-Formalin	0.5nmol, i.VL-PAG, LOCAL	Yes – 2 nd phase	Blocked by co-ad AM251, 0.5nmol, i.VL-PAG	-	Prevented with co-ad TRPV1 antagonist I-RTX, 0.5nmol, i.VL-PAG,	↑2AG and PEA in PAG in 1 st stage ↑AEA in PAG at 2 nd stage	(de Novellis et al., 2008)

Table 4.2. Comparison of the effects of inhibition of FAAH on inflammatory pain responses and levels of endocannabinoids.

Overall, these studies demonstrate that the analgesic effects of FAAH inhibition are mediated by the endocannabinoid system; however the contribution of peripheral versus central FAAH to these effects has been less widely studied and warrants further investigation (Table 4.3). An interesting observation from these previous studies is that the duration of analgesia produced by pharmacological inhibition of FAAH is shorter than the period over which FAAH activity is inhibited, however ECLs are remain elevated during enzyme inhibition. The consequence of this, in terms of the application of FAAH inhibition to a clinically relevant therapeutic treatment for pain, is unknown. One question that remains to be addressed is whether the effects of pharmacological inhibition of FAAH are sustained over longer periods of time treatment (repeated dosing). Indeed, it could be envisaged that alternative metabolising pathways for ECs play, such as MAG lipase and COX-2, may have increased prominence when FAAH is inhibited over a number of days.

FAAH Inhibitor		Model	EC Levels	Reference:
Single	Repeated			
-	10mg/kg Oral Once daily 4 days URB597 Mouse	Neuropathic Pain Chronic Constrictive Injury	Increase in spinal levels of AEA, OEA and PEA in URB597 treated animals versus vehicle CCI	(Russo et al., 2007)
0.3mg/kg i.p URB597 Rat	-	Naïve tissue Levels measured 30min, 1, 2, 6, and 24 hr post URB597	Increase in rat brain AEA levels 30min, 1 hr and 2 hr post URB597. Increase in PEA and OEA up to 6 hrs following URB597. No change in duodenum levels compared to vehicle	(Fegley et al., 2005)
-	5mg/kg i.p Once every 12 hrs for 48 hrs AA-5-HT Rat	Naïve Tissue Levels measured 1, 5, and 12 hr post AA-5-HT	Increase in AEA and 2AG levels in rat brain 1, 6, 12 hours post AA-5-HT compared to vehicle at each time point	(de Lago et al., 2005)
0.3mg/kg i.p URB597 Rat	-	Anti-anxiety Naïve tissue Levels measured 2 hours post URB597	Increase in brain levels of AEA, no change in 2-AG levels compared to vehicle.	(Kathuria et al., 2003b)

	0.3mg/kg i.p Once daily for 5 weeks	Chronic Mild Stress levels EC measured in midbrain, straitum, hippocampus, prefrontal cortex and thalamus	Increase in AEA levels in Midbrain, thalamus and striatum, not hippocampus and prefrontal cortex. Levels of OEA and PEA increased in all 5 areas compared to vehicle.	(Bortolato et al., 2007)
0.1mg/kg i.p URB597	0.1mg/kg i.p Once daily 4 days URB597	Anti-depressant ECs measured in Hippocampus, cortex and midbrain.	Increase in AEA 2 hours following single administration of URB597 in all 3 brain regions. Increase in AEA levels following repeated administration, although levels were approx 3 times lower than single URB597.	(Gobbi et al., 2005)
10mg/kg oral PF-3845 Rat		CFA model of Inflammatory Pain ECs measured in brain	Increase in brain and liver levels of AEA, PEA and OEA. Levels peaked at approx 3 hours, and maintained for up to 7-12 hrs post PF-3845.	(Ahn et al., 2009)

Table 4.3 Effects of systemic administration of FAAH inhibitors and on the levels of ECs in peripheral and brain tissue

4.1.4 COX-2 metabolism of ECs and its role in inflammatory pain

Both AEA and 2-AG can be oxidised by COX-2 *in vitro* (Kozak et al., 2001a, Kozak et al., 2001b, Kozak et al., 2003) to prostaglandin ethanolamides (PG-EA), and prostaglandin glycerol esters (PG-GE), respectively, see figure 4.1. There is some evidence that this route of metabolism has physiological / pathophysiological relevance. Bimatropast, a structural analogue of PGF₂α-EA, has anti-glaucoma

properties (Woodward et al., 2004) and PGE₂-GE modulates inhibitory synaptic transmission in hippocampal neurones (Sang et al., 2006).

COX-2 is constitutively expressed in some areas of the CNS (Yamagata et al., 1993, Ghilardi et al., 2004), reproductive tissues (Kniss, 1999), and kidneys (Harris et al., 1994). Constitutive levels of COX-2 are high in the spinal cord. Expression is up-regulated spinally following peripheral inflammation (Ichitani et al., 1997, Tonai et al., 1999, Samad et al., 2001) and neuropathic pain states (Zhao et al., 2000). Inhibition of COX-2 has well described analgesic effects in models of inflammatory pain (Zhang et al., 1997, Yaksh et al., 2001, Francischi et al., 2002). Synergistic analgesic actions of ECLs and COX2 inhibitors have been reported (Guindon et al., 2006) and a number of *in vivo* studies have provided evidence for a role of COX-2 in modulating levels of AEA and 2-AG. Intraplantar administration of the COX-2 inhibitor nimesulide, increased levels of AEA and PEA in the hindpaw, and reduced hindpaw inflammation (Jhaveri et al., 2008b), thus suggesting that there is a role for COX-2 metabolism of AEA under inflammatory conditions. By contrast, peripheral administration of another COX-2 inhibitor (rofecoxib) did not alter levels of AEA or PEA in the formalin model of pain (Guindon et al., 2006). The selectivity of the compounds used is an important issue. Several non-selective cyclooxygenase inhibitors also inhibit the activity of FAAH in a pH-dependent manner (Holt et al., 2001, Fowler et al., 2003a), whereas nimesulide is selective

for COX-2 (Fowler et al., 2003b), rofecoxib is also a weak inhibitor of FAAH (Holt et al., 2007). Interestingly, ECs are able to modulate COX2 activity, AEA and 2AG increase cyclooxygenase and 5-LOX activity in intact human neuroblastoma CHP100 cells (Maccarrone et al., 2000) and AEA produced a concentration-dependent increase in the expression of COX-2 in cerebral microvascular endothelium cells, which was partially inhibited by AM251 (Chen et al., 2005).

The detection of the COX-2 metabolites of AEA and 2-AG *in vivo* is central to the hypothesis that that route of metabolism has biological significance. There are, however, limited conflicting reports of the detection of COX-2 metabolites in naïve tissue. The first report of COX-2 metabolites of AEA was their identification in liver, kidney lung and small intestine following the exogenous administration of AEA in FAAH knock-out mice (Weber et al., 2004). PGE2-GE has been detected in the rat hindpaw under control conditions, levels were decreased by inhibition of COX-2 and MAG lipase, but were unaffected by the inflammatory stimulus carrageenan (Hu et al., 2008). Exogenous intraplantar administration of PGE2-GE produced mechanical allodynia and thermal hyperalgesia (Hu et al., 2008), indicating that the generation of COX-2 metabolites of AEA may contribute to pain responses.

Although evidence to date indicates that FAAH is the predominant metabolic enzyme for the ECLs, there may be an enhanced role of

alternative metabolic pathways when the EC system is activated, or when FAAH activity is compromised. To date, few studies have investigated whether inhibition of FAAH, when the EC system is activated, results in the metabolism of ECLs by alternative pathways in the CNS.

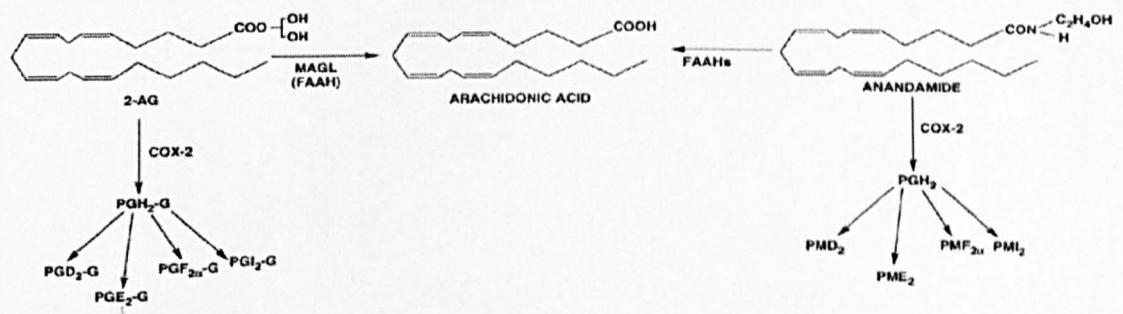


Figure 4.1. Metabolism pathways of anandamide and 2-AG (adapted from Woodward et al., 2007). Anandamide, via FAAH, and 2-AG predominately via MAGL, but also by FAAH are metabolised to arachidonic acid. Metabolism via Cyclooxygenase-2 produces the intermediate product prostaglandin H₂ (AEA), and prostaglandin H₂-glycerol (2-AG). This is then converted to corresponding prostamides (for AEA), and prostaglandin glycerol esters (for 2-AG) via specific prostaglandin synthases.

4.2 Aims

The aims of study;

- To investigate the effects of single and repeated systemic treatment with the FAAH inhibitor URB597 on carrageenan-evoked changes weight bearing and paw circumference.
- To measure levels of ECs and prostamides in the hindpaw and spinal cord and to compare behavioural changes due to carrageenan and URB597 treatment, with changes in levels of ECs in the tissues.

4.3 Methods

4.3.1 Overview of Studies

The effects of repeated systemic injection of URB597, in comparison with a single systemic injection of URB597, on levels of ECs and prostamides in the paw and spinal cord of carrageen or vehicle-treated rats were investigated. Rats were either treated once daily for 4 days with URB597 0.3mgkg^{-1} (*i.p.*) or vehicle, or received a single identical injection of URB597 or vehicle on the day of behavioural testing. A timeline of this study is shown in Figure 4.2. To summarise, treatment groups were:

- URB597 (0.3mgkg^{-1}) injection for 4 days in intraplantar saline-treated rats ($n = 6$).
- URB597 (0.3mgkg^{-1}) injection for 4 days in intraplantar carrageenan-treated rats for 4 days ($n = 12$).
- Single URB597 (0.3mgkg^{-1}) injection in intraplantar saline-treated rats ($n = 6$).
- Single URB597 (0.3mgkg^{-1}) injection in intraplantar carrageenan-treated rats ($n = 12$).
- Vehicle injection for 4 days in intraplantar saline-treated rats ($n = 6$).

- Vehicle injection for 4 days in intraplantar carrageenan-treated rats (n = 12).
- Single vehicle injection in intraplantar saline-treated rats (n = 6).
- Single vehicle in intraplantar carrageenan-treated rats (n = 12).

The development of hyperalgesia following intraplantar injection of carrageenan was assessed by monitoring changes in weight bearing on injected versus non-injected hindpaw. Paw circumference and oedema were measured immediately following each injection and 3 hours after intraplantar injection of carrageenan or vehicle.

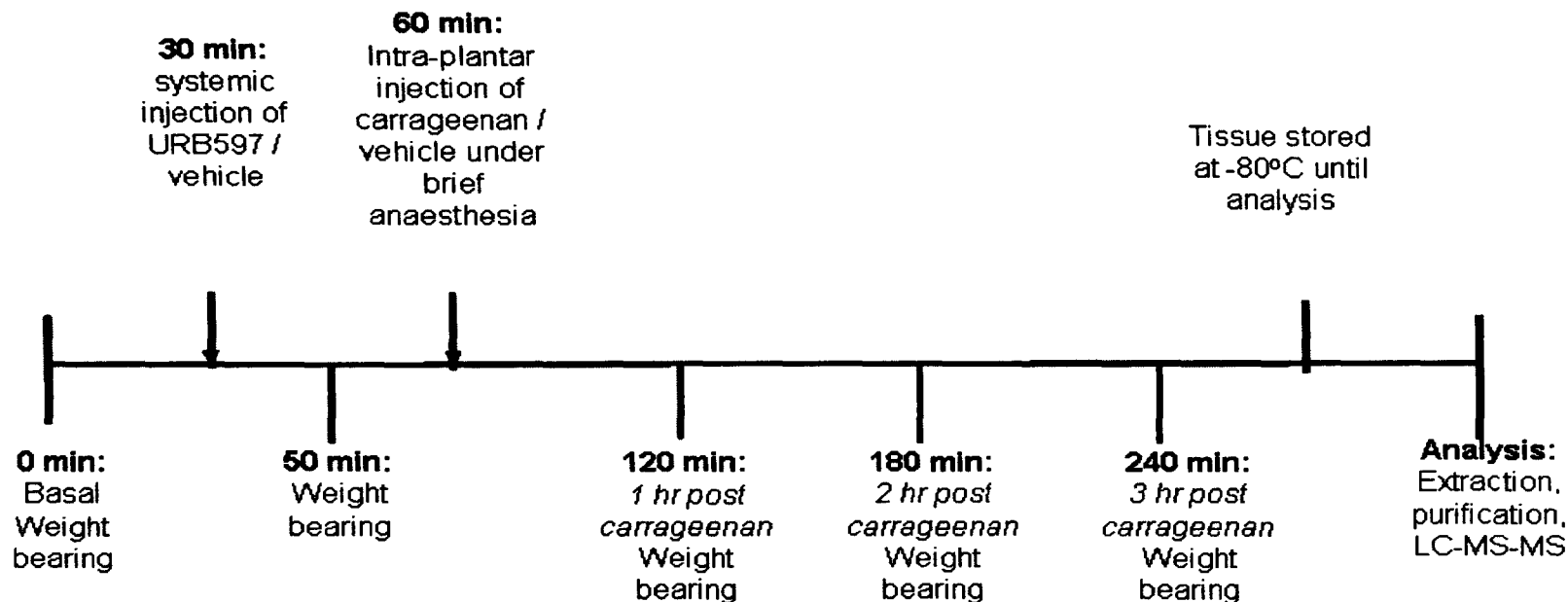


Figure 4.2 A timeline of interventions and measurements used in the study of the effects of URB597 on carrageenan-induced changes in weight bearing and levels of endocannabinoids and prostamides. Rats were pre-treated with URB597 or vehicle followed by injection of carrageenan or vehicle 30 minutes later. Weight bearing measurements were taken, as shown, to investigate effects of the different treatment combinations on pain sensitivity. The time from tissue collection until extraction and analysis of samples by LC-MS/MS was less than two months. Animals repeatedly treated received a single *i.p* injection on 3 consecutive days prior to behavioural testing at the same time of day.

4.3.2 Animals

Male Sprague Dawley rats (200 – 260 g, Charles River, UK) were group housed and maintained on a 12 hour light / dark cycle, with access to food and water *ad libitum*. All experiments were carried out in accordance with UK Home Office regulations (Scientific Procedures Act, 1986).

4.3.3 Measurement of carrageenan-induced inflammation and drug treatment

4.3.3.1 Weight bearing Behaviour

Rats normally distribute their weight evenly between their two hind paws; however when one paw is inflamed, the animals redistribute their weight, to reduce the pressure on the inflamed paw. Changes in weight bearing between the carrageenan-injected and contralateral paws were measured using an incapitance tester (Linton Instrumentation, UK). The incapitance tester measures the weight placed on each hindpaw at a given time point (Figure 4.3), providing a quantitative value which is independent of the experimenter. Care was taken to ensure weight bearing measurements were performed under comparable conditions and the experimenter was blind to the treatment groups. Measurements were taken when rats had settled with each hindpaw on the appropriate transducer, with their front paws on the sloping portion of the holder and their head up. Weight bearing scores were calculated over a 3 second period, repeated 3 times in succession and averaged for each time point. Weight

bearing values are expressed as a percentage of the weight on the injected paw, compared to the contralateral paw.



Figure 4.3 The incapacitance tester used in these experiments (taken from (Bove et al., 2003).

Baseline weight bearing measurements were made 30 minutes prior to the first systemic injection of drug. Rats then received an intraperitoneal injection of either URB597 (0.3mgkg^{-1}) in 3% Tween 80 in saline or vehicle (3% Tween 80 in saline). Thirty minutes following the first injection, rats were briefly anaesthetised under isoflurane/ N_2O / O_2 and received an intra-plantar injection of λ -carrageenan (100 μl , 2 mg in saline, Sigma, UK) or vehicle (saline) into the left hindpaw. The dose of carrageenan used has previously been shown to produce a robust inflammation and associated behavioural changes (Hargreaves et al., 1988b, Nackley et al., 2003, Jhaveri et al., 2005). Weight bearing measurements were taken at 1, 2, and 3 hours post carrageenan-injection.

4.3.3.2 Measurement of Paw Circumference and Volume

4.3.3.2.1 Paw Circumference

In order to measure the degree of carrageenan-induced hindpaw inflammation, the paw circumference was recorded. Nylon thread was tied tightly around the paw. The knot was cut in the middle, and the length of thread was measured to the nearest millimetre (figure4.4). Measurements were taken prior to the carrageenan / vehicle injection and after the 3 hour time point, at the end of the experiment. Changes in paw circumference were expressed as the difference from control values (before carrageenan/vehicle).

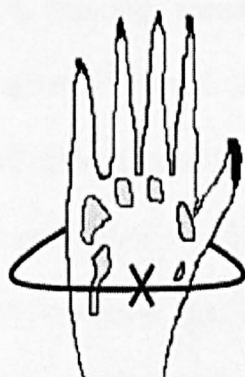


Figure4.4 A diagrammatic representation of rat hind paw, showing the area measured for hind paw circumference. Black nylon was tied around the paw, and cut at position x, and the piece of thread is then measured.

4.3.3.2.2 Paw Volume

To measure the degree of oedema, the volume of the paw was measured using Plethysmometer, which was calibrated using 0.5, 2 and 4g probes. The rat paw was inserted into a solution of KCl in clear acrylic cell, up to a planned point, such as the knee. The volume of liquid displaced was measured by a transducer. Measurements are taken before carrageenan / vehicle injection, and at 3 hour time point, at the end of the experiment. Oedema was expressed as the difference in these values.

4.3.4 Measurement of ECLs and prostamides in rat hindpaw and spinal cord

After the last weight bearing measurement, rats were killed by stunning and decapitation. The spinal cord and hindpaw tissue were rapidly removed and placed onto dry ice. A laminectomy was performed and approximately 2 cm of the lumbar region (L4 and L5) of the spinal cord was removed, and bisected into sections ipsilateral and contralateral sections. Paw tissue was also removed from both the ipsilateral and contralateral hindpaws.

Following collection, samples were stored at -80°C until analysis. The processing of samples with extraction and analysis of analytes was described in detail in chapter 2. Tissue was finely minced using scalpel blades and homogenised in ice-cold acetonitrile. Samples

were shaken twice at 4°C for 1 hour and the supernatant collected. The LC-MS/MS method was optimised for the quantification of AEA, 2-AG, virodhamine, OEA, PEA, and COX-2 metabolites of AEA, and 2-AG (PG-EA and vPG-GE, respectively). AEA-d8, 2-AG-d8 and PGF2 α -EA-d4 were used as internal standards.

4.3.5 FAAH enzyme activity

The *ex vivo* activity of FAAH was studied using a fluorimetric assay, as recently described (Patel et al., 2007) and was carried out by Annie Patel.

Dilute tissue preparations were assessed for hydrolysis of oleamide (100 μ M) as substrate, in a final volume of 100 μ L in 96-well plates. The evolved ammonia was quantified by the production of isoindole-1-sulfonate, following incubation at room temperature with o-phthalaldehyde for 30 min, measuring fluorescence at 360 nm (excitation) and 460 nm (emission). Protein content was determined by a modification of the method of Lowry et al. (1951).

4.3.6 Data Analysis

2 way analysis of variance (ANOVA) was used to compare weight-bearing data between different treatment groups at different time points, with Bonferroni post-hoc analysis. 2-way ANOVA was used to compare paw circumference and volume measurements at different time points and a t-test to compare individual time points. Comparison of levels of ECs and prostamides was carried out using a Mann-Whitney non-parametric test. The level of statistical

significance levels was set at $p < 0.05$. Data are expressed as mean \pm SEM or median + range. A correlation analysis was applied to investigate the relationship between n-acyl ethanolamines (AEA, OEA, PEA) and acyl-glycerols (2-AG) in tissue, a random spearman rank coefficient was calculated for levels of AEA, OEA, PEA and 2-AG within individual rats.

4.4 Results

4.4.1 Carrageenan-induced hyperalgesia

This study used two different dosing regimes, thus the effects of single versus repeated treatment with vehicle on behavioural responses and endocannabinoid levels were compared. There were no significant differences in the effects of intraplantar injection of carrageenan on paw volume, paw circumference, and weight bearing of animals receiving a single or repeated administration of vehicle. Similarly, levels of AEA, PEA, OEA and 2-AG in the hindpaw were not significantly different between rats that received single and repeated administration of vehicle prior to injection of carrageenan. These data were, therefore, combined for comparisons of the effects carrageenan-induced hyperalgesia to saline-treated animals. Comparisons of single versus repeated administration of URB597 were compared to the appropriate vehicle control group for the individual study.

Intraplantar injection of saline did not alter weight bearing on the ipsilateral and contralateral hindpaw, compared to pre-injection values. Intraplantar injection of carrageenan significantly reduced weight bearing on the ipsilateral hindpaw, compared to the contralateral hind-paw. At 2 and 3 hours post carrageenan injection, there was a significant difference between the change in weight bearing between the ipsilateral and contralateral hindpaw of carrageenan-treated rats, compared to saline treated rats (Figure

4.5). Note, both saline and carrageenan treated rats received an i.p injection of vehicle 30 mins prior to saline / carrageenan.

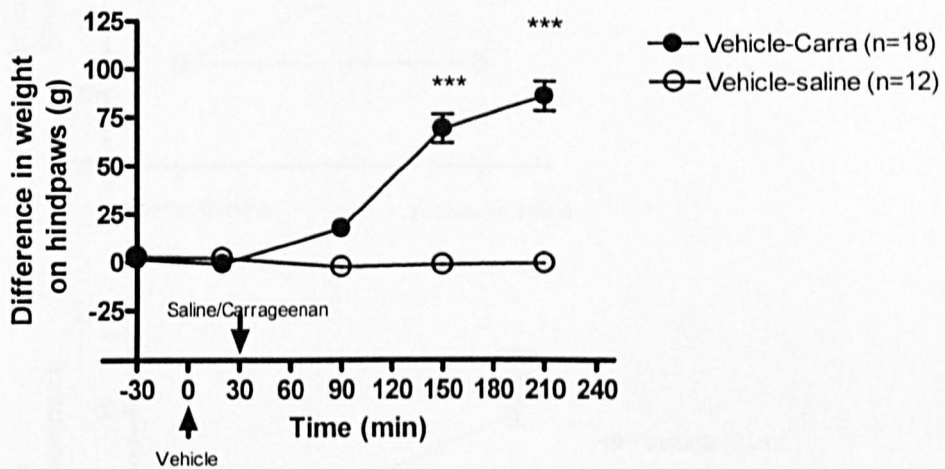


Figure 4.5: Intraplantar injection of carrageenan increased the difference in weight bearing on the ipsilateral and contralateral hindpaws. Rats received a systemic injection of vehicle (3%Tween80 in saline) 30min prior to saline or carrageenan (2mg in 100 μ l). Data were analysed using 2-way ANOVA followed by Bonferroni post hoc test, *** $P < 0.005$ vs. vehicle saline. Data are expressed as mean \pm SEM of differences in weight bearing between contralateral and ipsilateral hindpaw (n=12-18).

Hindpaw circumference was measured before injection of carrageenan / saline (baseline values) and immediately before tissue collection at 2 or 3 hours post carrageenan/saline injection.

There was a significant increase in paw diameter and paw volume of vehicle treated rats at both 2 hours and 3 hours post carrageenan compared to saline treated rats ($P < 0.005$). Intraplantar injection of carrageenan produced a robust increase in paw circumference at both 2 and 3 hours post injection, which was not seen in saline treated rats, (Figure 4.6 A+B).

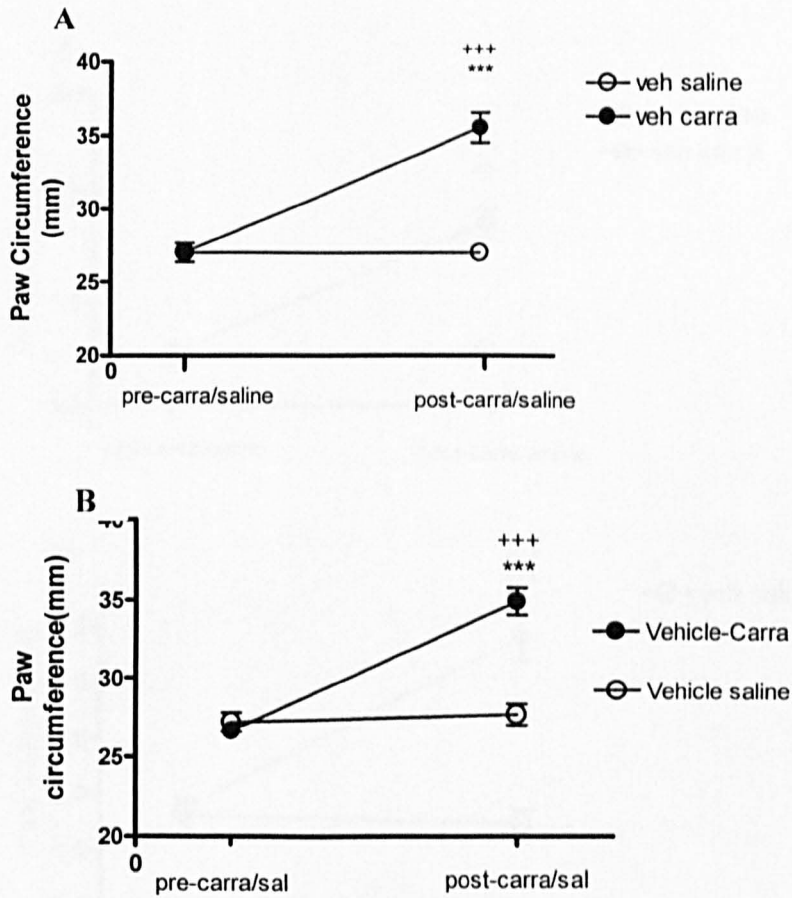


Figure 4.6 A+B: Intraplantar injection of carrageenan produced a significant increase in paw circumference at 2 (A) and 3 (B) hours post carrageenan injection. Data were analysed using unpaired t-test. ***P<0.005 vs. vehicle saline; ***P<0.01 vs. pre-carra. Data are expressed as mean \pm SEM (n=6-9)

Another device for measuring paw volume is the plethysmometer, measuring the whole paw volume, instead of specific cross-section. Hindpaw volume measurements were taken before intraplantar injection of carrageenan or saline (baseline value) and before tissue collection, 2 and 3 hours after injection of carrageenan / saline. Intraplantar injection of saline did not alter hindpaw volume, compared to baseline value. Intraplantar injection of carrageenan (2mg in 100 μ l) induced a significant increase in hindpaw volume at both 2 and 3 hours after carrageenan injection (Figure 4.7).

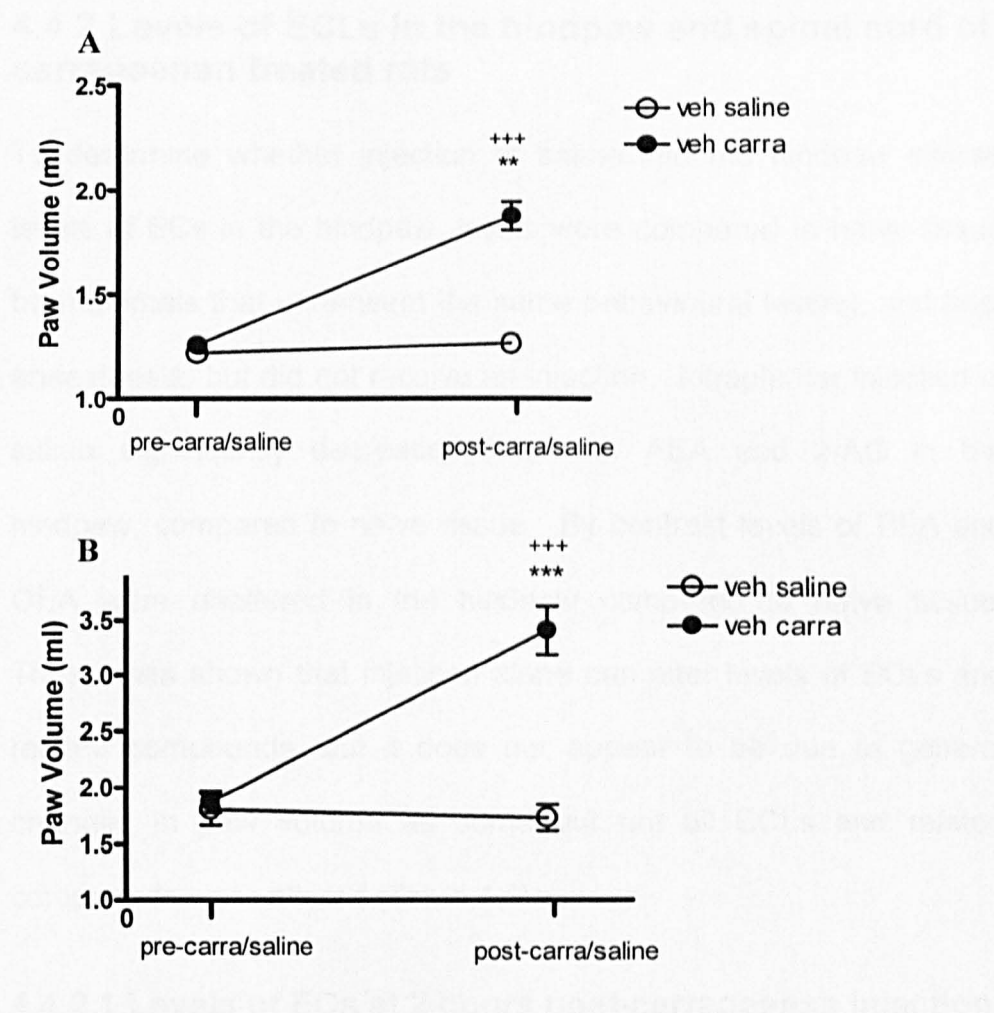


Figure 4.7: Intraplantar injection of carrageenan produced a significant increase in hindpaw volume at 2 (A) and 3 (B) hours post carrageenan injection. Data are expressed as mean \pm SEM (n=6-9) and analysed with an unpaired t-test. ***P<0.005 vs. vehicle saline, ***P<0.005 vs. pre-carra.

There was a strong correlation between paw circumference and paw volume of rats pre-treated with vehicle, receiving an intraplantar injection of carrageenan ($P<0.05$, $R^2=0.81$) (Data not shown)

4.4.2 Levels of ECLs in the hindpaw and spinal cord of carrageenan treated rats

To determine whether injection of saline into the hindpaw altered levels of ECs in the hindpaw, levels were compared to naïve tissue from animals that underwent the same behavioural testing, and brief anaesthesia, but did not receive an injection. Intraplantar injection of saline significantly decreased levels of AEA and 2-AG in the hindpaw, compared to naïve tissue. By contrast levels of PEA and OEA were unaltered in the hindpaw compared to naïve tissue. These data shown that injection alone can alter levels of ECLs and related compounds, but it does nor appear to be due to general changes in paw volume as some but not all ECLs and related compounds were altered (Table 4.4).

4.4.2.1 Levels of ECs at 2 hours post-carrageenan injection

Injection of carrageenan into the hindpaw significantly decreased levels of PEA, OEA and 2-AG in the ipsilateral hindpaw, compared to saline-treated rats, levels of AEA were unaltered (Figure 4.8). Levels of AEA, PEA, OEA and 2-AG in the ipsilateral hindpaw of carrageenan-treated rats were significantly lower than levels in the contralateral hindpaw of carrageenan treated rats (Figure 4.8).

Effects of inhibition of fatty acid amide hydrolase in the carrageenan model of inflammation

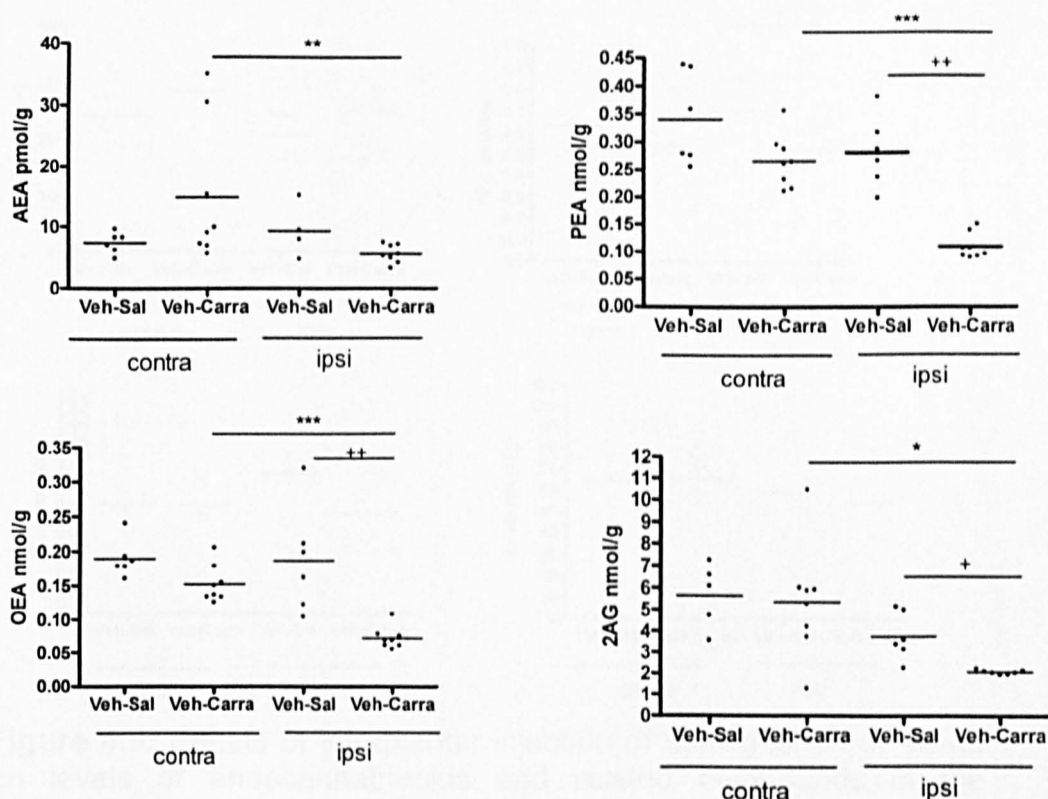


Figure 4.8: Effects of intraplantar injection of carrageenan (carra) or saline (sal) on the levels of endocannabinoids and related compounds in the ipsilateral and contralateral hindpaw of vehicle treated rats 2 hours post-carrageenan injection. Data are expressed as the median and range and were analysed using Mann-Whitney non-parametric test and, (n=6-8). *P<0.05, **P<0.01 vs. ipsilateral vehicle saline hindpaw, *P<0.05, **P<0.01, ***P<0.001 vs. contralateral hindpaw.

Intraplantar injection of carrageenan decreased levels of PEA in the ipsilateral spinal cord of vehicle treated rats, compared to the ipsilateral spinal cord of saline treated rats (Figure 4.9). By contrast, there were no differences in the levels of AEA, OEA or 2-AG in the ipsilateral or contralateral spinal cord of rats at 2 hours following intraplantar injection of saline or carrageenan (Figure 4.9).

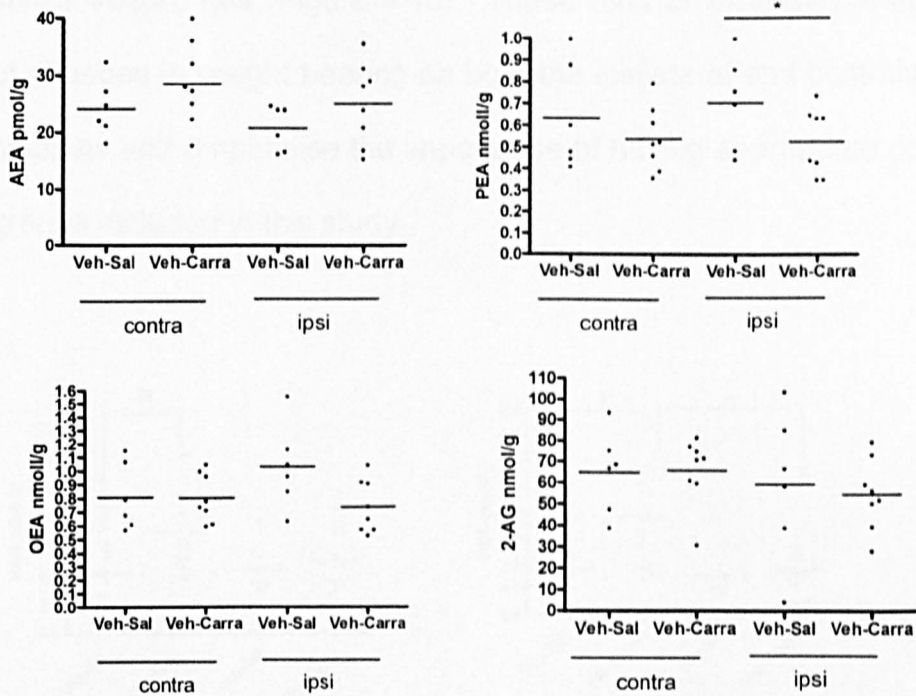


Figure 4.9: Effects of intraplantar injection of carrageenan or saline on levels of endocannabinoids and related compounds in the ipsilateral and contralateral spinal cord of vehicle treated rats 2 hours post injection. Data are expressed as the median and range and were analysed using Mann-Whitney non-parametric test and, (n=6-8). *P<0.05 vs. ipsilateral vehicle saline spinal cord, *P<0.05.

4.4.2.2 Levels of ECLs at 3 hours post-carrageenan injection

Injection of carrageenan into the hindpaw did not significantly alter levels of AEA, PEA, OEA or 2-AG in the ipsilateral hindpaw, compared to saline-treated rats (Figure 4.10). Levels of PEA, and OEA in the ipsilateral hindpaw of carrageenan-treated rats were significantly lower than levels in the contralateral hindpaw of carrageenan treated rats (Figure 4.10). This was not the case for the intraplantar injection of saline, with no differences observed between the ipsilateral and contralateral hindpaw of saline treated rats. Levels of AEA and PEA were higher in the contralateral hindpaw of carrageenan-treated rats compared to the contralateral hindpaw of

saline treated rats (Figure 4.10). These data emphasise the impact of changes in weight bearing on both the ipsilateral and contralateral hindpaw and emphasise the importance of having appropriate control groups included in this study.

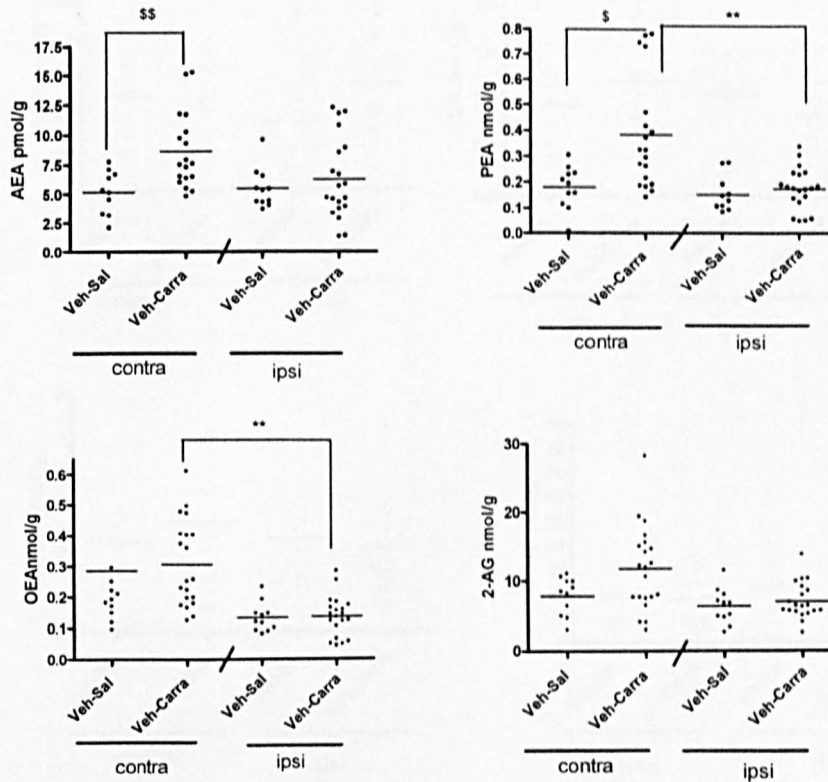


Figure 4.10 Effects of intraplantar injection of carrageenan (carra) or saline on the levels of endocannabinoids and related compounds in the contralateral and ipsilateral hindpaw of vehicle treated rats 3 hours post-injection. Data are expressed as the median and range and were analysed using Mann-Whitney non-parametric test (n=10-21). \$P<0.05, \$\$P<0.01 vs. contralateral vehicle saline hindpaw, **P<0.01 vs. contralateral hindpaw.

The impact of these treatments on levels of ECLs in the spinal cord was also assessed at 3 hours post-injection. Intraplantar injection of saline did not alter levels of AEA, PEA, OEA or 2-AG in the ipsilateral spinal cord compared to the contralateral spinal cord (Figure 4.11). Intraplantar injection of carrageenan was associated with a

significant increase in levels of AEA in the ipsilateral spinal cord ($P < 0.05$) compared to saline-treated rats (Figure 4.11). Note levels of AEA were also elevated in the contralateral spinal cord of carrageenan treated rats, however significance wasn't reached.

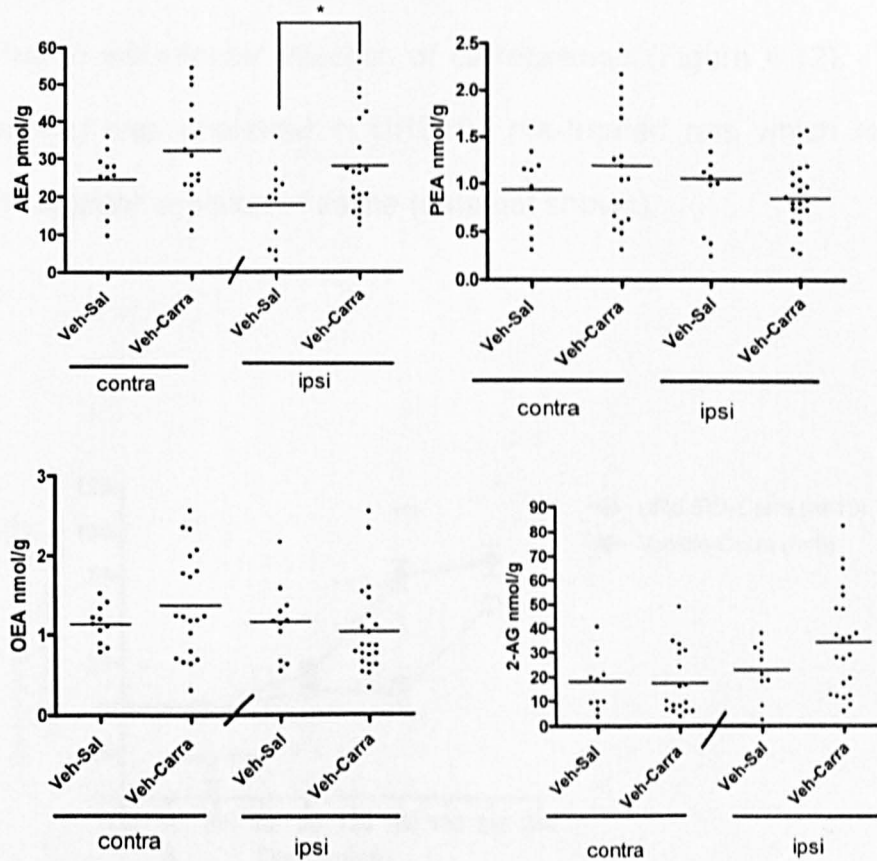


Figure 4.11: Effects of intraplantar injection of carrageenan or saline on levels of endocannabinoids and related compounds in the ipsilateral and contralateral spinal cord of vehicle treated rats 3 hours post-injection. Data are median and range and were analysed using Mann-Whitney non-parametric test ($n=11-19$). * $P < 0.05$ vs. ipsilateral vehicle saline hind-paw.

4.4.3 Effects of a single systemic administration of URB597 on carrageenan induced hyperalgesia

A single i.p injection of URB597 (0.3mgkg^{-1}) significantly delayed the onset and changes in weight bearing on the ipsilateral paw of carrageenan-treated rats, compared to rats pre-treated with vehicle prior to intraplantar injection of carrageenan (Figure 4.12). Weight bearing was unaltered in URB597 pre-treated rats which received intraplantar injection of saline (data not shown).

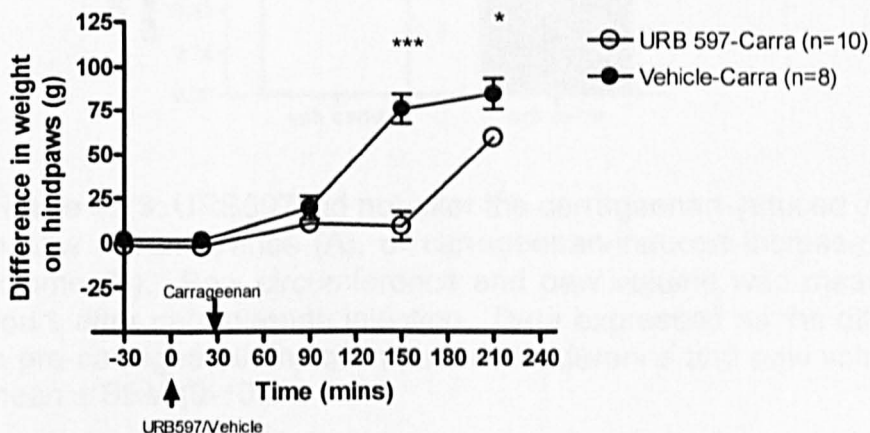


Figure 4.12: Effects of single systemic injection of URB597 on carrageenan induced changes in weight bearing. Rats received URB597 or vehicle 30mins prior to intraplantar injection of carrageenan (2mg in 100 μ l). Data are expressed as mean SEM of differences in weight bearing between contralateral and ipsilateral hindpaw (n=8-10). Data were analysed using 2-way ANOVA followed by Bonferroni post hoc test, * $P < 0.05$, *** $P < 0.005$ vs. vehicle Carra.

A single injection of URB597 did not alter the carrageenan-induced increase in paw circumference, or paw volume, compared to vehicle pre-treated rats receiving intraplantar carrageenan (Figure 4.13 A+B).

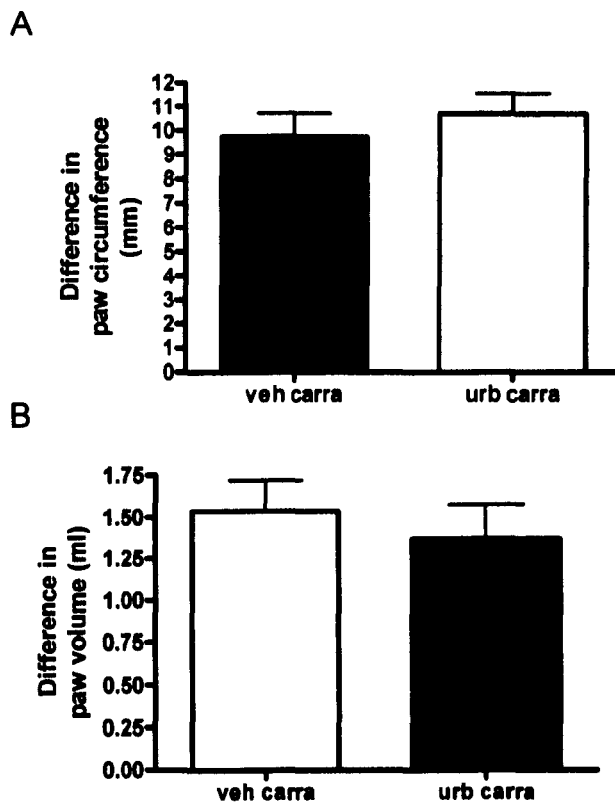


Figure 4.13: URB597 did not alter the carrageenan-induced increase in paw circumference (A), or carrageenan-induced increase in paw volume (B). Paw circumference and paw volume was measured 3 hours after carrageenan injection. Data expressed as the difference in pre-carrageenan injection paw circumference and paw volume, as mean \pm SEM (9-10).

URB597 treatment did not alter the normal progression in the increase in paw diameter and oedema formation between 2 and 3 hours post-carrageenan injection (Figure 4.14).

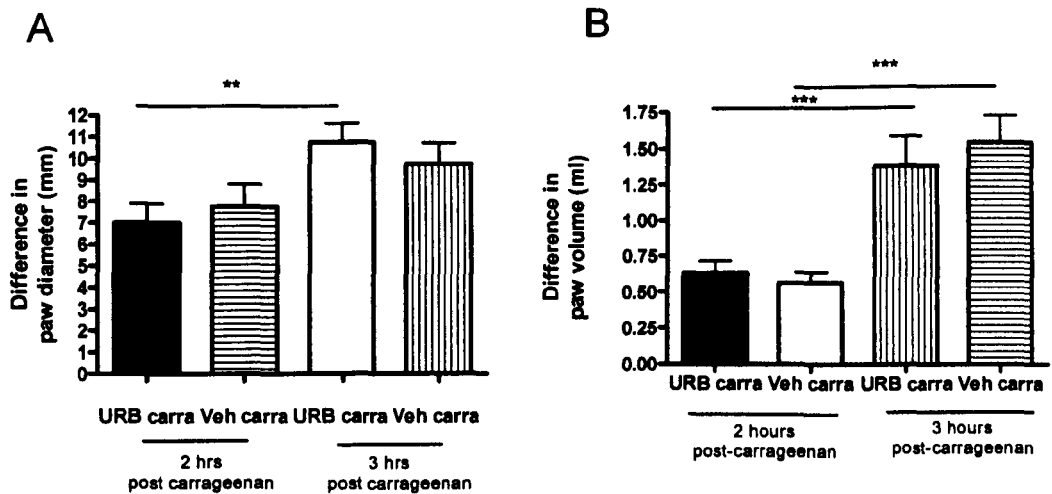


Figure 4.14: Effects of URB597 on paw circumference and volume 2 hours and 3 hours post-carrageenan injection. Data were analysed using 1-way ANOVA and expressed as the difference in pre-carrageenan injection paw circumference, as mean \pm SEM (n=8-9).

4.4.4 Effects of a single systemic administration of URB597 on FAAH enzyme activity in the Midbrain and Liver

To confirm that the single dose of URB597 used was appropriate, levels of FAAH activity in the liver and midbrain in these rats were determined.

URB597 (0.3mgkg^{-1}) produced a small, but non-significant decrease in FAAH activity in the liver and midbrain (Figure 4.15 A+B) Note, FAAH activity in the midbrain was lower than activity in the liver.

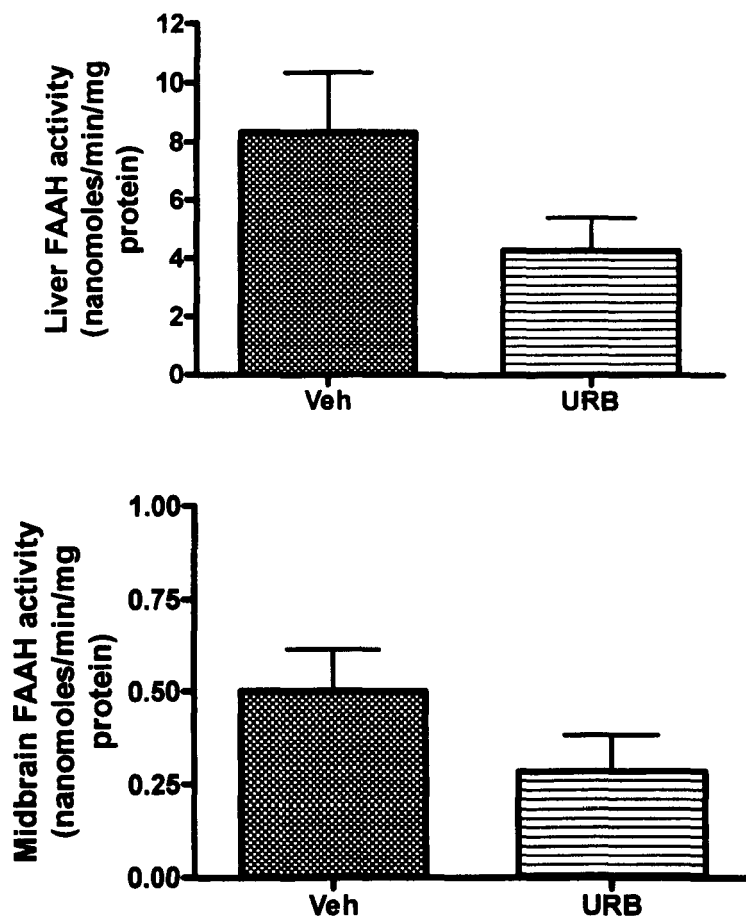


Figure 4.15: *Ex vivo* assessment of FAAH activity in liver (A) and midbrain (B) of vehicle or URB597 treated rats. Data are expressed as mean \pm SEM of fluorescence at 360nm (emission) and 460nm (excitation) from 6 animals using 1 μ M URB597 to define specific FAAH activity. Data were analysed by one-way ANOVA followed by Newman-Keuls post hoc test.

4.4.5 Effects of a single systemic administration of URB597 on levels of ECLs and related compounds

The effects of URB597 on ECL levels in the hindpaw and spinal cord at 2 hours and 3 hours post-carrageenan injection were also determined.

4.4.5.1 Levels of ECLs 2 hours post-carrageenan injection

Single injection of URB597 did not alter levels of AEA, PEA, OEA and 2-AG in the ipsilateral hindpaw at 2 hours post-carrageenan injection, compared to levels in the ipsilateral hindpaw of carrageenan treated rats which received vehicle (Table 4.5)

In all cases, levels of AEA, PEA, OEA and 2-AG in the ipsilateral hindpaw of URB597 pre-treated rats receiving intraplantar injection of carrageenan were significantly lower than levels in the contralateral hindpaw of these rats (Fig 4.16), which reflects the observation that levels of ECs in the ipsilateral hindpaw are lower following carrageenan injection, compared to the contralateral hindpaw (Page 4). A single injection of URB597 did not alter levels of ECLs in the hindpaw of rats which subsequently received an intraplantar injection of saline, compared to vehicle (Table 4.5).

Group	AEA pmol ⁻¹ median (range)		OEA nmol ⁻¹ median (range)		PEA nmol ⁻¹ median (range)		2AG nmol ⁻¹ median (range)	
	Ipsi	Contra	Ipsi	Contra	Ipsi	Contra	Ipsi	Contra
Naive	10.21(7.41-11.74)	10.57 (8.38-12.05)	0.14 (0.11-0.21)	0.15 (0.14-0.38)	0.18 (0.13-0.32)	0.17 (0.16-0.36)	15.01 (6.50-18.83)	13.46 (8.94-16.40)
Vehicle saline	9.40 (4.74-15.31)	7.36 (4.77-9.66)	0.19 (0.10-0.32)	0.19 (0.16-0.24)	0.28 (0.20-0.38)	0.34 (0.26-0.44)	3.78 (2.29-5.17) ^{^^}	5.65 (3.57-7.26) [~]
Vehicle carrageenan	5.62 (3.29-7.50) ^{***+}	15.00 (5.62-35.08)	0.07 (0.06-0.11) ^{*****}	0.14 (0.13-0.19) [§]	0.11 (0.09-0.15) ^{*****}	0.27 (0.21-0.36)	2.08 (1.93-2.25) ^{***}	5.35 (1.30-10.49)
URB597 saline	10.56 (6.84-15.0)	9.56 (6.42-18.33)	0.18 (0.14-0.22)	0.19 (0.15-0.24)	0.27 (0.21-0.44)	0.31 (0.22-0.52)	3.75 (2.42-6.30)	4.21 (3.26-7.22)
URB597 carrageenan	5.06 (2.68-7.58) ^{***}	20.44 (4.20-42.93) ^Δ	0.07 (0.05-0.10) ^{*****}	0.18 (0.14-0.27)	0.10 (0.07-0.16) ^{*****}	0.36 (0.17-0.55)	2.11 (1.47-3.57) ^{**}	5.12 (2.40-9.25)

Table 4.5 Levels of ECLs in the hindpaw of rats treated with a single dose URB597 0.3mgkg⁻¹ or vehicle (i.p), 2 hours following intraplantar injection of carrageenan or saline. Data expressed as median and range and were analysed using non-parametric Mann-Whitney test. ^{*}P<0.05, ^{**}P<0.01, ^{***}P<0.001 vs. contralateral hindpaw, ⁺P<0.05, ⁺⁺P<0.01 vs ipsilateral vehicle saline, ^{**}p<0.01 vs ipsilateral URB597 saline, [§] P<0.05 vs contralateral vehicle saline, ^{^^}P<0.01 vs ipsilateral naïve, [~]P<0.05 vs contralateral naïve.

Effects of inhibition of fatty acid amide hydrolase in the carrageenan model of inflammation

	AEA	OEA	PEA	2-AG
Vehicle	↓	↓	↓	↓
URB597	↓	↓	↓	↓

Table 4.5a summarises the effects of intraplantar injection of carrageenan on levels of ECLs in hindpaw of rats treated with a single injection of vehicle/ URB597 2 hrs post saline/carrageenan injection.

	AEA	OEA	PEA	2-AG
Saline	↔	↔	↔	↔
Carrageenan	↔	↔	↔	↔

Table 4.5b summarises the effects of a single injection of URB597 on levels of ECLs in hindpaw 2 hrs post saline/carrageenan injection.

Effects of inhibition of fatty acid amide hydrolase in the carrageenan model of inflammation

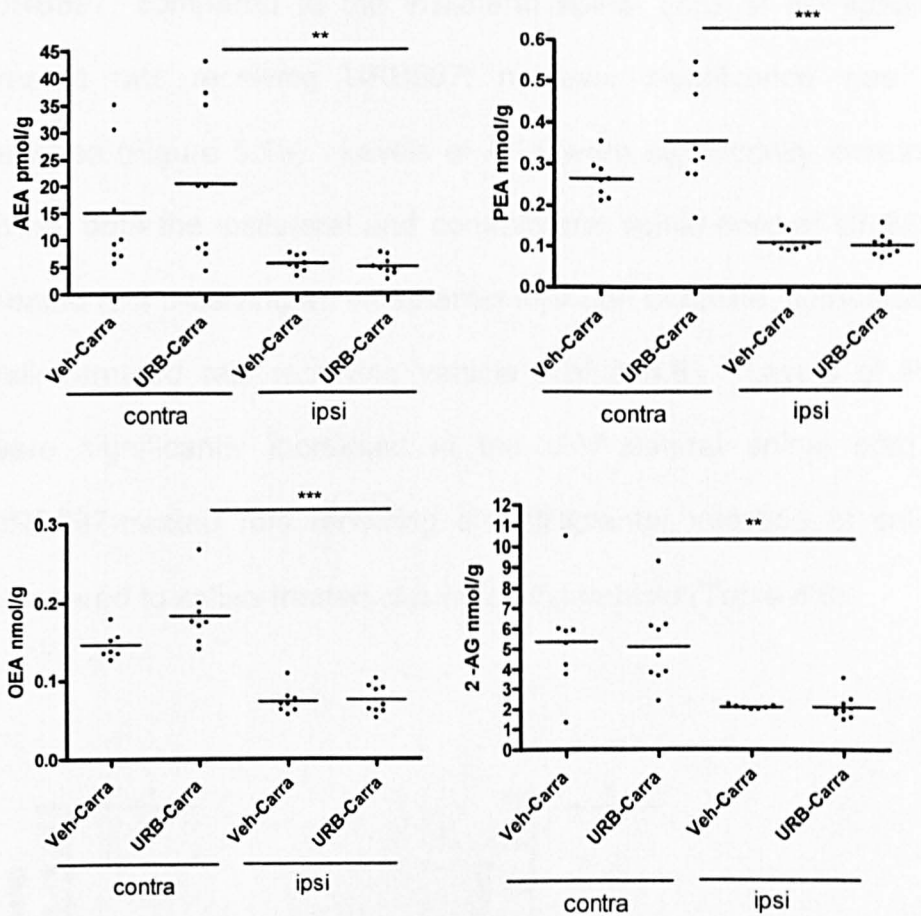


Figure 4.16: Effects of single systemic injection of URB597 or vehicle on carrageenan (carra) or saline (sal) induced changes in levels of endocannabinoids and related compounds in the ipsilateral and contralateral hindpaw at 2 hours post injection. Data were expressed as Median and range (n=8-9) and were analysed using Mann-Whitney non-parametric test. **P<0.01, ***P<0.005 vs. contralateral hindpaw.

Systemic injection of URB597 significantly ($P < 0.01$) increased levels of AEA, OEA, and PEA in the contralateral spinal cord of carrageenan-treated rats compared to the contralateral spinal cord of carrageenan-treated rats receiving systemic injection of vehicle. Levels of 2AG were unaltered (Figure 4.17). There was a trend towards an increase in levels of AEA, PEA and OEA in the ipsilateral spinal cord of carrageenan-treated rats receiving

URB597, compared to the ipsilateral spinal cord of carrageenan treated rats receiving URB597; however significance was not reached (Figure 5.19). Levels of AEA were significantly increased in the both the ipsilateral and contralateral spinal cord of URB597-treated rats receiving an intraplantar injection of saline, compared to saline-treated rats receiving vehicle (Table 4.6). Levels of PEA were significantly increased in the contralateral spinal cord of URB597-treated rats receiving an intraplantar injection of saline, compared to saline-treated rats receiving vehicle (Table 4.6).

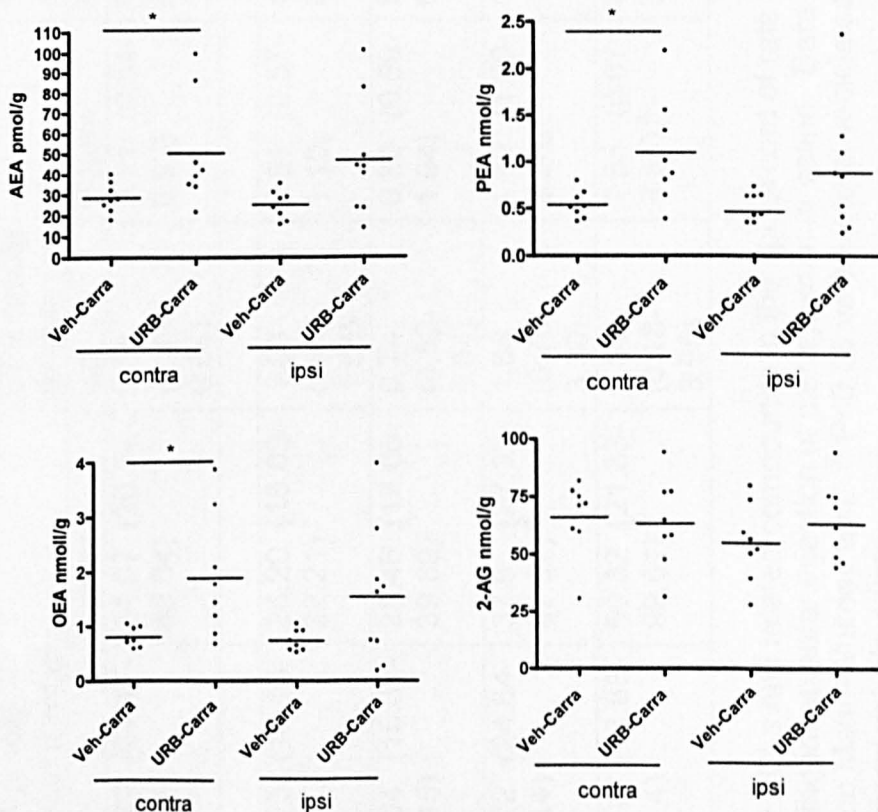


Figure 4.17: Effects of intraplantar injection of carrageenan or saline on levels of endocannabinoids and related compounds in the ipsilateral and contralateral spinal cord of vehicle treated rats 2 hours post injection. Data are expressed as the median and range and were analysed using Mann-Whitney non-parametric test, (n=8-9). *P<0.05 vs. contralateral vehicle carrageenan spinal cord.

Group	AEA pmolg ⁻¹ median (range)		OEA nmolg ⁻¹ median (range)		PEA nmolg ⁻¹ median (range)		2AG nmolg ⁻¹ median (range)	
	Ipsi	Contra	Ipsi	Contra	Ipsi	Contra	Ipsi	Contra
Naive	27.89 (21.17-34.84)	34.07 (30.14-40.04)	0.58 (0.40-0.64)	0.71 (0.54-0.92)	0.46 (0.27-0.58)	0.62 (0.39-0.81)	30.55 (24.63-35.42)	45.46 (32.88-48.05)
Vehicle saline	20.75 (16.16-24.6)	24.20 (18.03-32.21)	1.03 (0.63-1.55)	0.81 (0.57-1.15)	0.70 (0.44-0.99)	0.63 (0.41-1.0)	59.45 (4.09-103.8)	64.82 (38.53-93.13)
Vehicle carrageenan	25.04 (15.31-35.45)	28.46 (17.66-39.89)	0.74 (0.52-1.04)	0.80 (0.59-1.04)	0.53 (0.35-0.73) [%]	0.54 (0.35-0.79)	54.63 (27.99-79.48)	65.85 (30.54-81.52)
URB597 Saline	45.72 (24.64-92.14) [%]	37.6 (27.37-67.52) [#]	1.86 (0.70-3.30)	1.80 (1.00-3.68) [#]	1.06 (0.39-1.86)	1.01 (0.57-1.55)	53.72 (21.83-80.32)	71.87 (38.65-113.7)
URB597 Carrageenan	46.99 (13.68-101.4)	50.32 (21.63-99.61) ^Δ	1.53 (0.18-3.95)	1.88 (0.67-3.85) ^Δ	0.88 (0.24-2.36)	1.10 (0.38-2.19) ^Δ	63.07 (44.11-93.78)	63.22 (31.2-93.96)

Table 4.6 Levels of ECLs and related compounds in the spinal cord of rats treated with a single dose URB597 0.3mgkg⁻¹ or vehicle (i.p), 2 hours following intraplantar injection of carrageenan or saline. Data are expressed as median and range and were analysed using non-parametric Mann-Whitney test. [%] P<0.05 vs ipsilateral vehicle saline, ^Δ P<0.05 vs contralateral vehicle carrageenan, [#] P<0.05 vs contralateral vehicle saline.

	AEA	OEA	PEA	2-AG
Vehicle	↔	↔	↓	↔
URB597	↔	↔	↔	↔

Table 4.6a summarises the effects of intraplantar injection of carrageenan on levels of ECLs in the spinal cord of rats treated with a single injection of Vehicle/ URB597 2 hrs post saline/carrageenan injection.

	AEA	OEA	PEA	2-AG
Saline	↑	↔	↔	↔
Carrageenan	↔	↔	↔	↔

Table 4.6b. summarises the effects of a single injection of URB597 on levels of ECLs in spinal cord 2 hrs post intraplantar injection of saline/carrageenan injection compared to i.p administration of vehicle/URB597 saline.

A correlation analysis of the levels of ECLs in the ipsilateral spinal cord 2 hours post carrageenan / saline injection was undertaken in vehicle and URB597 treated rats to investigate the relationship between each of the N-acylethanolamines (AEA, OEA, and PEA) and acyl-glycerols (2-AG) in each individual rat. Spearman rank correlation coefficient (R^2) were calculated and are presented in Table 5.7. Representative correlation graphs are shown in Figure 4.18. This analysis demonstrates that irrespective of group, levels of 2-AG are not correlated with AEA, PEA or OEA. There was a significant correlation between levels of OEA and PEA for each

treatment group. AEA and OEA were correlated in both the vehicle carrageenan group and URB597 carrageenan group. Interestingly treatment with URB597 was associated with a significant correlation in AEA and PEA, which was not present in the absence of URB597 treatment or the absence of carrageenan treatment.

		R ²			
		URB Carra	Veh Carra	URB saline	Veh Saline
AEA	vs	0.87**	0.40	0.77	0.94*
PEA					
AEA	vs	0.83**	0.74**	0.77	0.94*
OEA					
AEA	vs 2-	-0.05	0.29	0.43	0.14
AG					
OEA	vs	0.97***	0.85*	0.83*	1.00*
PEA					
2-AG	vs	-0.18	-0.02	0.09	0.25
PEA					
2-AG	vs	-0.18	0.10	0.30	0.26
OEA					

Table 4.7 Spearman Rank coefficient correlating levels of ECLs following single systemic injection of URB597 or vehicle, in the spinal cord 2 hours post-injection of carrageenan/saline into the hindpaw. *P<0.05, **P<0.01, ***P<0.005 = significant correlation.

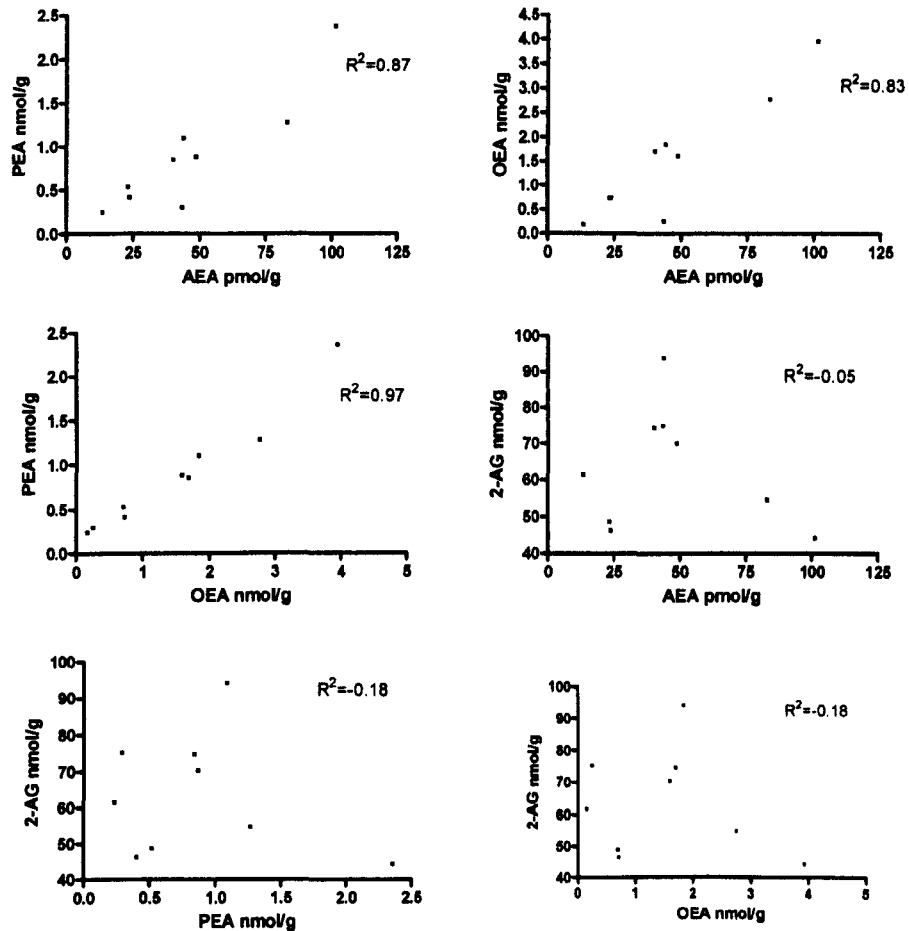


Figure 4.18 Representative graphs showing the correlation coefficient between AEA, OEA, PEA and 2-AG in ipsilateral spinal cord of URB597 treated rats receiving an intraplantar injection of carrageenan.

4.4.5.2 Levels of ECLs 3 hours post-carrageenan injection

Single injection of URB597 did not alter levels of AEA, PEA, OEA and 2-AG in the ipsilateral hindpaw of carrageenan-treated rats, compared to levels in the ipsilateral hindpaw of carrageenan treated rats, which received vehicle (table 4.8). Levels of AEA in the contralateral hindpaw of carrageenan-treated rats were increased in URB597 treated rats compared to rats pre-treated with vehicle (Figure 4.19).

In all cases levels of AEA, PEA, OEA and 2-AG in the ipsilateral hindpaw of URB597 pre-treated rats receiving intraplantar injection of carrageenan were significantly lower than levels in the contralateral hindpaw of these rats (Fig 4.19), which reflects the observation that levels of ECs in the ipsilateral hindpaw are lower following carrageenan treatment, compared to the contralateral hindpaw. A single injection of URB597 did not alter levels of ECLs in the hindpaw of rats receiving intraplantar injection of saline, compared to vehicle (Table 4.8).

Group	AEA pmol g^{-1} median (range)		OEA nmol g^{-1} median (range)		PEA nmol g^{-1} median (range)		2AG nmol g^{-1} median (range)	
	Ipsi	Contra	Ipsi	Contra	Ipsi	Contra	Ipsi	Contra
Naive	10.21(7.41-11.74)	10.57 (8.38-12.05)	0.14 (0.11-0.21)	0.15 (0.14-0.38)	0.18 (0.13-0.32)	0.17 (0.16-0.36)	15.01 (6.50-18.83)	13.46 (8.94-16.40)
Vehicle saline	5.4 (4.1-9.6) [^]	6.5 (5.4-7.8) [~]	0.09 (0.08-0.15)	0.13 (0.10-0.22)	0.11 (0.08-0.15)	0.14 (0.1-0.23)	7.16 (3.37-11.49) ^{^^}	9.90 (8.48-11.02) [~]
Vehicle carrageenan	5.22 (4.34-6.89)	8.55 (5.28-11.76)	0.12 (0.04-0.19) ^{**}	0.36 (0.12-0.48)	0.12 (0.05-0.34) ^{**}	0.39 (0.14-0.78) ^{\$}	5.71 (2.58-10.31)	12.15 (7.54-18.73)
URB597 saline	9.23(6.13-12.6)	8.25 (5.15-13.93)	0.13 (0.12-0.25)	0.14 (0.11-0.16)	0.13 (0.12-0.22)	0.13 (0.11-0.17)	3.55 (2.41-5.97) [*]	10.48 (7.95-14.16)
URB597 carrageenan	6.47 (4.26-11.15) [*]	12.68 (8.72-23.49) [^]	0.09 (0.07-0.17) ^{**}	0.29 (0.14-0.51)	0.14 (0.06-0.30) ^{**}	0.24 (0.15-0.93)	4.19 (2.52-6.55)	11.24(7.57-17.51)

Table 4.8 Levels of ECLs in the hindpaw of rats treated with a single dose URB597 0.3mgkg⁻¹ or vehicle (i.p), 3 hours following intraplantar injection of carrageenan or saline. Data were analysed using non-parametric Mann-Whitney test. Data expressed as median and range. ^{*}P<0.05, ^{**}P<0.01 vs. contralateral hindpaw, [^] P<0.05 vs contralateral vehicle-carrageenan, ^{\$}P<0.05 vs contralateral vehicle saline, [^]P<0.05, ^{^^}P<0.01 vs ipsilateral naive, [~] P<0.05 vs contralateral naive.

	AEA	OEA	PEA	2-AG
Vehicle	↔	↔	↔	↔
URB597	↔	↔	↔	↔

Tables4.8a summarises the effects of intraplantar injection of carrageenan on levels of ECLs in the hindpaw of rats treated with a single injection of Vehicle/ URB597 3 hrs post saline/carrageenan injection.

	AEA	OEA	PEA	2-AG
Saline	↔	↔	↔	↔
Carrageenan	↔	↔	↔	↔

Table4.8b summarises the effects of a single injection of URB597 on levels of ECLs in hindpaw 3 hrs post intraplantar injection of saline/carrageenan injection.

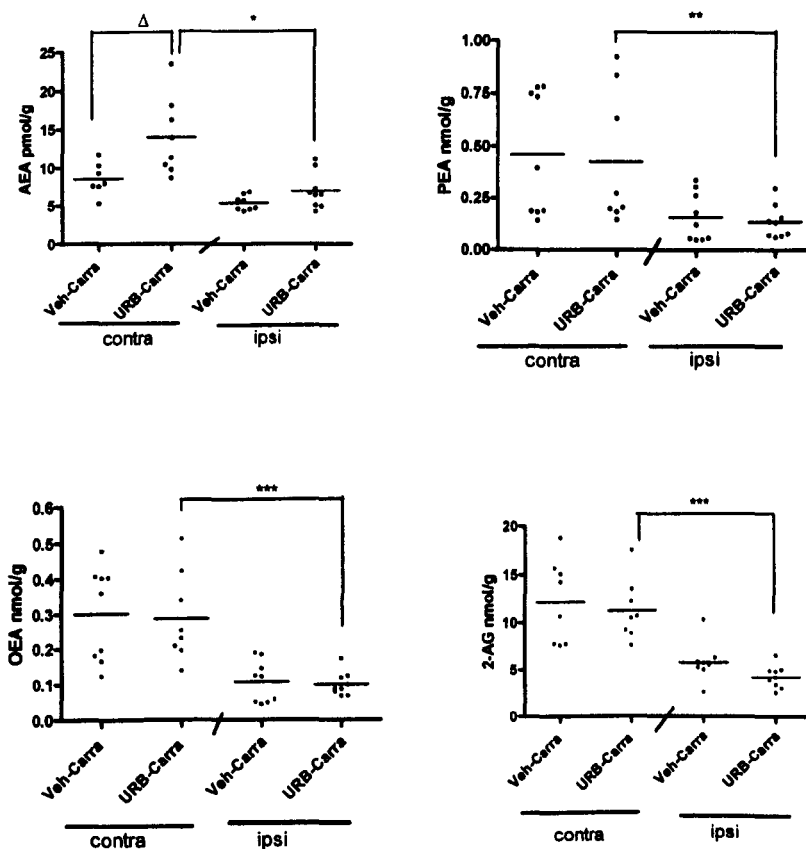


Figure 4.19: Effects of single systemic injection of URB597 or vehicle on carrageenan (carra) induced changes in levels of endocannabinoids and related compounds in the ipsilateral and contralateral hindpaw 3 hours post injection. Data are expressed as Median and range (n=7-9). Comparisons were made using Mann-Whitney non-parametric test. **P<0.01, ***P<0.005 vs. contralateral hindpaw, Δ P<0.05 vs. contralateral vehicle carrageenan hindpaw.

The effect of single systemic dose of URB597 on levels of ECLs in the spinal cord was also determined. Systemic injection of URB597 significantly (P<0.01) increased levels of AEA, OEA, and PEA in the ipsilateral spinal cord of carrageenan-treated rats, compared to the ipsilateral spinal cord of carrageenan-treated rats receiving systemic injection of vehicle. Levels of 2AG were unaltered (Figure 4.20). Levels of AEA were also significantly increased in the ipsilateral spinal cord of saline-treated rats receiving URB597, compared to

the ipsilateral spinal cord of saline treated rats receiving vehicle (Figure 4.20). Levels of PEA and OEA were significantly increased in the contralateral spinal cord of URB597-treated rats receiving an intraplantar injection of saline, compared to saline-treated rats receiving vehicle (Table 4.9).

Group	AEA pmol g^{-1} median (range)		OEA nmol g^{-1} median (range)		PEA nmol g^{-1} median (range)		2AG nmol g^{-1} median (range)	
	Ipsi	Contra	Ipsi	Contra	Ipsi	Contra	Ipsi	Contra
Naive	27.89 (21.17-34.84)	34.07 (30.14-40.04)	0.58 (0.40-0.64)	0.71 (0.54-0.92)	0.46 (0.27-0.58)	0.62 (0.39-0.81)	30.55 (24.63-35.42)	45.46 (32.88-48.05)
Vehicle saline	22.98 (10.43-27.25)	27.87 (17.22-35.94)	1.19 (0.55-1.38)	1.20 (0.78-1.52)	1.00 (0.24-1.51)	0.96 (0.54-1.60)	29.36 (18.55-33.57)	28.77 (3.77-40.67)
Vehicle carrageenan	20.16 (12.24-32.72) ^{**}	35.82 (25.9-49.98)	1.04 (0.74-1.60)	2.04 (1.02-2.56)	0.83 (0.48-1.52)	1.85 (0.81-2.42)	12.49 (8.34-68.73)	6.90 (3.83-29.74)
URB597 Saline	31.99 (27.77-52.64) [#]	72.02 (35.36-99.85) ^{%%}	1.68 (0.99-3.83)	4.72 (1.93-5.68) ^{%%}	1.32 (0.27-2.71)	3.53 (1.55-5.74) [%]	22.36 (8.92-31.74)	17.03 (2.60-28.29)
URB597 Carrageenan	51.29 (20.18-77.8) ⁺⁺	39.68 (10.56-95.46)	3.62 (0.96-8.54) ⁺⁺	3.25 (0.97-5.26)	2.19 (0.80-5.70) ⁺⁺	2.36 (0.83-3.47)	11.81 (5.98-37.69)	9.47 (6.71-46.88)

Table 4.9 Levels of ECLs in the spinal cord of rats treated with a single dose URB597 0.3mgkg⁻¹ or vehicle, 3 hours following injection of carrageenan or saline. Data were analysed using non-parametric Mann-Whitney test. Data expressed as median and range. *P<0.05, **P<0.01 vs contralateral spinal cord, %P<0.05, %%P<0.01 vs. contralateral vehicle saline, #P<0.05 vs. ipsilateral vehicle saline, ++P<0.01 vs ipsilateral vehicle carrageenan.

Effects of inhibition of fatty acid amide hydrolase in the carrageenan model of inflammation

	AEA	OEA	PEA	2-AG
Vehicle	↔	↔	↔	↔
URB597	↔	↔	↔	↔

Tables 4.9a summarises the effects of intraplantar injection of carrageenan on levels of ECLs in the spinal cord of rats treated with a single injection of Vehicle/ URB597 3 hrs post saline/carrageenan injection.

	AEA	OEA	PEA	2-AG
Saline	↑	↔	↔	↔
Carrageenan	↑	↑	↑	↔

Table 4.9b summarises the effects of a single injection of URB597 on levels of ECLs in spinal cord 3 hrs post intraplantar injection of saline/carrageenan injection.

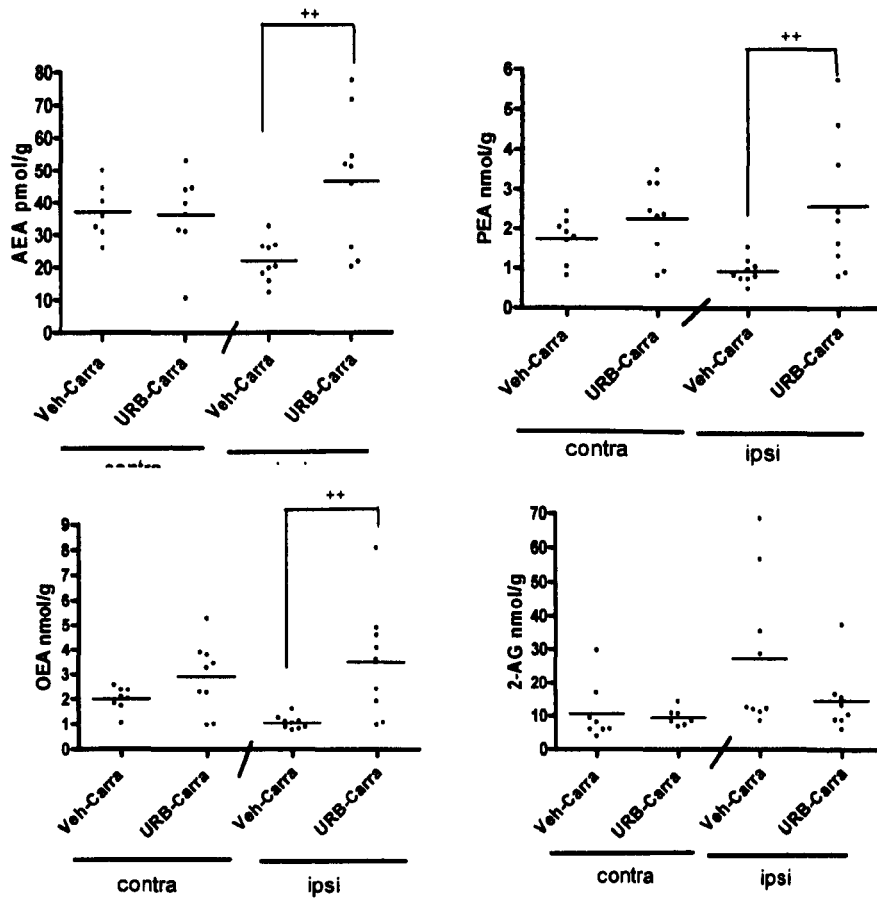


Figure 4.20: Effects of single systemic injection of URB597 or vehicle on carrageenan (carra) or saline (sal) induced changes in levels of endocannabinoids and related compounds in the contralateral and ipsilateral spinal cord 3 hours post injection. Data are expressed as Median and range (n=8-9) and analysed using a Mann Whitney non-parametric test. $^{**}P < 0.01$, ipsilateral vehicle carrageenan spinal cord.

To ease comparisons of the effects URB597 on levels of ECLs and related compounds, at the two different time points, in the hindpaw and spinal cord of URB597-carrageenan treated rats, data were expressed as a percentage of the mean level of ECL in the ipsilateral hindpaw or spinal cord of vehicle pre-treated rats receiving intraplantar injection of carrageenan. Single treatment with URB597 did not alter levels of ECs or related compounds in the hindpaw at 2 hours post-carrageenan, but increased levels of AEA

in the hindpaw at 3 hours post-carrageenan treatment. Levels of PEA, OEA and 2-AG in the hindpaw were unaltered by single treatment with URB597 at 2 or 3 hours post-carrageenan injection (Table 4.10). At the level of the spinal cord, there was a trend for single treatment with URB597 to increase levels of AEA, PEA and OEA in the spinal cord at 2 hours post-carrageenan-injection (Table 4.10). At 3 hours post-carrageenan injection, effects of URB597 on AEA were significant (Table 4.10).

		% of mean levels in vehicle carrageenan-treated rats			
		AEA	PEA	OEA	2-AG
Paw	Single	90.06±9.5	93.16±8.3	103.1±8.2	104.5±10.4
	2hr				
Paw	Single	139.6±15.8*	86.6±16.8	93.3±10.6	73.3±7.1
	3hr				
Spinal Cord	Single	187.6±38.1	168.4±42.2	208.0±56.1	115.5±10.1*
	2hr				
Spinal Cord	Single	213.0±31.5*	278.1±62.0	337.2±71.9	83.9±32.5
	3hr				

Table 4.10: Effects of a single injection of URB597 (0.3mgkg^{-1}) 2 and 3 hours post-carrageenan injection on levels of AEA, PEA, OEA, and 2-AG in the hindpaw and spinal cord of rats. Data were analysed using Mann-Whitney non-parametric test and are expressed as a percentage of the ipsilateral mean level of EC of vehicle treated rats, receiving an intraplantar injection of carrageenan. (n=7-9) *P<0.05, versus 2 hour URB597 administration.

4.4.6 Effects of a repeated systemic administration of URB597 on carrageenan induced hyperalgesia

Repeated i.p injection of URB597 (0.3mgkg^{-1}) once a day, for 4 days did not alter carrageenan-induced changes in weight bearing on the ipsilateral hindpaw, compared to rats receiving 4 day treatment with vehicle prior to intraplantar injection of carrageenan (Figure 4.21).

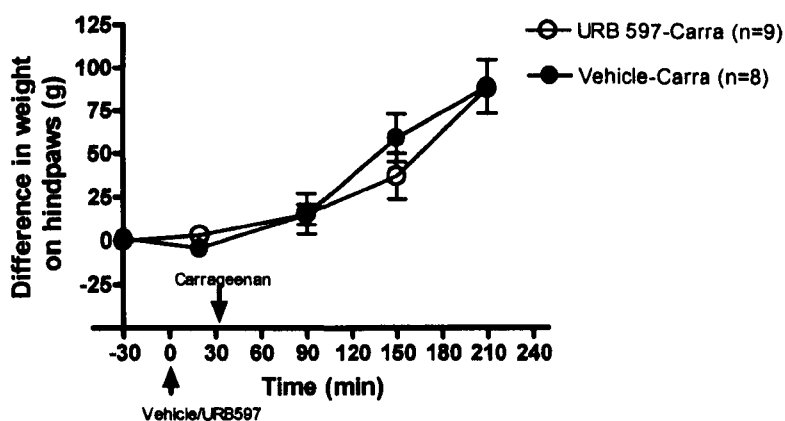


Figure 4.21: Effects of repeated systemic injection of 0.3mgkg^{-1} URB597 on carrageenan-induced changes in weight bearing. Rats received i.p injection of URB597 once daily for 4 days, receiving the final injection 30 mins prior to injection of carrageenan. Data are expressed as mean SEM of differences in weight bearing between contralateral and ipsilateral hind-paw ($n=8-9$). Data were analysed using 2-way ANOVA.

Repeated systemic injection of URB597 did not alter carrageenan-induced increases in paw circumference, or paw oedema, compared to rats receiving repeated injection of vehicle prior to intraplantar injection of carrageenan. (Figure 4.22 A+B).

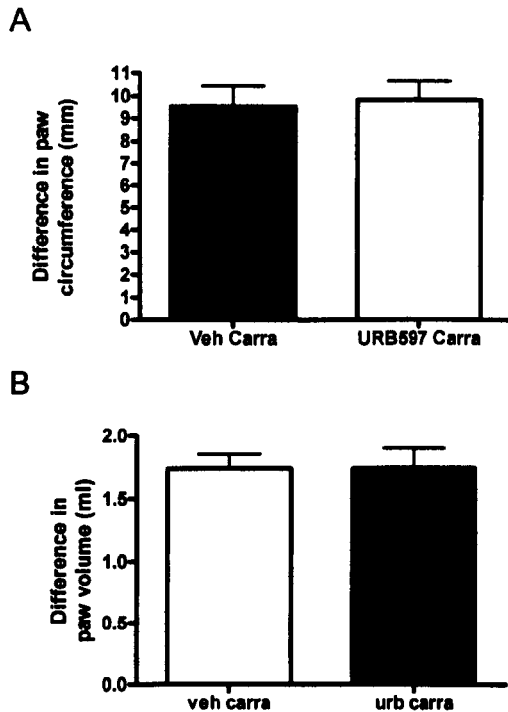


Figure 4.22: Repeated URB597 pre-treatment did not alter the carrageenan-induced increase in paw circumference (A), or carrageenan-induced increase in paw volume (B). Paw circumference and paw volume was measured 3 hours after carrageenan injection. Data are expressed as the difference in pre-carrageenan injection paw circumference and paw volume and presented as mean \pm SEM (6-9)

There was a strong correlation between paw circumference and paw volume of rats pre-treated with either vehicle or URB597, receiving an intraplantar injection of carrageenan ($P < 0.05$, $R = 0.72$) (Data not shown).

4.4.7 Effects of repeated systemic injection of URB597 on FAAH enzyme activity in the Midbrain and Liver

Repeated systemic injection of URB597 (0.3 mg kg^{-1}) significantly decreased FAAH activity in the liver (Figure 4.23A) and midbrain (Figure 4.23B).

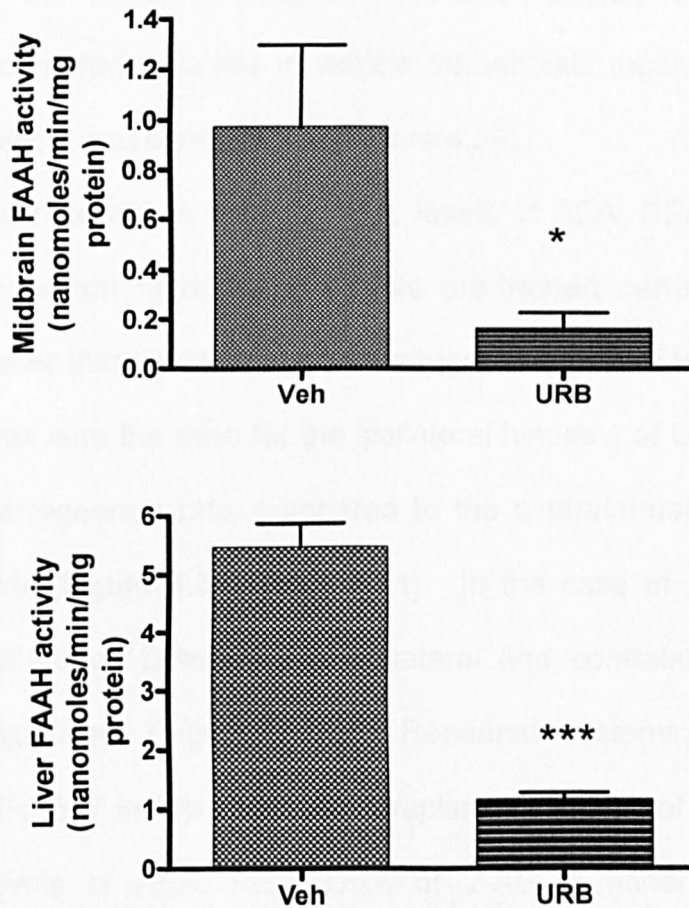


Figure 4.23: *Ex vivo* assessment of FAAH activity in liver (A) and midbrain (B) of repeated vehicle or URB597 treated animals. Data were analysed by one-way ANOVA followed by Newman-Keulis post hoc test, * $P < 0.05$, *** $P < 0.005$. Data are expressed as mean \pm SEM of fluorescence at 360nm (emission) and 460nm (excitation) from 6 animals using 1uM URB597 to define specific FAAH activity

4.4.8 Effects of repeated systemic injection of URB597 on levels of ECLs in the hindpaw and spinal cord of carrageenan treated rats

Repeated injection of URB597 (0.3mgkg^{-1}) did not alter levels of AEA, OEA or 2-AG in the ipsilateral hindpaw of carrageenan-treated rats, compared to levels in rats receiving repeated injection of vehicle prior to injection of carrageenan (Table 4.11). Levels of PEA

in the ipsilateral hindpaw of URB597 treated rats were decreased compared to levels in vehicle treated rats receiving an intraplantar injection of carrageenan (Figure 4.24).

As reported in section 4.3.5, levels of AEA, PEA, and OEA in the ipsilateral hindpaw of vehicle pre-treated carrageenan rats were lower than levels in the contralateral hindpaw of these animals. This was also the case for the ipsilateral hindpaw of URB597 pre-treated carrageenan rats, compared to the contralateral hindpaw of these rats (Figure 4.24, Table 4.11). In the case of AEA and PEA this difference between the ipsilateral and contralateral hindpaw was significant (Figure 4.24). Repeated systemic administration of URB597 in rats receiving intraplantar injection of saline did not alter levels of AEA, PEA, OEA or 2-AG in either the ipsilateral or contralateral hindpaw, compared to systemic vehicle treatment in rats receiving intraplantar injection of saline (Table 4.11).

Group	AEA pmol g ⁻¹ median (range)		OEA nmol g ⁻¹ median (range)		PEA nmol g ⁻¹ median (range)		2AG nmol g ⁻¹ median (range)	
	Ipsi	Contra	Ipsi	Contra	Ipsi	Contra	Ipsi	Contra
Naive	10.21(7.41-11.74)	10.57 (8.38-12.05)	0.14 (0.11-0.21)	0.15 (0.14-0.38)	0.18 (0.13-0.32)	0.17 (0.16-0.36)	15.01 (6.50-18.83)	13.46 (8.94-16.40)
Vehicle saline	5.35 (4.33-6.85) [^]	4.25 (2.14-7.12) [~]	0.16 (0.12-0.23)	0.21 (0.17-0.29)	0.19 (0.10-0.28)	0.22 (0.16-0.31)	5.87 (2.67-8.63) [^]	6.31 (2.67-8.68) ^{~~}
Vehicle carrageenan	7.24 (1.45-12.28)	9.05 (5.55-15.31)	0.15 (0.06-0.28) ^{**}	0.31 (0.14-0.61)	0.19 (0.14-0.24) ^{**}	0.31 (0.17-0.47)	7.99 (4.11-13.89)	8.13 (4.11-13.89)
URB597 Saline	5.35 (4.78-7.20)	5.02 (4.33-6.85)	0.23 (0.18-0.30)	0.20 (0.18-0.25)	0.12 (0.10-0.18)	0.20 (0.11-0.30)	7.20 (2.65-10.86)	6.73 (2.65-10.86)
URB597 Carrageenan	5.07 (1.38-14.14) ^{**}	9.04 (2.36-15.32)	0.16 (0.07-0.19)	0.20 (0.10-0.31) ^Δ	0.13 (0.08-0.19) ^{****+}	0.27 (0.15-0.45)	6.05 (1.81-9.41)	5.83 (1.81-9.41)

Table 4.11: Levels of ECLs and related compounds in the hindpaw of rats receiving repeated dosing with URB597 0.3mgkg⁻¹) or vehicle, and the intraplantar injection of carrageenan or saline. Tissue were collected 3 hours following injection of carrageenan or saline. Data expressed as median and range and were analysed using non-parametric Mann-Whitney test. ^{*}P<0.01, ^{***}P<0.005 vs. contralateral hindpaw, ^{**}P<0.01 vs ipsilateral vehicle carrageenan, ^Δ P<0.05 vs contralateral vehicle-carrageenan, [^]P<0.05 vs ipsilateral naïve, [~]P<0.05, ^{~~}P<0.01vscontralateral naïve.

	AEA	OEA	PEA	2-AG
Vehicle	↔	↔	↔	↔
URB597	↔	↔	↔	↔

Tables 4.11a summarises the effects of intraplantar injection of carrageenan on levels of ECLs in the hindpaw of rats treated with a single injection of Vehicle/ URB597 3 hrs post saline/carrageenan injection.

	AEA	OEA	PEA	2-AG
Saline	↔	↔	↔	↔
Carrageenan	↔	↔	↓	↔

Table 4.11b summarises the effects of a repeated injection of URB597 on levels of ECLs in the hindpaw 3 hrs post intraplantar injection of saline/carrageenan injection.

Effects of inhibition of fatty acid amide hydrolase in the carrageenan model of inflammation

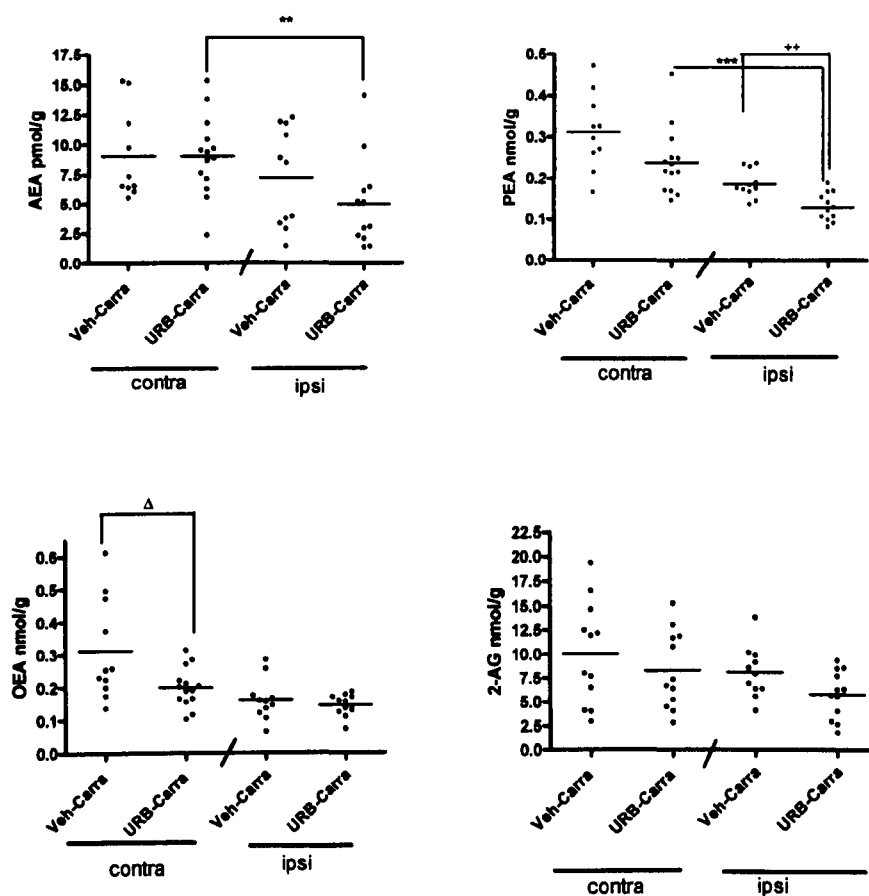


Figure 4.24: Effects of repeated systemic injection of URB597 or vehicle on carrageenan (carra) or saline (sal) induced changes in endocannabinoid levels in the contralateral and ipsilateral hindpaw 3 hours post carrageenan injection. Data were expressed as Median and range (n=9-14), and analysed using Mann-Whitney non-parametric test, **P<0.01, ***P<0.005 vs. contralateral hind-paw, **P<0.01 vs. ipsilateral vehicle-carrageenan hind-paw, ΔP<0.05 vs. contralateral vehicle carrageenan hind-paw.

Repeated URB597 treatment in rats receiving intraplantar injection of saline did not alter levels of AEA, PEA, OEA or 2-AG in the ipsilateral spinal cord, compared to vehicle saline treated rats (Table 4.12). This was also the case for the contralateral spinal cord, with the exception of PEA. Repeated URB597 treatment in rats receiving intraplantar injection of carrageenan did not alter levels of

AEA in the ipsilateral spinal cord compared to vehicle treated carrageenan rats. By contrast levels of OEA and PEA were increased (Figure 4.25, Table 4.12) in the ipsilateral spinal cord of rats repeatedly dosed with URB597 and receiving intraplantar injection of carrageenan, compared to vehicle treated carrageenan rats.

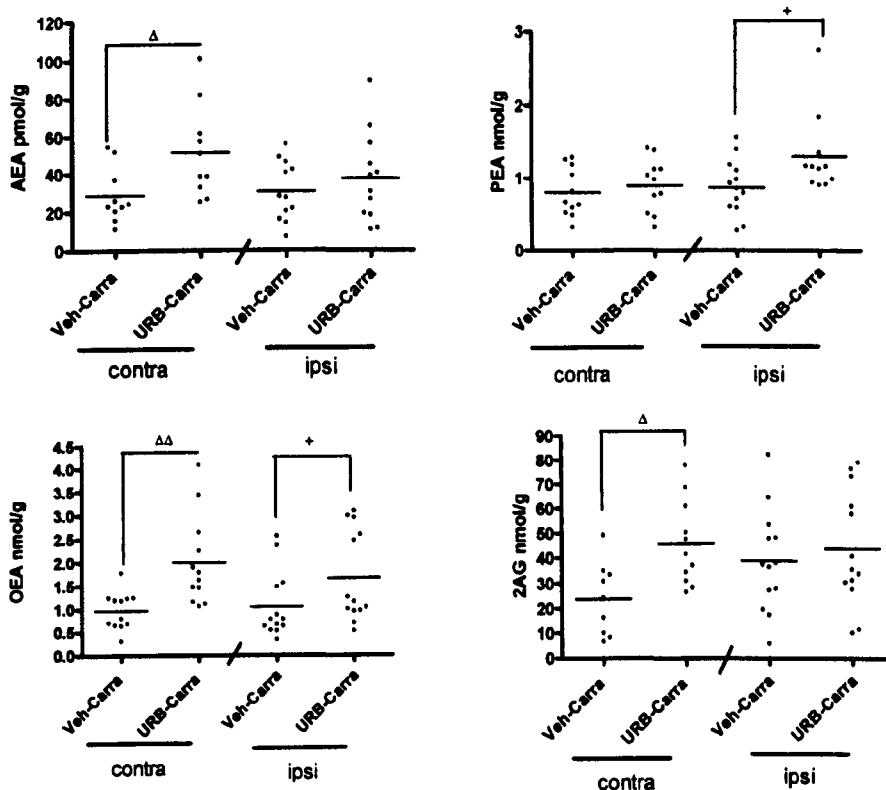


Figure 4.25: Effects of repeated systemic injection of URB597 or vehicle on carrageenan (carra) or saline (sal) induced changes in levels of endocannabinoids in the contralateral and ipsilateral spinal cord of vehicle treated rats 3 hours post-injection. Data are expressed as median and range (n=10-13) and analysed using Mann-Whitney non-parametric test, + $P < 0.05$, vs. ipsilateral vehicle-carrageenan spinal cord, Δ $P < 0.05$, ΔΔ $P < 0.01$ vs. vehicle carra contralateral spinal cord.

Group	AEA pmol g^{-1} median (range)		OEA nmol g^{-1} median (range)		PEA nmol g^{-1} median (range)		2AG nmol g^{-1} median (range)	
	Ipsi	Contra	Ipsi	Contra	Ipsi	Contra	Ipsi	Contra
Naïve	27.89(21.17-34.84)	34.07 (30.14-40.04)	0.58 (0.4-0.64)	0.71 (0.54-0.92)	0.46 (0.27-0.58)	0.62 (0.39-0.81)	30.55 (24.63-35.42)	45.46 (32.88-48.05)
Vehicle saline	12.55 (3.01-35.9) ^{^^}	25.09 (9.65-32.36) [~]	1.20 (0.63-2.18) ^{^^}	1.09 (0.83-1.41)	1.22(0.38-2.30) ^{^^}	0.87 (0.31-1.33) [~]	19.55 (2.38-37.98) [^]	14.73(9.27-20.96) ^{^^}
Vehicle carrageenan	30.77 (6.98-56.08)	23.59 (11.00-54.6)	1.05 (0.34-2.56)	0.99 (0.30-1.78)	0.86 (0.27-1.57)	0.80 (0.31-1.29)	38.84 (5.76-82.38)	24.88 (6.58-49.02)
URB597 Saline	18.93 (8.62-37.37)	35.08 (7.20-56.22)	1.39 (0.84-2.16)	1.79 (1.35-2.64) ^{^^}	1.34 (0.44-2.14)	1.68 (0.73-2.31) ⁺	23.68 (7.63-56.78)	24.73 (13.94-44.15)
URB597 carrageenan	37.77 (10.68-89.29)	51.50 (25.14-101.1) ^{Δ∞}	1.65 (0.52-3.08) ⁺	2.00(1.07-4.10)	1.31(0.91-2.74) ⁺	0.90 (0.38-1.47) [∞]	43.69(10.08-79.21)	45.73 (26.37-77.84) ^{Δ∞}

Table 4.12: Levels of ECLs and related compounds in the spinal cord of rats receiving repeated dosing with URB597 (0.3mgkg⁻¹) or vehicle, 3 hours following injection of carrageenan or saline. Data are expressed as median and range and were analysed using non-parametric Mann-Whitney test. ^{*}P<0.05, ^{**}P<0.01 vs contralateral vehicle saline, [∞]P<0.05 vs contralateral URB597 saline, ^ΔP<0.05 vs contralateral vehicle carrageenan, ⁺P<0.05 vs ipsilateral vehicle carrageenan, [~]P<0.05, ^{^^}P<0.01 vs contralateral naïve, [^]<0.05, ^{^^}0.01 vs ipsilateral naïve.

	AEA	OEA	PEA	2-AG
Vehicle	↔	↔	↔	↔
URB597	↔	↔	↔	↔

Table 4.12a summarises the effects of intraplantar injection of carrageen on levels of ECLs in the spinal cord of rats treated with a single injection of Vehicle/ URB597 3 hrs post saline/carrageenan injection.

	AEA	OEA	PEA	2-AG
Saline	↔	↔	↔	↔
Carrageenan	↔	↑	↑	↔

Table 4.12b summarises the effects of a repeated injection of URB597 on levels of ECLs in the spinal cord 3 hrs post intraplantar injection of saline/carrageenan injection.

To ease comparisons of the effects of acute versus repeated URB597 treatment on levels of ECLs in the ipsilateral hindpaw and spinal cord of URB597-carrageenan treated rats, data were expressed as a percentage of the mean level of ECL in the ipsilateral hindpaw or spinal cord of vehicle pre-treated rats receiving intraplantar injection of carrageenan. For the hindpaw, there was a higher percentage increase in levels of AEA in rats receiving a single dose of URB597, compared to repeated dose of URB597, at 3 hours post-carrageenan injection (Table4.13). There were no significant

differences in the increase in levels of PEA, OEA, and 2-AG in the hindpaw following repeated or single treatment with URB597.

In the spinal cord, there was a significantly larger increase in levels of AEA and OEA in rats receiving a single dose of URB597, compared to repeated treatment with URB597 at 3 hours post-carrageenan injection (Table 4.13). There was also a trend towards an increase in levels of PEA following the single dose of URB597 compared to repeated treatment; however this did not reach significance (Table 4.13).

		% of mean level in vehicle carrageenan-treated rats			
		AEA	PEA	OEA	2-AG
PAW	Single	139.6± 15.8**	86.6±1 6.8	93.3±10.6	73.3±7.1
	Repeated	69.4±1 5.2	69.7±5. 3	89.9±5.8	71.7±8.9
SPINAL CORD	Single	213.0± 31.5*	278.1± 62.0	337.2±71.9 3*	83.9±32.5
	Repeated	122.8± 22.2	168.5± 25.8	157.9±25.8	112.5±16.9

Table 4.13: Effects of intraplantar injection of carrageenan on levels of AEA, PEA, OEA, and 2-AG in the hindpaw and spinal cord of rats which received either a single or repeated treatment with URB597 (0.3mgkg⁻¹). Data were analysed using Mann-Whitney non-parametric test and are expressed as a percentage of the ipsilateral mean level of EC of vehicle treated rats, receiving an intraplantar injection of carrageenan. (n=7-9) *P<0.05, **P<0.01 versus repeated URB597 administration.

Overall, the greater increase in the levels of AEA, PEA and OEA in rats receiving a single dose of URB597 may explain the significant inhibitory effect of a single dose URB597 on pain behaviour, compared to the lack of effect of repeated URB597 treatment. The basis for the differential effect of repeated URB597 treatment compared to a single dose of URB597 is unknown.

A correlation analysis of the levels of ECs in the ipsilateral spinal cord 3 hours post carrageenan / saline injection was also undertaken in rats treated with a single systemic injection of vehicle or URB597 to investigate the relationship between each of the N-acylethanolamines (AEA, OEA, and PEA) and acyl-glycerols (2-AG) in each individual rat. Spearman rank correlation coefficient (R^2) are presented in Table 4.14 and representative correlation graphs are shown in Figure 4.26. This analysis demonstrates that irrespective of group levels of 2-AG are not correlated with AEA, PEA or OEA. There was a significant correlation between levels of OEA and PEA for each treatment group. AEA and OEA were correlated in both the vehicle carrageenan group and URB597 carrageenan group. Interestingly treatment with URB597 was associated with a significant correlation in AEA and PEA, which was not present in the absence of URB597 treatment.

		R ²			
		URB Carra	Veh Carra	URB saline	Veh Saline
AEA	vs	0.85**	0.68	0.80	0.60
PEA					
AEA	vs	0.85**	0.82*	0.40	0.51
OEA					
AEA	vs 2-	0.13	0.20	0.61	0.80
AG					
OEA	vs	0.97***	0.77*	0.80*	0.72*
PEA					
2-AG	vs	-0.03	0.02	0.41	0.24
PEA					
2-AG	vs	0.1	0.38	0.20	0.61
OEA					

Table 4.14 Spearman Rank coefficient correlating levels of ECLs in spinal cord 3 hours following intraplantar injection of carrageenan / saline, *P<0.05, **P<0.01, ***P<0.005.

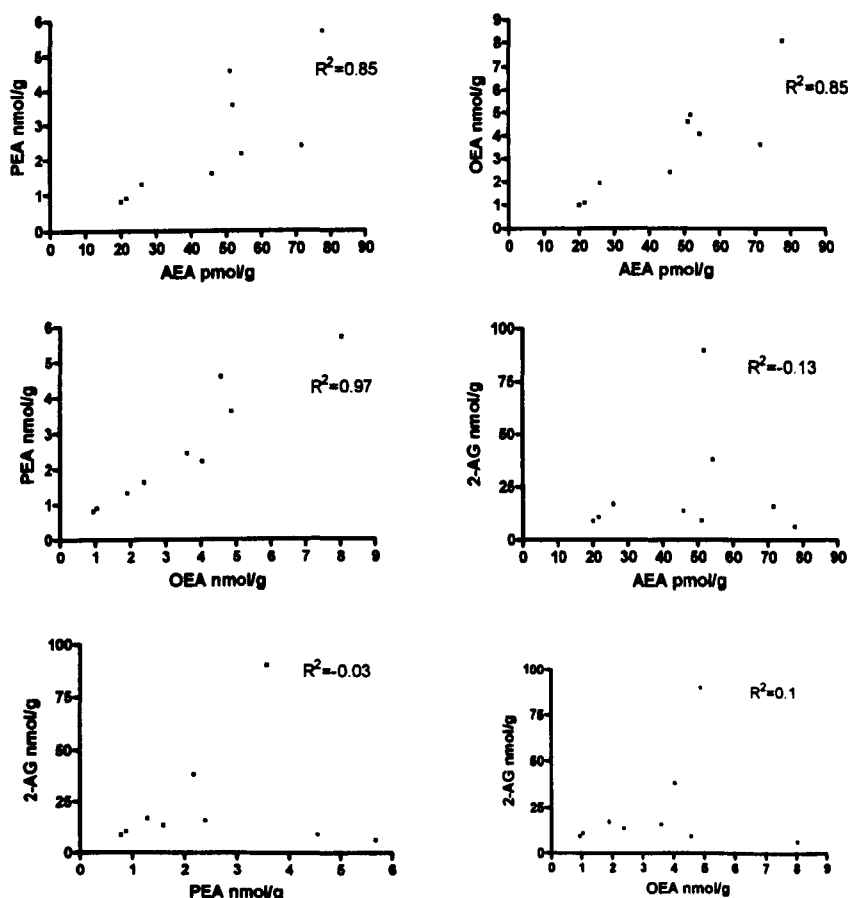


Figure 4.26 Representative graphs showing the correlation coefficient between AEA, OEA, PEA and 2-AG in ipsilateral spinal cord of URB597 treated rats 3 hours post following intraplantar injection of carrageenan.

In Chapter 2, I describe the development and validation of a sensitive LC-MS/MS method for the detection of COX-2 metabolites (PG E₂, PGD₂, PGF₂α EA, PGE₂ GE and PGF₂α GE) in biological tissue. This method was employed to determine whether COX-2 metabolites of AEA or 2-AG are present in the hindpaw or spinal cord following the induction of inflammation and / or the inhibition of FAAH. In particular, this analytical approach was used to identify if alternative catabolism pathways for AEA may account for the reduced effect of repeated URB597 treatment on pain behaviour. Neither COX-2 metabolites of AEA or 2-AG was detected in either the hindpaw or spinal cord of rats treated with single or repeated URB597 and intraplantar injection of carrageenan or saline. Prostaglandin ethanolamides and prostaglandin glycerol esters were detected if they were spiked into rat brain tissue (Figure 4.27), showing the functionality of the method. The limit of detection of PG-EAs and PG-GEs was 10pmol/g and 100pmol/g respectively. On this basis, we assume that if the COX-2 metabolites of AEA and 2-AG are present, they are below our limit of detection.

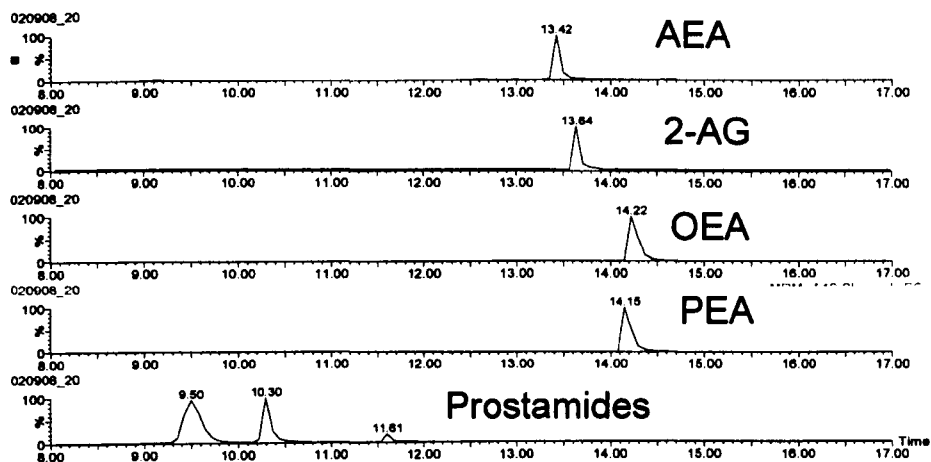


Figure 4.27: Representative chromatograms of the endocannabinoids detected in rat brain and COX-2 metabolites of AEA with the addition of synthetic standards.

4.5 Discussion

In this chapter I have shown that intraplantar injection of carrageenan results in hindpaw oedema and hyperalgesia 3 hours post carrageenan administration. A single systemic injection of URB597 did not alter carrageenan-induced hindpaw oedema, but did delay the onset of carrageenan-induced hyperalgesia at 2 hours post-carrageenan injection, and also attenuated carrageenan-induced hyperalgesia at 3 hours. By contrast repeated systemic administration of URB597 did not alter carrageenan-induced hyperalgesia or hindpaw oedema at either 2 or 3 hours post-carrageenan injection.

The analgesic effects of a single injection of URB597 on carrageenan-induced hyperalgesia were not associated with changes in levels of ECLs in the ipsilateral hindpaw of carrageenan-inflamed animals. It was, however, associated with an increase in levels of AEA, OEA and PEA in the ipsilateral spinal cord, compared to the ipsilateral spinal cord of vehicle treated animals. These data suggest that a spinal site of action contributes to the inhibitory effects of URB597 in this model of inflammatory pain. In line with the lack of effect of repeated URB597 on hyperalgesia, there was a modest effect of this treatment on levels of OEA and PEA in the ipsilateral spinal cord of carrageenan-treated rats, compared to vehicle. Comparison of the effects of a single versus repeated URB597 treated rats on levels of ECLs in the spinal cord revealed that there was a larger percentage increase in levels of AEA in both the

hindpaw and spinal cord of animals receiving a single injection of URB597, compared to repeated injection of URB597. Repeated injection of URB597 only elevated PEA and OEA in the spinal cord, suggesting that elevation of AEA, OEA and PEA is required to attenuate carrageenan induced hyperalgesia, which is in keeping with previous studies demonstrating a role of the CB₁ receptor in mediating the effects of URB597 (Jayamanne et al., 2006a, Maione et al., 2006, Ahn et al., 2009b).

4.5.1 The effects of carrageenan at 2 hours and 3 hours on carrageenan-induced hyperalgesia and levels of ECLs.

It is well established that intraplantar injection of carrageenan produces a behavioral pain response which is associated with hindpaw expansion of receptive field of spinal neurones innervating the inflamed site (Elmes et al., 2004). The behavioral pain response can be assessed through changes in behavioural responses such as withdrawal latency to mechanical or thermal stimuli and changes in weight bearing.

The increase in hindpaw oedema is associated with an increase in paw volume and circumference 3 hours following injection of carrageenan (Hargreaves et al., 1988a), which is consistent with our observations. Carrageenan-induced hyperalgesia was assessed by rats placing significantly less weight on the injected hindpaw and more weight on the non-injected hindpaw. In keeping with previous

studies, we show that the increase in hindpaw oedema and hyperalgesia is maximal after 3 hours, and significantly different from saline-treated rats (Hargreaves et al., 1988a, Clayton et al., 2002, Elmes et al., 2005).

The effect of inflammation on levels of ECLs is unclear and varies depending on the nature of inflammation and the tissue under investigation. For example in LPS induced pulmonary inflammation, levels of AEA and PEA were unaltered (Holt et al., 2004) and in a formalin model of hindpaw inflammation levels of AEA, PEA and 2-AG were also unaltered (De Petrocellis et al, 2000). While in the carrageenan model of inflammation, a decrease in AEA, PEA and OEA was observed in the hindpaw (Jhaveri et al., 2008b).

Carrageenan-induced inflammation peaks at 3 hours post injection and, although it could be argued that the increased activity, both at nociceptors and local immune cells, would be expected to increase levels of ECLs, this time point was associated with increased hindpaw levels of cytokines such as tumour necrosis factor- α (TNF- α), interleukin 1b (IL-1b), IL-6 ((Cunha et al., 2000, Loram et al., 2007)) and prostaglandins such as PGE2 (Guay et al., 2004) which contribute to neuronal sensitisation and an increase in nociceptive activity (for review see (Gold and Flake, 2005, Cheng and Ji, 2008) , which, in turn may contribute to the on-demand synthesis of endocannabinoids (see reviews (Howlett et al., 2002, Piomelli, 2003)). The carrageenan-induced hyperalgesia and hindpaw oedema observed in this study were, however, associated with a decrease in

levels of ECLs in the ipsilateral hindpaw, compared to levels in the contralateral hindpaw of carrageenan-inflamed hindpaw at both 2 and 3 hours post carrageenan. We also observed a decrease in levels of ECLs in the ipsilateral hindpaw at 2 hours post carrageenan injection, compared to saline treated rats, however, this was not apparent at 3 hours post-carrageenan.

Cannabinoid receptors have been shown to be up-regulated during inflammation (Izzo et al., 2001), which could be consistent with decreased local levels of endogenous ligands. Levels of AEA and 2-AG were significantly lower in the hindpaw of saline-treated rats compared to naïve tissue, indicating that injection alone can alter levels of ECs, possibly due to volume changes.

In the spinal cord of vehicle treated rats, there were no changes in levels of ECs 2 hours post-carrageenan injection, compared to saline treated rats. However, at 3 hours post carrageenan injection levels of AEA, were increased in the ipsilateral spinal cord of carrageenan-treated rats, compared to the ipsilateral spinal cord of saline treated controls, whilst levels of AEA, OEA, PEA and 2-AG were unaltered compared to naïve tissue. This suggests that the physiological noxious response to inflammation in the hindpaw increases levels of AEA at the spinal level where there is considerable processing of noxious inputs.

4.5.2 Effects of URB597 on carrageenan-induced changes in weight bearing and paw oedema.

Neither single nor repeated systemic injection of URB597 (0.3mg/kg) altered carrageenan-induced hindpaw oedema. These data are consistent with the earlier report that 3mg/kg, but not 0.3mg/kg URB597 attenuates carrageenan-induced changes in hindpaw (Holt et al., 2005b). It is clear that oedema formation is modulated by endocannabinoids as deletion of the FAAH gene reduced the development of carrageenan-induced oedema by less than half. This presumably reflects the capacity of the cannabinoid receptor system to modulate oedema as exogenous administration of AEA or PEA did not further decrease oedema in FAAH knockout mice (Wise et al., 2007). On this basis, only a proportion of carrageenan-induced oedema can be modulated by ECLs and related substances.

Despite the lack of effect of single injection of URB597 on oedema, this treatment delayed the onset, and attenuated carrageenan-induced hyperalgesia at 3 hours post carrageenan injection. These data are consistent with the reported anti-nociceptive effects of URB597(0.3mg/kg) in CFA model of inflammatory pain (Jayamanne et al., 2006a). It is of interest to note that URB597 did not reduce allodynia in the partial nerve ligation model of neuropathic pain, whereas the CB receptor agonist HU210 (0.03mg/kg) attenuated CFA-induced inflammation and allodynia in neuropathic pain model (Jayamanne et al., 2006). Thus, following peripheral inflammation URB597 mediated analgesia may be arise as a result of an

enhancement of peripheral endogenous cannabinoids acting at CB1/2 receptors, which may not be elevated following nerve injury.

4.5.3 Central versus peripheral effects of FAAH inhibition in inflammatory pain.

Inhibition of FAAH through the use of knock out mice and pharmacological inhibition of FAAH elevates levels of AEA in nervous tissue (Cravatt et al., 2004, Maione et al., 2007, Ahn et al., 2009b) and these increases have been associated with the analgesic effects of FAAH inhibition. Our finding that single dose of URB597 did not alter levels of ECLs in the hindpaw, but did increase levels in the spinal cord of carrageenan treated rats is consistent with the notion of a predominant central site of action mediating the analgesic effects of FAAH inhibitors. These increases were most apparent at 3 hours post-carrageenan injection, with levels of levels of AEA, OEA and PEA in the ipsilateral spinal cord of carrageenan treated rats significantly increased by URB597. These data are consistent with previous studies showing single systemic administration of URB597 time-dependently increased levels of AEA in brain from 30 minutes to 2 hours post URB597 (0.3mg/kg) administration while levels were unaltered in peripheral tissue (Fegley et al., 2005). An increase in levels of AEA in the hippocampus, cortex and midbrain was also reported 2 hours following URB597 (0.1mg/kg) treatment (Gobbi et al., 2005).

Comparison of the effects of pharmacological manipulation of FAAH versus genetic deletion identifies some interesting differences. As discussed above the dose of URB597 used in this study did not alter oedema formation. However, studies using tissue specific FAAH knock out mice demonstrated a contribution of peripheral FAAH to the reduction in oedema observed in the carrageenan model (Cravatt et al., 2004). Levels of ECLs in peripheral tissue were significantly elevated in FAAH-NS tissue, compared to wild-type, while levels in brain and spinal cord were unaltered, however analgesic effects was not mediated through CB₁ or CB₂ receptors (Cravatt et al., 2004). Collectively, these data suggest that the analgesic phenotype exhibited by FAAH^{-/-} mice is through the elevation of central ECLs, and the anti-inflammatory properties of are through the elevation of peripheral ECs. Consistent with these findings, we suggest that analgesic properties of URB597 are mediated through an elevation of ECs in the spinal cord, while we observed no effect on odema or levels of ECs in the hindpaw.

As would be expected, there was an increase in the levels of AEA in the ipsilateral spinal cord of URB597 treated rats receiving an intraplantar injection of saline compared to vehicle treated. This observation is in keeping with previous reports of increases in levels of AEA in the brain at 2 hours post URB597 treatment (Kathuria et al., 2003a, Gobbi et al., 2005, Ahn et al., 2009b)

4.5.4 Effects of repeated administration of URB597 on carrageenan-induced hindpaw inflammation and endocannabinoid levels.

Repeated administration of URB597 did not alter carrageenan-induced hyperalgesia or oedema, despite significantly decreasing FAAH activity in both midbrain and liver. The lack of analgesia was paralleled by a lack of effect of repeated administration of URB597 on levels of AEA in the ipsilateral hindpaw of carrageenan treated rats, compared to ipsilateral hindpaw of vehicle treated rats. Repeated URB597 treatment was associated with a small, but significant, decrease in PEA levels compared to vehicle. Levels of PEA and OEA, but not AEA, were elevated in the ipsilateral spinal cord following repeated URB597 treatment in carrageenan treated rats. Overall, levels of AEA were significantly higher in the hindpaw and spinal cord of rats treated with a single injection of URB597, compared to repeated administration URB597. The larger percentage increase, along with the elevation of AEA, OEA and PEA in the spinal cord of rats receiving a single injection of URB597 may explain the analgesic properties of this treatment.

Previous work has reported that repeated URB597 treatment (0.3mg/kg for 5 weeks) in a model of chronic mild stress, elevated levels of AEA in midbrain, thalamus and striatum, however levels were unaltered in the hippocampus and pre-frontal cortex, while levels of PEA and OEA were elevated in all brain regions. Thus, both our data, and this early work, suggests that the effects of URB597 on AEA versus OEA and PEA are not identical and that

elevations may be specific to one of these compounds and also tissue dependent. Our data demonstrating that the effects of URB597 on pain behavior are absent following repeated dosing is in keeping with the report that the ability of repeated URB597 treatment (0.1mg.kg once daily for 4 days) to elevate levels of AEA in rat brain is diminished compared to the effects of a single dose of URB597 (Gobbi et al., 2005).

4.5.5 Is the lack of effect of repeated administration of URB597 due to changes in endocannabinoid biosynthesis and catabolism?

The mechanisms behind the lack of effect of repeated injection of URB597 on pain behavior and levels of ECs are unclear and warrant further investigation. Previous work has suggested that prolonged exposure to the FAAH inhibitor may result in a down regulation of AEA mobilization in certain tissue (e.g. spinal tissue) and not in others such as thalamus. The mechanism underlying this hypothetical down-regulation of AEA signalling remains undetermined (Bortolato et al., 2007). Repeated administration with a FAAH inhibitor may also affect the synthesis and catabolism of ECs. It is generally accepted that AEA and other NAEs are principally biosynthesized from membrane phospholipids through a common two-step pathway, termed 'the transacylation-phosphodiesterase pathway. The first reaction in this pathway involves the formation of (N-acylated phosphatidylethanolamines

(NAPE) by a Ca^{2+} -dependent *N*-acyltransferase (NAT), followed by phospholipase type-D (PLD) hydrolysis of the resultant NAPE by NAPE-PLD, leading to the formation of AEA, (see Chapter 1 for further explanation). Since specific inhibitors of NAPE-PLD are not available, generation of gene-disrupted mice is of great importance to elucidate its physiological function. NAPE-PLD-deficient mice have decreased levels of long chain, saturated NAEs, however polyunsaturated NAEs, including AEA, were unaltered in these animals suggesting additional routes for AEA synthesis (Leung et al., 2006). Consistent with this finding, siRNA knockdown of NAPE-PLD in macrophages did not significantly reduce levels of AEA (Liu et al., 2006), again suggestive of additional routes of synthesis of AEA.

Further understanding of different routes of synthesis and how this may influence our data requires methods to study synthesis pathways. Screening through LC/MS/MS for AEA precursors such GP-NAEs (Simon and Cravatt, 2006, 2008), and pAEA (Liu et al., 2008) may provide some insight into the synthesis of these compounds.

In addition to their hydrolysis by FAAH, ECLs can also under go degradation and catabolism via alternative routes including COX-2 to generate prostaglandin ethanolamides (PG-EA) and prostaglandin glycerol esters (PG-GE) (Yu et al., 1997, Kozak et al., 2000, Kozak et al., 2001a, Kozak and Marnett, 2002, Kozak et al., 2004, Fowler, 2007), 12- and 15-lipoxygenase (LOX) to generate hydroperoxides ((Hampson et al., 1995, Ueda et al., 1995b, Kozak et al., 2002b),

cytochrome P450 (CYP450) to produce hydroxy and epoxide metabolites (Snider et al., 2007, Snider et al., 2008), and N-acylethanolamine-hydrolyzing acid amidase (NAAA), to produce ethanolamine and arachidonic acid. The lack of elevation of AEA with repeated treatment with URB597 may be due to the increased catabolism via other metabolic routes. The majority of evidence for COX-2 metabolism of AEA and 2-AG to PG-EA and the corresponding PG-GE is derived from *in vitro* studies (Yu et al., 1997, Kozak et al., 2002a) there is evidence for a role of this route of metabolism under certain conditions *in vivo*. Oxidative metabolites of AEA were detected following exogenous administration of AEA in FAAH knockout mice (Weber et al., 2004) and PGE2-GE, the COX-2 metabolite of 2-AG was detected in the rat hindpaw (Hu et al., 2008). Although increased catabolism via COX-2 is an attractive theory for the lack of effect of repeated dosing with URB597 on pain behaviour, we found no evidence that metabolism of ECs via COX-2 contributes to the lack of effect of repeated treatment with URB597. Of the two endocannabinoids AEA and 2-AG, endogenous levels of 2AG are more compatible with substrate affinities at COX-2 suggesting that 2AG may be a better substrate for COX-2 (Kozak and Marnett, 2002). The amount of PGE2-GE found in the rat hindpaw (fmol/g) was low relative to the nmol/g levels of 2-AG, which may indicate that very little 2-AG is metabolized by COX-2 *in vivo*, or it may be the result of the rapid hydrolysis of PGE2-GE into PGE2 (Kozak et al., 2001a, Hu et al., 2008). It appears that high levels of AEA are

required *in vivo* for prostamide formation (Weber et al., 2004), which may not occur due to other routes of inactivation.

An important consideration is the validity of the analytical method employed to quantify the COX-2 metabolites of AEA and 2-AG. As described in chapter 2, the methods used in this thesis for the identification and quantification of COX-2 metabolites has been validated in biological tissue to FDA guidelines, unlike previous methods (Weber et al., 2004, Hu et al., 2008). On this basis we are confident that if COX-2 metabolites of AEA and 2-AG are formed endogenously our method allows their quantification at levels down to 10 pmol/g. Nevertheless, it is possible that these metabolites fall below the limit of detection of our analytical method.

In conclusion, we have shown that single administration of URB597 delays the onset and attenuated carrageenan-induced hyperalgesia, which was associated with an increase in levels of AEA, OEA and PEA in the spinal cord. However repeated administration of URB597 did not alter carrageenan-induced hyperalgesia, possibly due to the lack of elevation in levels of AEA in the spinal cord. We found no evidence for the role of COX-2 metabolism in this model of inflammation, and further work will determine if these compounds are formed *in vivo* under other inflammatory conditions.

Chapter 5.

The role of the endocannabinoid system in MIA model of Osteoarthritis.

5 The role of the endocannabinoid system in MIA model of Osteoarthritis.

5.1 Introduction

Osteoarthritis (OA) is a degenerative joint disease commonly described as a non-inflammatory degenerative disease of articular cartilage resulting in changes in the underlying subchondral bone, synovium and capsule (Guilak, 2000). OA is the most common form of arthritis, and is particularly prevalent in the elderly, with 10 – 20% of over 65 year olds suffering from OA (ARC, 2005). OA is associated with chronic pain (Dieppe and Lohmander, 2005), however the aetiology of OA is poorly understood, with mechanical, metabolic and inflammatory causing other symptoms which may include tenderness, stiffness, inflammation, locking of joints, and pain.

The relationship between degeneration of the joint and the pain experienced is poorly understood. Currently there is a lack of drugs that delay the onset or repair joint damage caused by OA, and current NSAID treatments do not always provide adequate pain relief long-term, and have detrimental side-effects (Patrignani et al., 2005). Thus, there is a strong need for the identification of novel targets for safer drugs which alleviate OA pain (Berenbaum, 2008), with a reduced side-effect which can only be achieved by an improved

mechanistic understanding of the changes associated with this disease. Studies of animal models of degenerative joint disease, that replicate the major symptoms of the clinical condition, will improve our understanding of the mechanisms underlying OA pain (Ameje and Young, 2006).

5.2 Synovial Joint Histology

Synovial joints, such as the knee, consist of two bone ends covered by articular cartilage. The articular cartilage is smooth and flexible and enables frictionless movement of the joint; a normal joint is shown in Figure 5.1. The joint capsule is made up of the fibrous capsule which aids structural integrity and an inner lining layer, the synovial membrane. The synovial membrane secretes synovial fluid which provides lubrication within the joint. The joint is further stabilised by attached tendons and ligaments.

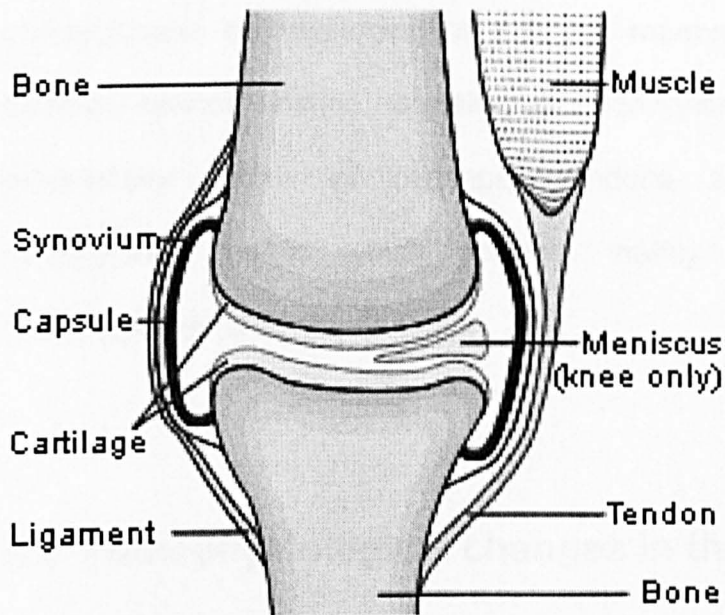


Figure 5.1 Normal physiology of a synovial joint. The two bones are held in place a short distance from each other with tendons and ligaments. Cartilage lines the areas of the bones which are in close proximity to each other, and is surrounded by a synovial fluid filled sac. Taken from (ARC, 2005)

Frictionless motion is provided by the combination of a smooth articular cartilage as well as lubrication of both the articular cartilage and the synovial membrane. Shock absorption to the joint is provided by a combination of structures, including articular cartilage, subchondral bone and the soft tissue structures namely the joint capsule and ligaments. Cartilage is mainly composed of a mixture of water, collagen, proteoglycans and various cellular constituents (Guilak, 2000), and is essential for structure and mechanical strength of the joint, providing cushioning and evenly distributing weight applied on the bones to ease movement. Both the collagen and proteoglycans are very important for normal function of articular cartilage. The synovial tissue and fluid add nourishment, rigidity for cartilage, and prevent excess movement (Guilak, 2000). Loss of

proteoglycans or breakdown of collagen means that the articular cartilage cannot function normally. Chondrocytes, which are in the extracellular matrix of cartilage, produce and maintain the cartilaginous matrix, which consists mainly of collagen and proteoglycans (Goldring, 2006).

5.3 Pathophysiological changes in the joint in OA

OA is characterised by a loss of cartilage due to faster degradation of the extracellular matrix (ECM) compared to synthesis, and subsequent changes in the underlying bone (for a review see (Sarzi-Puttini et al., 2005). During the development of OA, the cartilage gradually roughens and thins, while the bone underneath thickens. The bone at the edge of the joint grows outwards and forms osteophytes (bony spurs). The synovium produces extra fluid, causing a swelling of the joint, along with the thickening and contraction of ligaments trying to stabilise the joint as it changes shape (See Figure 5.2). The release of cytokines, such as IL-1, inhibits the synthesis of matrix constituents such as collagen and proteoglycans, and stimulates the synthesis and release of some eicosanoids, including prostaglandins and leukotrienes from the synovium and chondrocytes. Collectively, this contributes to cartilage degradation and the roughening of the cartilage surface, slight inflammation of the joint and apoptotic events in the chondrocytes (Pelletier et al., 1999, Mathy-Hartert et al., 2002,

Barksby et al., 2006). Instability and inflammation in the joint also induce alterations in other cells: osteoblasts proliferate along the joint margin, resulting in osteophyte formation (Mankin and Lippiello, 1970), synovial cells proliferate resulting in synovial cell hyperplasia (Goldenberg et al., 1982, Lindblad and Hedfors, 1987) and new subchondral bone formation results in sclerosis underlying damaged cartilage (Bendele and Hulman, 1988).

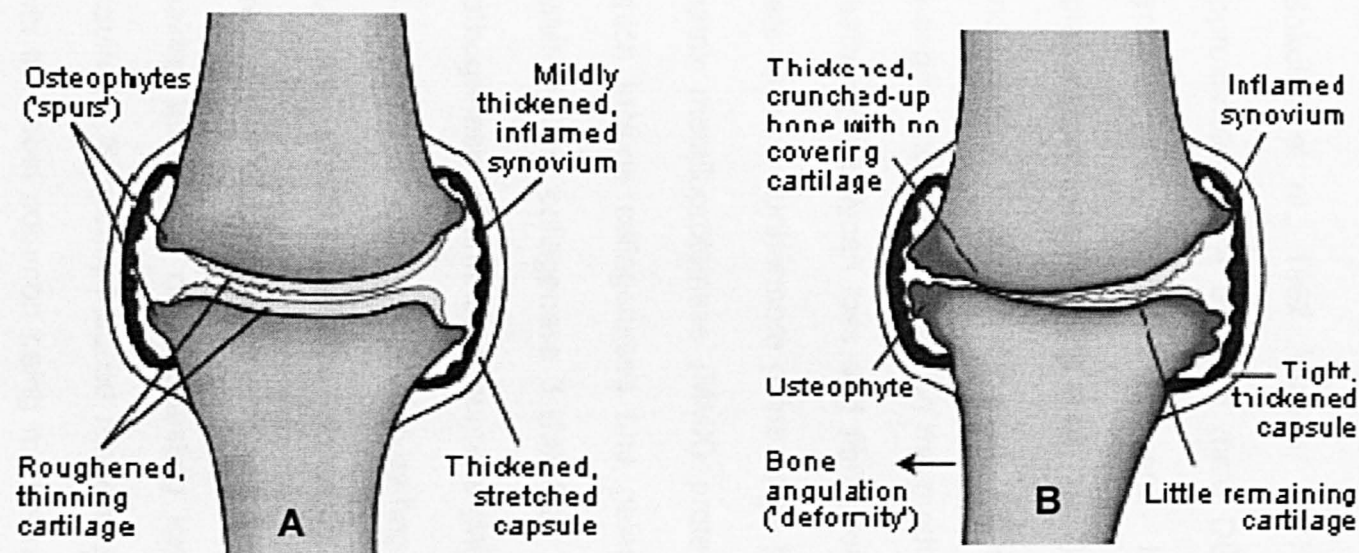


Figure 5.2 A comparison of the physiological changes in the joint observed in patients suffering with **(A)** mild osteoarthritis, with thinning and roughening of cartilage and production of 'spurs'. The joint becomes swollen due to excess synovium fluid or **(B)** severe osteoarthritis, with a destruction of cartilage, severely inflamed synovium and bone deformity due to lack of stabilisation of knee joint by tendons. A key difference between the severities of the two diseases is the lack of cartilage, bone deformity and inflamed synovium. Taken from (ARC, 2005).

5.3.1 Animal models of OA

Animal models of OA frequently study the pathogenesis of cartilage degeneration and potential therapeutic modulation of disease. These models are either naturally occurring or surgically-induced.

Spontaneous OA occurs in the knee joints of various strains of mice (Sokoloff et al., 1962, Walton, 1977) where arthritis occurs in approximately 80% of aging male DBA/1 mice, characterized by synovial lining proliferation and infiltration of mononuclear inflammatory cells (Nordling et al., 1992) and in guinea pigs (Bendele and Hulman, 1988, Bendele et al., 1989), which note the histological changes, including lesions on the medial tibial plateau, chondrocyte death, proteoglycan loss and fibrillation progressing as the animal gets older. Furthermore guinea pigs have been shown to express matrix metalloproteinase (MMX) proteins (Huebner et al., 1998), which include collagenases and gelatinases., and collagenase 1 (MMP-1) and collagenase 3 (MMP-3) have been implicated in the pathogenesis of arthritis in humans (Mitchell et al., 1996, Reboul et al., 1996). The pathology and pathogenesis of naturally occurring OA are similar to those occurring in humans, however the progression of OA in these models are slow, and inevitably costly, making the period of drug testing long, hence other models are required. Surgically-induced models of OA have also been used, with the most common being medial meniscal tear (MMT). In the MMT model, the joint space is exposed through the transaction of the

medial collateral ligament of the femorotibial joint. The medial meniscus is then cut to mimic a meniscal tear. Histologically, the MMT model is similar to that of human OA, with cartilage damage starting with fibrillation and loss of proteoglycan, progressing to complete loss of the cartilage layer and exposure of the subchondral bone (Bendele, 2001). The advantage of a rat model is it quick, and allows evaluation of potential pharmacological agents. Rats, also have very little spontaneous degradation in their knees (Smale et al., 1995), thus the lesions are generally as a result of surgical/chemical manipulation.

5.3.2 MIA model of OA pain

However, to date, the vast majority of studies of animal models of osteoarthritis have investigated the pathophysiology and progression of joint damage with little characterisation of the associated pain. More recently a number of studies have investigated pain behaviour in some of these models of OA (Guingamp et al., 1997, Bove et al., 2003, Kobayashi et al., 2003, Pomonis et al., 2005, Vermeirsch et al., 2007).

The monosodium iodoacetate (MIA) induced arthritis model was first described around 20 years ago (Kalbhen, 1987). MIA is an inhibitor of glycolysis, which induces chondrocyte death and produces cartilage degeneration (Dunham et al., 1993). The histopathology of the MIA-injected joint has some similarities to that seen in human osteoarthritic joints, with exposed subchondral bone, loss of cartilage

and damaged synovium (Bove et al., 2003, Guzman et al., 2003, Kobayashi et al., 2003, Combe et al., 2004, Ivanavicius et al., 2007). The degradation of the joint is therefore associated with chronic pain behaviour, first described by Fernihough (Fernihough et al., 2004). This joint pathology is associated with a pronounced decrease in weight-bearing on the injected hind-paw (Bove et al. 2003; Kobayashi et al. 2003; Combe et al. 2004), a correlate of behavioural hyperalgesia. The MMT and MIA models produce comparable joint pathology, but more robust, and clinically relevant, pain behaviour is produced in the MIA model (Combe et al., 2004, Fernihough et al., 2004). In addition, the hindpaw ipsilateral to MIA knee joint injection has decreased thresholds for mechanical withdrawal (tactile allodynia), indicative of central sensitisation (Combe et al., 2004, Fernihough et al., 2004).

The advantage of the MIA model is the relatively rapid onset of the disease, which produces robust pain behaviour, whilst being non-invasive, allows for evaluation of analgesic compounds. The main problem associated with MIA is the dose given (Pomonis et al., 2005), too low a dose produces histological changes associated with OA, whilst not producing robust pain behaviour, too high dose results in severe cartilage and bone destruction, differing from the human condition.

The treatment of patients with OA is often directed at relieving pain and restoring function through the use of pharmacologic therapies. Intra-articular injections of corticosteroids have been demonstrated to

relieve inflammation and associated pain, but due to their shortness of effect are rarely used. The effects of analgesic drugs, including the opioid morphine and the non-steroidal anti-inflammatory drugs (NSAIDs), on MIA-induced pain behaviour have been reported. Administration of non-selective NSAIDs and morphine attenuates MIA-induced changes in weight bearing (Bove et al., 2003, Fernihough et al., 2004, Pomonis et al., 2005, Beyreuther et al., 2007, Ivanavicius et al., 2007), but not mechanical allodynia (Fernihough et al., 2004, Beyreuther et al., 2007).

5.3.3 The cannabinoid receptor system: implications for OA

Cannabinoids have also been shown to play an important role in the treatment of chronic pain (see reviews (Hohmann, 2002, Iversen and Chapman, 2002, Goya et al., 2003). The endocannabinoids, AEA and 2-AG inhibit neuronal responses and attenuate nociceptive processing (for review see Jhaveri et al., 2007a). Constitutive expression of both CB1 and CB2 receptors have been isolated on chondrocytes and implicated in a potential disease modifying role in OA (Mbvundula et al., 2006), hence, the phytocannabinoid preparation Sativex has been reported to significantly attenuate pain associated with rheumatoid arthritis (Blake et al., 2006, Wright et al., 2006), while ajulemic acid, a synthetic cannabinoid acid, has anti-inflammatory properties in human synovial cells through an increase

in COX-2 mRNA expression and prostaglandin 15d-PGJ₂ synthesis (Stebulis et al., 2008), which has anti-inflammatory properties, possibly through the activation of PPAR γ . (1995 ,.Forman et al) Furthermore local administration of the CB1 agonist arachidonyl-2-chloroethylamide (ACEA) reduced the mechanosensitivity of afferent knee fibres in control and MIA-treated rats (Schuelert and McDougall, 2008), while SR141716A reduced thermal hyperalgesia and mechanical allodynia in CFA model of arthritis (Croci and Zarini, 2007), which may be mediated through the endocannabinoid system. Previous work from Nottingham has shown that levels of endocannabinoids and related compounds are altered in the synovial fluid taken from patients with endstage osteoarthritis and rheumatoid arthritis (Richardson et al., 2008), however it is unknown if these changes are associated with an increase in pain behaviour and cartilage damage.

5.3.4 Aims

The aim of this study was to investigate whether the behavioural and histological changes associated with intra-articular injection of MIA is associated with changes in the levels of ECs in the hindpaw and spinal cord in this model of OA.

5.4 Methods

Rats were purchased from Charles River U.K. All studies were carried out in accordance with UK Home Office Animals (Scientific Procedures) Act (1986) and follow guidelines of the International Association for the Study of Pain. Male Sprague Dawley rats weighing 120-190g were used for these studies.

5.4.1 Intra-articular injections

The following procedures were carried out by Dr D Sagar.

Rats were anaesthetised with isoflurane (1.5-2% in 66% N₂O -33% O₂) and received a single intra-articular injection of monosodium iodoacetate (MIA; 1mg/50µl) in saline through the infra-patellar ligament of the left knee. The dose of MIA was chosen from the previous literature (Bove et al., 2003, Guzman et al., 2003, Kobayashi et al., 2003, Pomonis et al., 2005). Control animals received a single injection of saline (50µl) into the left knee in an identical manner.

5.4.2 Behavioural testing

The following procedures were carried out by Dr D Sagar.

After surgery, rats were maintained under the same conditions as during the pre-operative period. The posture and behaviour of the rats were carefully monitored following recovery from the anaesthesia and then on the first postoperative (PO) day. Baseline

measurements were taken immediately prior to intra-articular injection (PO day 0) and then from PO day 2 onwards. Behavioural tests assessing changes in weight-distribution and sensitivity to mechanical stimuli were performed for up to 28 days post-injection. The weight gain and general behaviour of the rats was monitored throughout the PO period.

Effects of joint damage on weight-distribution through the left (ipsilateral) and right (contralateral) knee were assessed using an incapacitance tester (Linton Instrumentation, U.K.). The two hind-paws were placed on separate sensors and the force (in grams) exerted by each hind-limb was calculated and averaged over a period of 3 seconds as previously described (Clayton et al., 2002, Elmes et al., 2005). Each data point was taken as the mean of three 3 sec readings. Effects of an intra-articular injection of MIA or saline on weight distribution were assessed between post-operative days 2-28. Naïve and saline-treated rats distribute their weight evenly between both paws. Changes in weight distribution has been used as an indicator of hypersensitivity of the joint (Bove et al., 2003, Kobayashi et al., 2003) and hindpaw (Clayton et al., 1997). The development of tactile allodynia was assessed using von Frey monofilaments (Semmes-Weinstein monofilaments of bending forces 0.6, 1, 1.4, 2, 4, 6, 8, 10 and 15 g). Rats were placed in transparent plastic cubicles on a mesh floored table and a period of acclimatization was allowed prior to testing. Von Frey monofilaments were applied, in ascending order of bending force, to the plantar

surface of both hind-paws. Each von Frey was applied for a 3 sec period. Once a withdrawal reflex was established, the paw was re-tested with the next descending von Frey monofilament until no response occurred. The lowest weight of monofilament which elicited a withdrawal reflex was noted as the paw withdrawal threshold (PWT). On post-operative days 14-17 and 28-31, rats were killed by stunning decapitation. The spinal cord and hind paw tissue were rapidly removed and placed onto dry ice. A laminectomy was performed and approximately 2 cm of the lumbar region (L4 and L5) of the spinal cord was removed, and bisected into sections ipsilateral and contralateral sections. Paw tissue was also removed from both the ipsilateral and contralateral paws. In separate experiments knee joints were cut horizontally at the end of the femur and tibia, and vertically along the tibia and fibula. Muscle was cut away and knee joint lifted out.

5.4.3 Histology

(Histological studies of joints from MIA or saline-treated rats were performed by Dr Rich Pearson at post-operative days 14-17 and 28-31). Knee joints removed and fixed in 10% formal saline and subsequently decalcified in an aqueous ethylenediaminetetracetic acid (EDTA) solution (14% in distilled water; pH 7.0, 20°C) until completely decalcified. Samples were paraffin embedded, and 5-8 μ M sections of the central portion of each MIA ipsilateral and contralateral knee joint in the coronal plane were stained by safranin-

O fast green to show matrix proteoglycan and overall joint morphology. Each knee was scored using a modified Mankin osteoarthritis grading system by 2 independent observers and a mean derived (Mankin et al. 2004). The worst affected area was scored; for example, a focal lesion with hypocellularity and decreased safranin-O staining would result in a high score even if the rest of the joint looked relatively normal and bare bone scored the maximum grade of 6 for structure. The maximum score was 13 (not 14) as the tidemark is ill defined in the rat.

5.4.4 Measurement of endocannabinoids

Endocannabinoid (EC) measurement was carried out using a method similar to that of Richardson *et al.*, (2007). Paw and spinal cord tissue was stored at -80°C ; it was then finely minced and added to ice cold acetonitrile containing internal standards (0.42 nmol d8-anandamide, 1.5 nmol d8-2AG). Samples were shaken at 4°C , followed by repeated cycles of centrifugation, and supernatant layer collection. Simultaneous measurement of ECs and related compounds was then performed using liquid chromatography-tandem mass spectrometry (LC-MS/MS). Analysis was carried out on an Agilent 1100 system (Agilent Technologies, Waldbrunn, Germany) coupled to a triple quadrupole Quattro Ultima MS (Waters, Manchester, UK) in electrospray positive mode.

Analytes were separated chromatographically on a C18 column (150×21. mm internal diameter, 3.5 μm particle size; Waters

Symmetry, Hertfordshire, UK) with a mobile phase flow rate of 0.3 ml/min. A gradient elution was used, with mobile phases consisting of A (water, 1g/L ammonium acetate, 0.1% formic acid) and B (acetonitrile, 1g/L ammonium acetate, 0.1% formic acid). Samples were injected from a cooled auto sampler maintained at 4°C. Multiple reaction monitoring of individual compounds, using specific precursor and product mass to charge (m/z) ratios allowed simultaneous measurement of anandamide (AEA), 2-arachidonoyl glycerol (2-AG), palmitoylethanolamide (PEA) and oleoylethanolamide (OEA).

5.5 Results

5.5.1 MIA-induced changes in pain behaviour

Intra-articular injection of MIA (1mg) produced significant decreases in weight-bearing on the hind-limb ipsilateral to injection, compared to pre-injection values and saline-treated rats (Figure 5.3A). There was an marked decrease in weight-bearing at PO day 2/3, which was followed by a small recovery by PO day 7. A significant decrease in weight-bearing was then maintained from PO day 7 to PO day 28. Changes in weight-bearing were accompanied by significant decreases in paw withdrawal thresholds for ipsilateral hindpaw withdrawal, indicative of mechanical allodynia (Figure 5.3B).

Contralateral paw withdrawal thresholds were not altered over the course of the study (data not shown). Intra-articular injection of saline did not significantly alter paw withdrawal thresholds on the ipsilateral paw, compared to baseline values (Figure 5.3A, B)

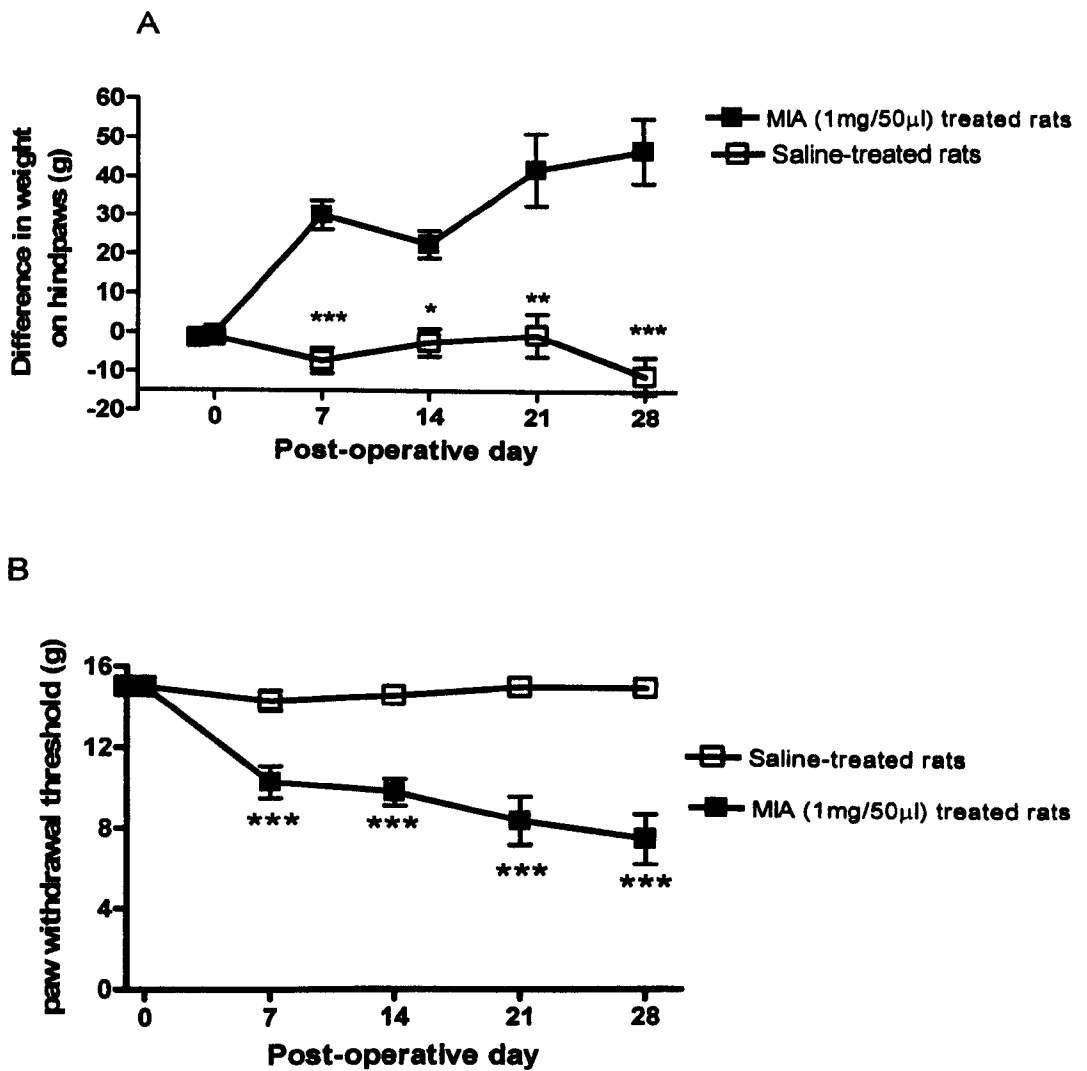


Figure 5.2 Time course of changes in (A) weight distribution on the ipsilateral hind-limb and (B) hindpaw-withdrawal thresholds intra-articular injection of MIA (1-/50µl) or saline. Statistical analyses comparing MIA-treated rats to saline-treated rats were performed using a 2-way ANOVA with a Bonferroni post hoc test. * $p < 0.05$, ** $p < 0.01$ and *** $p < 0.001$ for MIA-treated rats versus saline.

Histological analysis of the normal (saline) treated joints shows clear red glycosaminoglycan (GAG) staining of articular cartilage on both the femur and tibia. There is also articular cartilage present on the meniscus, and dense red staining in the epiphysis, with chondrocytes (nuclei stained blue) present in bone marrow (Figure 5.5). MIA treated rats at PO day 14 revealed that there is a loss of

red staining in the meniscus and superficial zone of articular cartilage. There is a loss of dark blue staining of chondrocytes, indicating hypocellular bone marrow, and fibrous tissue is also present in the meniscus and subchondral bone on both the femoral and tibial side. Horizontal clefts have also appeared between cartilage and bone on femoral side. The median Mankin score at this time point was 8.08 ± 1.54 (Figure 5.4). By day 28, virtually all of the articular cartilage was had lost significant safranin-O staining with pronounced loss of articular cartilage and subchondral bone. Fibrous tissue is present down to the epiphysis, with large horizontal cleft between the bone and cartilage on the femoral side. Furthermore, virtually all of the bone marrow present in hypocellular, (Figure 5.5). The median Mankin score at this time point was 7.00 ± 1.37 (Figure 5.4).

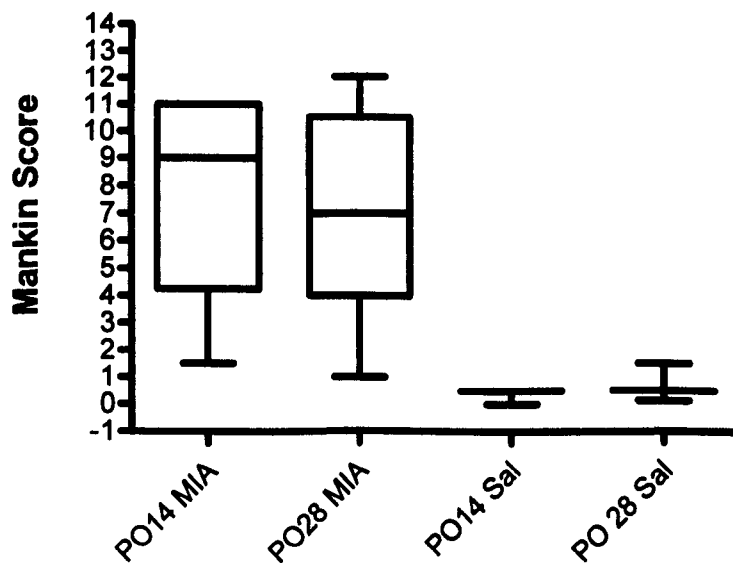


Figure 5.4 Box and whisker plot of the range of scores from the Mankin osteoarthritis grading system for ipsilateral knee joints from saline and MIA (1mg) treated rats. The horizontal line is the median score.

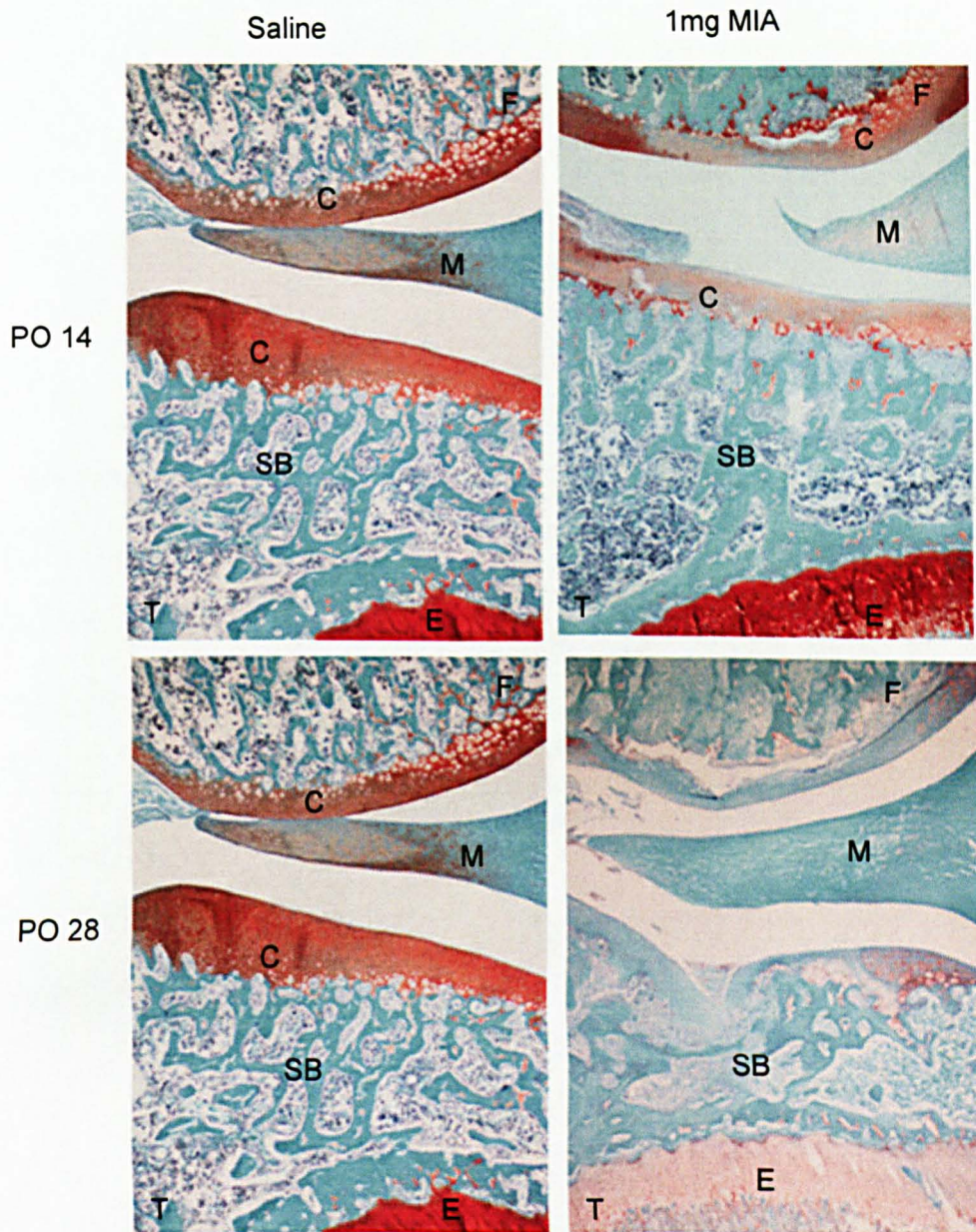


Figure 5.5 Histological changes following MIA injection at PO 14 and PO28. Intra-articular injection of MIA (1mg /50 μ l) produces degeneration of the articular cartilage (C) with a loss of structure in the subchondral bone (SB) layer in rats 14 and 28 days post-MIA injection. (E) – epiphyses; (M) meniscus, (F) Fibia, (T) Tibia.

5.5.2 Levels of ECLs in the hindpaw and spinal cord of MIA and saline treated rats

5.5.2.1 ECL levels in rat hindpaw PO14 and PO28

Levels of ECLs and related compounds in the hindpaw and spinal cord of rats were measured at PO days 14-17 and PO days 28-31 following intra-articular injection of MIA or saline.

Intra-articular injection of saline did not significantly alter levels of AEA, 2AG, PEA or OEA in the ipsilateral hindpaw, compared to contralateral hindpaw at PO days 14-17 (Figure 5.6). Levels of AEA, PEA and OEA were significantly elevated in the ipsilateral hindpaw of MIA-treated rats, compared to the contralateral hindpaw (Figure 5.6) and the ipsilateral hindpaw of saline-treated rats at PO days 14-17 (Figure 5.6). Levels of 2-AG in the ipsilateral hindpaw were comparable in the ipsilateral and contralateral hindpaw of MIA-treated rats, and were consistent with levels in the hindpaw of saline-treated rats.

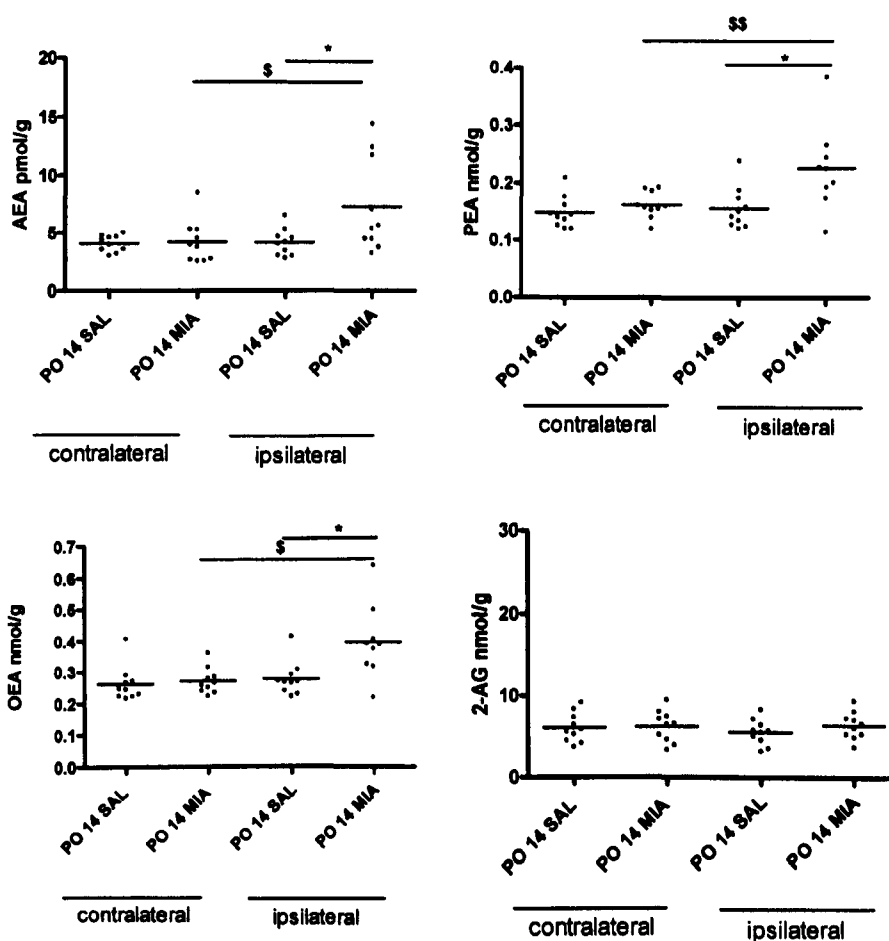


Figure 5.6: Levels of endocannabinoids and related compounds in the skin of the hindpaw taken from rats receiving intra-articular injection of MIA (1mg/50 μ l) or saline at post-operative days 14. Statistical analyses were carried out using a Mann Whitney test. * $p < 0.05$, vs ipsilateral saline-treated rats, $^{\&}$ $p < 0.05$, $^{\&\&}$ $p < 0.01$ vs contralateral hindpaw.

In keeping with the changes seen at the earlier time point, levels of AEA, PEA and OEA were significantly elevated in the ipsilateral hindpaw, compared to the contralateral hindpaw of MIA-treated rats at PO days 28-31 (Figure 5.7). In the case of PEA and OEA, levels were also significantly elevated in the ipsilateral hindpaw of MIA-treated rats, compared to levels in the ipsilateral hindpaw of saline-

treated rats (Figure 5.7). As seen at days PO14-17, levels of 2-AG were unaltered in the hindpaw in any of the treatment groups.

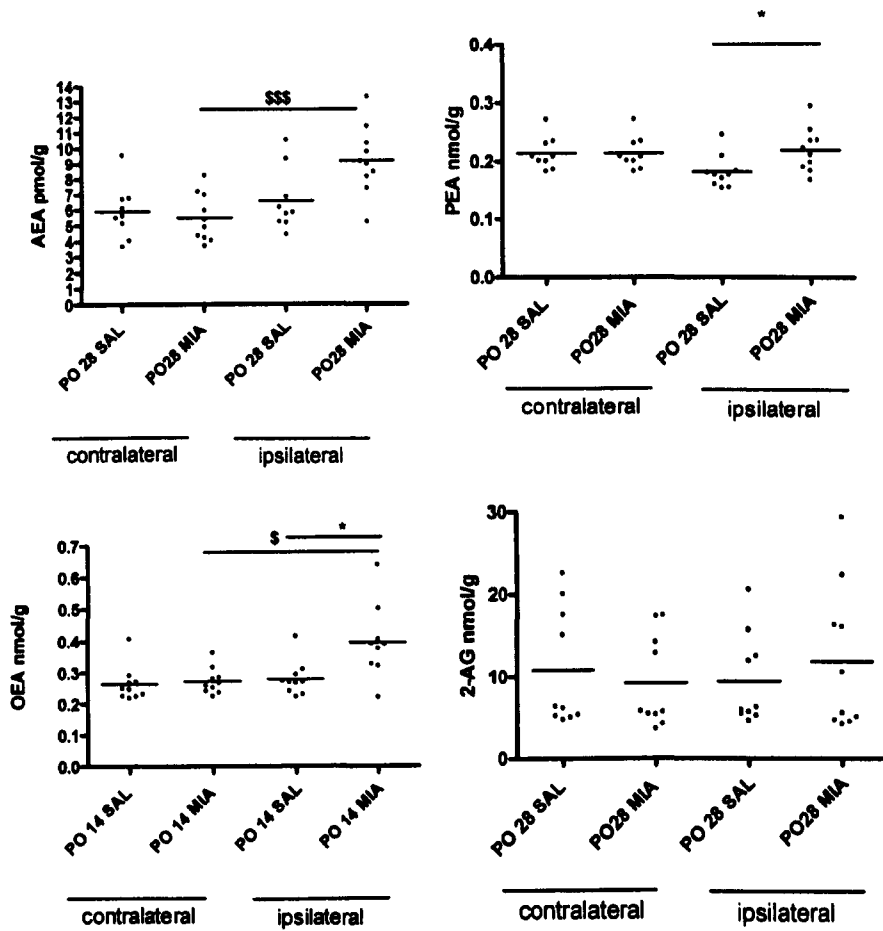


Figure 5.7 Levels of endocannabinoids in the skin from the hind paw of MIA (1mg/50 μ l) and saline-treated rats at post-operative day 28. Statistical analyses were carried out using a Mann Whitney test. * $p < 0.05$, vs ipsilateral saline-treated rats, & $p < 0.05$, && $p < 0.005$ vs contralateral hindpaw.

Note, there were significant differences in levels of AEA and PEA in the ipsilateral and contralateral hindpaw taken from saline treated rats, compared to PO28 compared to saline treated rats PO14 (table 5.1).

Group	AEA pmolg ⁻¹		OEA nmolg ⁻¹		PEA nmolg ⁻¹		2AG nmolg ⁻¹	
	median (range)		median (range)		median (range)		median (range)	
	Ipsi	Contra	Ipsi	Contra	Ipsi	Contra	Ipsi	Contra
PO 14 saline	14 4.11 (2.81-6.51)	4.14 (3.01-5.00)	0.27 (0.22-0.42)	0.25 (0.22-0.41)	0.15 (0.12-0.24)	0.14 (0.12-0.21)	5.61 (3.20-8.38)	5.71 (3.69-9.16)
PO 14 MIA	5.53 (3.25-14.39) ^{**}	3.86 (2.56-8.49) [§]	0.39 (0.22-0.64) ^{**}	0.25 (0.22-0.36)	0.23 (0.12-0.39) ^{**}	0.16 (0.12-0.19)	6.35 (3.73-9.51)	6.52 (3.35-9.57)
PO 28 saline	28 5.85 (4.44-10.53) [*]	5.62 (3.64-9.55)	0.25 (0.22-0.44)	0.29 (0.25-0.37)	0.17 (0.15-0.25) [*]	0.21 (0.18-0.27) ^{\$\$\$}	6.15 (4.65-20.56)	6.29 (4.79-22.53)
PO 28 MIA	9.12 (5.25-13.33) ^{***}	5.86 (3.64-17.99)	0.34 (0.25-0.41) ^{****}	0.26 (0.16-0.38)	0.22 (0.17-0.29) [†]	0.21 (0.18-0.27) ^{^^^}	8.10 (4.23-29.35)	5.76 (3.62-17.39)

Table 5.1 Levels of ECs and related compounds in the skin from the hindpaw of rats treated with intra-articular injection of MIA or saline. Data were analysed using non-parametric Mann-Whitney test. Data expressed as median and range. ^{*}P<0.05, ^{**}P<0.01, ^{***}P<0.001 vs. contralateral hindpaw, [†]P<0.05, ^{**}P<0.01 vs PO28 ipsilateral saline, ^{*}p<0.05, ^{**}p<0.01 vs ipsilateral PO14 saline, [§]P<0.05, ^{\$\$\$} P<0.005 vs contralateral PO14 saline, ^{^^^}P<0.005 vs contralateral PO14 MIA.

5.5.3 ECL levels in rat spinal cord PO14 and PO28

At the level of the ipsilateral spinal cord, we observed a significant increase in levels of PEA, OEA and 2AG in the ipsilateral spinal cord of MIA treated rats, compared to the ipsilateral spinal cord of saline-treated rats, at PO day 14-17 (Figure 5.8). There was a trend towards an increase in levels of AEA in the ipsilateral spinal cord of MIA-treated rats compared to the ipsilateral spinal cord of saline-treated rats at PO days 14-17 (Figure 5.8). Levels of 2-AG in the ipsilateral spinal cord of MIA treated rats were elevated compared to the contralateral spinal cord (Figure 5.8), which was also the case for levels of AEA, OEA and PEA. Levels of AEA, PEA and OEA were also significantly elevated in the contralateral spinal cord of MIA-treated rats compared to the contralateral spinal cord of saline-treated rats at PO day 14-17 (Figure 5.8).

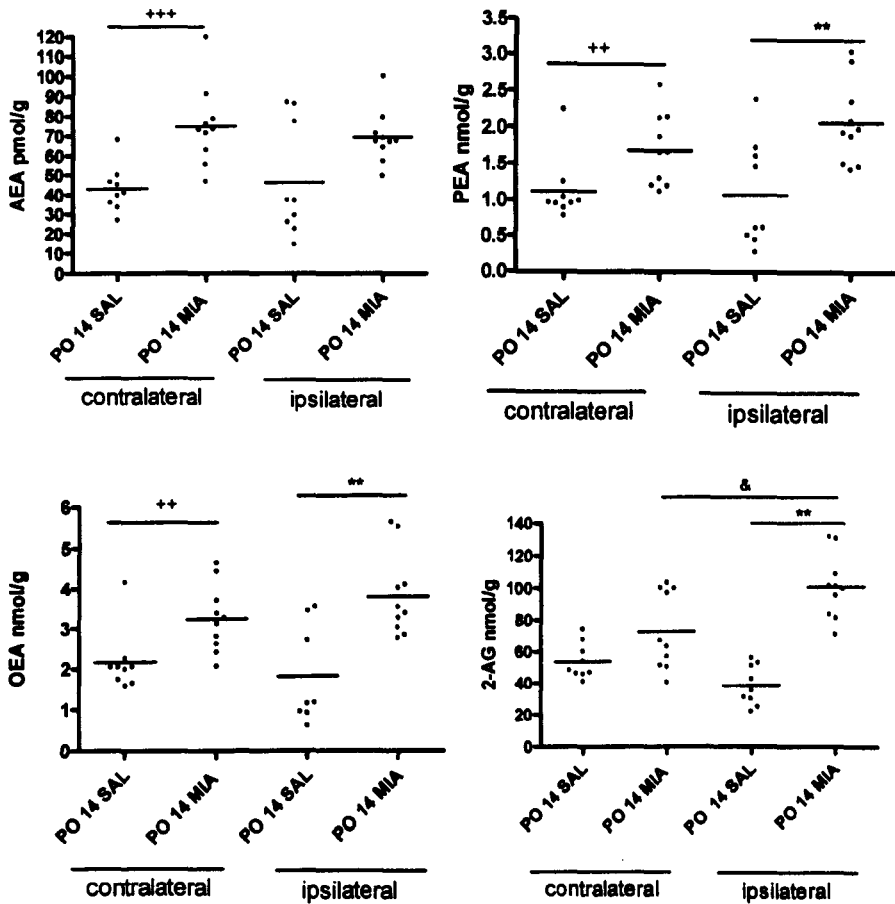


Figure 5.8. Levels of endocannabinoids and related compounds in the spinal cord of MIA (1mg/50 μ l) and saline-treated rats at post-operative day 14. Statistical analyses were carried out using a Mann Whitney test. * $p < 0.05$, vs ipsilateral saline-treated rats, & $p < 0.05$, vs contralateral hindpaw, ** $p < 0.01$, *** $p < 0.005$ vs contralateral saline-treated rats.

At the later timepoint (PO 28-31), there was a trend towards an increase in levels of AEA in the ipsilateral spinal cord of MIA-treated rats, compared to the ipsilateral spinal cord of saline-treated rats (Figure 5.9). Levels of AEA were significantly increased in the contralateral spinal cord of MIA-treated rats, compared to saline-treated rats, at PO days 28-31 (Figure 5.9). Levels of OEA, PEA and 2-AG were significantly increased in the ipsilateral spinal cord of MIA-treated rats, compared to the ipsilateral spinal cord of saline-treated

rats (Figure 5.9 and Table 5.2). Furthermore, there was a significant decrease in levels of OEA and PEA in the ipsilateral spinal cord of MIA treated rats at PO days 28-31, compared to MIA treated rats at PO days 14-17 (Table 5.2).

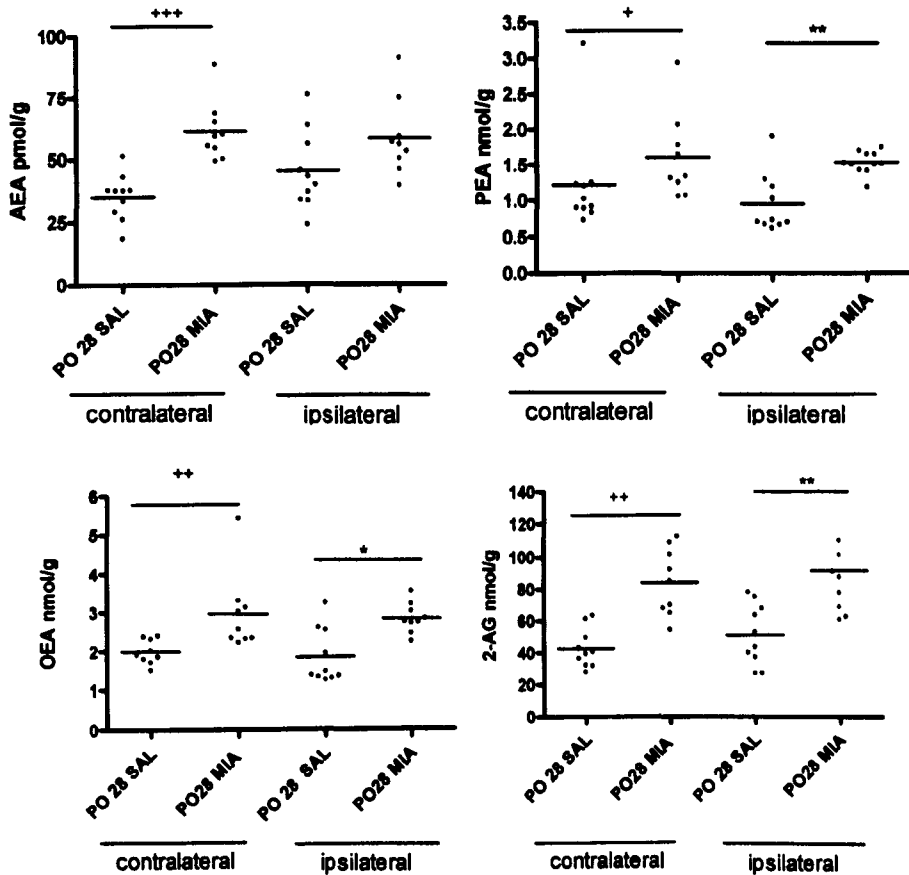


Figure 5.9: Levels of endocannabinoids and related compounds in the spinal cord of MIA (1mg/50 μ l) and saline-treated rats at post-operative day 28-31. Statistical analyses were carried out using a Mann Whitney test. * $p < 0.05$, ** $p < 0.01$ vs ipsilateral saline-treated rats, + $p < 0.05$, ** $p < 0.01$, *** $p < 0.005$ vs contralateral saline-treated rats

Note: Levels of ECLs in the spinal cord at PO14 and PO28 were comparable.

Group	AEA pmol g^{-1} median (range)		OEA nmol g^{-1} median (range)		PEA nmol g^{-1} median (range)		2AG nmol g^{-1} median (range)	
	Ipsi	Contra	Ipsi	Contra	Ipsi	Contra	Ipsi	Contra
PO 14 saline	37.14 (14.66- 87.05)	40.75 (26.78- 67.94)	1.16 (0.60- 3.56)	2.04 (1.57- 4.15)	0.62 (0.28- 2.39)	0.96 (0.78- 2.25)	35.78 (22.19- 56.39)*	48.33 (41.24- 74.47)
PO 14 MIA	67.87 (50.16- 100.5)	73.21 (46.85- 119.7) \$\$\$	3.78 (2.78- 5.63)**	3.20 (2.06- 4.64) \$\$	1.96 (1.43- 3.05) **	1.67 (1.12- 2.59) \$\$	100.6 (71.6- 131.7)* **	65.42 (40.8- 103.5)
PO 28 saline	41.27 (23.88- 76.28)	37.45 (18.53- 51.27)	1.45 (1.27- 3.26)	1.98 (1.52- 7.77)	0.71 (0.61- 1.91)	0.97 (0.73- 3.21)	49.68 (27.09- 78.3)	40.07 (27.77- 63.39) \$
PO 28 MIA	56.03 (39.33-91.36)	59.15 (49.17- 88.53) $\Delta\Delta\Delta$	2.78 (2.77- 3.58) ##%	5.57 (2.24- 5.43) Δ	1.52 (1.20- 1.76) ###%	1.35 (1.06- 2.95) Δ	87.53 (61.36- 161.7) **	85.37 (54.79- 112.4) $\Delta\Delta\Delta$

Table 5.2 Levels of ECLs in the spinal cord of rats treated with a intra-articular injection of MIA or saline. Data were analysed using non-parametric Mann-Whitney test. Data expressed as median and range. *P<0.05 vs. contralateral spinal cord, †P<0.05,

****P<0.01 vs PO14 ipsilateral saline, %P<0.05vs ipsilateral PO14 MIA, *p<0.05, **p<0.01 vs ipsilateral PO28 saline, † P<0.05, **P<0.01 *** P<0.005 vs contralateral PO14 saline, ΔP<0.05, ΔΔΔ P<0.001 vs contralateral PO28 saline.**

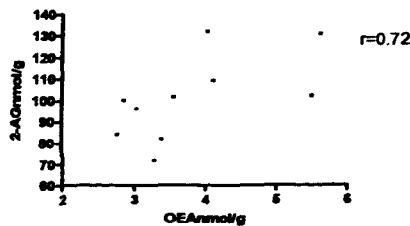
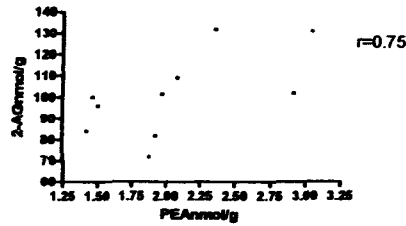
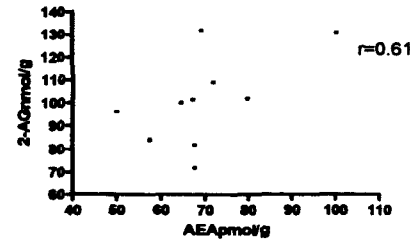
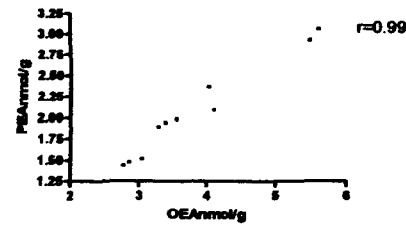
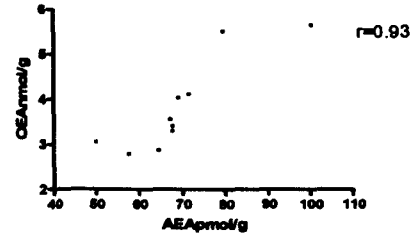
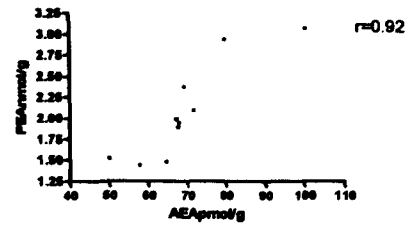
The relationship between each of the N-acylethanolamines (AEA, OEA, and PEA) and acyl-glycerols (2-AG) in each individual rat in the ipsilateral spinal cord of MIA and saline-treated rats, at day PO14 and PO28, was investigated with a correlation analysis. Spearman rank correlation coefficients (R^2) were calculated and are presented in Table 5.3, representative correlation graphs are shown in Figure 5.10. In PO14 saline treated rats, there is significant correlation between levels of AEA, OEA and PEA, and following MIA injection, there is a further correlation of levels of 2-AG with OEA and PEA. In saline-treated rats at day there is a correlation of levels of OEA with PEA and AEA, as well as levels of 2-AG correlating with AEA. However, following MIA treatment there is a loss of correlation between AEA, OEA PEA and 2-AG (Figure 5.10). This lack of correlation in MIA-treated rats PO28 and the further correlation in MIA-treated rats at PO14 may explain the degree of alloydnia observed at each time point.

	R^2			
	PO14 MIA	PO14 Saline	PO28 MIA	PO28 Saline
AEA vs PEA	0.92***	0.95***	0.00	0.64
AEA vs OEA	0.93***	0.90***	0.12	0.68*
AEA vs 2-AG	0.61	0.13	0.13	0.70*
OEA vs PEA	0.99***	0.96***	0.55	0.93***
2-AG vs PEA	0.75*	0.20	0.05	0.61
2-AG vs OEA	0.72*	0.30	0.21	0.56

Table 5.3 Spearman Rank coefficient correlating levels of ECs in spinal cord of MIA and saline treated rats at days PO14 and PO28. * $P < 0.05$, ** $P < 0.01$, *** $P < 0.005$ = significant correlation.

In Chapter 2, I describe the development and validation of a sensitive LC-MS/MS method for the detection of COX-2 metabolites PG-EAs (PGE₂-EA, PGD₂-EA, PGF₂ α -EA) and PG-GEs (PGE₂-GE and PGF₂ α -GE) in biological tissue. This method was employed to determine whether COX-2 metabolites of AEA or 2-AG are present in the hindpaw or spinal cord following the induction of arthritis. This analytical approach was used to identify if alternative catabolism pathways for AEA and 2-AG in chronic pain models. Neither COX-2 metabolites of AEA or 2-AG was detected in either the hindpaw or spinal cord of rats treated with single or repeated URB597 and intraplantar injection of carrageenan or saline. PG-EA and PG-GE were detected if they were spiked into rat brain tissue (Chapter 4, Figure 4.26), showing the functionality of the method. The limit of detection of PG-EAs and PG-GEs was 10 pmol/g and 100 pmol/g respectively. On this basis, we assume that if the COX-2 metabolites of AEA and 2-AG are present, they are below our limit of detection.

A



B

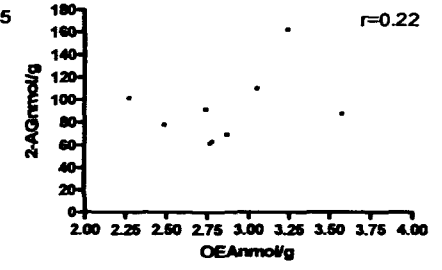
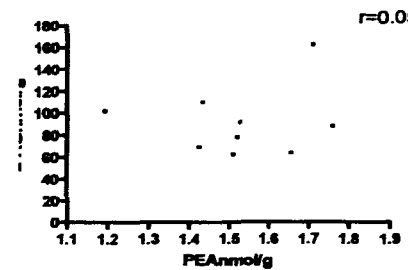
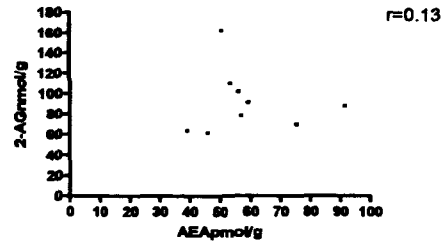
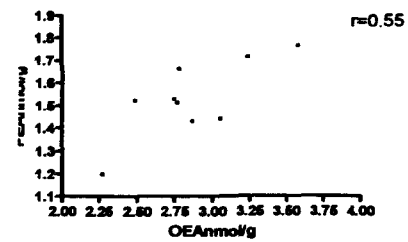
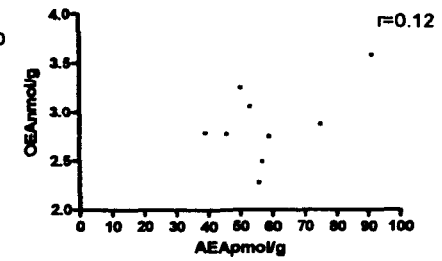
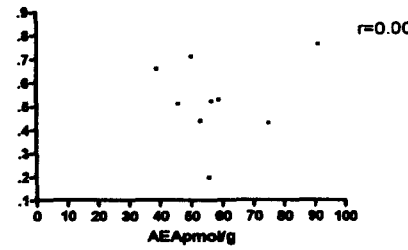


Figure 5.10 Representative graphs showing the correlation coefficient between AEA, OEA, PEA and 2-AG in ipsilateral spinal cord MIA-treated rats at day PO14 (A), and the lack of correlation between AEA, OEA, PEA and 2-AG in ipsilateral spinal cord MIA-treated rats at day PO28 (B).

5.6 Discussion

The major finding of this study is that intra-articular injection of MIA produces time-dependent increase in pain behaviour and that these effects are associated with increased levels of endocannabinoids and related compounds in the hindpaw and spinal cord, which is comparable to our recent finding in the synovium OA patients (Richardson et al., 2008).

This is the first study to assess the effect of MIA-induced joint degeneration in relation to changes in pain behaviour and levels of ECLs. MIA-treated joints show a time-dependant decrease in GAG staining, which corresponds to loss of cartilage matrix. There is also an increase in hypocellular bone matrix at PO14, compared to saline treated, with only fibrous tissue present at day 28. At PO 28, there were large horizontal clefts present, articular surface was a lot thinner, and comprised of mineralized cartilage, or bone, compared to saline-treated joints. This type of joint damage is reminiscent of the type of damage seen in patients with end stage OA (Pritzker et al., 2006), with the main difference in the pathology of rats and humans is the presence of an open epiphysis, which is not present in humans. Thus, this model has a clinical validity, in terms of joint pathology and pain behaviour.

Intra-articular injection of MIA produced a time-dependant decrease in paw withdrawal thresholds and weight bearing on the ipsilateral (injured) side. The observed biphasic changes in pain behaviour concurs with previous reports of an early robust change in weight

bearing (Pomonis et al., 2005), due to an initial inflammatory phase as indicated by mild swelling of the MIA-treated knee joint. Intra-articular MIA injection results in acute inflammation (Bove et al., 2003) which can lead to the release of pro-inflammatory mediators, such as TNF α , bradykinin and prostaglandins (Farahat et al., 1993, Nishimura et al., 2002, Pulichino et al., 2006) in the knee joint, and an increase in the expression of spinal COX-2 mRNA (Prochazkova et al., 2009). The inflammatory response following intra-articular injection of MIA has been shown to be largely resolved by day 7 and is not expected to play a role in pain at later time points (Guzman et al., 2003, Pulichino et al., 2006). Consistent with this finding, administration of the TNF- α inhibitor etanercept during the first week, but not the second week, following intr-articular injection of MIA attenuated pain behaviour in MIA-treated rats (Vonsy et al., 2008). The sharp decrease in weight bearing on the injured paw in the days following MIA injection which we, and others, have observed is likely to reflect the initial inflammatory response. Despite the inflammation being resolved by PO day 7, hyperalgesia and allodynia is maintained until later timepoints (Combe et al., 2004, Pomonis et al., 2005). Changes in paw withdrawal thresholds of the hindpaw (allodynia) did not develop as early as the changes in weight-bearing. This is consistent with previous studies, with a rapid decrease in weight placed on the ipsilateral hindpaw (Combe et al., 2004, Fernihough et al., 2004, Pomonis et al., 2005, Vermeirsch et al., 2007). Damage to the joint, includes the initial inflammatory

response, and may induce a sensitisation of peripheral receptors with changes in the response characteristics of primary afferent fibres (Petersen-Felix and Curatolo, 2002) includes decreased thresholds of C-fibre mediated of an increased input to the spinal cord (Woolf and Salter, 2000). Sustained activation of nociceptive pathways may lead to moderate or severe pain as seen in patients with chronic pain. Noxious mechanoreceptive inputs from the knee joint are processed by dorsal horn neurones, which also receives inputs from the paw and skin (Schaible and Grubb, 1993). The articular nerves supplying the knee project to superficial lamina I and deep laminae V-VII (Schaible and Grubb, 1993), while afferent fibers from rat hind paw project predominantly to lamina I II at L4/5 (Abbadie and Besson, 1992, Takahashi et al., 2003, Todd et al., 2005). Previously, sensitisation of joint nociceptors has been shown to increase peripheral receptive fields of neurones innervating the knee joint, paw and ankle, presumably due to sensitisation of spinal neurones (Neugebauer et al., 1993). The outcome of these studies using animal models are consistent with the referred pain reported by osteoarthritic patients (Kean et al., 2004, Kidd, 2006). It has been proposed that the bone pathology in the MIA model initiates nerve damage and neuropathic type behavioural pain responses (Ivanavicius et al., 2007), which may also contribute to changes in excitability of spinal neurones. Increased levels of CGRP mRNA and TRPV1 receptor mRNA in the DRG innervated by joint afferents have been reported at 28 days post MIA treatment (Fernihough et al.,

2005), both of which are likely to impact upon excitability of primary afferent fibres and post-synaptic responses of spinal neurones. Electrophysiological recordings from primary afferent fibres in MIA-treated rats at the earlier time point (PO day 14) reported increased mechanical responses of C and A- δ fibres (Kelly et al., 2008, Schuelert and McDougall, 2008). Increases in the spontaneous activity and noxious-evoked activity of afferent fibres have also been demonstrated in the aged (36 month) guinea pig model of OA (McDougall et al., 2009). Thus, changes in spinal neuronal responses in MIA-treated rats may arise as the result of increased primary afferent input producing long term changes in spinal processing of inputs and the appearance of spinal excitability at later time points. Increases in neuronal responses can develop from an increase in synaptic input from afferent fibres which are sensitised during injury and inflammation, which can increase input from both injured and non-injured area (peripheral sensitisation).

It is well known that increases neuronal activity can drive the generation of ECLs and related compounds. Intra-articular injection of MIA increased levels of the endocannabinoid AEA in the ipsilateral hindpaw of MIA-treated rats both at 14 and 28 days post-injection. Levels of two related compounds, PEA and OEA, were also elevated in the ipsilateral hindpaw of MIA-treated rats. The robust changes in levels of AEA, PEA and OEA in the hindpaw of the MIA-treated rats occurred in parallel with the allodynia at both PO14 and PO28. Furthermore, we observed an increase in levels of AEA, OEA and

PEA, however levels of 2-AG were unaltered following intra-articular injection of MIA compared to saline at both PO14 and PO28. This suggests changes in activity of either synthetic or catabolic pathway that is specific to the NAEs. Future work will determine whether catabolic or synthetic enzyme expression is altered. These data demonstrate that the MIA-induced joint damage produces changes at sites distal to the joint. The effects of MIA treatment on levels of endocannabinoids and related compounds are reminiscent of changes in ECL levels demonstrated in the synovial fluid of OA patients, compared to control subjects (Richardson et al., 2008). Currently, the measurement of ECLs in the synovial fluid of rats is not achievable due to the small sample volume, however future studies will attempt to address this issue.

At the level of the spinal cord, there was a trend towards increases in levels of AEA in the ipsilateral spinal cord of MIA treated rats, but significance was not reached at either time point. There was, however, a significant increase in AEA in the contralateral spinal cord of MIA-treated rats at both timepoints. Levels of PEA and OEA were significantly increased in the ipsilateral and contralateral spinal cord of MIA-treated rats, compared to saline-treated rats, at both 14 and 28 days post-injection. Bilateral changes are also observed in other models of chronic pain including CFA model of monoarthritis and CCI model of neuropathic pain (Besse et al., 1992, Malcangio and Bowery, 1994, Ibuki et al., 1997, Lombard et al., 1999). Bilateral

decreases in κ -opoid binding sites in spinal cord are observed in CFA model of monoarthritis (Besse et al., 1992), as well as a loss of GABA-IR in the spinal cord of rats following peripheral nerve injury (Ibuki et al., 1997) and increased spinal substance C in a *Mycobacterium tuberculosis* model of monoarthritis (Malcangio and Bowery, 1994). Collectively these changes underlie exaggerated sensory processing, and demonstrate bilateral changes at the level of the spinal cord following unilateral injury.

Increases in levels of AEA, 2AG, PEA and OEA in the spinal cord of MIA-treated rats may arise as a result of the increased nociceptive drive into the spinal cord and spinal excitability increasing the activity dependent synthesis of these compounds. Although it has not been shown directly, the activity-dependent release of endocannabinoids has been suggested from *in vitro* pharmacological studies (Maejima et al., 2001b, Wilson and Nicoll, 2001, Gerdeman et al., 2002, Brown et al., 2003, Di et al., 2005). Conversely the elevated levels may be due to a decreased catabolism of the endocannabinoids either by FAAH or other catabolic enzymes. It is important to note, however, I did not detect COX-2 metabolites of AEA or 2-AG in rat hindpaw and spinal cord suggesting little contribution of this pathway in MIA treated rats. We observed an increase in 2-AG in MIA-treated rats in the spinal cord, however not the hindpaw, which maybe associated with an increase in 2-AG synthesis via DAGL. DAGL is expressed in superficial lamina of the spinal cord, which also coincides with input from knee (Schaible and Grubb, 1993, Nyilas et al., 2009), thus when

neuronal activity is increased such as in chronic pain states, lead to an activity dependant increase in 2-AG synthesis. Nevertheless, despite the increase in ECLs in the spinal cord of MIA-treated rats, animals still show pain behaviour, at PO14 and PO28. However, the measured increased ECLs, may be attenuating pain behaviour compared if none were present, if so we may see an exaggerated pain state, thus if we were to block CB₁ receptor, would we see embellished pain behaviour. Indeed, acute administration of SR141716 in chronic pain animal models has been demonstrated to have hyperalgesic effects (Meng et al., 1998, Richardson et al., 1998a, Strangman et al., 1998, Chapman, 1999) suggesting that endogenous cannabinoids serve naturally to modulate the maintenance of pain.

In conclusion, the present study has demonstrated that MIA-induced joint degeneration produced aberrant pain behaviour and is associated with increased levels of inhibitory endocannabinoids and related compounds in the hindpaw and spinal cord, which have been shown to tonically control nociceptive responses in other models of pain (Jhaveri et al., 2007a).

Chapter 6

General Discussion

6 General Discussion

Cannabis-based medicines have been suggested as potential treatments for a wide variety of diseases, with positive results in the symptomatic relief of neuropathic pain in multiple sclerosis and cancer pain, as well as suppressing chemotherapy-induced nausea and emesis (Seamon, 2006). Direct targetting of CB₁ receptors has met with limited success; indeed the selective CB₁ receptor antagonist rimonabant was withdrawn from the European market due to the risk of serious psychiatric problems. However, indirect modulation of the endocannabinoid system, by targeting ECL metabolism, has been demonstrated to produce anti-nociception in models of inflammatory pain (for reviews (Jhaveri et al., 2007a, Di Marzo, 2008). Whilst modulation of ECL synthesis has not been investigated in models of pain, it has been shown that disruption of ECL synthesising enzymes, such as NAPE-PLD decreases levels of ECLs. Since the elevation of ECLs, through inhibition of metabolism, is thought to be the main route of analgesia, decreasing levels would presumably be hyperalgesic. Therefore, the identification of alternative routes of ECL metabolism and synthesis is essential for understanding the mechanisms involving ECL turnover, which could lead to the development of alternative medicines.

The data presented in this thesis demonstrate the presence and functionality of the endocannabinoid system in pain pathways *in vitro* and *in vivo*. Following the successful development of an LC-MS/MS method for the simultaneous measurement of ECLs and COX-2

metabolites of AEA and 2-AG, I was able to use this method to quantify levels of AEA, 2-AG, OEA and PEA in cell, hindpaw and spinal cord tissue. Using this method, we investigated the effects of increased intracellular calcium on the levels of ECLs *in vitro*, levels of ECLs in rat models of acute and chronic inflammation, and the effects of FAAH inhibition on nociceptive behaviour and levels of ECLs, PG-EA and PG-GE in the carrageenan model of inflammatory pain.

In models of pain and inflammation, ECL levels in tissues involved in nociceptive processing (namely the spinal cord, brain and skin of rodents) are usually elevated following treatment with irritants and inflammatory stimuli (Oka et al., 2006, Jhaveri et al., 2008b) Levels are also elevated in animal models of neuropathic pain (Mitirattanakul et al., 2006, Agarwal et al., 2007, Petrosino et al., 2007) and are thought to represent adaptive changes aimed at reducing pain and inflammation.

What is apparent from the data presented in this thesis is that the general conception that an increase in ECL levels is analgesic is actually more complex than first anticipated. The impact appears to depend greatly on the tissue in question, the disease state, and also on the degree of disease progression. In order to manipulate the ECL system to provide analgesia, a better understanding of the ECL system in various pain states at differing times is needed, which may lead to the development of clinically relevant compounds targetted to enhance or decrease the activity of the ECL system at certain time

points associated with hyperalgesia. Indeed, in the hindpaw, a decrease in ECL levels was observed 2 hours post carrageenan, with no change in the spinal cord, while at 3 hours post carrageenan, we see no change in levels of ECLs in the hindpaw, but an increase in AEA in the spinal cord. Thus, elevating ECLs in tissues specific to nociception may be required in order to achieve analgesia. This can possibly be achieved through systemic administration of ECL metabolising enzyme inhibitors such as URB597, which in theory should elevate levels of ECLs in tissues specific to nociception. The systemic administration of a single injection of URB597 did, however, elevate levels of ECLs in the spinal cord, but not in the hindpaw, 3 hours post carrageenan injection, which proved to be analgesic, suggesting that an increase in ECL levels is required for analgesia. Interestingly, repeated administration of URB597, a more clinically relevant dosing regimen, did not elevate levels of ECLs in either the hindpaw or spinal cord. These data suggest that the dosing schedule and possibly the route of administration are key to elevating levels of ECL, and thus analgesia. Indeed, intraplantar administration of URB597 was reported to elevate levels of ECLs in the hindpaw, which attenuated hyperalgesia (Jhaveri et al., 2008b). Not surprisingly, the correct dose also appears important to achieve analgesia. High oral doses of URB597 (10-50 mg/kg) are required to attenuate neuropathic pain (Russo et al., 2007a), whereas lower i.p doses are not effective in this model (Jayamanne et al., 2006b). Thus, using the correct dose, and combination of local and systemic

administration of FAAH inhibitors may elevate levels of ECLs in the desired tissues and provide analgesia.

The lack of effect of repeated administration of URB597 in an acute model of inflammatory pain should not be overlooked and may be more therapeutically relevant in chronic pain states, such as neuropathic pain, where repeated dosing of URB597 has been reported to produce anti-nociceptive effects (Russo et al., 2007a).

In the MIA model of chronic inflammation, elevation of ECLs in the hindpaw and spinal cord did not produce analgesia. Thus, there is a question about whether further elevation of levels, through the use of FAAH inhibitors, can produce analgesia, or whether levels are elevated beyond physiological levels, perhaps activating other targets, such as TRPV1 (Starowicz et al., 2007). Increased levels of ECLs are thought, in the case of central neurones, to act to inhibit excitatory neurotransmitter release (Pertwee, 2006, Di Marzo and Petrosino, 2007), however high levels/concentrations of CB₁ ligands, such as ECLs (Maione et al., 2006), or under pathological conditions where there is an elevation in ECLs, such as nociception, ECLs may reduce inhibitory neurotransmission, such as through GABAergic neurones (Hohmann and Suplita, 2006, Maione et al., 2006). These may elicit a reduced activity of the desired inhibitory nociceptive pathway, leading to a decrease in analgesia. Thus, perhaps a TRPV1 antagonist, or a GABA agonist, in combination with a FAAH inhibitor may elevate ECL levels without activating other off-target receptors.

High concentrations of URB597 have been found to activate TRPA1 channels (Niforatos et al., 2007) also involved in pain transduction, thus potentially altering the analgesic efficacy of this compound. Hence there is the need for a more selective FAAH inhibitor, which produces analgesia through the elevation of ECLs, without hitting other, potentially pro-nociceptive targets.

A lot of attention has been focussed on the use of FAAH inhibitors in elevating levels of ECLs producing analgesia, however ECLs are also metabolised by other routes such as COX-2, LOX and CYP450 (see review (Kozak and Marnett, 2002) and Figure 1.5). Thus, there is the potential for other compensatory metabolising pathways to be activated when FAAH is inhibited. We found no evidence for COX-2 metabolism of AEA and 2-AG in the carrageenan model of inflammation when FAAH was inhibited, however, further development of other analytical methods for the simultaneous measurement of ECLs and metabolites of ECLs, would provide additional information on patterns of change, as well as identifying potential therapeutic compounds of interest involved in the deactivation of the EC system. Thus instead of focussing on inhibiting one ECL metabolising enzyme, such as FAAH, the combination of FAAH, LOX, COX-2 and/or CYP450 inhibitors may be better analgesic candidates.

The ECL levels determined in this thesis are a relatively quick 'snapshot' in time of inflammatory and pain states. Quantification of

ECLs using microdialysis sample collection would provide important information regarding changes in time. This technique has been previously used to measure ECLs in awake, behaving rats (Giuffrida et al., 1999, Porter et al., 2002, Orio et al., 2009), however, many methods do not have sufficient sensitivity to measure ECLs (particularly AEA) in microdialysis samples collected over minute time scales and often require pooling of samples. The method developed in this thesis may provide the extra sensitivity required to measure small amounts of ECLs in the low volumes of biological samples obtained following acute and chronic inflammation, and, combined with a method for global profiling of ECL precursors and metabolites, may provide potential therapeutic targets for modulating endocannabinoid synthesis and metabolism.

In summary, an analytical method for the simultaneous quantification of AEA, OEA, PEA, 2-AG, and COX-2 metabolites of AEA and 2-AG has been developed and applied to the measurement of ECLs following noxious stimulation. Data obtained in this thesis show an increase in ECL levels following noxious stimulation and that modulation of the EC system provides a potential therapeutic target for the treatment of inflammatory pain states.

Chapter 7

References.

7 Reference:

- Abbadie C, Besson JM (c-fos expression in rat lumbar spinal cord during the development of adjuvant-induced arthritis. *Neuroscience* 48:985-993.1992).
- Abrams DI, Jay CA, Shade SB, Vizoso H, Reda H, Press S, Kelly ME, Rowbotham MC, Petersen KL (Cannabis in painful HIV-associated sensory neuropathy: a randomized placebo-controlled trial. *Neurology* 68:515-521.2007).
- Afrah AW, Fiska A, Gjerstad J, Gustafsson H, Tjolsen A, Olgart L, Stiller CO, Hole K, Brodin E (Spinal substance P release in vivo during the induction of long-term potentiation in dorsal horn neurons. *Pain* 96:49-55.2002).
- Agarwal N, Pacher P, Tegeder I, Amaya F, Constantin CE, Brenner GJ, Rubino T, Michalski CW, Marsicano G, Monory K, Mackie K, Marian C, Batkai S, Parolaro D, Fischer MJ, Reeh P, Kunos G, Kress M, Lutz B, Woolf CJ, Kuner R (Cannabinoids mediate analgesia largely via peripheral type 1 cannabinoid receptors in nociceptors. *Nat Neurosci* 10:870-879.2007).
- Ahern GP, Brooks IM, Miyares RL, Wang XB (Extracellular cations sensitize and gate capsaicin receptor TRPV1 modulating pain signaling. *J Neurosci* 25:5109-5116.2005).
- Ahluwalia J, Urban L, Bevan S, Capogna M, Nagy I (Cannabinoid 1 receptors are expressed by nerve growth factor- and glial cell-derived neurotrophic factor-responsive primary sensory neurones. *Neuroscience* 110:747-753.2002).
- Ahluwalia J, Urban L, Bevan S, Nagy I (Anandamide regulates neuropeptide release from capsaicin-sensitive primary sensory neurons by activating both the cannabinoid 1 receptor and the vanilloid receptor 1 in vitro. *Eur J Neurosci* 17:2611-2618.2003a).
- Ahluwalia J, Urban L, Capogna M, Bevan S, Nagy I (Cannabinoid 1 receptors are expressed in nociceptive primary sensory neurons. *Neuroscience* 100:685-688.2000).
- Ahluwalia J, Yaqoob M, Urban L, Bevan S, Nagy I (Activation of capsaicin-sensitive primary sensory neurones induces anandamide production and release. *J Neurochem* 84:585-591.2003b).
- Ahmadi S, Lippross S, Neuhuber WL, Zeilhofer HU (PGE(2) selectively blocks inhibitory glycinergic neurotransmission onto rat superficial dorsal horn neurons. *Nat Neurosci* 5:34-40.2002).
- Ahn K, Johnson DS, Mileni M, Beidler D, Long JZ, McKinney MK, Weerapana E, Sadagopan N, Liimatta M, Smith SE, Lazerwith S, Stiff C, Kamtekar S, Bhattacharya K, Zhang Y, Swaney S, Van Becelaere K, Stevens RC, Cravatt BF (Discovery and characterization of a highly selective FAAH inhibitor that reduces inflammatory pain. *Chem Biol* 16:411-420.2009).
- Al-Haboubi HA, Zeitlin IJ (Re-appraisal of the role of histamine in carrageenan-induced paw oedema. *Eur J Pharmacol* 88:169-176.1983).

- Alexander SP, Kendall DA (The complications of promiscuity: endocannabinoid action and metabolism. *Br J Pharmacol* 152:602-623.2007).
- Amaya F, Oh-hashii K, Naruse Y, Iijima N, Ueda M, Shimosato G, Tominaga M, Tanaka Y, Tanaka M (Local inflammation increases vanilloid receptor 1 expression within distinct subgroups of DRG neurons. *Brain Res* 963:190-196.2003).
- Ameye LG, Young MF (Animal models of osteoarthritis: lessons learned while seeking the "Holy Grail". *Curr Opin Rheumatol* 18:537-547.2006).
- Amrani Y, Krymskaya V, Maki C, Panettieri RA, Jr. (Mechanisms underlying TNF-alpha effects on agonist-mediated calcium homeostasis in human airway smooth muscle cells. *Am J Physiol* 273:L1020-1028.1997).
- Amrani Y, Panettieri RA, Jr., Frossard N, Bronner C (Activation of the TNF alpha-p55 receptor induces myocyte proliferation and modulates agonist-evoked calcium transients in cultured human tracheal smooth muscle cells. *Am J Respir Cell Mol Biol* 15:55-63.1996).
- ARC (2005) Osteoarthritis. In: *Arthritis Research Campaign - About Arthritis*: York, UK.
- Artmann A, Petersen G, Hellgren LI, Boberg J, Skonberg C, Nellemann C, Hansen SH, Hansen HS (Influence of dietary fatty acids on endocannabinoid and N-acyl ethanolamine levels in rat brain, liver and small intestine. *Biochim Biophys Acta* 1781:200-212.2008).
- Astarita G, Rourke BC, Andersen JB, Fu J, Kim JH, Bennett AF, Hicks JW, Piomelli D (Postprandial increase of oleoylethanolamide mobilization in small intestine of the Burmese python (*Python molurus*). *Am J Physiol Regul Integr Comp Physiol* 290:R1407-1412.2006).
- Averill S, McMahon SB, Clary DO, Reichardt LF, Priestley JV (Immunocytochemical localization of trkA receptors in chemically identified subgroups of adult rat sensory neurons. *Eur J Neurosci* 7:1484-1494.1995).
- Avraham Y, Magen I, Zolotarev O, Vorobiev L, Nachmias A, Pappo O, Ilan Y, Berry EM, Ackerman Z (2-Arachidonoylglycerol, an endogenous cannabinoid receptor agonist, in various rat tissues during the evolution of experimental cholestatic liver disease. *Prostaglandins Leukot Essent Fatty Acids* 79:35-40.2008).
- Baba H, Ji RR, Kohno T, Moore KA, Ataka T, Wakai A, Okamoto M, Woolf CJ (Removal of GABAergic inhibition facilitates polysynaptic A fiber-mediated excitatory transmission to the superficial spinal dorsal horn. *Mol Cell Neurosci* 24:818-830.2003).
- Bach FW, Yaksh TL (Release of beta-endorphin immunoreactivity into ventriculo-cisternal perfusate by lumbar intrathecal capsaicin in the rat. *Brain Res* 701:192-200.1995).
- Balvers MG, Verhoeckx KC, Witkamp RF (Development and validation of a quantitative method for the determination of 12 endocannabinoids and related compounds in human plasma using liquid chromatography-tandem mass spectrometry. *J Chromatogr B Analyt Technol Biomed Life Sci* 877:1583-1590.2009).
- Barksby HE, Hui W, Wappler I, Peters HH, Milner JM, Richards CD, Cawston TE, Rowan AD (Interleukin-1 in combination with oncostatin M up-regulates multiple genes in chondrocytes: implications for cartilage destruction and repair. *Arthritis Rheum* 54:540-550.2006).

- Basavarajappa BS (Critical enzymes involved in endocannabinoid metabolism. *Protein Pept Lett* 14:237-246.2007).
- Batetta B, Griinari M, Carta G, Murru E, Ligresti A, Cordeddu L, Giordano E, Sanna F, Bisogno T, Uda S, Collu M, Bruheim I, Di Marzo V, Banni S (Endocannabinoids may mediate the ability of (n-3) fatty acids to reduce ectopic fat and inflammatory mediators in obese Zucker rats. *J Nutr* 139:1495-1501.2009).
- Beaulieu P, Bisogno T, Punwar S, Farquhar-Smith WP, Ambrosino G, Di Marzo V, Rice AS (Role of the endogenous cannabinoid system in the formalin test of persistent pain in the rat. *Eur J Pharmacol* 396:85-92.2000).
- Beck PW, Handwerker HO, Zimmermann M (Nervous outflow from the cat's foot during noxious radiant heat stimulation. *Brain Res* 67:373-386.1974).
- Behbehani MM, Fields HL (Evidence that an excitatory connection between the periaqueductal gray and nucleus raphe magnus mediates stimulation produced analgesia. *Brain Res* 170:85-93.1979).
- Beltramo M, Bernardini N, Bertorelli R, Campanella M, Nicolussi E, Fredduzzi S, Reggiani A (CB2 receptor-mediated antihyperalgesia: possible direct involvement of neural mechanisms. *Eur J Neurosci* 23:1530-1538.2006).
- Beltramo M, Stella N, Calignano A, Lin SY, Makriyannis A, Piomelli D (Functional role of high-affinity anandamide transport, as revealed by selective inhibition. *Science* 277:1094-1097.1997).
- Bendele AM (Animal models of osteoarthritis. *J Musculoskelet Neuronal Interact* 1:363-376.2001).
- Bendele AM, Hulman JF (Spontaneous cartilage degeneration in guinea pigs. *Arthritis Rheum* 31:561-565.1988).
- Bendele AM, White SL, Hulman JF (Osteoarthrosis in guinea pigs: histopathologic and scanning electron microscopic features. *Lab Anim Sci* 39:115-121.1989).
- Bennett GJ, Xie YK (A peripheral mononeuropathy in rat that produces disorders of pain sensation like those seen in man. *Pain* 33:87-107.1988).
- Berenbaum F (New horizons and perspectives in the treatment of osteoarthritis. *Arthritis Res Ther* 10 Suppl 2:S1.2008).
- Besse D, Weil-Fugazza J, Lombard MC, Butler SH, Besson JM (Monoarthritis induces complex changes in mu-, delta- and kappa-opioid binding sites in the superficial dorsal horn of the rat spinal cord. *Eur J Pharmacol* 223:123-131.1992).
- Besson JM (The neurobiology of pain. *Lancet* 353:1610-1615.1999).
- Bevan S, Szolcsanyi J (Sensory neuron-specific actions of capsaicin: mechanisms and applications. *Trends Pharmacol Sci* 11:330-333.1990).
- Beyreuther B, Callizot N, Stohr T (Antinociceptive efficacy of lacosamide in the monosodium iodoacetate rat model for osteoarthritis pain. *Arthritis Res Ther* 9:R14.2007).
- Bhave G, Zhu W, Wang H, Brasier DJ, Oxford GS, Gereau RWt (cAMP-dependent protein kinase regulates desensitization of the capsaicin receptor (VR1) by direct phosphorylation. *Neuron* 35:721-731.2002).
- Bick RJ, Liao JP, King TW, LeMaistre A, McMillin JB, Buja LM (Temporal effects of cytokines on neonatal cardiac myocyte Ca²⁺ transients and adenylate cyclase activity. *Am J Physiol* 272:H1937-1944.1997).

- Binzen U, Greffrath W, Hennessy S, Bausen M, Saaler-Reinhardt S, Treede RD (Co-expression of the voltage-gated potassium channel Kv1.4 with transient receptor potential channels (TRPV1 and TRPV2) and the cannabinoid receptor CB1 in rat dorsal root ganglion neurons. *Neuroscience* 142:527-539.2006).
- Bisogno T, Howell F, Williams G, Minassi A, Cascio MG, Ligresti A, Matias I, Schiano-Moriello A, Paul P, Williams EJ, Gangadharan U, Hobbs C, Di Marzo V, Doherty P (Cloning of the first sn1-DAG lipases points to the spatial and temporal regulation of endocannabinoid signaling in the brain. *J Cell Biol* 163:463-468.2003).
- Bisogno T, Ligresti A, Di Marzo V (The endocannabinoid signalling system: biochemical aspects. *Pharmacol Biochem Behav* 81:224-238.2005).
- Bisogno T, Maurelli S, Melck D, De Petrocellis L, Di Marzo V (Biosynthesis, uptake, and degradation of anandamide and palmitoylethanolamide in leukocytes. *J Biol Chem* 272:3315-3323.1997).
- Bisogno T, Ortar G, Petrosino S, Morera E, Palazzo E, Nalli M, Maione S, Di Marzo V (Development of a potent inhibitor of 2-arachidonoylglycerol hydrolysis with antinociceptive activity in vivo. *Biochim Biophys Acta* 1791:53-60.2009).
- Blake DR, Robson P, Ho M, Jubb RW, McCabe CS (Preliminary assessment of the efficacy, tolerability and safety of a cannabis-based medicine (Sativex) in the treatment of pain caused by rheumatoid arthritis. *Rheumatology (Oxford)* 45:50-52.2006).
- Bleakman D, Brorson JR, Miller RJ (The effect of capsaicin on voltage-gated calcium currents and calcium signals in cultured dorsal root ganglion cells. *Br J Pharmacol* 101:423-431.1990a).
- Bleakman D, Thayer SA, Glaum SR, Miller RJ (Bradykinin-induced modulation of calcium signals in rat dorsal root ganglion neurons in vitro. *Mol Pharmacol* 38:785-796.1990b).
- Bortolato M, Mangieri RA, Fu J, Kim JH, Arguello O, Duranti A, Tontini A, Mor M, Tarzia G, Piomelli D (Antidepressant-like activity of the fatty acid amide hydrolase inhibitor URB597 in a rat model of chronic mild stress. *Biol Psychiatry* 62:1103-1110.2007).
- Bottorff JL, Johnson JL, Moffat BM, Mulvogue T (Relief-oriented use of marijuana by teens. *Subst Abuse Treat Prev Policy* 4:7.2009).
- Bove SE, Calcaterra SL, Brooker RM, Huber CM, Guzman RE, Juneau PL, Schrier DJ, Kilgore KS (Weight bearing as a measure of disease progression and efficacy of anti-inflammatory compounds in a model of monosodium iodoacetate-induced osteoarthritis. *Osteoarthritis Cartilage* 11:821-830.2003).
- Boyle DL, Jones TL, Hammaker D, Svensson CI, Rosengren S, Albani S, Sorkin L, Firestein GS (Regulation of peripheral inflammation by spinal p38 MAP kinase in rats. *PLoS Med* 3:e338.2006).
- Bradshaw HB, Rimmerman N, Hu SS, Benton VM, Stuart JM, Masuda K, Cravatt BF, O'Dell DK, Walker JM (The endocannabinoid anandamide is a precursor for the signaling lipid N-arachidonoyl glycine by two distinct pathways. *BMC Biochem* 10:14.2009).
- Bradshaw HB, Rimmerman N, Krey JF, Walker JM (Sex and Hormonal Cycle Differences in Brain Levels of Pain-related Cannabimimetic Lipid Mediators. *Am J Physiol Regul Integr Comp Physiol*.2006).
- Brenowitz SD, Regehr WG (Calcium dependence of retrograde inhibition by endocannabinoids at synapses onto Purkinje cells. *J Neurosci* 23:6373-6384.2003).

- Breyer RM, Bagdassarian CK, Myers SA, Breyer MD (Prostanoid receptors: subtypes and signaling. *Annu Rev Pharmacol Toxicol* 41:661-690.2001).
- Bridges D, Rice AS, Egertova M, Elphick MR, Winter J, Michael GJ (Localisation of cannabinoid receptor 1 in rat dorsal root ganglion using in situ hybridisation and immunohistochemistry. *Neuroscience* 119:803-812.2003).
- Bron R, Klesse LJ, Shah K, Parada LF, Winter J (Activation of Ras is necessary and sufficient for upregulation of vanilloid receptor type 1 in sensory neurons by neurotrophic factors. *Mol Cell Neurosci* 22:118-132.2003).
- Brown AJ (Novel cannabinoid receptors. *Br J Pharmacol* 152:567-575.2007).
- Brown SP, Brenowitz SD, Regehr WG (Brief presynaptic bursts evoke synapse-specific retrograde inhibition mediated by endogenous cannabinoids. *Nat Neurosci* 6:1048-1057.2003).
- Bruce-Keller AJ (Microglial-neuronal interactions in synaptic damage and recovery. *J Neurosci Res* 58:191-201.1999).
- Burgess GM, Mullaney I, McNeill M, Dunn PM, Rang HP (Second messengers involved in the mechanism of action of bradykinin in sensory neurons in culture. *J Neurosci* 9:3314-3325.1989).
- Burstein SH, Huang SM, Petros TJ, Rossetti RG, Walker JM, Zurier RB (Regulation of anandamide tissue levels by N-arachidonylglycine. *Biochem Pharmacol* 64:1147-1150.2002).
- Burstein SH, Rossetti RG, Yagen B, Zurier RB (Oxidative metabolism of anandamide. *Prostaglandins Other Lipid Mediat* 61:29-41.2000).
- Cadas H, Gaillet S, Beltramo M, Venance L, Piomelli D (Biosynthesis of an endogenous cannabinoid precursor in neurons and its control by calcium and cAMP. *J Neurosci* 16:3934-3942.1996).
- Campbell JN, Raja SN, Meyer RA, Mackinnon SE (Myelinated afferents signal the hyperalgesia associated with nerve injury. *Pain* 32:89-94.1988).
- Carlton SM, Coggeshall RE (Peripheral capsaicin receptors increase in the inflamed rat hindpaw: a possible mechanism for peripheral sensitization. *Neurosci Lett* 310:53-56.2001).
- Caterina MJ, Leffler A, Malmberg AB, Martin WJ, Trafton J, Petersen-Zeit KR, Koltzenburg M, Basbaum AI, Julius D (Impaired nociception and pain sensation in mice lacking the capsaicin receptor. *Science* 288:306-313.2000).
- Caterina MJ, Schumacher MA, Tominaga M, Rosen TA, Levine JD, Julius D (The capsaicin receptor: a heat-activated ion channel in the pain pathway. *Nature* 389:816-824.1997).
- Cesare P, Dekker LV, Sardini A, Parker PJ, McNaughton PA (Specific involvement of PKC-epsilon in sensitization of the neuronal response to painful heat. *Neuron* 23:617-624.1999a).
- Cesare P, McNaughton P (A novel heat-activated current in nociceptive neurons and its sensitization by bradykinin. *Proc Natl Acad Sci U S A* 93:15435-15439.1996).
- Cesare P, Moriondo A, Vellani V, McNaughton PA (Ion channels gated by heat. *Proc Natl Acad Sci U S A* 96:7658-7663.1999b).
- Chan CC, Boyce S, Brideau C, Ford-Hutchinson AW, Gordon R, Guay D, Hill RG, Li CS, Mancini J, Penneton M, et al. (Pharmacology of a selective cyclooxygenase-2 inhibitor, L-745,337: a novel nonsteroidal anti-inflammatory agent with an ulcerogenic sparing

- effect in rat and nonhuman primate stomach. *J Pharmacol Exp Ther* 274:1531-1537.1995).
- Chang L, Luo L, Palmer JA, Sutton S, Wilson SJ, Barbier AJ, Breitenbucher JG, Chaplan SR, Webb M (Inhibition of fatty acid amide hydrolase produces analgesia by multiple mechanisms. *Br J Pharmacol* 148:102-113.2006).
- Chapman CR, Casey KL, Dubner R, Foley KM, Gracely RH, Reading AE (Pain measurement: an overview. *Pain* 22:1-31.1985).
- Chapman V (The cannabinoid CB1 receptor antagonist, SR141716A, selectively facilitates nociceptive responses of dorsal horn neurones in the rat. *Br J Pharmacol* 127:1765-1767.1999).
- Chen G, Goeddel DV (TNF-R1 signaling: a beautiful pathway. *Science* 296:1634-1635.2002).
- Chen JK, Chen J, Imig JD, Wei S, Hachey DL, Guthi JS, Falck JR, Capdevila JH, Harris RC (Identification of novel endogenous cytochrome p450 arachidonate metabolites with high affinity for cannabinoid receptors. *J Biol Chem* 283:24514-24524.2008).
- Chen P, Hu S, Yao J, Moore SA, Spector AA, Fang X (Induction of cyclooxygenase-2 by anandamide in cerebral microvascular endothelium. *Microvasc Res* 69:28-35.2005).
- Cheng JK, Ji RR (Intracellular signaling in primary sensory neurons and persistent pain. *Neurochem Res* 33:1970-1978.2008).
- Chin CL, Tovcimak AE, Hradil VP, Seifert TR, Hollingsworth PR, Chandran P, Zhu CZ, Gauvin D, Pai M, Wetter J, Hsieh GC, Honore P, Frost JM, Dart MJ, Meyer MD, Yao BB, Cox BF, Fox GB (Differential effects of cannabinoid receptor agonists on regional brain activity using pharmacological MRI. *Br J Pharmacol* 153:367-379.2008).
- Cholewinski A, Burgess GM, Bevan S (The role of calcium in capsaicin-induced desensitization in rat cultured dorsal root ganglion neurons. *Neuroscience* 55:1015-1023.1993).
- Chu CJ, Huang SM, De Petrocellis L, Bisogno T, Ewing SA, Miller JD, Zipkin RE, Daddario N, Appendino G, Di Marzo V, Walker JM (N-oleoyldopamine, a novel endogenous capsaicin-like lipid that produces hyperalgesia. *J Biol Chem* 278:13633-13639.2003).
- Chuang HH, Prescott ED, Kong H, Shields S, Jordt SE, Basbaum AI, Chao MV, Julius D (Bradykinin and nerve growth factor release the capsaicin receptor from PtdIns(4,5)P2-mediated inhibition. *Nature* 411:957-962.2001).
- Clarke CE, Guttman M (Dopamine agonist monotherapy in Parkinson's disease. *Lancet* 360:1767-1769.2002).
- Clayton N, Marshall FH, Bountra C, O'Shaughnessy CT (CB1 and CB2 cannabinoid receptors are implicated in inflammatory pain. *Pain* 96:253-260.2002).
- Clayton NM, Oakley I, Thompson S, Wheeldon A, Sargent B, Bountra C (Validation of the dual channel averager as an instrument of the measure of clinically relevant pain. *British Journal of Pharmacology* 120 supplement:219P.1997).
- Clerk A, Sugden PH (The p38-MAPK inhibitor, SB203580, inhibits cardiac stress-activated protein kinases/c-Jun N-terminal kinases (SAPKs/JNKs). *FEBS Lett* 426:93-96.1998).
- Combe R, Bramwell S, Field MJ (The monosodium iodoacetate model of osteoarthritis: a model of chronic nociceptive pain in rats? *Neurosci Lett* 370:236-240.2004).
- Comelli F, Giagnoni G, Bettoni I, Colleoni M, Costa B (The inhibition of monoacylglycerol lipase by URB602 showed an anti-inflammatory

- and anti-nociceptive effect in a murine model of acute inflammation. *Br J Pharmacol* 152:787-794.2007).
- Consroe P, Musty R, Rein J, Tillery W, Pertwee R (The perceived effects of smoked cannabis on patients with multiple sclerosis. *Eur Neurol* 38:44-48.1997).
- Constantin CE, Mair N, Sailer CA, Andratsch M, Xu ZZ, Blumer MJ, Scherbakov N, Davis JB, Bluethmann H, Ji RR, Kress M (Endogenous tumor necrosis factor alpha (TNFalpha) requires TNF receptor type 2 to generate heat hyperalgesia in a mouse cancer model. *J Neurosci* 28:5072-5081.2008).
- Costa B, Comelli F, Bettoni I, Colleoni M, Giagnoni G (The endogenous fatty acid amide, palmitoylethanolamide, has anti-allodynic and anti-hyperalgesic effects in a murine model of neuropathic pain: involvement of CB(1), TRPV1 and PPARgamma receptors and neurotrophic factors. *Pain*.2008).
- Craft RM, Porreca F (Treatment parameters of desensitization to capsaicin. *Life Sci* 51:1767-1775.1992).
- Craib SJ, Ellington HC, Pertwee RG, Ross RA (A possible role of lipoxygenase in the activation of vanilloid receptors by anandamide in the guinea-pig bronchus. *Br J Pharmacol* 134:30-37.2001).
- Cravatt BF, Demarest K, Patricelli MP, Bracey MH, Giang DK, Martin BR, Lichtman AH (Supersensitivity to anandamide and enhanced endogenous cannabinoid signaling in mice lacking fatty acid amide hydrolase. *Proc Natl Acad Sci U S A* 98:9371-9376.2001).
- Cravatt BF, Giang DK, Mayfield SP, Boger DL, Lerner RA, Gilula NB (Molecular characterization of an enzyme that degrades neuromodulatory fatty-acid amides. *Nature* 384:83-87.1996).
- Cravatt BF, Saghatelian A, Hawkins EG, Clement AB, Bracey MH, Lichtman AH (Functional disassociation of the central and peripheral fatty acid amide signaling systems. *Proc Natl Acad Sci U S A* 101:10821-10826.2004).
- Croci T, Zarini E (Effect of the cannabinoid CB1 receptor antagonist rimonabant on nociceptive responses and adjuvant-induced arthritis in obese and lean rats. *Br J Pharmacol* 150:559-566.2007).
- Cunha JM, Cunha FQ, Poole S, Ferreira SH (Cytokine-mediated inflammatory hyperalgesia limited by interleukin-1 receptor antagonist. *Br J Pharmacol* 130:1418-1424.2000).
- Cunha Q, Poole S, Lorenzetti BB, Ferreira SH (The Pivotal Role of Tumor-Necrosis-Factor-Alpha in the Development of Inflammatory Hyperalgesia. *British Journal of Pharmacology* 107:660-664.1992).
- Cunha TM, Verri WA, Jr., Silva JS, Poole S, Cunha FQ, Ferreira SH (A cascade of cytokines mediates mechanical inflammatory hypernociception in mice 10.1073/pnas.0409225102. *PNAS* 102:1755-1760.2005).
- Curtis JR, Xi J, Patkar N, Xie A, Saag KG, Martin C (Drug-specific and time-dependent risks of bacterial infection among patients with rheumatoid arthritis who were exposed to tumor necrosis factor alpha antagonists. *Arthritis Rheum* 56:4226-4227.2007).
- Cuzzocrea S, Mazzon E, Di Paola R, Peli A, Bonato A, Britti D, Genovese T, Muia C, Crisafulli C, Caputi AP (The role of the peroxisome proliferator-activated receptor-alpha (PPAR-alpha) in the regulation of acute inflammation. *J Leukoc Biol* 79:999-1010.2006).
- Davis AJ, Perkins MN (The involvement of bradykinin B1 and B2 receptor mechanisms in cytokine-induced mechanical hyperalgesia in the rat. *Br J Pharmacol* 113:63-68.1994).

- Davis JB, Gray J, Gunthorpe MJ, Hatcher JP, Davey PT, Overend P, Harries MH, Latcham J, Clapham C, Atkinson K, Hughes SA, Rance K, Grau E, Harper AJ, Pugh PL, Rogers DC, Bingham S, Randall A, Sheardown SA (Vanilloid receptor-1 is essential for inflammatory thermal hyperalgesia. *Nature* 405:183-187.2000).
- de Lago E, Petrosino S, Valenti M, Morera E, Ortega-Gutierrez S, Fernandez-Ruiz J, Di Marzo V (Effect of repeated systemic administration of selective inhibitors of endocannabinoid inactivation on rat brain endocannabinoid levels. *Biochem Pharmacol* 70:446-452.2005).
- de Novellis V, Palazzo E, Rossi F, de Petrocellis L, Petrosino S, Guida F, Luongo L, Migliozi A, Cristino L, Marabese I, Starowicz K, Di Marzo V, Maione S (The analgesic effect of N-arachidonoyl-serotonin, a FAAH inhibitor and TRPV1 receptor antagonist, associated with changes in rostral ventromedial medulla and locus coeruleus cell activity in rats. *Neuropharmacology* 55:1105-1113.2008).
- De Petrocellis L, Bisogno T, Davis JB, Pertwee RG, Di Marzo V (Overlap between the ligand recognition properties of the anandamide transporter and the VR1 vanilloid receptor: inhibitors of anandamide uptake with negligible capsaicin-like activity. *FEBS Lett* 483:52-56.2000).
- De Petrocellis L, Bisogno T, Maccarrone M, Davis JB, Finazzi-Agro A, Di Marzo V (The activity of anandamide at vanilloid VR1 receptors requires facilitated transport across the cell membrane and is limited by intracellular metabolism. *J Biol Chem* 276:12856-12863.2001a).
- De Petrocellis L, Davis JB, Di Marzo V (Palmitoylethanolamide enhances anandamide stimulation of human vanilloid VR1 receptors. *FEBS Lett* 506:253-256.2001b).
- De Petrocellis L, Harrison S, Bisogno T, Tognetto M, Brandi I, Smith GD, Creminon C, Davis JB, Geppetti P, Di Marzo V (The vanilloid receptor (VR1)-mediated effects of anandamide are potently enhanced by the cAMP-dependent protein kinase. *J Neurochem* 77:1660-1663.2001c).
- Desarnaud F, Cadas H, Piomelli D (Anandamide amidohydrolase activity in rat brain microsomes. Identification and partial characterization. *J Biol Chem* 270:6030-6035.1995).
- Desroches J, Guindon J, Lambert C, Beaulieu P (Modulation of the antinociceptive effects of 2-arachidonoyl glycerol by peripherally administered FAAH and MGL inhibitors in a neuropathic pain model. *Br J Pharmacol* 155:913-924.2008).
- Deutsch DG, Chin SA (Enzymatic synthesis and degradation of anandamide, a cannabinoid receptor agonist. *Biochem Pharmacol* 46:791-796.1993).
- Devane WA, Hanus L, Breuer A, Pertwee RG, Stevenson LA, Griffin G, Gibson D, Mandelbaum A, Etinger A, Mechoulam R (Isolation and structure of a brain constituent that binds to the cannabinoid receptor. *Science* 258:1946-1949.1992).
- Di Marzo V (Biosynthesis and inactivation of endocannabinoids: relevance to their proposed role as neuromodulators. *Life Sci* 65:645-655.1999).
- Di Marzo V (Endocannabinoids: synthesis and degradation. *Rev Physiol Biochem Pharmacol* 160:1-24.2008).
- Di Marzo V, Bisogno T, Sugiura T, Melck D, De Petrocellis L (The novel endogenous cannabinoid 2-arachidonoylglycerol is inactivated by

- neuronal- and basophil-like cells: connections with anandamide. *Biochem J* 331 (Pt 1):15-19.1998).
- Di Marzo V, Breivogel CS, Tao Q, Bridgen DT, Razdan RK, Zimmer AM, Zimmer A, Martin BR (Levels, metabolism, and pharmacological activity of anandamide in CB(1) cannabinoid receptor knockout mice: evidence for non-CB(1), non-CB(2) receptor-mediated actions of anandamide in mouse brain. *J Neurochem* 75:2434-2444.2000 (a)).
- Di Marzo V, Cote M, Matias I, Lemieux I, Arsenault BJ, Cartier A, Piscitelli F, Petrosino S, Almeras N, Despres JP (Changes in plasma endocannabinoid levels in viscerally obese men following a 1 year lifestyle modification programme and waist circumference reduction: associations with changes in metabolic risk factors. *Diabetologia* 52:213-217.2009).
- Di Marzo V, Fontana A, Cadas H, Schinelli S, Cimino G, Schwartz JC, Piomelli D (Formation and inactivation of endogenous cannabinoid anandamide in central neurons. *Nature* 372:686-691.1994).
- Di Marzo V, Petrosino S (Endocannabinoids and the regulation of their levels in health and disease. *Curr Opin Lipidol* 18:129-140.2007).
- Di Rosa M, Giroud JP, Willoughby DA (Studies on the mediators of the acute inflammatory response induced in rats in different sites by carrageenan and turpentine. *J Pathol* 104:15-29.1971).
- Di S, Boudaba C, Popescu IR, Weng FJ, Harris C, Marcheselli VL, Bazan NG, Tasker JG (Activity-dependent release and actions of endocannabinoids in the rat hypothalamic supraoptic nucleus. *J Physiol* 569:751-760.2005).
- Diana MA, Levenes C, Mackie K, Marty A (Short-term retrograde inhibition of GABAergic synaptic currents in rat Purkinje cells is mediated by endogenous cannabinoids. *J Neurosci* 22:200-208.2002).
- Dieppe PA, Lohmander LS (Pathogenesis and management of pain in osteoarthritis. *Lancet* 365:965-973.2005).
- Dinh TP, Carpenter D, Leslie FM, Freund TF, Katona I, Sensi SL, Kathuria S, Piomelli D (Brain monoglyceride lipase participating in endocannabinoid inactivation. *Proceedings of the National Academy of Sciences of the United States of America* 99:10819-10824.2002).
- Djoughri L, Dawbarn D, Robertson A, Newton R, Lawson SN (Time course and nerve growth factor dependence of inflammation-induced alterations in electrophysiological membrane properties in nociceptive primary afferent neurons. *J Neurosci* 21:8722-8733.2001).
- Docherty RJ, Robertson B, Bevan S (Capsaicin causes prolonged inhibition of voltage-activated calcium currents in adult rat dorsal root ganglion neurons in culture. *Neuroscience* 40:513-521.1991).
- Dostrovsky JOC, A.D. (2006) Ascending projection systems. In: Wall and Melzack's Textbook of Pain(McMahon, S. B. K., M., ed), pp 187-205: Elsevier Churchill Livingstone.
- Dray A (Inflammatory mediators of pain. *Br J Anaesth* 75:125-131.1995).
- Dray A, Patel IA, Perkins MN, Rueff A, Urban L (Desensitization of bradykinin-induced activation of peripheral nociceptors. *Agents Actions Suppl* 38 (Pt 2):93-97.1992).
- Dunham J, Hoedt-Schmidt S, Kalbhen DA (Prolonged effect of iodoacetate on articular cartilage and its modification by an anti-rheumatic drug. *Int J Exp Pathol* 74:283-289.1993).
- Edgmond WS, Hillard CJ, Falck JR, Kearn CS, Campbell WB (Human platelets and polymorphonuclear leukocytes synthesize oxygenated

- derivatives of arachidonylethanolamide (anandamide): their affinities for cannabinoid receptors and pathways of inactivation. *Mol Pharmacol* 54:180-188.1998).
- Egertova M, Elphick MR (Localisation of cannabinoid receptors in the rat brain using antibodies to the intracellular C-terminal tail of CB1. *Journal of Comparative Neurology* 422:159-171.2000).
- Egertova M, Giang DK, Cravatt BF, Elphick MR (A new perspective on cannabinoid signalling: complementary localization of fatty acid amide hydrolase and the CB1 receptor in rat brain. *Proc Biol Sci* 265:2081-2085.1998).
- Egertova M, Simon GM, Cravatt BF, Elphick MR (Localization of N-acyl phosphatidylethanolamine phospholipase D (NAPE-PLD) expression in mouse brain: A new perspective on N-acylethanolamines as neural signaling molecules. *J Comp Neurol* 506:604-615.2008).
- Eissner G, Kirchner S, Lindner H, Kolch W, Janosch P, Grell M, Scheurich P, Andreesen R, Holler E (Reverse signaling through transmembrane TNF confers resistance to lipopolysaccharide in human monocytes and macrophages. *J Immunol* 164:6193-6198.2000).
- Eissner G, Kolch W, Scheurich P (Ligands working as receptors: reverse signaling by members of the TNF superfamily enhance the plasticity of the immune system. *Cytokine Growth Factor Rev* 15:353-366.2004).
- Elmes SJ, Jhaveri MD, Smart D, Kendall DA, Chapman V (Cannabinoid CB2 receptor activation inhibits mechanically evoked responses of wide dynamic range dorsal horn neurons in naive rats and in rat models of inflammatory and neuropathic pain. *Eur J Neurosci* 20:2311-2320.2004).
- Elmes SJ, Winyard LA, Medhurst SJ, Clayton NM, Wilson AW, Kendall DA, Chapman V (Activation of CB1 and CB2 receptors attenuates the induction and maintenance of inflammatory pain in the rat. *Pain* 118:327-335.2005).
- Farahat MN, Yanni G, Poston R, Panayi GS (Cytokine expression in synovial membranes of patients with rheumatoid arthritis and osteoarthritis. *Annals of the Rheumatic Diseases* 52:870-875.1993).
- Fegley D, Gaetani S, Duranti A, Tontini A, Mor M, Tarzia G, Piomelli D (Characterization of the fatty acid amide hydrolase inhibitor cyclohexyl carbamic acid 3'-carbamoyl-biphenyl-3-yl ester (URB597): effects on anandamide and oleoylethanolamide deactivation. *J Pharmacol Exp Ther* 313:352-358.2005).
- Fegley D, Kathuria S, Mercier R, Li C, Goutopoulos A, Makriyannis A, Piomelli D (Anandamide transport is independent of fatty-acid amide hydrolase activity and is blocked by the hydrolysis-resistant inhibitor AM1172. *Proc Natl Acad Sci U S A* 101:8756-8761.2004).
- Feldmann M, Brennan FM, Maini RN (Role of cytokines in rheumatoid arthritis. *Annu Rev Immunol* 14:397-440.1996).
- Fernihough J, Gentry C, Bevan S, Winter J (Regulation of calcitonin gene-related peptide and TRPV1 in a rat model of osteoarthritis. *Neurosci Lett* 388:75-80.2005).
- Fernihough J, Gentry C, Malcangio M, Fox A, Rediske J, Pellas T, Kidd B, Bevan S, Winter J (Pain related behaviour in two models of osteoarthritis in the rat knee. *Pain* 112:83-93.2004).

- Fields HL, Heinricher MM (Anatomy and physiology of a nociceptive modulatory system. *Philos Trans R Soc Lond B Biol Sci* 308:361-374.1985).
- Fields HL, Heinricher MM, Mason P (Neurotransmitters in nociceptive modulatory circuits. *Annu Rev Neurosci* 14:219-245.1991).
- Forman BM, Tontonoz P, Chen J, Brun RP, Spiegelman BM, Evans RM (15-Deoxy-delta 12, 14-prostaglandin J2 is a ligand for the adipocyte determination factor PPAR gamma. *Cell* 83:803-812.1995).
- Fowler CJ (The contribution of cyclooxygenase-2 to endocannabinoid metabolism and action. *Br J Pharmacol* 152:594-601.2007).
- Fowler CJ, Holt S, Nilsson O, Jonsson KO, Tiger G, Jacobsson SO (The endocannabinoid signaling system: pharmacological and therapeutic aspects. *Pharmacol Biochem Behav* 81:248-262.2005).
- Fowler CJ, Holt S, Tiger G (Acidic nonsteroidal anti-inflammatory drugs inhibit rat brain fatty acid amide hydrolase in a pH-dependent manner. *J Enzyme Inhib Med Chem* 18:55-58.2003a).
- Fowler CJ, Tiger G, Lopez-Rodriguez ML, Viso A, Ortega-Gutierrez S, Ramos JA (Inhibition of fatty acid amidohydrolase, the enzyme responsible for the metabolism of the endocannabinoid anandamide, by analogues of arachidonoyl-serotonin. *J Enzyme Inhib Med Chem* 18:225-231.2003b).
- Francischi JN, Chaves CT, Moura AC, Lima AS, Rocha OA, Ferreira-Alves DL, Bakhle YS (Selective inhibitors of cyclo-oxygenase-2 (COX-2) induce hypoalgesia in a rat paw model of inflammation. *Br J Pharmacol* 137:837-844.2002).
- Friedman WJ, Larkfors L, Ayer-LeLievre C, Ebendal T, Olson L, Persson H (Regulation of beta-nerve growth factor expression by inflammatory mediators in hippocampal cultures. *J Neurosci Res* 27:374-382.1990).
- Fu J, Astarita G, Gaetani S, Kim J, Cravatt BF, Mackie K, Piomelli D (Food intake regulates oleoylethanolamide formation and degradation in the proximal small intestine. *J Biol Chem* 282:1518-1528.2007).
- Fu J, Kim J, Oveisi F, Astarita G, Piomelli D (Targeted enhancement of oleoylethanolamide production in proximal small intestine induces across-meal satiety in rats. *Am J Physiol Regul Integr Comp Physiol* 295:R45-50.2008).
- Fu KY, Light AR, Matsushima GK, Maixner W (Microglial reactions after subcutaneous formalin injection into the rat hind paw. *Brain Res* 825:59-67.1999).
- Galiegue S, Mary S, Marchand J, Dussossoy D, Carriere D, Carayon P, Bouaboula M, Shire D, Le Fur G, Casellas P (Expression of central and peripheral cannabinoid receptors in human immune tissues and leukocyte subpopulations. *Eur J Biochem* 232:54-61.1995).
- Gauldie SD, McQueen DS, Pertwee R, Chessell IP (Anandamide activates peripheral nociceptors in normal and arthritic rat knee joints. *Br J Pharmacol* 132:617-621.2001).
- Genovese T, Mazzon E, Di Paola R, Cannavo G, Muia C, Bramanti P, Cuzzocrea S (Role of endogenous ligands for the peroxisome proliferators activated receptors alpha in the secondary damage in experimental spinal cord trauma. *Exp Neurol* 194:267-278.2005).
- Gerdeman GL, Ronesi J, Lovinger DM (Postsynaptic endocannabinoid release is critical to long-term depression in the striatum. *Nat Neurosci* 5:446-451.2002).

- Ghilardi JR, Svensson CI, Rogers SD, Yaksh TL, Mantyh PW (Constitutive spinal cyclooxygenase-2 participates in the initiation of tissue injury-induced hyperalgesia. *J Neurosci* 24:2727-2732.2004).
- Giuffrida A, Parsons LH, Kerr TM, Rodriguez de Fonseca F, Navarro M, Piomelli D (Dopamine activation of endogenous cannabinoid signaling in dorsal striatum. *Nat Neurosci* 2:358-363.1999).
- Giuffrida A, Piomelli D (Isotope dilution GC/MS determination of anandamide and other fatty acylethanolamides in rat blood plasma. *FEBS Lett* 422:373-376.1998).
- Giuffrida A, Rodriguez de Fonseca F, Nava F, Loubet-Lescoulie P, Piomelli D (Elevated circulating levels of anandamide after administration of the transport inhibitor, AM404. *Eur J Pharmacol* 408:161-168.2000a).
- Giuffrida A, Rodriguez de Fonseca F, Piomelli D (Quantification of bioactive acylethanolamides in rat plasma by electrospray mass spectrometry. *Anal Biochem* 280:87-93.2000b).
- Glaser ST, Kaczocha M, Deutsch DG (Anandamide transport: a critical review. *Life Sci* 77:1584-1604.2005).
- Go VL, Yaksh TL (Release of substance P from the cat spinal cord. *J Physiol* 391:141-167.1987).
- Gobbi G, Bambico FR, Mangieri R, Bortolato M, Campolongo P, Solinas M, Cassano T, Morgese MG, Debonnel G, Duranti A, Tontini A, Tarzia G, Mor M, Trezza V, Goldberg SR, Cuomo V, Piomelli D (Antidepressant-like activity and modulation of brain monoaminergic transmission by blockade of anandamide hydrolysis. *Proc Natl Acad Sci U S A* 102:18620-18625.2005).
- Gold MS, Flake NM (Inflammation-mediated hyperexcitability of sensory neurons. *Neurosignals* 14:147-157.2005).
- Goldenberg DL, Egan MS, Cohen AS (Inflammatory synovitis in degenerative joint disease. *J Rheumatol* 9:204-209.1982).
- Goldring MB (Update on the biology of the chondrocyte and new approaches to treating cartilage diseases. *Best Pract Res Clin Rheumatol* 20:1003-1025.2006).
- Gong JP, Onaivi ES, Ishiguro H, Liu QR, Tagliaferro PA, Brusco A, Uhl GR (Cannabinoid CB2 receptors: immunohistochemical localization in rat brain. *Brain Res* 1071:10-23.2006).
- Gonthier MP, Hoareau L, Festy F, Matias I, Valenti M, Bes-Houtmann S, Rouch C, Robert-Da Silva C, Chesne S, Lefebvre d'Hellencourt C, Cesari M, Di Marzo V, Roche R (Identification of endocannabinoids and related compounds in human fat cells. *Obesity (Silver Spring)* 15:837-845.2007).
- Gonzalez S, Cascio MG, Fernandez-Ruiz J, Fezza F, Di Marzo V, Ramos JA (Changes in endocannabinoid contents in the brain of rats chronically exposed to nicotine, ethanol or cocaine. *Brain Res* 954:73-81.2002).
- Goodin D (Marijuana and multiple sclerosis. *Lancet Neurol* 3:79-80.2004).
- Goparaju SK, Ueda N, Yamaguchi H, Yamamoto S (Anandamide amidohydrolase reacting with 2-arachidonoylglycerol, another cannabinoid receptor ligand. *FEBS Lett* 422:69-73.1998).
- Goya P, Jagerovic N, Hernandez-Folgado L, Martin MI (Cannabinoids and neuropathic pain. *Mini Rev Med Chem* 3:765-772.2003).
- Grassi F, Mileo AM, Monaco L, Punturieri A, Santoni A, Eusebi F (TNF-alpha increases the frequency of spontaneous miniature synaptic currents in cultured rat hippocampal neurons. *Brain Res* 659:226-230.1994).

- Guay J, Bateman K, Gordon R, Mancini J, Riendeau D (Carrageenan-induced paw edema in rat elicits a predominant prostaglandin E2 (PGE2) response in the central nervous system associated with the induction of microsomal PGE2 synthase-1. *J Biol Chem* 279:24866-24872.2004).
- Guijarro A, Osei-Hyiaman D, Harvey-White J, Kunos G, Suzuki S, Nadochiy S, Brookes PS, Meguid MM (Sustained weight loss after Roux-en-Y gastric bypass is characterized by down regulation of endocannabinoids and mitochondrial function. *Ann Surg* 247:779-790.2008).
- Guilak FS, L.A. (2000) Structure and Function of Articular Cartilage. In: *Orthopaedic Sports Medicine*(Garrett, W. E., Speer, K.P. & Kirkendall, D.T., ed), pp 53-75 Philadelphia: Lippincott Williams & Wilkins.
- Guindon J, De Lean A, Beaulieu P (Local interactions between anandamide, an endocannabinoid, and ibuprofen, a nonsteroidal anti-inflammatory drug, in acute and inflammatory pain. *Pain* 121:85-93.2006).
- Guindon J, Desroches J, Beaulieu P (The antinociceptive effects of intraplantar injections of 2-arachidonoyl glycerol are mediated by cannabinoid CB2 receptors. *Br J Pharmacol* 150:693-701.2007).
- Guindon J, Hohmann AG (Cannabinoid CB2 receptors: a therapeutic target for the treatment of inflammatory and neuropathic pain. *Br J Pharmacol* 153:319-334.2008).
- Guingamp C, Gegout-Pottie P, Philippe L, Terlain B, Netter P, Gillet P (Mono-iodoacetate-induced experimental osteoarthritis: a dose-response study of loss of mobility, morphology, and biochemistry. *Arthritis Rheum* 40:1670-1679.1997).
- Gunthorpe MJ, Chizh BA (Clinical development of TRPV1 antagonists: targeting a pivotal point in the pain pathway. *Drug Discov Today* 14:56-67.2009).
- Gunthorpe MJ, Szallasi A (Peripheral TRPV1 receptors as targets for drug development: new molecules and mechanisms. *Curr Pharm Des* 14:32-41.2008).
- Guzman M, Lo Verme J, Fu J, Oveisi F, Blazquez C, Piomelli D (Oleoylethanolamide stimulates lipolysis by activating the nuclear receptor peroxisome proliferator-activated receptor alpha (PPAR-alpha). *J Biol Chem* 279:27849-27854.2004).
- Guzman RE, Evans MG, Bove S, Morenko B, Kilgore K (Mono-iodoacetate-induced histologic changes in subchondral bone and articular cartilage of rat femorotibial joints: an animal model of osteoarthritis. *Toxicol Pathol* 31:619-624.2003).
- Hains BC, Waxman SG (Activated microglia contribute to the maintenance of chronic pain after spinal cord injury. *J Neurosci* 26:4308-4317.2006).
- Hampson AJ, Hill WA, Zan-Phillips M, Makriyannis A, Leung E, Eglen RM, Bornheim LM (Anandamide hydroxylation by brain lipoxygenase:metabolite structures and potencies at the cannabinoid receptor. *Biochim Biophys Acta* 1259:173-179.1995).
- Hansen HH, Hansen SH, Bjornsdottir I, Hansen HS (Electrospray ionization mass spectrometric method for the determination of cannabinoid precursors: N-acylethanolamine phospholipids (NAPEs). *J Mass Spectrom* 34:761-767.1999).
- Hansen HS, Lauritzen L, Strand AM, Moesgaard B, Frandsen A (Glutamate stimulates the formation of N-acylphosphatidylethanolamine and N-

- acylethanolamine in cortical neurons in culture. *Biochim Biophys Acta* 1258:303-308.1995).
- Hanus L, Abu-Lafi S, Fride E, Breuer A, Vogel Z, Shalev DE, Kustanovich I, Mechoulam R (2-arachidonyl glyceryl ether, an endogenous agonist of the cannabinoid CB1 receptor. *Proceedings of the National Academy of Sciences of the United States of America* 98:3662-3665.2001).
- Harashima S, Horiuchi T, Hatta N, Morita C, Higuchi M, Sawabe T, Tsukamoto H, Tahira T, Hayashi K, Fujita S, Niho Y (Outside-to-inside signal through the membrane TNF-alpha induces E-selectin (CD62E) expression on activated human CD4+ T cells. *J Immunol* 166:130-136.2001).
- Hargreaves K, Dubner R, Brown F, Flores C, Joris J (A new and sensitive method for measuring thermal nociception in cutaneous hyperalgesia. *Pain* 32:77-88.1988).
- Harris RC, McKanna JA, Akai Y, Jacobson HR, Dubois RN, Breyer MD (Cyclooxygenase-2 is associated with the macula densa of rat kidney and increases with salt restriction. *J Clin Invest* 94:2504-2510.1994).
- Hashimoto-dani Y, Ohno-Shosaku T, Maejima T, Fukami K, Kano M (Pharmacological evidence for the involvement of diacylglycerol lipase in depolarization-induced endocannabinoid release. *Neuropharmacology* 54:58-67.2008).
- Hashizume H, DeLeo JA, Colburn RW, Weinstein JN (Spinal glial activation and cytokine expression after lumbar root injury in the rat. *Spine (Phila Pa 1976)* 25:1206-1217.2000).
- Hayes P, Meadows HJ, Gunthorpe MJ, Harries MH, Duckworth DM, Cairns W, Harrison DC, Clarke CE, Ellington K, Prinjha RK, Barton AJ, Medhurst AD, Smith GD, Topp S, Murdock P, Sanger GJ, Terrett J, Jenkins O, Benham CD, Randall AD, Gloger IS, Davis JB (Cloning and functional expression of a human orthologue of rat vanilloid receptor-1. *Pain* 88:205-215.2000).
- Helliwell RJ, McLatchie LM, Clarke M, Winter J, Bevan S, McIntyre P (Capsaicin sensitivity is associated with the expression of the vanilloid (capsaicin) receptor (VR1) mRNA in adult rat sensory ganglia. *Neurosci Lett* 250:177-180.1998).
- Hensellek S, Brell P, Schaible HG, Brauer R, Segond von Banchet G (The cytokine TNFalpha increases the proportion of DRG neurones expressing the TRPV1 receptor via the TNFR1 receptor and ERK activation. *Mol Cell Neurosci* 36:381-391.2007).
- Herkenham M (Characterization and localization of cannabinoid receptors in brain: an in vitro technique using slide-mounted tissue sections. *NIDA Res Monogr* 112:129-145.1991).
- Herkenham M, Lynn AB, Johnson MR, Melvin LS, Decosta BR, Rice KC (Characterization and Localization of Cannabinoid Receptors in Rat-Brain - a Quantitative Invitro Autoradiographic Study. *Journal of Neuroscience* 11:563-583.1991).
- Herkenham M, Lynn AB, Little MD, Johnson MR, Melvin LS, Decosta BR, Rice KC (CANNABINOID RECEPTOR LOCALIZATION IN BRAIN. *Proceedings of the National Academy of Sciences of the United States of America* 87:1932-1936.1990).
- Hermann A, Kaczocha M, Deutsch DG (2-Arachidonoylglycerol (2-AG) membrane transport: history and outlook. *Aaps J* 8:E409-412.2006).
- Hermann H, De Petrocellis L, Bisogno T, Schiano Moriello A, Lutz B, Di Marzo V (Dual effect of cannabinoid CB1 receptor stimulation on a

- vanilloid VR1 receptor-mediated response. *Cell Mol Life Sci* 60:607-616.2003).
- Hillard CJ, Edgemond WS, Jarrahan A, Campbell WB (Accumulation of N-arachidonylethanolamine (anandamide) into cerebellar granule cells occurs via facilitated diffusion. *J Neurochem* 69:631-638.1997).
- Hillard CJ, Wilkison DM, Edgemond WS, Campbell WB (Characterization of the kinetics and distribution of N-arachidonylethanolamine (anandamide) hydrolysis by rat brain. *Biochim Biophys Acta* 1257:249-256.1995).
- Hingtgen CM, Waite KJ, Vasko MR (Prostaglandins facilitate peptide release from rat sensory neurons by activating the adenosine 3',5'-cyclic monophosphate transduction cascade. *J Neurosci* 15:5411-5419.1995).
- Ho WS, Hillard CJ (Modulators of endocannabinoid enzymic hydrolysis and membrane transport. *Handb Exp Pharmacol* 187-207.2005).
- Ho WS, Randall MD (Endothelium-dependent metabolism by endocannabinoid hydrolases and cyclooxygenases limits vasorelaxation to anandamide and 2-arachidonoylglycerol. *Br J Pharmacol* 150:641-651.2007).
- Hohmann A, Suplita R (Endocannabinoid mechanisms of pain modulation. *Aaps J* 8:E693-708.2006).
- Hohmann AG (Spinal and peripheral mechanisms of cannabinoid antinociception: behavioral, neurophysiological and neuroanatomical perspectives. *Chem Phys Lipids* 121:173-190.2002).
- Hohmann AG, Herkenham M (Localization of central cannabinoid CB1 receptor messenger RNA in neuronal subpopulations of rat dorsal root ganglia: a double-label in situ hybridization study. *Neuroscience* 90:923-931.1999).
- Hohmann AG, Tsou K, Walker JM (Cannabinoid modulation of wide dynamic range neurons in the lumbar dorsal horn of the rat by spinally administered WIN55,212-2. *Neurosci Lett* 257:119-122.1998).
- Holt S, Comelli F, Costa B, Fowler CJ (Inhibitors of fatty acid amide hydrolase reduce carrageenan-induced hind paw inflammation in pentobarbital-treated mice: comparison with indomethacin and possible involvement of cannabinoid receptors. *British journal of pharmacology* 146:467-476.2005).
- Holt S, Nilsson J, Omeir R, Tiger G, Fowler CJ (Effects of pH on the inhibition of fatty acid amidohydrolase by ibuprofen. *Br J Pharmacol* 133:513-520.2001).
- Holt S, Paylor B, Boldrup L, Alajakku K, Vandevoorde S, Sundstrom A, Cocco MT, Onnis V, Fowler CJ (Inhibition of fatty acid amide hydrolase, a key endocannabinoid metabolizing enzyme, by analogues of ibuprofen and indomethacin. *Eur J Pharmacol* 565:26-36.2007).
- Holt S, Rocksén D, Bucht A, Petersen G, Hansen HS, Valenti M, Di Marzo V, Fowler CJ (Lipopolysaccharide-induced pulmonary inflammation is not accompanied by a release of anandamide into the lavage fluid or a down-regulation of the activity of fatty acid amide hydrolase. *Life Sci* 76:461-472.2004).
- Holzer P (Local effector functions of capsaicin-sensitive sensory nerve endings: involvement of tachykinins, calcitonin gene-related peptide and other neuropeptides. *Neuroscience* 24:739-768.1988).

- Howlett AC, Barth F, Bonner TI, Cabral G, Casellas P, Devane WA, Felder CC, Herkenham M, Mackie K, Martin BR, Mechoulam R, Pertwee RG (International Union of Pharmacology. XXVII. Classification of Cannabinoid Receptors. *Pharmacol Rev* 54:161-202.2002).
- Hu SS, Bradshaw HB, Chen JS, Tan B, Walker JM (Prostaglandin E2 glycerol ester, an endogenous COX-2 metabolite of 2-arachidonoylglycerol, induces hyperalgesia and modulates NFkappaB activity. *Br J Pharmacol* 153:1538-1549.2008).
- Huang SM, Bisogno T, Petros TJ, Chang SY, Zavitsanos PA, Zipkin RE, Sivakumar R, Coop A, Maeda DY, De Petrocellis L, Burstein S, Di Marzo V, Walker JM (Identification of a new class of molecules, the arachidonyl amino acids, and characterization of one member that inhibits pain. *J Biol Chem* 276:42639-42644.2001).
- Huang SM, Bisogno T, Trevisani M, Al-Hayani A, De Petrocellis L, Fezza F, Tognetto M, Petros TJ, Krey JF, Chu CJ, Miller JD, Davies SN, Geppetti P, Walker JM, Di Marzo V (An endogenous capsaicin-like substance with high potency at recombinant and native vanilloid VR1 receptors. *Proceedings of the National Academy of Sciences of the United States of America* 99:8400-8405.2002).
- Huebner JL, Otterness IG, Freund EM, Caterson B, Kraus VB (Collagenase 1 and collagenase 3 expression in a guinea pig model of osteoarthritis. *Arthritis Rheum* 41:877-890.1998).
- Hunt SP, Mantyh PW (The molecular dynamics of pain control. *Nat Rev Neurosci* 2:83-91.2001).
- Ibrahim MM, Rude ML, Stagg NJ, Mata HP, Lai J, Vanderah TW, Porreca F, Buckley NE, Makriyannis A, Malan TP, Jr. (CB2 cannabinoid receptor mediation of antinociception. *Pain* 122:36-42.2006).
- Ibuki T, Hama AT, Wang XT, Pappas GD, Sagen J (Loss of GABA-immunoreactivity in the spinal dorsal horn of rats with peripheral nerve injury and promotion of recovery by adrenal medullary grafts. *Neuroscience* 76:845-858.1997).
- Ichitani Y, Shi T, Haeggstrom JZ, Samuelsson B, Hokfelt T (Increased levels of cyclooxygenase-2 mRNA in the rat spinal cord after peripheral inflammation: an in situ hybridization study. *Neuroreport* 8:2949-2952.1997).
- Ignatowski TA, Covey WC, Knight PR, Severin CM, Nickola TJ, Spengler RN (Brain-derived TNFalpha mediates neuropathic pain. *Brain Res* 841:70-77.1999).
- Ikeda K, Kobayashi T, Kumanishi T, Yano R, Sora I, Niki H (Molecular mechanisms of analgesia induced by opioids and ethanol: is the GIRK channel one of the keys? *Neurosci Res* 44:121-131.2002).
- Ivanavicius SP, Ball AD, Heapy CG, Westwood FR, Murray F, Read SJ (Structural pathology in a rodent model of osteoarthritis is associated with neuropathic pain: increased expression of ATF-3 and pharmacological characterisation. *Pain* 128:272-282.2007).
- Iversen L, Chapman V (Cannabinoids: a real prospect for pain relief? *Curr Opin Pharmacol* 2:50-55.2002).
- Izzo AA, Fezza F, Capasso R, Bisogno T, Pinto L, Iuvone T, Esposito G, Mascolo N, Di Marzo V, Capasso F (Cannabinoid CB1-receptor mediated regulation of gastrointestinal motility in mice in a model of intestinal inflammation. *Br J Pharmacol* 134:563-570.2001).
- Jarrahian A, Manna S, Edgemond WS, Campbell WB, Hillard CJ (Structure-activity relationships among N-arachidonylethanolamine (Anandamide) head group analogues for the anandamide transporter. *J Neurochem* 74:2597-2606.2000).

- Jayamanne A, Greenwood R, Mitchell VA, Aslan S, Piomelli D, Vaughan CW (Actions of the FAAH inhibitor URB597 in neuropathic and inflammatory chronic pain models. *Br J Pharmacol* 147:281-288.2006).
- Jerman JC, Gray J, Brough SJ, Ooi L, Owen D, Davis JB, Smart D (Comparison of effects of anandamide at recombinant and endogenous rat vanilloid receptors. *Br J Anaesth* 89:882-887.2002).
- Jhaveri MD, Elmes SJ, Kendall DA, Chapman V (Inhibition of peripheral vanilloid TRPV1 receptors reduces noxious heat-evoked responses of dorsal horn neurons in naive, carrageenan-inflamed and neuropathic rats. *Eur J Neurosci* 22:361-370.2005).
- Jhaveri MD, Elmes SJ, Richardson D, Barrett DA, Kendall DA, Mason R, Chapman V (Evidence for a novel functional role of cannabinoid CB receptors in the thalamus of neuropathic rats. *Eur J Neurosci* 27:1722-1730.2008a).
- Jhaveri MD, Richardson D, Chapman V (Endocannabinoid metabolism and uptake: novel targets for neuropathic and inflammatory pain. *Br J Pharmacol* 152:624-632.2007a).
- Jhaveri MD, Richardson D, Kendall DA, Barrett DA, Chapman V (Analgesic effects of fatty acid amide hydrolase inhibition in a rat model of neuropathic pain. *J Neurosci* 26:13318-13327.2006).
- Jhaveri MD, Richardson D, Robinson I, Garle MJ, Patel A, Sun Y, Sagar DR, Bennett AJ, Alexander SP, Kendall DA, Barrett DA, Chapman V (Inhibition of fatty acid amide hydrolase and cyclooxygenase-2 increases levels of endocannabinoid related molecules and produces analgesia via peroxisome proliferator-activated receptor-alpha in a model of inflammatory pain. *Neuropharmacology* 55:85-93.2008b).
- JJhaveri MD, Sagar DR, Elmes SJ, Kendall DA, Chapman V (Cannabinoid CB(2) Receptor-Mediated Anti-nociception in Models of Acute and Chronic Pain. *Molecular neurobiology* 36:26-35.2007b).
- Ji R, Samad T, Jin S, Schmoll R, Woolf C (p38 MAPK activation by NGF in primary sensory neurons after inflammation increases TRPV1 levels and maintains heat hyperalgesia. *Neuron* 36:57-68.2002a).
- Jin X, Gereau RWt (Acute p38-mediated modulation of tetrodotoxin-resistant sodium channels in mouse sensory neurons by tumor necrosis factor-alpha. *J Neurosci* 26:246-255.2006).
- Jin XH, Okamoto Y, Morishita J, Tsuboi K, Tonai T, Ueda N (Discovery and characterization of a Ca²⁺-independent phosphatidylethanolamine N-acyltransferase generating the anandamide precursor and its congeners. *J Biol Chem* 282:3614-3623.2007).
- Johns DG, Behm DJ, Walker DJ, Ao Z, Shapland EM, Daniels DA, Riddick M, Dowell S, Staton PC, Green P, Shabon U, Bao W, Aiyar N, Yue TL, Brown AJ, Morrison AD, Douglas SA (The novel endocannabinoid receptor GPR55 is activated by atypical cannabinoids but does not mediate their vasodilator effects. *Br J Pharmacol* 152:825-831.2007).
- Jonakait GM (Neural-immune interactions in sympathetic ganglia. *Trends Neurosci* 16:419-423.1993).
- Jordt SE, Bautista DM, Chuang HH, McKemy DD, Zygmunt PM, Hogestatt ED, Meng ID, Julius D (Mustard oils and cannabinoids excite sensory nerve fibres through the TRP channel ANKTM1. *Nature* 427:260-265.2004).
- Joseph EK, Levine JD (Caspase signalling in neuropathic and inflammatory pain in the rat. *Eur J Neurosci* 20:2896-2902.2004).

- Junger H, Sorkin LS (Nociceptive and inflammatory effects of subcutaneous TNF[alpha]. *Pain* 85:145-151.2000).
- Kalant H (Adverse effects of cannabis on health: an update of the literature since 1996. *Prog Neuropsychopharmacol Biol Psychiatry* 28:849-863.2004).
- Kalshen DA (Chemical model of osteoarthritis--a pharmacological evaluation. *J Rheumatol* 14 Spec No:130-131.1987).
- Karbarz MJ, Luo L, Chang L, Tham CS, Palmer JA, Wilson SJ, Wennerholm ML, Brown SM, Scott BP, Apodaca RL, Keith JM, Wu J, Breitenbucher JG, Chaplan SR, Webb M (Biochemical and biological properties of 4-(3-phenyl-[1,2,4] thiadiazol-5-yl)-piperazine-1-carboxylic acid phenylamide, a mechanism-based inhibitor of fatty acid amide hydrolase. *Anesth Analg* 108:316-329.2009).
- Karsak M, Gaffal E, Date R, Wang-Eckhardt L, Rehnelt J, Petrosino S, Starowicz K, Steuder R, Schlicker E, Cravatt B, Mechoulam R, Buettner R, Werner S, Di Marzo V, Tuting T, Zimmer A (Attenuation of allergic contact dermatitis through the endocannabinoid system. *Science* 316:1494-1497.2007).
- Kasai M, Mizumura K (Increase in spontaneous action potentials and sensitivity in response to norepinephrine in dorsal root ganglion neurons of adjuvant inflamed rats. *Neurosci Res* 39:109-113.2001).
- Kathuria S, Gaetani S, Fegley D, Valino F, Duranti A, Tontini A, Mor M, Tarzia G, La Rana G, Calignano A, Giustino A, Tattoli M, Palmery M, Cuomo V, Piomelli D (Modulation of anxiety through blockade of anandamide hydrolysis. *Nature Medicine* 9:76-81.2003a).
- Kathuria S, Gaetani S, Fegley D, Valino F, Duranti A, Tontini A, Mor M, Tarzia G, La Rana G, Calignano A, Giustino A, Tattoli M, Palmery M, Cuomo V, Piomelli D (Modulation of anxiety through blockade of anandamide hydrolysis. *Nat Med* 9:76-81.2003b).
- Kean WF, Kean R, Buchanan WW (Osteoarthritis: symptoms, signs and source of pain. *Inflammopharmacology* 12:3-31.2004).
- Kelly S, Chapman V (Selective cannabinoid CB1 receptor activation inhibits spinal nociceptive transmission in vivo. *J Neurophysiol* 86:3061-3064.2001).
- Kelly S, Chapman V (Spinal administration of capsazepine inhibits noxious evoked responses of dorsal horn neurons in non-inflamed and carrageenan inflamed rats. *Brain Res* 935:103-108.2002).
- Kelly S, Chapman V (Cannabinoid CB(1) receptor inhibition of mechanically evoked responses of spinal neurones in control rats, but not in rats with hindpaw inflammation. *Eur J Pharmacol* 474:209-216.2003).
- Kelly S, Dunham JP, Murray F, Read S, Donaldson LF, Lawson SN (2008) Nociceptors in MIA osteoarthritic knee joints : Spontaneous firing in C-fibres and increased mechanosensitivity of Adelta fibres. In: International Association for the Study of Pain 12th World Congress on Pain, p PW145 Glasgow, Scotland, U.K.
- Kelly S, Jhaveri MD, Sagar DR, Kendall DA, Chapman V (Activation of peripheral cannabinoid CB1 receptors inhibits mechanically evoked responses of spinal neurons in noninflamed rats and rats with hindpaw inflammation. *Eur J Neurosci* 18:2239-2243.2003).
- Khanolkar AD, Makriyannis A (Structure-activity relationships of anandamide, an endogenous cannabinoid ligand. *Life Sci* 65:607-616.1999).
- Khasabov SG, Rogers SD, Ghilardi JR, Peters CM, Mantyh PW, Simone DA (Spinal neurons that possess the substance P receptor are

- required for the development of central sensitization. *J Neurosci* 22:9086-9098.2002).
- Kidd BL (Osteoarthritis and joint pain. *Pain* 123:6-9.2006).
- Kidd BL, Urban LA (Mechanisms of inflammatory pain. *Br J Anaesth* 87:3-11.2001).
- Kim J, Alger BE (Inhibition of cyclooxygenase-2 potentiates retrograde endocannabinoid effects in hippocampus. *Nat Neurosci* 7:697-698.2004).
- Kim J, Isokawa M, Ledent C, Alger BE (Activation of muscarinic acetylcholine receptors enhances the release of endogenous cannabinoids in the hippocampus. *J Neurosci* 22:10182-10191.2002a).
- Kim SY, Bae JC, Kim JY, Lee HL, Lee KM, Kim DS, Cho HJ (Activation of p38 MAP kinase in the rat dorsal root ganglia and spinal cord following peripheral inflammation and nerve injury. *Neuroreport* 13:2483-2486.2002b).
- Kingsley PJ, Marnett LJ (Analysis of endocannabinoids by Ag⁺ coordination tandem mass spectrometry. *Anal Biochem* 314:8-15.2003).
- Kingsley PJ, Rouzer CA, Saleh S, Marnett LJ (Simultaneous analysis of prostaglandin glyceryl esters and prostaglandins by electrospray tandem mass spectrometry. *Anal Biochem* 343:203-211.2005).
- Klegeris A, Bissonnette CJ, McGeer PL (Reduction of human monocytic cell neurotoxicity and cytokine secretion by ligands of the cannabinoid-type CB2 receptor. *Br J Pharmacol* 139:775-786.2003).
- Kniss DA (Cyclooxygenases in reproductive medicine and biology. *J Soc Gynecol Investig* 6:285-292.1999).
- Kobayashi K, Imaizumi R, Sumichika H, Tanaka H, Goda M, Fukunari A, Komatsu H (Sodium iodoacetate-induced experimental osteoarthritis and associated pain model in rats. *J Vet Med Sci* 65:1195-1199.2003).
- Kohno T, Wang H, Amaya F, Brenner GJ, Cheng JK, Ji RR, Woolf CJ (Bradykinin enhances AMPA and NMDA receptor activity in spinal cord dorsal horn neurons by activating multiple kinases to produce pain hypersensitivity. *J Neurosci* 28:4533-4540.2008).
- Koller H, Thiem K, Siebler M (Tumour necrosis factor-alpha increases intracellular Ca²⁺ and induces a depolarization in cultured astroglial cells. *Brain* 119 (Pt 6):2021-2027.1996).
- Koltzenburg M, Torebjork HE, Wahren LK (Nociceptor modulated central sensitization causes mechanical hyperalgesia in acute chemogenic and chronic neuropathic pain. *Brain* 117 (Pt 3):579-591.1994).
- Kong SK, Fung KP, Choy YM, Lee CY (Slow increase in intranuclear and cytosolic free calcium concentrations in L929 cells is important in tumour necrosis factor-alpha-mediated cell death. *Oncology* 54:55-62.1997).
- Koplas PA, Rosenberg RL, Oxford GS (The role of calcium in the desensitization of capsaicin responses in rat dorsal root ganglion neurons. *J Neurosci* 17:3525-3537.1997).
- Koppel J, Bradshaw H, Goldberg TE, Khalili H, Marambaud P, Walker MJ, Pazos M, Gordon ML, Christen E, Davies P (Endocannabinoids in Alzheimer's disease and their impact on normative cognitive performance: a case-control and cohort study. *Lipids Health Dis* 8:2.2009).
- Kozak KR, Crews BC, Morrow JD, Wang LH, Ma YH, Weinander R, Jakobsson PJ, Marnett LJ (Metabolism of the endocannabinoids, 2-arachidonylglycerol and anandamide, into prostaglandin,

- thromboxane, and prostacyclin glycerol esters and ethanolamides. *J Biol Chem* 277:44877-44885.2002a).
- Kozak KR, Crews BC, Ray JL, Tai HH, Morrow JD, Marnett LJ (Metabolism of prostaglandin glycerol esters and prostaglandin ethanolamides in vitro and in vivo. *J Biol Chem* 276:36993-36998.2001a).
- Kozak KR, Gupta RA, Moody JS, Ji C, Boeglin WE, DuBois RN, Brash AR, Marnett LJ (15-Lipoxygenase metabolism of 2-arachidonylglycerol. Generation of a peroxisome proliferator-activated receptor alpha agonist. *J Biol Chem* 277:23278-23286.2002b).
- Kozak KR, Marnett LJ (Oxidative metabolism of endocannabinoids. *Prostaglandins Leukot Essent Fatty Acids* 66:211-220.2002).
- Kozak KR, Prusakiewicz JJ, Marnett LJ (Oxidative metabolism of endocannabinoids by COX-2. *Curr Pharm Des* 10:659-667.2004).
- Kozak KR, Prusakiewicz JJ, Rowlinson SW, Prudhomme DR, Marnett LJ (Amino acid determinants in cyclooxygenase-2 oxygenation of the endocannabinoid anandamide. *Biochemistry* 42:9041-9049.2003).
- Kozak KR, Prusakiewicz JJ, Rowlinson SW, Schneider C, Marnett LJ (Amino acid determinants in cyclooxygenase-2 oxygenation of the endocannabinoid 2-arachidonylglycerol. *J Biol Chem* 276:30072-30077.2001b).
- Kozak KR, Rowlinson SW, Marnett LJ (Oxygenation of the endocannabinoid, 2-arachidonylglycerol, to glyceryl prostaglandins by cyclooxygenase-2. *J Biol Chem* 275:33744-33749.2000).
- Kreitzer AC, Regehr WG (Retrograde inhibition of presynaptic calcium influx by endogenous cannabinoids at excitatory synapses onto Purkinje cells. *Neuron* 29:717-727.2001).
- Kumar RN, Chambers WA, Pertwee RG (Pharmacological actions and therapeutic uses of cannabis and cannabinoids. *Anaesthesia* 56:1059-1068.2001).
- Lam PM, Hainsworth AH, Smith GD, Owen DE, Davies J, Lambert DG (Activation of recombinant human TRPV1 receptors expressed in SH-SY5Y human neuroblastoma cells increases $[Ca^{2+}]_i$, initiates neurotransmitter release and promotes delayed cell death. *J Neurochem* 102:801-811.2007).
- Lam PM, McDonald J, Lambert DG (Characterization and comparison of recombinant human and rat TRPV1 receptors: effects of exo- and endocannabinoids. *Br J Anaesth* 94:649-656.2005).
- LaMotte RH, Shain CN, Simone DA, Tsai EF (Neurogenic hyperalgesia: psychophysical studies of underlying mechanisms. *J Neurophysiol* 66:190-211.1991).
- Lauckner JE, Jensen JB, Chen HY, Lu HC, Hille B, Mackie K (GPR55 is a cannabinoid receptor that increases intracellular calcium and inhibits M current. *Proceedings of the National Academy of Sciences of the United States of America* 105:2699-2704.2008).
- Le Bars D, Gozariu M, Cadden SW (Animal models of nociception. *Pharmacol Rev* 53:597-652.2001).
- Ledeen RW, Chakraborty G (Cytokines, signal transduction, and inflammatory demyelination: review and hypothesis. *Neurochem Res* 23:277-289.1998).
- Lee SY, Lee JH, Kang KK, Hwang SY, Choi KD, Oh U (Sensitization of vanilloid receptor involves an increase in the phosphorylated form of the channel. *Arch Pharm Res* 28:405-412.2005).
- Lembeck F, Popper H, Juan H (Release of prostaglandins by bradykinin as an intrinsic mechanism of its algescic effect. *Naunyn Schmiedeberg's Arch Pharmacol* 294:69-73.1976).

- Leon A, Buriani A, Dal Toso R, Fabris M, Romanello S, Aloe L, Levi-Montalcini R (Mast cells synthesize, store, and release nerve growth factor. *Proc Natl Acad Sci U S A* 91:3739-3743.1994).
- Lester G, McGowan J, Panagis J, Serrate-Sztejn S, Tyree B (Osteoarthritis, National Institutes of Health. National Institute of Arthritis and Musculoskeletal and Skin Diseases 06-4617.2002).
- Leung D, Saghatelian A, Simon GM, Cravatt BF (Inactivation of N-acyl phosphatidylethanolamine phospholipase D reveals multiple mechanisms for the biosynthesis of endocannabinoids. *Biochemistry* 45:4720-4726.2006).
- Levine JDR, D.B (1999) Peripheral mechanisms of Inflammatory Pain. In: *Textbook of Pain*, vol. 4 (Wall, P. D., Melzack, R, ed): Churchill Livingstone.
- Lewis M, Tartaglia LA, Lee A, Bennett GL, Rice GC, Wong GH, Chen EY, Goeddel DV (Cloning and expression of cDNAs for two distinct murine tumor necrosis factor receptors demonstrate one receptor is species specific. *Proc Natl Acad Sci U S A* 88:2830-2834.1991).
- Li S, Kaur PP, Chan V, Berney S (Use of tumor necrosis factor-alpha (TNF-alpha) antagonists infliximab, etanercept, and adalimumab in patients with concurrent rheumatoid arthritis and hepatitis B or hepatitis C: a retrospective record review of 11 patients. *Clin Rheumatol* 28:787-791.2009).
- Lichtman A, Leung D, Shelton C, Saghatelian A, Hardouin C, Boger D, Cravatt B (Reversible Inhibitors of Fatty Acid Amide Hydrolase That Promote Analgesia: Evidence for an Unprecedented Combination of Potency and Selectivity. *Journal of Pharmacology and Experimental Therapeutics* 311:441-448.2004a).
- Lichtman AH, Cook SA, Martin BR (Investigation of brain sites mediating cannabinoid-induced antinociception in rats: evidence supporting periaqueductal gray involvement. *J Pharmacol Exp Ther* 276:585-593.1996).
- Lichtman AH, Hawkins EG, Griffin G, Cravatt BF (Pharmacological activity of fatty acid amides is regulated, but not mediated, by fatty acid amide hydrolase in vivo. *J Pharmacol Exp Ther* 302:73-79.2002).
- Lichtman AH, Shelton CC, Advani T, Cravatt BF (Mice lacking fatty acid amide hydrolase exhibit a cannabinoid receptor-mediated phenotypic hypoalgesia. *Pain* 109:319-327.2004b).
- Ligresti A, Bisogno T, Matias I, De Petrocellis L, Cascio MG, Cosenza V, D'Argenio G, Scaglione G, Bifulco M, Sorrentini I, Di Marzo V (Possible endocannabinoid control of colorectal cancer growth. *Gastroenterology* 125:677-687.2003).
- Lindblad S, Hedfors E (Arthroscopic and immunohistologic characterization of knee joint synovitis in osteoarthritis. *Arthritis Rheum* 30:1081-1088.1987).
- Liu J, Wang L, Harvey-White J, Huang BX, Kim HY, Luquet S, Palmiter RD, Krystal G, Rai R, Mahadevan A, Razdan RK, Kunos G (Multiple pathways involved in the biosynthesis of anandamide. *Neuropharmacology* 54:1-7.2008).
- Liu J, Wang L, Harvey-White J, Osei-Hyiaman D, Razdan R, Gong Q, Chan AC, Zhou Z, Huang BX, Kim HY, Kunos G (A biosynthetic pathway for anandamide. *Proc Natl Acad Sci U S A* 103:13345-13350.2006).
- Lombard MC, Weil-Fugazza J, Ries C, Allard M (Unilateral joint inflammation induces bilateral and time-dependent changes in neuropeptide FF binding in the superficial dorsal horn of the rat

- spinal cord: implication of supraspinal descending systems. *Brain Res* 816:598-608.1999).
- Long JZ, Li WW, Booker L, Burston JJ, Kinsey SG, Schlosburg JE, Pavon FJ, Serrano AM, Selley DE, Parsons LH, Lichtman AH, Cravatt BF (Selective blockade of 2-arachidonoylglycerol hydrolysis produces cannabinoid behavioral effects. *Nature Chemical Biology* 5:37-44.2009).
- Lopshire JC, Nicol GD (The cAMP transduction cascade mediates the prostaglandin E2 enhancement of the capsaicin-elicited current in rat sensory neurons: whole-cell and single-channel studies. *J Neurosci* 18:6081-6092.1998).
- Loram LC, Fuller A, Fick LG, Cartmell T, Poole S, Mitchell D (Cytokine profiles during carrageenan-induced inflammatory hyperalgesia in rat muscle and hind paw. *J Pain* 8:127-136.2007).
- LoVerme J, Guzman M, Gaetani S, Piomelli D (Cold exposure stimulates synthesis of the bioactive lipid oleoylethanolamide in rat adipose tissue. *J Biol Chem* 281:22815-22818.2006a).
- LoVerme J, Russo R, La Rana G, Fu J, Farthing J, Mattace-Raso G, Meli R, Hohmann A, Calignano A, Piomelli D (Rapid broad-spectrum analgesia through activation of peroxisome proliferator-activated receptor-alpha. *J Pharmacol Exp Ther* 319:1051-1061.2006b).
- Lowry OH, Rosebrough NJ, Farr AL, Randall RJ (Protein measurement with the Folin phenol reagent. *J Biol Chem* 193:265-275.1951).
- Luo H, Cheng J, Han JS, Wan Y (Change of vanilloid receptor 1 expression in dorsal root ganglion and spinal dorsal horn during inflammatory nociception induced by complete Freund's adjuvant in rats. *Neuroreport* 15:655-658.2004).
- Maccarrone M, Attina M, Carboni A, Bari M, Finazzi-Agro A (Gas chromatography-mass spectrometry analysis of endogenous cannabinoids in healthy and tumoral human brain and human cells in culture. *J Neurochem* 76:594-601.2001).
- Maccarrone M, Bari M, Battista N, Finazzi-Agro A (Estrogen stimulates arachidonoyl ethanolamide release from human endothelial cells and platelet activation. *Blood* 100:4040-4048.2002).
- Maccarrone M, Rossi S, Bari M, De Chiara V, Fezza F, Musella A, Gasperi V, Prosperetti C, Bernardi G, Finazzi-Agro A, Cravatt BF, Centonze D (Anandamide inhibits metabolism and physiological actions of 2-arachidonoylglycerol in the striatum. *Nat Neurosci* 11:152-159.2008).
- Maccarrone M, Salvati S, Bari M, Finazzi A (Anandamide and 2-arachidonoylglycerol inhibit fatty acid amide hydrolase by activating the lipoxygenase pathway of the arachidonate cascade. *Biochem Biophys Res Commun* 278:576-583.2000).
- Maejima T, Hashimoto K, Yoshida T, Aiba A, Kano M (Presynaptic inhibition caused by retrograde signal from metabotropic glutamate to cannabinoid receptors. *Neuron* 31:463-475.2001a).
- Maejima T, Ohno-Shosaku T, Kano M (Endogenous cannabinoid as a retrograde messenger from depolarized postsynaptic neurons to presynaptic terminals. *Neurosci Res* 40:205-210.2001b).
- Maggi CA, Patacchini R, Tramontana M, Amann R, Giuliani S, Santicioli P (Similarities and differences in the action of resiniferatoxin and capsaicin on central and peripheral endings of primary sensory neurons. *Neuroscience* 37:531-539.1990).
- Maini R, St Clair EW, Breedveld F, Furst D, Kalden J, Weisman M, Smolen J, Emery P, Harriman G, Feldmann M, Lipsky P (Infliximab

- (chimeric anti-tumour necrosis factor alpha monoclonal antibody) versus placebo in rheumatoid arthritis patients receiving concomitant methotrexate: a randomised phase III trial. ATTRACT Study Group. *Lancet* 354:1932-1939.1999a).
- Maini RN, Taylor PC, Paleolog E, Charles P, Ballara S, Brennan FM, Feldmann M (Anti-tumour necrosis factor specific antibody (infliximab) treatment provides insights into the pathophysiology of rheumatoid arthritis. *Ann Rheum Dis* 58 Suppl 1:156-60.1999b).
- Maione S, Bisogno T, de Novellis V, Palazzo E, Cristino L, Valenti M, Petrosino S, Guglielmotti V, Rossi F, Di Marzo V (Elevation of endocannabinoid levels in the ventrolateral periaqueductal grey through inhibition of fatty acid amide hydrolase affects descending nociceptive pathways via both cannabinoid receptor type 1 and transient receptor potential vanilloid type-1 receptors. *J Pharmacol Exp Ther* 316:969-982.2006).
- Maione S, De Petrocellis L, de Novellis V, Moriello AS, Petrosino S, Palazzo E, Rossi FS, Woodward DF, Di Marzo V (Analgesic actions of N-arachidonoyl-serotonin, a fatty acid amide hydrolase inhibitor with antagonistic activity at vanilloid TRPV1 receptors. *Br J Pharmacol* 150:766-781.2007).
- Malan TP, Jr., Ibrahim MM, Deng H, Liu Q, Mata HP, Vanderah T, Porreca F, Makriyannis A (CB2 cannabinoid receptor-mediated peripheral antinociception. *Pain* 93:239-245.2001).
- Malcangio M, Bowery NG (Spinal cord SP release and hyperalgesia in monoarthritic rats: involvement of the GABAB receptor system. *Br J Pharmacol* 113:1561-1566.1994).
- Malcangio M, Bowery NG (GABA and its receptors in the spinal cord. *Trends Pharmacol Sci* 17:457-462.1996).
- Mankin HJ, Lippiello L (Biochemical and metabolic abnormalities in articular cartilage from osteo-arthritic human hips. *J Bone Joint Surg Am* 52:424-434.1970).
- Marchand F, Perretti M, McMahon SB (Role of the immune system in chronic pain. *Nat Rev Neurosci* 6:521-532.2005).
- Maresz K, Carrier EJ, Ponomarev ED, Hillard CJ, Dittel BN (Modulation of the cannabinoid CB2 receptor in microglial cells in response to inflammatory stimuli. *J Neurochem* 95:437-445.2005).
- Marini P, Moriello AS, Cristino L, Palmery M, De Petrocellis L, Di Marzo V (Cannabinoid CB1 receptor elevation of intracellular calcium in neuroblastoma SH-SY5Y cells: Interactions with muscarinic and delta-opioid receptors. *Biochim Biophys Acta*.2009).
- Martin WJ, Coffin PO, Attias E, Balinsky M, Tsou K, Walker JM (Anatomical basis for cannabinoid-induced antinociception as revealed by intracerebral microinjections. *Brain Res* 822:237-242.1999).
- Masferrer JL, Zweifel BS, Seibert K, Needleman P (Selective regulation of cellular cyclooxygenase by dexamethasone and endotoxin in mice. *J Clin Invest* 86:1375-1379.1990).
- Massa F, Marsicano G, Hermann H, Cannich A, Monory K, Cravatt BF, Ferri GL, Sibaev A, Storr M, Lutz B (The endogenous cannabinoid system protects against colonic inflammation. *J Clin Invest* 113:1202-1209.2004).
- Mathy-Hartert M, Deby-Dupont GP, Reginster JY, Ayache N, Pujol JP, Henrotin YE (Regulation by reactive oxygen species of interleukin-1beta, nitric oxide and prostaglandin E(2) production by human chondrocytes. *Osteoarthritis Cartilage* 10:547-555.2002).

- Matias I, Chen J, De Petrocellis L, Bisogno T, Ligresti A, Fezza F, Krauss AH, Shi L, Protzman CE, Li C, Liang Y, Nieves AL, Kedzie KM, Burk RM, Di Marzo V, Woodward DF (Prostaglandin ethanolamides (prostamides): in vitro pharmacology and metabolism. *J Pharmacol Exp Ther* 309:745-757.2004).
- Matias I, Gonthier MP, Petrosino S, Docimo L, Capasso R, Hoareau L, Monteleone P, Roche R, Izzo AA, Di Marzo V (Role and regulation of acylethanolamides in energy balance: focus on adipocytes and beta-cells. *Br J Pharmacol* 152:676-690.2007).
- Matias I, Pochard P, Orlando P, Salzet M, Pestel J, Di Marzo V (Presence and regulation of the endocannabinoid system in human dendritic cells. *Eur J Biochem* 269:3771-3778.2002).
- Matsuda LA, Lolait SJ, Brownstein MJ, Young AC, Bonner TI (Structure of a Cannabinoid Receptor and Functional Expression of the Cloned Cdna. *Nature* 346:561-564.1990).
- Maubach KA, Grundy D (The role of prostaglandins in the bradykinin-induced activation of serosal afferents of the rat jejunum in vitro. *J Physiol* 515 (Pt 1):277-285.1999).
- Mbvundula EC, Bunning RA, Rainsford KD (Arthritis and cannabinoids: HU-210 and Win-55,212-2 prevent IL-1 α -induced matrix degradation in bovine articular chondrocytes in-vitro. *J Pharm Pharmacol* 58:351-358.2006).
- McLarnon JG, Franciosi S, Wang X, Bae JH, Choi HB, Kim SU (Acute actions of tumor necrosis factor- α on intracellular Ca²⁺ and K⁺ currents in human microglia. *Neuroscience* 104:1175-1184.2001).
- McNearney T, Baethge BA, Cao S, Alam R, Lisse JR, Westlund KN (Excitatory amino acids, TNF- α , and chemokine levels in synovial fluids of patients with active arthropathies. *Clinical & Experimental Immunology*137(3):621-7.2004).
- Mechoulam R, Ben-Shabat S, Hanus L, Ligumsky M, Kaminski NE, Schatz AR, Gopher A, Almog S, Martin BR, Compton DR, et al. (Identification of an endogenous 2-monoglyceride, present in canine gut, that binds to cannabinoid receptors. *Biochem Pharmacol* 50:83-90.1995).
- Mechoulam R, Gaoni Y (The absolute configuration of delta-1-tetrahydrocannabinol, the major active constituent of hashish. *Tetrahedron Lett* 12:1109-1111.1967).
- Melnikova I (Future of COX2 inhibitors. *Nat Rev Drug Discov* 4:453-454.2005).
- Melzack R, Wall PD (Pain mechanisms: a new theory. *Science* 150:971-979.1965).
- Meng ID, Manning BH, Martin WJ, Fields HL (An analgesia circuit activated by cannabinoids. *Nature* 395:381-383.1998).
- Meng J, Ovsepian SV, Wang J, Pickering M, Sasse A, Aoki KR, Lawrence GW, Dolly JO (Activation of TRPV1 mediates calcitonin gene-related peptide release, which excites trigeminal sensory neurons and is attenuated by a retargeted botulinum toxin with anti-nociceptive potential. *J Neurosci* 29:4981-4992.2009).
- Merskey HB, N. (ed.) (1994) Classification of chronic pain. Seattle: IASP press.
- Meyer RA, Ringkamp, M., Campbell, J.N. & Raja, S.N. (2006) Peripheral mechanisms of cutaneous nociception. In: Wall and Melzack's Textbook of Pain(McMahon, S. B. K., M., ed), pp 3-35: Elsevier Churchill Livingstone.

- Millan MJ (The induction of pain: an integrative review. *Prog Neurobiol* 57:1-164.1999).
- Millan MJ (Descending control of pain. *Prog Neurobiol* 66:355-474.2002).
- Millns PJ, Chapman V, Kendall DA (Cannabinoid inhibition of the capsaicin-induced calcium response in rat dorsal root ganglion neurones. *Br J Pharmacol* 132:969-971.2001).
- Millns PJ, Chimenti M, Ali N, Ryland E, de Lago E, Fernandez-Ruiz J, Chapman V, Kendall DA (Effects of inhibition of fatty acid amide hydrolase vs. the anandamide membrane transporter on TRPV1-mediated calcium responses in adult DRG neurons; the role of CB receptors. *Eur J Neurosci* 24:3489-3495.2006).
- Mitchell JM, Lowe D, Fields HL (The contribution of the rostral ventromedial medulla to the antinociceptive effects of systemic morphine in restrained and unrestrained rats. *Neuroscience* 87:123-133.1998).
- Mitchell PG, Magna HA, Reeves LM, Lopresti-Morrow LL, Yocum SA, Rosner PJ, Geoghegan KF, Hambor JE (Cloning, expression, and type II collagenolytic activity of matrix metalloproteinase-13 from human osteoarthritic cartilage. *J Clin Invest* 97:761-768.1996).
- Mitrirattanakul S, Ramakul N, Guerrero AV, Matsuka Y, Ono T, Iwase H, Mackie K, Faull KF, Spigelman I (Site-specific increases in peripheral cannabinoid receptors and their endogenous ligands in a model of neuropathic pain. *Pain* 126:102-114.2006).
- Mizushima T, Obata K, Yamanaka H, Dai Y, Fukuoka T, Tokunaga A, Mashimo T, Noguchi K (Activation of p38 MAPK in primary afferent neurons by noxious stimulation and its involvement in the development of thermal hyperalgesia. *Pain* 113:51-60.2005).
- Moalem G, Tracey DJ (Immune and inflammatory mechanisms in neuropathic pain. *Brain Res Brain Res Rev* 51:240-264.2006).
- Molliver DC, Wright DE, Leitner ML, Parsadanian AS, Doster K, Wen D, Yan Q, Snider WD (IB4-binding DRG neurons switch from NGF to GDNF dependence in early postnatal life. *Neuron* 19:849-861.1997).
- Morrison DL, Yee A, Paddon HB, Vilimek D, Aebersold R, Pelech SL (Regulation of the meiosis-inhibited protein kinase, a p38(MAPK) isoform, during meiosis and following fertilization of seastar oocytes. *J Biol Chem* 275:34236-34244.2000).
- Nackley AG, Suplita RL, 2nd, Hohmann AG (A peripheral cannabinoid mechanism suppresses spinal fos protein expression and pain behavior in a rat model of inflammation. *Neuroscience* 117:659-670.2003).
- Naef M, Curatolo M, Petersen-Felix S, Arendt-Nielsen L, Zbinden A, Brenneisen R (The analgesic effect of oral delta-9-tetrahydrocannabinol (THC), morphine, and a THC-morphine combination in healthy subjects under experimental pain conditions. *Pain* 105:79-88.2003).
- Nagy I, Santha P, Jancso G, Urban L (The role of the vanilloid (capsaicin) receptor (TRPV1) in physiology and pathology. *Eur J Pharmacol* 500:351-369.2004).
- Narang S, Gibson D, Wasan AD, Ross EL, Michna E, Nedeljkovic SS, Jamison RN (Efficacy of dronabinol as an adjuvant treatment for chronic pain patients on opioid therapy. *J Pain* 9:254-264.2008).
- Narumiya S, FitzGerald GA (Genetic and pharmacological analysis of prostanoid receptor function. *J Clin Invest* 108:25-30.2001).
- Narumiya S, Sugimoto Y, Ushikubi F (Prostanoid receptors: structures, properties, and functions. *Physiol Rev* 79:1193-1226.1999).

- Neugebauer V, Lucke T, Schaible HG (N-methyl-D-aspartate (NMDA) and non-NMDA receptor antagonists block the hyperexcitability of dorsal horn neurons during development of acute arthritis in rat's knee joint. *Journal of neurophysiology* 70:1365-1377.1993).
- Nicol GD, Lopshire JC, Pafford CM (Tumor necrosis factor enhances the capsaicin sensitivity of rat sensory neurons. *J Neurosci* 17:975-982.1997).
- Niforatos W, Zhang XF, Lake MR, Walter KA, Neelands T, Holzman TF, Scott VE, Faltynek CR, Moreland RB, Chen J (Activation of TRPA1 channels by the fatty acid amide hydrolase inhibitor 3'-carbamoylbiphenyl-3-yl cyclohexylcarbamate (URB597). *Mol Pharmacol* 71:1209-1216.2007).
- Nishimura M, Segami N, Kaneyama K, Suzuki T, Miyamaru M (Relationships between pain-related mediators and both synovitis and joint pain in patients with internal derangements and osteoarthritis of the temporomandibular joint. *Oral Surg Oral Med Oral Pathol Oral Radiol Endod* 94:328-332.2002).
- Noga M, Sucharski F, Suder P, Silberring J (A practical guide to nano-LC troubleshooting. *J Sep Sci* 30:2179-2189.2007).
- Nordling C, Karlsson-Parra A, Jansson L, Holmdahl R, Klareskog L (Characterization of a spontaneously occurring arthritis in male DBA/1 mice. *Arthritis Rheum* 35:717-722.1992).
- Numazaki M, Tominaga T, Takeuchi K, Murayama N, Toyooka H, Tominaga M (Structural determinant of TRPV1 desensitization interacts with calmodulin. *Proc Natl Acad Sci U S A* 100:8002-8006.2003).
- Nurmikko TJ, Serpell MG, Hoggart B, Toomey PJ, Morlion BJ, Haines D (Sativex successfully treats neuropathic pain characterised by allodynia: a randomised, double-blind, placebo-controlled clinical trial. *Pain* 133:210-220.2007).
- Nyilas R, Gregg LC, Mackie K, Watanabe M, Zimmer A, Hohmann AG, Katona I (Molecular architecture of endocannabinoid signaling at nociceptive synapses mediating analgesia. *Eur J Neurosci* 29:1964-1978.2009).
- O'Sullivan SE (Cannabinoids go nuclear: evidence for activation of peroxisome proliferator-activated receptors. *Br J Pharmacol* 152:576-582.2007).
- Ohno-Shosaku T, Hashimoto-dani Y, Maejima T, Kano M (Calcium signaling and synaptic modulation: regulation of endocannabinoid-mediated synaptic modulation by calcium. *Cell Calcium* 38:369-374.2005).
- Ohno-Shosaku T, Maejima T, Kano M (Endogenous cannabinoids mediate retrograde signals from depolarized postsynaptic neurons to presynaptic terminals. *Neuron* 29:729-738.2001).
- Ohno-Shosaku T, Matsui M, Fukudome Y, Shosaku J, Tsubokawa H, Taketo MM, Manabe T, Kano M (Postsynaptic M1 and M3 receptors are responsible for the muscarinic enhancement of retrograde endocannabinoid signalling in the hippocampus. *Eur J Neurosci* 18:109-116.2003).
- Ohno-Shosaku T, Shosaku J, Tsubokawa H, Kano M (Cooperative endocannabinoid production by neuronal depolarization and group I metabotropic glutamate receptor activation. *Eur J Neurosci* 15:953-961.2002).
- Oka S, Wakui J, Ikeda S, Yanagimoto S, Kishimoto S, Gokoh M, Nasui M, Sugiura T (Involvement of the cannabinoid CB2 receptor and its

- endogenous ligand 2-arachidonoylglycerol in oxazolone-induced contact dermatitis in mice. *J Immunol* 177:8796-8805.2006).
- Okamoto Y, Morishita J, Wang J, Schmid PC, Krebsbach RJ, Schmid HH, Ueda N (Mammalian cells stably overexpressing N-acylphosphatidylethanolamine-hydrolysing phospholipase D exhibit significantly decreased levels of N-acylphosphatidylethanolamines. *Biochem J* 389:241-247.2005).
- Olah Z, Karai L, Iadarola MJ (Anandamide activates vanilloid receptor 1 (VR1) at acidic pH in dorsal root ganglia neurons and cells ectopically expressing VR1. *J Biol Chem* 276:31163-31170.2001).
- Orio L, Edwards S, George O, Parsons LH, Koob GF (A role for the endocannabinoid system in the increased motivation for cocaine in extended-access conditions. *J Neurosci* 29:4846-4857.2009).
- Pacher P, Batkai S, Kunos G (The endocannabinoid system as an emerging target of pharmacotherapy. *Pharmacol Rev* 58:389-462.2006).
- Parada CA, Yeh JJ, Joseph EK, Levine JD (Tumor necrosis factor receptor type-1 in sensory neurons contributes to induction of chronic enhancement of inflammatory hyperalgesia in rat. *Eur J Neurosci* 17:1847-1852.2003).
- Parris JR, Cobban HJ, Littlejohn AF, MacEwan DJ, Nixon GF (Tumour necrosis factor-alpha activates a calcium sensitization pathway in guinea-pig bronchial smooth muscle. *J Physiol* 518 (Pt 2):561-569.1999).
- Patrignani P, Tacconelli S, Sciulli MG, Capone ML (New insights into COX-2 biology and inhibition. *Brain Res Brain Res Rev* 48:352-359.2005).
- Pelletier JP, Lascau-Coman V, Jovanovic D, Fernandes JC, Manning P, Connor JR, Currie MG, Martel-Pelletier J (Selective inhibition of inducible nitric oxide synthase in experimental osteoarthritis is associated with reduction in tissue levels of catabolic factors. *J Rheumatol* 26:2002-2014.1999).
- Perkins MN, Kelly D (Interleukin-1 beta induced-desArg9bradykinin-mediated thermal hyperalgesia in the rat. *Neuropharmacology* 33:657-660.1994).
- Pertwee RG (Cannabinoid receptors and pain. *Prog Neurobiol* 63:569-611.2001).
- Pertwee RG (The pharmacology of cannabinoid receptors and their ligands: an overview. *Int J Obes (Lond)* 30 Suppl 1:S13-18.2006).
- Petersen-Felix S, Curatolo M (Neuroplasticity--an important factor in acute and chronic pain. *Swiss Med Wkly* 132:273-278.2002).
- Petrosino S, Palazzo E, de Novellis V, Bisogno T, Rossi F, Maione S, Di Marzo V (Changes in spinal and supraspinal endocannabinoid levels in neuropathic rats. *Neuropharmacology* 28:28.2006).
- Petrosino S, Palazzo E, de Novellis V, Bisogno T, Rossi F, Maione S, Di Marzo V (Changes in spinal and supraspinal endocannabinoid levels in neuropathic rats. *Neuropharmacology* 52:415-422.2007).
- Piomelli D (The molecular logic of endocannabinoid signalling. *Nat Rev Neurosci* 4:873-884.2003).
- Piomelli D, Beltramo M, Giuffrida A, Stella N (Endogenous cannabinoid signaling isotope dilution GC/MS determination of anandamide and other fatty acylethanolamides in rat blood plasma. *Neurobiol Dis* 5:462-473.1998).
- Piomelli D, Tarzia G, Duranti A, Tontini A, Mor M, Compton TR, Dasse O, Monaghan EP, Parrott JA, Putman D (Pharmacological profile of the

- selective FAAH inhibitor KDS-4103 (URB597). *CNS Drug Rev* 12:21-38.2006).
- Pitchford S, Levine JD (Prostaglandins sensitize nociceptors in cell culture. *Neurosci Lett* 132:105-108.1991).
- Pollock J, McFarlane SM, Connell MC, Zehavi U, Vandenabeele P, MacEwan DJ, Scott RH (TNF-alpha receptors simultaneously activate Ca²⁺ mobilisation and stress kinases in cultured sensory neurones. *Neuropharmacology* 42:93-106.2002).
- Pomonis JD, Boulet JM, Gottshall SL, Phillips S, Sellers R, Bunton T, Walker K (Development and pharmacological characterization of a rat model of osteoarthritis pain. *Pain* 114:339-346.2005).
- Porcella A, Marchese G, Casu MA, Rocchitta A, Lai ML, Gessa GL, Pani L (Evidence for functional CB1 cannabinoid receptor expressed in the rat thyroid. *European Journal of Endocrinology* 147:255-261.2002).
- Porter AC, Sauer JM, Knierman MD, Becker GW, Berna MJ, Bao J, Nomikos GG, Carter P, Bymaster FP, Leese AB, Felder CC (Characterization of a novel endocannabinoid, virodhamine, with antagonist activity at the CB1 receptor. *J Pharmacol Exp Ther* 301:1020-1024.2002).
- Premkumar LS, Ahern GP (Induction of vanilloid receptor channel activity by protein kinase C. *Nature* 408:985-990.2000).
- Prentiss D, Power R, Balmas G, Tzuang G, Israelski DM (Patterns of marijuana use among patients with HIV/AIDS followed in a public health care setting. *J Acquir Immune Defic Syndr* 35:38-45.2004).
- Price TJ, Helesic G, Parghi D, Hargreaves KM, Flores CM (The neuronal distribution of cannabinoid receptor type 1 in the trigeminal ganglion of the rat. *Neuroscience* 120:155-162.2003).
- Pritzker KP, Gay S, Jimenez SA, Ostergaard K, Pelletier JP, Revell PA, Salter D, van den Berg WB (Osteoarthritis cartilage histopathology: grading and staging. *Osteoarthritis Cartilage* 14:13-29.2006).
- Prochazkova M, Zanvit P, Dolezal T, Prokesova L, Krsiak M (Increased gene expression and production of spinal cyclooxygenase 1 and 2 during experimental osteoarthritis pain. *Physiol Res* 58:419-425.2009).
- Pulichino AM, Rowland S, Wu T, Clark P, Xu D, Mathieu MC, Riendeau D, Audoly LP (Prostacyclin antagonism reduces pain and inflammation in rodent models of hyperalgesia and chronic arthritis. *J Pharmacol Exp Ther* 319:1043-1050.2006).
- Racz I, Nadal X, Alferink J, Banos JE, Rehnelt J, Martin M, Pintado B, Gutierrez-Adan A, Sanguino E, Manzanares J, Zimmer A, Maldonado R (Crucial role of CB(2) cannabinoid receptor in the regulation of central immune responses during neuropathic pain. *J Neurosci* 28:12125-12135.2008).
- Rakhshan F, Day TA, Blakely RD, Barker EL (Carrier-mediated uptake of the endogenous cannabinoid anandamide in RBL-2H3 cells. *J Pharmacol Exp Ther* 292:960-967.2000).
- Ralevic V, Kendall DA, Jerman JC, Middlemiss DN, Smart D (Cannabinoid activation of recombinant and endogenous vanilloid receptors. *Eur J Pharmacol* 424:211-219.2001).
- Rankin EC, Choy EH, Kassimos D, Kingsley GH, Sopwith AM, Isenberg DA, Panayi GS (The therapeutic effects of an engineered human anti-tumour necrosis factor alpha antibody (CDP571) in rheumatoid arthritis. *Br J Rheumatol* 34:334-342.1995).

- Rao P, Knaus EE (Evolution of nonsteroidal anti-inflammatory drugs (NSAIDs): cyclooxygenase (COX) inhibition and beyond. *J Pharm Pharm Sci* 11:81s-110s.2008).
- Rathee PK, Distler C, Obreja O, Neuhuber W, Wang GK, Wang SY, Nau C, Kress M (PKA/AKAP/VR-1 module: A common link of Gs-mediated signaling to thermal hyperalgesia. *J Neurosci* 22:4740-4745.2002).
- Reboul P, Pelletier JP, Tardif G, Cloutier JM, Martel-Pelletier J (The new collagenase, collagenase-3, is expressed and synthesized by human chondrocytes but not by synoviocytes. A role in osteoarthritis. *J Clin Invest* 97:2011-2019.1996).
- Rice AS, Farquhar-Smith WP, Nagy I (Endocannabinoids and pain: spinal and peripheral analgesia in inflammation and neuropathy. *Prostaglandins Leukot Essent Fatty Acids* 66:243-256.2002).
- Richardson D, Ortori CA, Chapman V, Kendall DA, Barrett DA (Quantitative profiling of endocannabinoids and related compounds in rat brain using liquid chromatography-tandem electrospray ionization mass spectrometry. *Anal Biochem* 360:216-226.2007).
- Richardson D, Pearson RG, Kurian N, Latif ML, Garle MJ, Barrett DA, Kendall DA, Scammell BE, Reeve AJ, Chapman V (Characterisation of the cannabinoid receptor system in synovial tissue and fluid in patients with osteoarthritis and rheumatoid arthritis. *Arthritis Res Ther* 10:R43.2008).
- Richardson JD, Aanonsen L, Hargreaves KM (Hypoactivity of the spinal cannabinoid system results in NMDA-dependent hyperalgesia. *J Neurosci* 18:451-457.1998a).
- Richardson JD, Kilo S, Hargreaves KM (Cannabinoids reduce hyperalgesia and inflammation via interaction with peripheral CB1 receptors. *Pain* 75:111-119.1998b).
- Richardson JD, Vasko MR (Cellular mechanisms of neurogenic inflammation. *J Pharmacol Exp Ther* 302:839-845.2002).
- Rockwell CE, Raman P, Kaplan BL, Kaminski NE (A COX-2 metabolite of the endogenous cannabinoid, 2-arachidonyl glycerol, mediates suppression of IL-2 secretion in activated Jurkat T cells. *Biochem Pharmacol* 76:353-361.2008).
- Rockwell CE, Snider NT, Thompson JT, Vanden Heuvel JP, Kaminski NE (Interleukin-2 suppression by 2-arachidonyl glycerol is mediated through peroxisome proliferator-activated receptor gamma independently of cannabinoid receptors 1 and 2. *Mol Pharmacol* 70:101-111.2006).
- Rodriguez de Fonseca F, Navarro M, Gomez R, Escuredo L, Nava F, Fu J, Murillo-Rodriguez E, Giuffrida A, LoVerme J, Gaetani S, Kathuria S, Gall C, Piomelli D (An anorexic lipid mediator regulated by feeding. *Nature* 414:209-212.2001).
- Rog DJ, Nurmikko TJ, Young CA (Oromucosal delta9-tetrahydrocannabinol/cannabidiol for neuropathic pain associated with multiple sclerosis: an uncontrolled, open-label, 2-year extension trial. *Clin Ther* 29:2068-2079.2007).
- Romero-Sandoval A, Natile-McMenemy N, DeLeo JA (Spinal microglial and perivascular cell cannabinoid receptor type 2 activation reduces behavioral hypersensitivity without tolerance after peripheral nerve injury. *Anesthesiology* 108:722-734.2008).
- Ross RA (The enigmatic pharmacology of GPR55. *Trends Pharmacol Sci* 30:156-163.2009).
- Ross RA, Gibson TM, Brockie HC, Leslie M, Pashmi G, Craib SJ, Di Marzo V, Pertwee RG (Structure-activity relationship for the endogenous

- cannabinoid, anandamide, and certain of its analogues at vanilloid receptors in transfected cells and vas deferens. *Br J Pharmacol* 132:631-640.2001).
- Russo R, Loverme J, La Rana G, Compton T, Parrot J, Duranti A, Tontini A, Mor M, Tarzia G, Calignano A, Piomelli D (The fatty-acid amide hydrolase inhibitor URB597 (cyclohexyl carbamic acid 3'-carbamoyl-biphenyl-3-yl ester) reduces neuropathic pain after oral administration in mice. *J Pharmacol Exp Ther* 322:236-242.2007a).
- Russo R, LoVerme J, La Rana G, D'Agostino G, Sasso O, Calignano A, Piomelli D (Synergistic antinociception by the cannabinoid receptor agonist anandamide and the PPAR-alpha receptor agonist GW7647. *Eur J Pharmacol* 566:117-119.2007b).
- Ryberg E, Larsson N, Sjogren S, Hjorth S, Hermansson NO, Leonova J, Elebring T, Nilsson K, Drmota T, Greasley PJ (The orphan receptor GPR55 is a novel cannabinoid receptor. *Br J Pharmacol* 152:1092-1101.2007).
- Ryu S, Liu B, Qin F (Low pH potentiates both capsaicin binding and channel gating of VR1 receptors. *J Gen Physiol* 122:45-61.2003).
- Sagar DR, Kelly S, Millns PJ, O'Shaughnessey C T, Kendall DA, Chapman V (Inhibitory effects of CB1 and CB2 receptor agonists on responses of DRG neurons and dorsal horn neurons in neuropathic rats. *Eur J Neurosci* 22:371-379.2005).
- Sagar DR, Kendall DA, Chapman V (Inhibition of fatty acid amide hydrolase produces PPAR-alpha-mediated analgesia in a rat model of inflammatory pain. *Br J Pharmacol* 155:1297-1306.2008).
- Samad TA, Moore KA, Sapirstein A, Billet S, Allchorne A, Poole S, Bonventre JV, Woolf CJ (Interleukin-1beta-mediated induction of Cox-2 in the CNS contributes to inflammatory pain hypersensitivity. *Nature* 410:471-475.2001).
- Sang N, Zhang J, Chen C (PGE2 glycerol ester, a COX-2 oxidative metabolite of 2-arachidonoyl glycerol, modulates inhibitory synaptic transmission in mouse hippocampal neurons. *J Physiol* 572:735-745.2006).
- Sang N, Zhang J, Chen C (COX-2 oxidative metabolite of endocannabinoid 2-AG enhances excitatory glutamatergic synaptic transmission and induces neurotoxicity. *J Neurochem* 102:1966-1977.2007).
- Sanghi S, MacLaughlin EJ, Jewell CW, Chaffer S, Naus PJ, Watson LE, Dostal DE (Cyclooxygenase-2 inhibitors: a painful lesson. *Cardiovasc Hematol Disord Drug Targets* 6:85-100.2006).
- Sarzi-Puttini P, Cimmino MA, Scarpa R, Caporali R, Parazzini F, Zaninelli A, Atzeni F, Canesi B (Osteoarthritis: An Overview of the Disease and Its Treatment Strategies. *Seminars in Arthritis and Rheumatism* 35:1-10.2005).
- Sasamura T, Kuraishi Y (Peripheral and central actions of capsaicin and VR1 receptor. *Jpn J Pharmacol* 80:275-280.1999).
- Sauer SK, Schafer D, Kress M, Reeh PW (Stimulated prostaglandin E2 release from rat skin, in vitro. *Life Sci* 62:2045-2055.1998).
- Schafers M, Geis C, Brors D, Yaksh TL, Sommer C (Anterograde Transport of Tumor Necrosis Factor-alpha in the Intact and Injured Rat Sciatic Nerve. *J Neurosci* 22:536-545.2002).
- Schafers M, Geis C, Svensson CI, Luo ZD, Sommer C (Selective increase of tumour necrosis factor-alpha in injured and spared myelinated primary afferents after chronic constrictive injury of rat sciatic nerve. *European Journal of Neuroscience* 17:791-804.2003a).

- Schafers M, Svensson CI, Sommer C, Sorkin LS (Tumor necrosis factor- α induces mechanical allodynia after spinal nerve ligation by activation of p38 MAPK in primary sensory neurons. *J Neurosci* 23:2517-2521.2003b).
- Schaible HG, Grubb BD (Afferent and spinal mechanisms of joint pain. *Pain* 55:5-54.1993).
- Schaible HG, Schmidt RF (Time course of mechanosensitivity changes in articular afferents during a developing experimental arthritis. *J Neurophysiol* 60:2180-2195.1988).
- Schicho R, Florian W, Liebmann I, Holzer P, Lippe IT (Increased expression of TRPV1 receptor in dorsal root ganglia by acid insult of the rat gastric mucosa. *Eur J Neurosci* 19:1811-1818.2004).
- Schmid PC, Krebsbach RJ, Perry SR, Dettmer TM, Maasson JL, Schmid HH (Occurrence and postmortem generation of anandamide and other long-chain N-acylethanolamines in mammalian brain. *FEBS Lett* 375:117-120.1995).
- Schmid PC, Reddy PV, Natarajan V, Schmid HH (Metabolism of N-acylethanolamine phospholipids by a mammalian phosphodiesterase of the phospholipase D type. *J Biol Chem* 258:9302-9306.1983).
- Schmid PC, Schwartz KD, Smith CN, Krebsbach RJ, Berdyshev EV, Schmid HH (A sensitive endocannabinoid assay. The simultaneous analysis of N-acylethanolamines and 2-monoacylglycerols. *Chem Phys Lipids* 104:185-191.2000).
- Schmid PC, Zuzarte-Augustin ML, Schmid HH (Properties of rat liver N-acylethanolamine amidohydrolase. *J Biol Chem* 260:14145-14149.1985).
- Schmidt R, Schmelz M, Forster C, Ringkamp M, Torebjork E, Handwerker H (Novel classes of responsive and unresponsive C nociceptors in human skin. *J Neurosci* 15:333-341.1995).
- Schmidt R, Schmelz M, Ringkamp M, Handwerker HO, Torebjork HE (Innervation territories of mechanically activated C nociceptor units in human skin. *J Neurophysiol* 78:2641-2648.1997).
- Schmidt R, Schmelz M, Torebjork HE, Handwerker HO (Mechano-insensitive nociceptors encode pain evoked by tonic pressure to human skin. *Neuroscience* 98:793-800.2000).
- Schreiber D, Harffinger S, Nolden BM, Gerth CW, Jaehde U, Schomig E, Klosterkötter J, Giuffrida A, Astarita G, Piomelli D, Markus Leweke F (Determination of anandamide and other fatty acyl ethanolamides in human serum by electrospray tandem mass spectrometry. *Anal Biochem* 361:162-168.2007).
- Schuelert N, McDougall JJ (Cannabinoid-mediated antinociception is enhanced in rat osteoarthritic knees. *Arthritis Rheum* 58:145-153.2008).
- Scott DA, Wright CE, Angus JA (Evidence that CB-1 and CB-2 cannabinoid receptors mediate antinociception in neuropathic pain in the rat. *Pain* 109:124-131.2004).
- Seamon MJ (The legal status of medical marijuana. *Ann Pharmacother* 40:2211-2215.2006).
- Seybold VS, Jia YP, Abrahams LG (Cyclo-oxygenase-2 contributes to central sensitization in rats with peripheral inflammation. *Pain* 105:47-55.2003).
- Sherrington CS (1906) *The Integrative Action of the Nervous System*. New York: Scribner.

- Shubayev VI, Myers RR (Axonal transport of TNF-alpha in painful neuropathy: distribution of ligand tracer and TNF receptors. *J Neuroimmunol* 114:48-56.2001).
- Simon GM, Cravatt BF (Endocannabinoid biosynthesis proceeding through glycerophospho-N-acyl ethanolamine and a role for alpha/beta-hydrolase 4 in this pathway. *J Biol Chem* 281:26465-26472.2006).
- Simon GM, Cravatt BF (Anandamide biosynthesis catalyzed by the phosphodiesterase GDE1 and detection of glycerophospho-N-acyl ethanolamine precursors in mouse brain. *J Biol Chem* 283:9341-9349.2008).
- Sivilotti L, Woolf CJ (The contribution of GABAA and glycine receptors to central sensitization: disinhibition and touch-evoked allodynia in the spinal cord. *J Neurophysiol* 72:169-179.1994).
- Smale G, Bendele A, Horton WE, Jr. (Comparison of age-associated degeneration of articular cartilage in Wistar and Fischer 344 rats. *Lab Anim Sci* 45:191-194.1995).
- Smart D, Gunthorpe MJ, Jerman JC, Nasir S, Gray J, Muir AI, Chambers JK, Randall AD, Davis JB (The endogenous lipid anandamide is a full agonist at the human vanilloid receptor (hVR1). *Br J Pharmacol* 129:227-230.2000).
- Smith JA, Davis CL, Burgess GM (Prostaglandin E2-induced sensitization of bradykinin-evoked responses in rat dorsal root ganglion neurons is mediated by cAMP-dependent protein kinase A. *Eur J Neurosci* 12:3250-3258.2000).
- Smith WL, Dewitt DL (Prostaglandin endoperoxide H synthases-1 and -2. *Adv Immunol* 62:167-215.1996).
- Snider NT, Kornilov AM, Kent UM, Hollenberg PF (Anandamide metabolism by human liver and kidney microsomal cytochrome p450 enzymes to form hydroxyeicosatetraenoic and epoxyeicosatrienoic acid ethanolamides. *J Pharmacol Exp Ther* 321:590-597.2007).
- Snider NT, Nast JA, Tesmer LA, Hollenberg PF (A cytochrome P450-derived epoxygenated metabolite of anandamide is a potent cannabinoid receptor 2-selective agonist. *Mol Pharmacol* 75:965-972.2009).
- Snider NT, Sikora MJ, Sridar C, Feuerstein TJ, Rae JM, Hollenberg PF (The endocannabinoid anandamide is a substrate for the human polymorphic cytochrome P450 2D6. *J Pharmacol Exp Ther* 327:538-545.2008).
- Sokoloff L, Crittenden LB, Yamamoto RS, Jay GE, Jr. (The genetics of degenerative joint disease in mice. *Arthritis Rheum* 5:531-546.1962).
- Soliven B, Albert J (Tumor necrosis factor modulates Ca²⁺ currents in cultured sympathetic neurons. *J Neurosci* 12:2665-2671.1992).
- Sommer C, Kress M (Recent findings on how proinflammatory cytokines cause pain: peripheral mechanisms in inflammatory and neuropathic hyperalgesia. *Neurosci Lett* 361:184-187.2004).
- Song C, Howlett AC (Rat brain cannabinoid receptors are N-linked glycosylated proteins. *Life Sciences* 56 1983-1989.1995).
- Spuler S, Yousry T, Scheller A, Voltz R, Holler E, Hartmann M, Wick M, Hohlfeld R (Multiple sclerosis: prospective analysis of TNF-alpha and 55 kDa TNF receptor in CSF and serum in correlation with clinical and MRI activity. *J Neuroimmunol* 66:57-64.1996).
- Squire LR, Bloom, F.E., McConnell, S.K., Roberts, J.L., Spitzer, N.C., Zigmond, M.J. (2003) *The Somatosensory System*. In: *Fundamental*

- Neuroscience, p 681 London, UK: Academic Press, Elsevier Science (c).
- Starowicz K, Nigam S, Di Marzo V (Biochemistry and pharmacology of endovanilloids. *Pharmacol Ther* 114:13-33.2007).
- Staumont-Salle D, Abboud G, Brenuchon C, Kanda A, Roumier T, Lavogiez C, Fleury S, Remy P, Papin JP, Bertrand-Michel J, Terce F, Staels B, Delaporte E, Capron M, Dombrowicz D (Peroxisome proliferator-activated receptor alpha regulates skin inflammation and humoral response in atopic dermatitis. *J Allergy Clin Immunol* 121:962-968 e966.2008).
- Stebulis JA, Johnson DR, Rossetti RG, Burstein SH, Zurier RB (Ajulemic acid, a synthetic cannabinoid acid, induces an antiinflammatory profile of eicosanoids in human synovial cells. *Life Sci* 83:666-670.2008).
- Steen KH, Steen AE, Reeh PW (A dominant role of acid pH in inflammatory excitation and sensitization of nociceptors in rat skin, in vitro. *J Neurosci* 15:3982-3989.1995).
- Steiner F (Applications of narrow-bore columns in HPLC.1991).
- Stella N, Piomelli D (Receptor-dependent formation of endogenous cannabinoids in cortical neurons. *Eur J Pharmacol* 425:189-196.2001).
- Stochla K, Maslinski S (Carrageenan-induced oedema in the rat paw - histamine participation. *Agents Actions* 12:201-202.1982).
- Strangman NM, Patrick SL, Hohmann AG, Tsou K, Walker JM (Evidence for a role of endogenous cannabinoids in the modulation of acute and tonic pain sensitivity. *Brain Res* 813:323-328.1998).
- Stucky CL, Koltzenburg M, Schneider M, Engle MG, Albers KM, Davis BM (Overexpression of nerve growth factor in skin selectively affects the survival and functional properties of nociceptors. *J Neurosci* 19:8509-8516.1999).
- Suarez J, Bermudez-Silva FJ, Mackie K, Ledent C, Zimmer A, Cravatt BF, de Fonseca FR (Immunohistochemical description of the endogenous cannabinoid system in the rat cerebellum and functionally related nuclei. *J Comp Neurol* 509:400-421.2008).
- Sugiura T, Kodaka T, Kondo S, Nakane S, Kondo H, Waku K, Ishima Y, Watanabe K, Yamamoto I (Is the cannabinoid CB1 receptor a 2-arachidonoylglycerol receptor? Structural requirements for triggering a Ca²⁺ transient in NG108-15 cells. *J Biochem* 122:890-895.1997).
- Sugiura T, Kodaka T, Nakane S, Miyashita T, Kondo S, Suhara Y, Takayama H, Waku K, Seki C, Baba N, Ishima Y (Evidence that the cannabinoid CB1 receptor is a 2-arachidonoylglycerol receptor. Structure-activity relationship of 2-arachidonoylglycerol, ether-linked analogues, and related compounds. *J Biol Chem* 274:2794-2801.1999).
- Sugiura T, Kondo S, Kishimoto S, Miyashita T, Nakane S, Kodaka T, Suhara Y, Takayama H, Waku K (Evidence that 2-arachidonoylglycerol but not N-palmitoylethanolamine or anandamide is the physiological ligand for the cannabinoid CB2 receptor. Comparison of the agonistic activities of various cannabinoid receptor ligands in HL-60 cells. *J Biol Chem* 275:605-612.2000).
- Sugiura T, Kondo S, Sukagawa A, Nakane S, Shinoda A, Itoh K, Yamashita A, Waku K (2-Arachidonoylglycerol: a possible endogenous cannabinoid receptor ligand in brain. *Biochem Biophys Res Commun* 215:89-97.1995).

- Sugiura T, Tominaga M, Katsuya H, Mizumura K (Bradykinin lowers the threshold temperature for heat activation of vanilloid receptor 1. *J Neurophysiol* 88:544-548.2002).
- Sugiura T, Yoshinaga N, Waku K (Rapid generation of 2-arachidonoylglycerol, an endogenous cannabinoid receptor ligand, in rat brain after decapitation. *Neurosci Lett* 297:175-178.2001).
- Sun RQ, Tu YJ, Lawand NB, Yan JY, Lin Q, Willis WD (Calcitonin gene-related peptide receptor activation produces PKA- and PKC-dependent mechanical hyperalgesia and central sensitization. *J Neurophysiol* 92:2859-2866.2004).
- Sun Y, Alexander SP, Garle MJ, Gibson CL, Hewitt K, Murphy SP, Kendall DA, Bennett AJ (Cannabinoid activation of PPAR alpha; a novel neuroprotective mechanism. *Br J Pharmacol* 152:734-743.2007).
- Suplita RL, 2nd, Gutierrez T, Fegley D, Piomelli D, Hohmann AG (Endocannabinoids at the spinal level regulate, but do not mediate, nonopioid stress-induced analgesia. *Neuropharmacology* 50:372-379.2006).
- Svendsen KB, Jensen TS, Bach FW (Does the cannabinoid dronabinol reduce central pain in multiple sclerosis? Randomised double blind placebo controlled crossover trial. *BMJ* 329:253.2004).
- Svensson CI, Marsala M, Westerlund A, Calcutt NA, Campana WM, Freshwater JD, Catalano R, Feng Y, Protter AA, Scott B, Yaksh TL (Activation of p38 mitogen-activated protein kinase in spinal microglia is a critical link in inflammation-induced spinal pain processing. *J Neurochem* 86:1534-1544.2003).
- Szallasi A (The vanilloid (capsaicin) receptor: receptor types and species differences. *Gen Pharmacol* 25:223-243.1994).
- Szallasi A, Blumberg PM (Vanilloid (Capsaicin) receptors and mechanisms. *Pharmacol Rev* 51:159-212.1999).
- Szallasi A, Nilsson S, Farkas-Szallasi T, Blumberg PM, Hokfelt T, Lundberg JM (Vanilloid (capsaicin) receptors in the rat: distribution in the brain, regional differences in the spinal cord, axonal transport to the periphery, and depletion by systemic vanilloid treatment. *Brain Res* 703:175-183.1995).
- Szolcsanyi J, Helyes Z, Oroszi G, Nemeth J, Pinter E (Release of somatostatin and its role in the mediation of the anti-inflammatory effect induced by antidromic stimulation of sensory fibres of rat sciatic nerve. *Br J Pharmacol* 123:936-942.1998a).
- Szolcsanyi J, Pinter E, Helyes Z, Oroszi G, Nemeth J (Systemic anti-inflammatory effect induced by counter-irritation through a local release of somatostatin from nociceptors. *Br J Pharmacol* 125:916-922.1998b).
- Takahashi Y, Chiba T, Kurokawa M, Aoki Y (Dermatomes and the central organization of dermatomes and body surface regions in the spinal cord dorsal horn in rats. *J Comp Neurol* 462:29-41.2003).
- Thalhammer JG, LaMotte RH (Spatial properties of nociceptor sensitization following heat injury of the skin. *Brain Res* 231:257-265.1982).
- Thomas EA, Cravatt BF, Danielson PE, Gilula NB, Sutcliffe JG (Fatty acid amide hydrolase, the degradative enzyme for anandamide and oleamide, has selective distribution in neurons within the rat central nervous system. *J Neurosci Res* 50:1047-1052.1997).
- Thomas H (A community survey of adverse effects of cannabis use. *Drug Alcohol Depend* 42:201-207.1996).

- Todd AJ, Spike RC, Young S, Puskar Z (Fos induction in lamina I projection neurons in response to noxious thermal stimuli. *Neuroscience* 131:209-217.2005).
- Todd AJ, Sullivan AC (Light microscope study of the coexistence of GABA-like and glycine-like immunoreactivities in the spinal cord of the rat. *J Comp Neurol* 296:496-505.1990).
- Todd AJ, H.R. (2006) Neuroanatomical substrates of spinal nociception. In: Wall and Melzack's Textbook of Pain(McMahon, S. B. K., M., ed), pp 73-91: Elsevier Churchill Livingstone.
- Tominaga M, Caterina MJ, Malmberg AB, Rosen TA, Gilbert H, Skinner K, Raumann BE, Basbaum AI, Julius D (The cloned capsaicin receptor integrates multiple pain-producing stimuli. *Neuron* 21:531-543.1998).
- Tominaga M, Wada M, Masu M (Potentiation of capsaicin receptor activity by metabotropic ATP receptors as a possible mechanism for ATP-evoked pain and hyperalgesia. *Proc Natl Acad Sci U S A* 98:6951-6956.2001).
- Tonai T, Taketani Y, Ueda N, Nishisho T, Ohmoto Y, Sakata Y, Muraguchi M, Wada K, Yamamoto S (Possible involvement of interleukin-1 in cyclooxygenase-2 induction after spinal cord injury in rats. *J Neurochem* 72:302-309.1999).
- Torsney C, MacDermott AB (Disinhibition opens the gate to pathological pain signaling in superficial neurokinin 1 receptor-expressing neurons in rat spinal cord. *J Neurosci* 26:1833-1843.2006).
- Tsou K, Brown S, Sanudo-Pena MC, Mackie K, Walker JM (Immunohistochemical distribution of cannabinoid CB1 receptors in the rat central nervous system. *Neuroscience* 83:393-411.1998).
- Tsuboi K, Takezaki N, Ueda N (The N-acylethanolamine-hydrolyzing acid amidase (NAAA). *Chemistry & biodiversity* 4:1914-1925.2007).
- Ueda N, Kurahashi Y, Yamamoto S, Tokunaga T (Partial purification and characterization of the porcine brain enzyme hydrolyzing and synthesizing anandamide. *J Biol Chem* 270:23823-23827.1995a).
- Ueda N, Yamamoto K, Kurahashi Y, Yamamoto S, Ogawa M, Matsuki N, Kudo I, Shinkai H, Shirakawa E, Tokunaga T (Oxygenation of arachidonylethanolamide (anandamide) by lipoxygenases. *Adv Prostaglandin Thromboxane Leukot Res* 23:163-165.1995b).
- Valenti M, Viganò D, Casico MG, Rubino T, Steardo L, Parolaro D, Di Marzo V, McPartland JM, Carrier EJ, Kearn CS, Barkmeier AJ, Breese NM, Yang W, Nithipatikom K, Pfister SL, Campbell WB, Hillard CJ (Differential diurnal variations of anandamide and 2-arachidonoyl-glycerol levels in rat brain phylogenomic and chemotaxonomic analysis of the endocannabinoid system cultured rat microglial cells synthesize the endocannabinoid 2-arachidonylglycerol, which increases proliferation via a CB2 receptor-dependent mechanism. *Cell Mol Life Sci* 61:945-950.2004).
- Valenzano KJ, Tafesse L, Lee G, Harrison JE, Boulet JM, Gottshall SL, Mark L, Pearson MS, Miller W, Shan S, Rabadi L, Rotshteyn Y, Chaffer SM, Turchin PI, Elsemore DA, Toth M, Koetzner L, Whiteside GT (Pharmacological and pharmacokinetic characterization of the cannabinoid receptor 2 agonist, GW405833, utilizing rodent models of acute and chronic pain, anxiety, ataxia and catalepsy. *Neuropharmacology* 48:658-672.2005).

- Van Der Stelt M, Di Marzo V (Endovanilloids. Putative endogenous ligands of transient receptor potential vanilloid 1 channels. *Eur J Biochem* 271:1827-1834.2004).
- van der Stelt M, Di Marzo V (Anandamide as an intracellular messenger regulating ion channel activity. *Prostaglandins Other Lipid Mediat* 77:111-122.2005).
- van der Stelt M, Trevisani M, Vellani V, De Petrocellis L, Schiano Moriello A, Campi B, McNaughton P, Geppetti P, Di Marzo V (Anandamide acts as an intracellular messenger amplifying Ca²⁺ influx via TRPV1 channels. *Embo J* 24:3026-3037.2005).
- Van Sickle MD, Duncan M, Kingsley PJ, Mouihate A, Urbani P, Mackie K, Stella N, Makriyannis A, Piomelli D, Davison JS, Marnett LJ, Di Marzo V, Pittman QJ, Patel KD, Sharkey KA (Identification and functional characterization of brainstem cannabinoid CB2 receptors. *Science* 310:329-332.2005).
- Vanden Berghe W, Plaisance S, Boone E, De Bosscher K, Schmitz ML, Fiers W, Haegeman G (p38 and extracellular signal-regulated kinase mitogen-activated protein kinase pathways are required for nuclear factor-kappaB p65 transactivation mediated by tumor necrosis factor. *J Biol Chem* 273:3285-3290.1998).
- Vandevoorde S, Jonsson KO, Labar G, Persson E, Lambert DM, Fowler CJ (Lack of selectivity of URB602 for 2-oleoylglycerol compared to anandamide hydrolysis in vitro. *Br J Pharmacol* 150:186-191.2007).
- Vandevoorde S, Lambert DM (The multiple pathways of endocannabinoid metabolism: a zoom out. *Chemistry & biodiversity* 4:1858-1881.2007).
- Vane JR (Inhibition of prostaglandin synthesis as a mechanism of action for aspirin-like drugs. *Nat New Biol* 231:232-235.1971).
- Vane JR (The mode of action of aspirin and similar compounds. *J Allergy Clin Immunol* 58:691-712.1976).
- Varma N, Carlson GC, Ledent C, Alger BE (Metabotropic glutamate receptors drive the endocannabinoid system in hippocampus. *J Neurosci* 21:RC188.2001).
- Vellani V, Petrosino S, De Petrocellis L, Valenti M, Prandini M, Magherini PC, McNaughton PA, Di Marzo V (Functional lipidomics. Calcium-independent activation of endocannabinoid/endovanilloid lipid signalling in sensory neurons by protein kinases C and A and thrombin. *Neuropharmacology* 55:1274-1279.2008).
- Vermeirsch H, Biermans R, Salmon PL, Meert TF (Evaluation of pain behavior and bone destruction in two arthritic models in guinea pig and rat. *Pharmacol Biochem Behav* 87:349-359.2007).
- Vonsy JL, Ghandehari J, Dickenson AH (Differential analgesic effects of morphine and gabapentin on behavioural measures of pain and disability in a model of osteoarthritis pain in rats. *European Journal of Pain* In Press, Corrected Proof.2008).
- Vyklicky L, Knotkova-Urbancova H, Vitaskova Z, Vlachova V, Kress M, Reeh PW (Inflammatory mediators at acidic pH activate capsaicin receptors in cultured sensory neurons from newborn rats. *J Neurophysiol* 79:670-676.1998).
- Wager-Miller J, Westenbroek R, Mackie K (Dimerization of G protein-coupled receptors: CB1 cannabinoid receptors as an example. *Chemistry and Physics of Lipids* 121:83-89.2002).
- Walker JM, Huang SM (Cannabinoid analgesia. *Pharmacol Ther* 95:127-135.2002a).

- Walker JM, Huang SM (Endocannabinoids in pain modulation. Prostaglandins Leukot Essent Fatty Acids 66:235-242.2002b).
- Walker JM, Huang SM, Strangman NM, Tsou K, Sanudo-Pena MC (Pain modulation by release of the endogenous cannabinoid anandamide. Proc Natl Acad Sci U S A 96:12198-12203.1999).
- Walker K, Fox AJ, Urban LA (Animal models for pain research. Mol Med Today 5:319-321.1999c).
- Walton M (Degenerative joint disease in the mouse knee; histological observations. J Pathol 123:109-122.1977).
- Wang J, Ueda N (Biology of endocannabinoid synthesis system. Prostaglandins Other Lipid Mediat.2008).
- Ware CF (Network communications: lymphotoxins, LIGHT, and TNF. Annu Rev Immunol 23:787-819.2005).
- Watanabe K, Ogi H, Nakamura S, Kayano Y, Matsunaga T, Yoshimura H, Yamamoto I (Distribution and characterization of anandamide amidohydrolase in mouse brain and liver. Life Sci 62:1223-1229.1998).
- Watkins LR, Goehler LE, Relton J, Brewer MT, Maier SF (Mechanisms of tumor necrosis factor-alpha (TNF-alpha) hyperalgesia. Brain Res 692:244-250.1995).
- Weber A, Ni J, Ling KH, Acheampong A, Tang-Liu DD, Burk R, Cravatt BF, Woodward D (Formation of prostamides from anandamide in FAAH knockout mice analyzed by HPLC with tandem mass spectrometry. J Lipid Res 45:757-763.2004).
- Wei BQ, Mikkelsen TS, McKinney MK, Lander ES, Cravatt BF (A second fatty acid amide hydrolase with variable distribution among placental mammals. J Biol Chem 281:36569-36578.2006).
- Welch SP, Huffman JW, Lowe J (Differential blockade of the antinociceptive effects of centrally administered cannabinoids by SR141716A. J Pharmacol Exp Ther 286:1301-1308.1998).
- Welch SP, Stevens DL (Antinociceptive activity of intrathecally administered cannabinoids alone, and in combination with morphine, in mice. J Pharmacol Exp Ther 262:10-18.1992).
- Wendling D, Streit G, Toussiroit E, Prati C (Herpes zoster in patients taking TNFalpha antagonists for chronic inflammatory joint disease. Joint Bone Spine 75:540-543.2008).
- Williams J, Wood J, Pandarinathan L, Karanian DA, Bahr BA, Vouros P, Makriyannis A (Quantitative method for the profiling of the endocannabinoid metabolome by LC-atmospheric pressure chemical ionization-MS. Anal Chem 79:5582-5593.2007).
- Willis WDC, R.E (Sensory mechanisms of the spinal cord. New York Kluwer Academic/ Plenum Publishers.2004).
- Wilson RI, Nicoll RA (Endogenous cannabinoids mediate retrograde signalling at hippocampal synapses. Nature 410:588-592.2001).
- Winter CA, Risley EA, Nuss GW (Carrageenin-induced edema in hind paw of the rat as an assay for antiinflammatory drugs. Proc Soc Exp Biol Med 111:544-547.1962).
- Winter J, Forbes CA, Sternberg J, Lindsay RM (Nerve growth factor (NGF) regulates adult rat cultured dorsal root ganglion neuron responses to the excitotoxin capsaicin. Neuron 1:973-981.1988).
- Wise LE, Shelton CC, Cravatt BF, Martin BR, Lichtman AH (Assessment of anandamide's pharmacological effects in mice deficient of both fatty acid amide hydrolase and cannabinoid CB1 receptors. Eur J Pharmacol 557:44-48.2007).

- Wood JN, Winter J, James IF, Rang HP, Yeats J, Bevan S (Capsaicin-induced ion fluxes in dorsal root ganglion cells in culture. *J Neurosci* 8:3208-3220.1988).
- Woodward DF, Phelps RL, Krauss AH, Weber A, Short B, Chen J, Liang Y, Wheeler LA (Bimatoprost: a novel antiglaucoma agent. *Cardiovasc Drug Rev* 22:103-120.2004).
- Woolf C, Wiesenfeld-Hallin Z (Substance P and calcitonin gene-related peptide synergistically modulate the gain of the nociceptive flexor withdrawal reflex in the rat. *Neurosci Lett* 66:226-230.1986).
- Woolf CJ, Allchorne A, Safieh-Garabedian B, Poole S (Cytokines, nerve growth factor and inflammatory hyperalgesia: the contribution of tumour necrosis factor alpha. *Br J Pharmacol* 121:417-424.1997).
- Woolf CJ, Salter MW (Neuronal plasticity: increasing the gain in pain. *Science* 288:1765-1769.2000).
- Wotherspoon G, Fox A, McIntyre P, Colley S, Bevan S, Winter J (Peripheral nerve injury induces cannabinoid receptor 2 protein expression in rat sensory neurons. *Neuroscience* 135:235-245.2005).
- Wright S, Ware M, Guy G (The use of a cannabis-based medicine (Sativex) in the treatment of pain caused by rheumatoid arthritis. *Rheumatology (Oxford)* 45:781; author reply 781-782.2006).
- Wu H (Assembly of post-receptor signaling complexes for the tumor necrosis factor receptor superfamily. *Adv Protein Chem* 68:225-279.2004).
- Xie WL, Chipman JG, Robertson DL, Erikson RL, Simmons DL (Expression of a mitogen-responsive gene encoding prostaglandin synthase is regulated by mRNA splicing. *Proc Natl Acad Sci U S A* 88:2692-2696.1991).
- Yaksh TL (Behavioral and autonomic correlates of the tactile evoked allodynia produced by spinal glycine inhibition: effects of modulatory receptor systems and excitatory amino acid antagonists. *Pain* 37:111-123.1989).
- Yaksh TL, Dirig DM, Conway CM, Svensson C, Luo ZD, Isakson PC (The acute antihyperalgesic action of nonsteroidal, anti-inflammatory drugs and release of spinal prostaglandin E2 is mediated by the inhibition of constitutive spinal cyclooxygenase-2 (COX-2) but not COX-1. *J Neurosci* 21:5847-5853.2001).
- Yamagata K, Andreasson KI, Kaufmann WE, Barnes CA, Worley PF (Expression of a mitogen-inducible cyclooxygenase in brain neurons: regulation by synaptic activity and glucocorticoids. *Neuron* 11:371-386.1993).
- Yamamoto W, Mikami T, Iwamura H (Involvement of central cannabinoid CB2 receptor in reducing mechanical allodynia in a mouse model of neuropathic pain. *European Journal of Pharmacology* 583:56-61.2008).
- Yang W, Ni J, Woodward DF, Tang-Liu DD, Ling KH (Enzymatic formation of prostamide F2alpha from anandamide involves a newly identified intermediate metabolite, prostamide H2. *J Lipid Res* 46:2745-2751.2005).
- Yorek M, Jaipaul N, Dunlap J, Bielefeldt K (Endothelin-stimulated Ca²⁺ mobilization by 3T3-L1 adipocytes is suppressed by tumor necrosis factor-alpha. *Arch Biochem Biophys* 361:241-251.1999).
- Yoshida T, Fukaya M, Uchigashima M, Miura E, Kamiya H, Kano M, Watanabe M (Localization of diacylglycerol lipase-alpha around postsynaptic spine suggests close proximity between production

- site of an endocannabinoid, 2-arachidonoyl-glycerol, and presynaptic cannabinoid CB1 receptor. *J Neurosci* 26:4740-4751.2006).
- Yoshida T, Hashimoto K, Zimmer A, Maejima T, Araishi K, Kano M (The cannabinoid CB1 receptor mediates retrograde signals for depolarization-induced suppression of inhibition in cerebellar Purkinje cells. *J Neurosci* 22:1690-1697.2002).
- Yu M, Ives D, Ramesha CS (Synthesis of prostaglandin E2 ethanolamide from anandamide by cyclooxygenase-2. *J Biol Chem* 272:21181-21186.1997).
- Zhang Y, Shaffer A, Portanova J, Seibert K, Isakson PC (Inhibition of cyclooxygenase-2 rapidly reverses inflammatory hyperalgesia and prostaglandin E2 production. *J Pharmacol Exp Ther* 283:1069-1075.1997).
- Zhao Z, Chen SR, Eisenach JC, Busija DW, Pan HL (Spinal cyclooxygenase-2 is involved in development of allodynia after nerve injury in rats. *Neuroscience* 97:743-748.2000).
- Zygmunt PM, Chuang H, Movahed P, Julius D, Hogestatt ED (The anandamide transport inhibitor AM404 activates vanilloid receptors. *Eur J Pharmacol* 396:39-42.2000).
- Zygmunt PM, Petersson J, Andersson DA, Chuang H, Sorgard M, Di Marzo V, Julius D, Hogestatt ED (Vanilloid receptors on sensory nerves mediate the vasodilator action of anandamide. *Nature* 400:452-457.1999).

8 Appendix

Calcium Imaging Buffer

145 mM NaCl,

5 mM KCl, CaCl₂

1 mM MgSO₄·7H₂O

10 mM HEPES

10 mM glucose

Make up to 1 liter dH₂O 37°C, pH 7.4.

Fura-2-AM

5 µl of a 10 mg/ml solution in anhydrous dimethyl sulfoxide in 900 µl Ca²⁺ buffer with 100 µl fetal calf serum.

Lowry A solution

2.85 g NaOH

14.30 g Na₂ CO₃

Make up to 500 ml in dH₂O

Lowry AB solution

20mls of solution A to 100µl 2% NaK tartrate and 100µl 1% CuSO₄

2.5mM Probenecid Solution

0.71g probenecid in 5ml 1M NaOH + 5ml HBSS

Brilliant Black Solution

10 g prepared to 50mM in dH₂O

HEPES buffered saline (HBSS)

0.22g Sodium Pyruvate

8.47g NaCl

1.8g Glucose

0.37g KCl

0.246g MgSO₄·7H₂O

2.384g HEPES

0.191g CaCl₂

0.126g NaHCO₃

Make up to 1L with dH₂O. pH to 7.45.

Fluo-4 loading solution

50µg Fluo-4 to a 1mM solution in 10% pluronic acid in DMSO (22.8µl DMSO + 22.8µl 20% pluronic acid). Add to 20ml loading buffer (supplemented HBSS plus final concentration of 2.5mM probenecid and 0.5mM brilliant black).

Transfer buffer

30.3 g Tris

144 g Glycine

Dissolve in 8 Ltr dH₂O, and 2 Ltr methanol

TBST blocking buffer 0.1% tween

30.29 g Tris

73.12 g NaCl

Dissolve in 1ltr dH₂O

Adjust pH 7.6

Make up to 10ltr in big container

Add 10ml Tween 20 to a final conc of 0.1%

Lysis Buffer pH 7.6

12.1 g Tris

1,9 g EGTA

51.7 g Sucrose

500µl 0.1% Triton X100

0.021g NaF

1.08 g β-glycerophosphate

Dissolve in 500ml DH₂O pH 7.6

Add 1 Protease tablet in 10ml lysis buffer before use

6X solubalisation Buffer

2.5ml 0.5M Tris

2.0ml Glycerol

2.0ml 10%SDS

2.5ml dH₂O

1.0ml β-mercaptoethanol

40μl 2.5% Bromophenol Blue